COMPLETION REPORT

NGR 25-001-012
UMKC 2140-2228

REFLECTANCE OF AQUEOUS SOLUTIONS

Submitted to

Grant Monitor
Mr. Robert Drummond
Goddard Space Flight Center
Greenbelt, Maryland

from the

Optical Physics Laboratory
Department of Physics
University of Missouri-Kansas City

Marvin R. Querry
Principal Investigator

Richard C. Waring
Senior Investigator

George M. Hale
Research Assistant

Wayne E. Holland
Research Associate

21 July 1972

FOREWORD

This is the final report for a two year research project NGR-25-001-012 to investigate the optical properties and the optical constants of water and aqueous solutions. The ultimate objective of the research project was to produce an accurate tabulation of graphical representation of the optical constants of water and aqueous solutions throughout a broad region of the electromagnetic spectrum. This report shows we have made significant progress toward fulfillment of that objective. The report is in four separate parts. The first three parts are manuscripts of articles submitted to either the Journal of the Optical Society of America or Applied Optics for review and hopefully for eventual publication. The fourth part is a series of graphical presentations of some optical properties and optical constants in the infrared for water, heavy water, and 26 aqueous solutions.

We invite your comments and discussion of the material included in the report.

Marvin R. Querry
21 July 1972

TABLE OF CONTENTS

THE REFLECTANCE OF AQUEOUS SOLUTIONS

M.R. Querry, R.C. Waring
W.E. Holland and G.M. Hale

INTRODUCTION

This is the final report for a two year research project to investigate the optical properties and the optical constants of water and aqueous solutions. The ultimate objective of the research project was to produce an accurate tabulation of graphical representation of the optical constants of water and aqueous solutions throughout a broad region of the electromagnetic spectrum. This report shows we have made significant progress toward fulfillment of that objective. The report is in four separate parts. The first three parts are manuscripts of articles submitted to either the Journal of the Optical Society of America or Applied Optics for review and hopefully for eventual publication. The fourth part is a series of graphical presentations of some optical properties and optical constants of water, heavy water, and 26 aqueous solutions.

Part I is a manuscript entitled "Optical Constants of Water in the 200-nm to 200-μm Wavelength Region". The abstract reads:

Extinction coefficients $k(\lambda)$ for water at 25°C were determined through a broad spectral region by

manually smoothing a point by point graph of $k(\lambda)$ versus wavelength λ which was plotted for data obtained from a review of the scientific literature on the optical constants of water. Absorption bands representing $k(\lambda)$ were postulated where data were not available in the vacuum ultraviolet and soft x-ray regions. A subtractive Kramers-Kronig analysis of the combined postulated and smoothed portions of the $k(\lambda)$-spectrum provided the index of refraction $n(\lambda)$ for the spectral region 200 nm $\leq \lambda \leq$ 200 μm.

Part II is a manuscript entitled "Kramers-Kronig analysis of Relative Reflectance Spectra Measured at an Oblique Angle." The abstract reads:

> Relative specular reflectance R is defined as $R = R_s/R_w$, where R_s and R_w are absolute reflectances of a sample material s and a material w for which the index of refraction n_w and the extinction coefficient k_w are known quantities. An algorithm was developed for computing n_s and k_s from the sample's R-spectrum measured for radiant flux polarized perpendicular to the plane of incidence and reflected at oblique angle θ. Kramers-Kronig analysis of the R-spectrum provides $\Delta\phi$ the difference between phase shifts for electromagnetic waves reflected at the surfaces of materials s and w. Real and imaginary parts of a Fresnel equation for relative reflectivity provides equations for computing n_s and k_s when θ, $\Delta\phi$, n_w, and k_w are known quantities. Optical constants for aqueous solutions containing NaCl were computed in this manner; distilled water was the reflectance standard.

Part III is a manuscript entitled "The Influence of Temperature on the Spectrum of Water". The abstract reads:

> The normal-incidence spectral reflectance of water at 5°C, 27°C, and 70°C has been measured in the spectral region between 5000 and 350 cm^{-1}. From the measured values of spectral reflectance we have determined the optical constants n_r and n_i by Kramers-Kronig methods. The band strengths $S_B = \int n_i(\nu)d\nu$ and band widths have been determined for the absorption bands near 3400 cm^{-1}, 1640 cm^{-1}, and 600 cm^{-1} at each temperature. A similar study of deuterium oxide at 27°C has been conducted for purposes of comparison.

Part IV is a series of graphical presentations of absolute reflectance, phase shifts, index of refraction, and extinction coefficients for water, heavy water, and 26 aqueous solutions. The measurements of absolute reflectance were supplied by Dr. Dudley Williams of Kansas State University. The reflectance was measured at near normal incidence through the spectral region 5,000 cm^{-1} to 300 cm^{-1}. We made a Kramers-Kronig analysis of the reflectance spectra in order to determine the phase-shift for electromagnetic waves reflected at the surface of the water and the aqueous solutions. We then determined the index of refraction and the extinction coefficients by use of the computed phase-shifts and measured values for reflectance. A full analysis of all the data presented in

Part IV will probably take about two more years. Several manuscripts should result from these future investigations. The manuscripts also will be forwarded to the NASA when they are submitted for publication.

Additionally, the report contains as an appendix a comprehensive list of lasing organic dyes and the conditions under which they lase. The list is based on a critical review of the scientific literature which was conducted by Mr. Wayne Holland of our staff. We have found the list of dye helpful in our work with the organic-dye-laser spectrophotometer that was described in the first annual report for this program of research. We include the list here in the hope that it will be helpful to others.

PART I

Optical Constants of Water in the 200-nm to 200-μm Wavelength Region*

George M. Hale and Marvin R. Querry

Department of Physics

University of Missouri, Kansas City 64110

Extinction coefficients $k(\lambda)$ for water at 25°C were determined through a broad spectral region by manually smoothing a point by point graph of $k(\lambda)$ versus wavelength λ which was plotted for data obtained from a review of the scientific literature on the optical constants of water. Absorption bands representing $k(\lambda)$ were postulated where data were not available in the vacuum ultraviolet and soft x-ray regions. A substractive Kramers-Kronig analysis of the combined postulated and smoothed portions of the $k(\lambda)$-spectrum provided the index of refraction $n(\lambda)$ for the spectral region 200 nm $\leq \lambda \leq$ 200 μm.

I. INTRODUCTION

The index of refraction $n(\lambda)$ and the extinction coefficient $k(\lambda)$ of water are respectively the real and imaginary parts of its spectral complex refractive index $\tilde{n} = n - ik$, where λ is the wavelength of an electromagnetic wave in vacuum and $i = (-1)^{\frac{1}{2}}$. The quantities $n(\lambda)$ and $k(\lambda)$ are called optical constants. They are physical parameters that together with the complex Fresnel equations and the generalized Fresnel equations provide the basis for computing the optical properties of water. In recent years knowledge of the optical properties of water has been of greater interest because of its application in (1) computing radiation transport through atmospheres containing water droplets and other aerosols or through oceans containing hydrosols, (2) development of optical remote sensing instruments for measuring the chemical and thermal quality or turbidity of environmental waters and for measuring the water content of soils, (3) computing the optical properties of plant leaves, and (4) investigations of the optical properties and optical constants of aqueous solutions.

In 1968 Irvine and Pollack[1/] published results from a critical review of the existing literature on the optical properties of water for the 0.2-200-μm wavelength region. They tabulated measured values of both $k(\lambda)$ and the Lambert absorption coefficient $\alpha(\lambda) = 4\pi k(\lambda)/\lambda$ from about thirty different papers appearing in

the scientific literature. Next, using the only four reports on measurements of the reflectance of water that were available at that time, they tabulated values for the reflectance $R(\lambda)$ measured at near normal incidence for a free water surface. The tabulated values for $k(\lambda)$ and the generalized Fresnel reflectance equation for $R(\lambda)$, i.e. the Cauchy equation, then provided values for $n(\lambda)$.

Zolotarev et al.[2] in 1969 reported values for the optical constants of water throughout the spectral region $1\text{-}10^6$ μm. They determined both $k(\lambda)$ and $n(\lambda)$ from their measurements of $\alpha(\lambda)$ and $R(\lambda)$ for water at 25°C in the 2-50-μm region and measurements of internal reflectance spectra in the 2-10-μm region. Their measurements and reliable data from thirteen other papers in the scientific literature provided values of $k(\lambda)$ throughout the spectral region $1\text{-}10^6$ μm. Values of $n(\lambda)$ were then obtained from a Kramers-Kronig (K-K) analysis of the $k(\lambda)$-spectrum:

$$n(\lambda_o) = 1 + \frac{2\lambda_o^2}{\pi} \int_o^\infty \frac{k(\lambda)\, d\lambda}{\lambda(\lambda_o^2 - \lambda^2)} \quad . \tag{1}$$

For making the integration indicated by Eq. (1) a model absorption band with central position at 100 nm was constructed for $k(\lambda)$ in in the ultraviolet region. The band was reported to have no significant affect on calculated values of $n(\lambda)$ for $\lambda \geq 1$ μm. Zolotarev et al. noted discrepancies in the 20-50-μm region between their values for $n(\lambda)$ and those reported by Irvine and Pollack. They noted that in the 6.5-9-μm region the values of

$k(\lambda)$ measured by Pointier and Dechambenoy[3] were 30% smaller than their measured values for that quantity, and also that values for both $n(\lambda)$ and $k(\lambda)$ at the infrared band centers were in disagreement with those measured by Pointier and Dechambenoy.

Since Zolotarev et al. completed their investigation of the optical constants of water in 1968 at least nine other papers[4-13] appearing in the literature have reported measurements of the optical properties of water in the vacuum ultraviolet, visible, infrared, or microwave spectral regions. Of particular interest are the careful measurements reported by Robertson and Williams[6] for $\alpha(\lambda)$ in the 2.5-38.4-μm region, and the measurements of reflectance and subsequent computations of $n(\lambda)$ and $k(\lambda)$ reported by Painter et al.[9,10] and Kerr et al.[8] for which, when combined, extend through the 80-300-nm region of the vacuum ultraviolet.

For three reasons; (1) because a current knowledge of the optical constants of water is essential to our investigations of aqueous solutions,[14,15] (2) because of the discrepancies between values reported for both $n(\lambda)$ and $k(\lambda)$, and (3) because of the additional measurements of these quantities in the infrared and ultraviolet regions that have been reported since 1968; we felt a need at this time for an updated review of the literature on the optical constants of water. From the scientific literature we compiled and then point by point manually plotted graphs of measured values for $k(\lambda)$ verses λ through the microwave, far infrared,

infrared, visible, x-ray, and part of the ultraviolet regions of the electromagnetic spectrum. A smooth continuous curve considered to be a mutually consistent fit to the best data for $k(\lambda)$ and to be representative of $k(\lambda)$ for water at 25°C was drawn manually through the plotted points. Two absorption bands each of adjustable height and width were postulated for $k(\lambda)$ in the vacuum ultraviolet and soft x-ray regions where data were not available from the literature. A subtractive Kramers-Kronig (K-K) analysis of the combined postulated and smoothed portions of the $k(\lambda)$-spectrum then provided values of $n(\lambda)$ for the spectral region 200 nm $\leq \lambda \leq$ 200 μm.

II. ACQUISITION OF DATA

A search was made for literature reporting measurements of the electromagnetic absorption characteristics of liquid water in any spectral region. A total of 58 articles and books[1-13,16-60] were selected from the literature of the past 81 years. The selected references were examined individually for specific or tabulated values of the extinction coefficient $k(\lambda)$. Often the information was presented in graphical form. In most cases the absorption characteristics were expressed as Lambert absorption coefficient $\alpha(\lambda)$; as molecular absorption coefficient $\xi(\lambda)_m = \alpha(\lambda)/(2.3026C)$ where C is the concentration of the substance in units of moles/liter; as absorption index $K(\lambda) = k(\lambda)/n(\lambda)$; as real $\xi_r(\lambda) = 2n(\lambda)k(\lambda)$ and imaginary $\xi_i(\lambda) = n(\lambda)^2 - k(\lambda)^2$ parts of the complex dielectric constant; or as mass absorption coefficient (μ/ρ) where μ is the linear absorption coefficient and ρ is the mass per unit volume. In the x-ray region $k(\lambda)$ for water was determined by use of the relation

$$k(\lambda) = \frac{\lambda\rho}{4\pi}\left[\, 0.111\left(\frac{\mu}{\rho}\right)_{H\lambda} + 0.889\left(\frac{\mu}{\rho}\right)_{o\lambda} - \frac{\sigma}{\rho}\right], \qquad (2)$$

where 0.111 and 0.889 are respectively the fractional masses of hydrogen and oxygen present in a water molecule, $(\mu/\rho)_{H\lambda}$ and $(\mu/\rho)_{o\lambda}$ are respectively the mass absorption coefficients of hydrogen and oxygen for x rays of wavelength λ, and $(\sigma/\rho) = 0.2\ cm^2/g$

is the mass scattering coefficient calculated according to the classical Thompson theory for x-ray scattering by atoms of low atomic number. The density ρ was 1 g/cm^3. A listing of all accumulated values for $k(\lambda)$ ordered with respect to increasing λ was provided by an IBM 360/50 computer. In many cases significant discrepancies were noted between values of $k(\lambda)$ at the same λ but obtained from different references. All points in the listing then were plotted manually on graphs of $k(\lambda)$ versus λ. The best visual fit to the plotted data for $k(\lambda)$ was obtained by manually drawing a smooth curve through the points while weighting the curve in favor of data reported by some authors and data for water at 25°C. Two postulated absorption bands of Gaussian shape were constructed for $k(\lambda)$ in the soft x-ray and vacuum ultraviolet regions where data were not available from the literature. The final values for $k(\lambda)$ are shown graphically in Figs. 1-5 and in Table I are tabulated at selected positions between 200 nm and 200 μm.

III. DISCUSSION OF GRAPHS FOR $k(\lambda)$ vs. λ

A. Figure 1, Graph 0 - 0.5 Å: The smooth curve shown in this graph was based on values for absorption coefficients of water for x-rays and γ-rays as reported by Allen[27].

B. Figure 1, Graph 0 - 55 Å: The smooth solid-line curve shown in this graph was based on values for the absorption coefficients of x-rays and γ-rays as reported by Allen[27] for the 0.25 - 0.7-Å region, and on Eq. (2) and values for the mass absorption coefficients taken from reference 52 for the 0.71 - 2.5 Å region and from Engstrom[51] for the 5 - 22-Å region. The smooth dashed-line curve was the short wavelength side of an absorption band postulated for $k(\lambda)$ in the soft x-ray region.

C. Figure 1, Graph 0 - 2000 Å

1. Spectral region 22 - 849 Å: Data for this region were not available from the literature. The dashed-line curve for $k(\lambda)$ in this region was postulated in a very subjective manner. The curve was made Gaussian shaped between 850 Å and about 300 Å. The peak in the curve at about 80 Å was added in order to continuously join the solid-line curve ending at 22 Å with the Gaussian shaped curve at about 300 Å.

2. Spectral region 849 - 1250 Å: The only data available for this region were those of Kerr et al.[8] Their values for $k(\lambda)$ were calculated by K-K analysis of reflectance data for water at 1°C. For $\lambda \geq 1250$ Å their values of $k(\lambda)$ are greater than those reported by other investigators. Therefore, we chose for this region the similar shaped but smaller-in-magnitude dashed-line curve which was thought to represent $k(\lambda)$ for water at 25°C.

3. Spectral region 1250 - 2000 Å: The solid-line curve was based on data from Painter et al.[9,10] and data from references 42, 44, 46, 47, and 49. Because the curve is rapidly rising in the 1,700 - 1,850-Å region, individual values of $k(\lambda)$ read from this curve are subject to a significant amount of error.

D. Figure 2, Graph 180 - 1,000 nm: The smooth solid-line curve was based mostly on values of $k(\lambda)$ from references 11, 16, 17, 18, 19, 31, 34, and 40. Notable exceptions to the curve selected for $k(\lambda)$ are data of Lenoble and Saint-Guilly[31] (LSG) and of Tyler, Smith, and Wilson[11] (TSW). The paper by TSW was a recent one predicting the optical properties of clear natural water. Data reported by LSG, when compared to our curve, are lower for $\lambda < 370$ nm and are greater for $\lambda > 370$ nm. At 400 nm, values of $k(\lambda)$ from LSG were significantly greater than values of

$k(\lambda)$ from Clarke and James[40] (CJ) and from several of the other references. Data from CJ suggested a more highly structured curve for $k(\lambda)$ than the one we constructed in the 380-580-nm region, but data from the other references supported the selected curve. Sullivan[18] provided a consistent set of data for $k(\lambda)$ throughout the region 580-790 nm. The structure of our curve for $k(\lambda)$, however, departed slightly from that suggested by Sullivan's data in the region of the maximum for $k(\lambda)$ at about 760 nm. In the 800-1,000 nm region the curve for $k(\lambda)$ was based primarily on data from Curcio and Petty[34] and Kondrat'yev[19]. Values for $k(\lambda)$ reported by Bayly, Kartha, and Stevens[26] seemed to be consistently too large.

E. Figure 3, Graph 0.95-2.6 μm: The smooth solid-line curve for $k(\lambda)$ was based on data from references 1-7, 16, 17, 19, 20, 23, 25, 28, 34, 39, 53, and 54. In the 0.95-2.0-μm region the primary references were Kondrat'yev[19], Curcio and Petty[34] and Zolotarev et al.[2] In the 2.0-2.6-μm region Centeno's data were in poor agreement with data from several of the other references. The small shoulder band at 2.5 μm originally reported by Collins[39] and recently commented on by Robertson and Williams[6] was included in our curve for $k(\lambda)$.

F. Figure 4, Graph 2.5-18.5 μm: The smooth solid-line curve for $k(\lambda)$ was based on data from references 1-7, 17, 19, 23, 25, 26, 28, 29, 38, and 54. The better data seemed to be those of Robertson and Williams[6] and Zolotarev et al.[2] The maximum value of $k(\lambda)$, $k(17.2\ \mu m) = 0.430$, for the libration band was estimated in both position and magnitude from data of Hale, Querry, Rusk, and Williams[7]. Values of $k(\lambda)$ from Irvine and Pollack[1] agree fairly well with the curve selected through this spectral region.

G. Figure 5, Graph 10 - 100 μm: Data through this spectral region were selected from references 1-7, 17, 19, 22, 24, 28, 29, 50, and 54. Many discrepancies existed between values for $k(\lambda)$ reported by different investigators. Data from Rusk, Williams, and Querry[5] (RWQ) seemed to assign values for $k(\lambda)$ that were too large; this was attributed to an inefficient polarizer for $\lambda \gtrsim 20\ \mu m$. Data from Robertson and Williams[6] (ROW) seemed to assign values for $k(\lambda)$ that were too small; as noted in the original paper this was perhaps due in part to scattered radiant flux that remained undetected. Temperature influences the shape and position of the libration band as indicated by Hale et al[7] and by Pointier and Dechambenoy[3] (PD, 1966). Temperature of

the water was not indicated by ROW. Our smooth curve for $k(\lambda)$ was based on a median estimate between ROW and PD; the estimate coincides very well with data from Zolotarev et al.[2]. In the 58-84-μm region the curve for $k(\lambda)$ follows closely data from Draegert et al.[22], Zolotarev et al.[2] and Irvine and Pollack[1]. Above 84 μm the curve was primarily based on data from Zolotarev et al.

H. Figure 5, Graph 50-100 μm: Data from Chamberlain, Chantry, and Gebbie[21] and from Zolotarev et al.[2] were used for $k(\lambda)$ in this spectral region.

J. Figure 5, Graph 0-10 cm: Data from Rabinovich and Melent'yev[13] (RBM) and from Zolotarev et al.[2] were used for $k(\lambda)$ in this spectral region.

K. Figure 5, Graph 0-1.0 meter: (curve begins at 10 cm). The solid-line curve was a smooth fit to scattered data points selected from references 2 and 37. There were probably some regions of absorption that were not shown in the final curve.

IV. INDEX OF REFRACTION

Values of the index of refraction $n(\lambda)$ for the spectral region 200 nm to 200 μm were computed by applying a subtractive Kramers-Kronig analysis[58,59] (SKK) to the continuous spectrum for $k(\lambda)$ shown in Figs. 1-5. Accordingly, the index of refraction $n(\lambda_o)$ at wavelength λ_o is

$$n(\lambda_o) = n(\lambda_1) + \text{Prin.}\left[\frac{2(\lambda_1^2 - \lambda_o^2)}{\pi}\int_0^\infty \frac{\lambda k(\lambda)\, d\lambda}{(\lambda_o^2 - \lambda^2)(\lambda_1^2 - \lambda^2)}\right], \quad (3)$$

where $n(\lambda_1)$ is a known value for the index of refraction at wavelength λ_1 and Prin. denotes the Cauchy principal value of the integral. We chose the value[52] $n(\lambda_1) = n(589.3\ \text{nm}) = 1.3325$. The integral was evaluated by use of Simpson's rule numerical approximation in the 0-1-M region and by use of analytical methods with $k(\lambda) = k(1M)$ throughout the $1M \leq \lambda \leq \infty$ spectral region. The resultant values for $n(\lambda)$ are given in Table I and are shown graphically by the solid-line curves in Fig. 6.

The influence of the shape and height of the postulated ultraviolet and soft x-ray bands for $k(\lambda)$ on calculated values for $n(\lambda)$ was investigated in four different ways. First, the SKK analysis was made with a straight line for $k(\lambda)$ between the ends of the solid-line curves at 22 Å and 1,250 Å. At 400 nm this gave $n = 1.3558$ as compared with 1.343 from Irvine and Pollack[1] and at 2 μm 1.2947 as compared with 1.304 and 1.302

from Irvine and Pollack[1] and Zolotarev et al.[2] respectively. Second, the SKK analysis was made for $k = 1.55 \times 10^{-3}$ throughout the 50-1,200 Å region and then a straight line joining $k = 1.55 \times 10^{-3}$ at 1,200 Å to the end of the solid-line curve at 1,250 Å. This gave $n = 1.336$ at 400 nm, and $n = 1.309$ at 2 μm. Third, the SKK analysis was made with the curve marked KHW joined smoothly to the dashed-line curve. This gave $n = 1.3449$ at 350 nm as compared with 1.349 from Irvine and Pollack[1]. Fourth, the effect of the amplitude of the curve for $k(\lambda)$ at about 880 Å was determined by raising only the peak value of the dashed-line curve to that for the KHW curve while other parts of the dashed-line curve remained fixed. This changed n at 200 nm from 1.3954 to 1.3957. The final values for $n(\lambda)$ were obtained by applying the SKK analysis to the continuous curve described in Section III of this paper.

Values of $n(\lambda)$ from references 1, 2, 5 and 8 are compared graphically in Fig. 6 with $n(\lambda)$ obtained during the present investigation. In the 0.2-0.6-μm region $n(\lambda)$ from the present work are less than those from Irvine and Pollack[1] (IP) and from Kerr et al.[8] (KHW). In part this is attributed to the influence of the curve postulated for $k(\lambda)$ in the ultraviolet on results of the SKK analysis in the 0.2-0.6-μm region. Additional investigations of the height, width, and shape of the vacuum-ultraviolet absorption band are needed in the future in order to resolve these discrepancies. In the 1.0-6.0-μm region $n(\lambda)$ from IP and

from Rusk, Williams, and Querry[5] (RWQ) are slightly lower than $n(\lambda)$ determined during the present investigation. The maximum and minimum values of $n(\lambda)$ in the region of the water band centered at 2.95 μm are respectively less than and greater than values for similar quantities from IP and from Zolotarev *et al.*[2] (ZMA). Values of $n(\lambda)$ from ZMA and RWQ are in best agreement with $n(\lambda)$ from the present investigations in the regions 3.1-6.0 μm and 7.5-9.0 μm respectively. Values of $n(\lambda)$ from reference 2 (ZMA) for the 10-200-μm region are in good general agreement while those from reference 1(IP) do not agree with $n(\lambda)$ determined during the present investigations. We feel the values from reference 1 are in error in the long wavelength region.

We repeat the encouragement[1] that authors in the future present their data in tabular form because many of the graphs were very difficult to read accurately.

We thank Miss Sue Riley for assisting with the plotting and reading of the graphs, Mrs. Marie Light for typing the manuscript, and the staff of Linda Hall Library of Science and Technology, Kansas City, Missouri for their cooperation during the survey of the scientific literature.

FOOTNOTES AND REFERENCES

*Supported in part by the National Aeronautics and Space Administration through grant number 25-001-012 to the University of Missouri. Paper presented at the Autumn Meeting of the Optical Society, San Francisco [J. Opt. Soc. Am. 62, _____A(1972)].

1. W. M. Irvine and J. B. Pollack, Icarus 8, 324 (1968).

2. V. M. Zolotarev, B. A. Mikhailov, L. I. Aperovich and S. I. Popov, Opt. Spektrosk. 27, 790 (1969) [Opt. Spectrosc. 27, 430 (1969)].

3. L. Pontier and C. Dechambenoy, Ann. Geophys. 22, 633 (1966); Ann. Geophys. 21, 462 (1965).

4. M. R. Querry, B. Curnutte, and D. Williams, J. Opt. Soc. Am. 59, 1299 (1969).

5. A. N. Rusk, D. Williams, and M. R. Querry, J. Opt. Soc. Am. 61, 895 (1971)

6. C. W. Robertson and D. Williams, J. Opt. Soc. Am. 61, 1316 (1971).

7. G. M. Hale, M. R. Querry, A. N. Rusk, and D. Williams, J. Opt. Soc. Am. 62, _____(1972) in press.

8. G. D. Kerr, R. N. Hamm, M. W. Williams, R. D. Birkhoff, and L. R. Painter, Phys. Rev. A 5, 2523 (1972).

9. L. R. Painter, R. D. Birkhoff, and E. T. Arakawa, J. Chem. Phys. 51, 243 (1969).

10. L. R. Painter, R. N. Hamm, E. T. Arakawa, and R. D. Birkhoff, Phys. Rev. Letters 21, 282 (1968).

11. J. E. Tyler, R. C. Smith, and W. H. Wilson, Jr., J. Opt. Soc. Am. 62, 83 (1972).

12. K. S. Shifrin, Yu. I. Rabinovich, and V. V. Melent'yev, Izvestia-Atmos. Ocea. Phys. 7, 661 (1971).

13. Yu. I. Rabinovich and V. V. Melent'yev, Trans. Glav. Geof. Observ. 235, 78 (1970).

14. M. R. Querry, R. C. Waring, W. E. Holland, G. M. Hale, and W. Nijm, J. Opt. Soc. Am. 62, 849 (1972).

15. G. M. Hale, W. E. Holland, and M. R. Querry, Appl. Opts. submitted on 29 June 1972 for review.

16. N. G. Jerlov, Optical Oceanography (Elsevier Publ. Co., Amsterdam, 1968) pp. 47-62.

17. R. M. Goody, Atmospheric Radiation I: Theoretical Basis (Oxford Univ. Press, London, 1964) pp. 415-416.

18. S. A. Sullivan, J. Opt. Soc. Am. 53, 962 (1963).

19. K. Kondratyev, Radiation in the Atmosphere, Vol. 12, Internat. Geophys. Series (academic Press, New York, 1969) pp. 107-123.

20. J. Schiffer and D. F. Hornig, J. Chem. Phys. 49, 4150 (1968).

21. J. E. Chamberlain, G. W. Chantry, H. A. Gebbie, N. W. B. Stone, T. B. Taylor, and G. Nyllie, Nature 210, 790 (1966).

22. D. A. Dragert, N. W. B. Stone, B. Curnutte, and D. Williams, J. Opt. Soc. Am. 56, 64 (1966).

23. E. K. Plyler and N. Griff, Appl. Opts. 4, 1663 (1965).

24. W. Bagdade and M. Tinkham, Bull. Am. Phys. Soc. 10, 1209 (1965).

25. W. K. Thompson, Trans. Faraday Soc. (London) 61, 2635 (1965).

26. J. G. Bayly, V. B. Kartha, and W. H. Stevens, Infrared Phys. 3, 211 (1963).

27. A. O. Allen, The Radiation Chemistry of Water and Aqueous Solutions (D. Van Nostrand Co., Inc., Princeton, N. J., 1961) pp. 1-3.

28. E. K. Plyler and N. Acquista, J. Opt. Soc. Am. 44, 505 (1954).

29. L. D. Kislovskii, Opt. Spektrosk. 7, 311 (1959); Opt. Spektrosk. 7, 201 (1959).

30. R. M. Rampolla, R. C. Miller, and C. P. Smyth, J. Chem. Phys. 30, 566 (1959).

31. J. Lenoble et B. Saint-Guilly, Compt. Rend. (Acad. Sci., Paris) 240, 954 (1955).

32. J. A. Lane and J. A. Saxton, Proc. Roy. Soc. (London) A213, 400 (1952).

33. J. A. Saxton, Proc. Roy. Soc. (London) A213, 473 (1952).

34. J. A. Curcio and C. C. Petty, J. Opt. Soc. Am. 41, 302 (1951).

35. C. H. Collie, J. B. Hasted, and D. M. Ritson, Proc. Phys. Soc. (London) 60, 71 (1948). Proc. Phys. Soc. (London) 60, 145 (1948)

36. M. Centeno, J. Opt. Soc. Am. 31, 244 (1941).

37. N. E. Dorsey, Properties of Ordinary Water-Substance (Reinhold Publ. Corp., New York, 1940) pp. 279-395. Optical Absorption Characteristics of Water as listed in this book are based on material from 49 references that date back to the year 1895.

38. J. J. Fox and A. E. Martin, Proc. Roy. Soc. (London) A174, 234 (1940).

39. J. R. Collins, Phys. Rev. 55, 470 (1939).

40. G. L. Clarke and H. R. James, J. Opt. Soc. Am. 29, 43 (1939).

41. A. Esau and G. Baz, Phys. Zeit. 38, 774 (1937).

42. M. Halmann and I. Platzner, J. Phys. Chem. 70, 580 (1966).

43. D. Eisenberg and W. Kauzmann, The Structures and Properties of Water (Oxford Univ. Press, New York, 1969).

44. J. L. Weeks, G. M. A. C. Meaburn, and S. Gordon, Radiation Res. 19, 559 (1963).

45. J. Barrett and J. H. Bakendale, Trans. Faraday Soc. (London) 56, 37 (1960).

46. J. Barrett and A. L. Mansell, Nature 187, 138 (1960).

47. W. C. Price, P. V. Harris, G. H. Beaven, and E. A. Johnson, Nature 188, 45 (1960).

48. C. D. Hodgman, J. Opt. Soc. Am. 23, 426 (1933).

49. M. K. Tsukamoto, Rev. Opt. 7, 89 (1928).

50. A. E. Stanevich and N. G. Yaroslavskii, Opt. Spektrosk 10, 538 (1961); Opt. Spektrosk. 10, 278 (1961).

51. A. Engstrom, X-Ray Microanalysis in Biology and Medicine (Elsevier Pub. Co., Amsterdam, 1962) p. 50.

52. CRC Handbook of Chemistry and Physics, 48th edition (Chemical Rubber Co., Cleveland, Ohio, 1967) p. E-121.

53. R. Goldstein and S. S. Penner, J. Quant. Spectrosc. Radiat. Transfer 4, 441 (19).

54. K. Y. Kondratyev, M. P. Burgova, I. F. Gainulin, and G. F. Totunova, Problems in the Physics of the Atmosphere 2 (Publ. House Leningrad State Univ. 1964).

55. H. R. James and E. A. Birge, Trans. Wisc. Acad. Sci. 31, 154 (1938).

56. R. P. Young and R. N. Jones, Chem. Rev. 71, 219 (1971).

57. S. R. Erlander, Sci. J. 5A, 60 (1969).

58. R. Z. Bachrach and F. C. Brown, Phys. Rev. B1, 818 (1970).

59. R. K. Ahrenkiel, J. Opt. Soc. Am. 61, 1651 (1971).

FIGURE CAPTIONS

Figure 1. Extinction coefficients of water for the 0-2,000 Å spectral region. Notation and curves are described in the text.

Figure 2. Extinction coefficients of water for the 200-1,000-nm spectral region. Notation and curves are described in the text.

Figure 3. Extinction coefficients of water for the 0.95-2.6-μm spectral region. Curves are described in the text.

Figure 4. Extinction coefficients of water for the 2.5-18.5-μm spectral region. Curves are described in the text.

Figure 5. Extinction coefficients of water for the $10\text{-}10^6$-μm spectral region. Notation and curves are described in the text.

Figure 6. Index of refraction of water for the spectral regions 0.2-200 μm. Descriptions of the curves and the symbols are presented in the text.

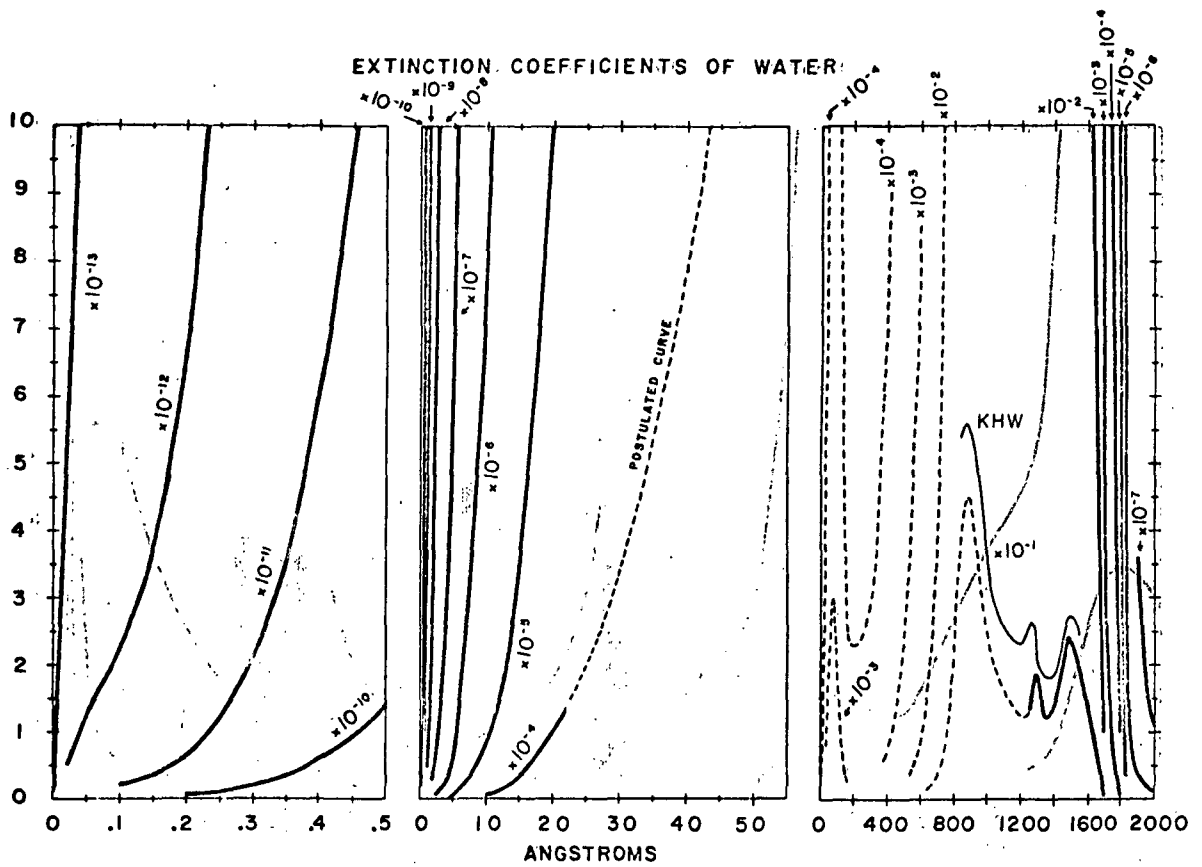
EXTINCTION COEFFICIENTS OF WATER
POSTULATED CURVE
KHW
ANGSTROMS
0
.1
.2
.3
.4
.5
10
20
30
40
50
400
800
1200
1600
2000

EXTINCTION COEFFICIENTS OF WATER

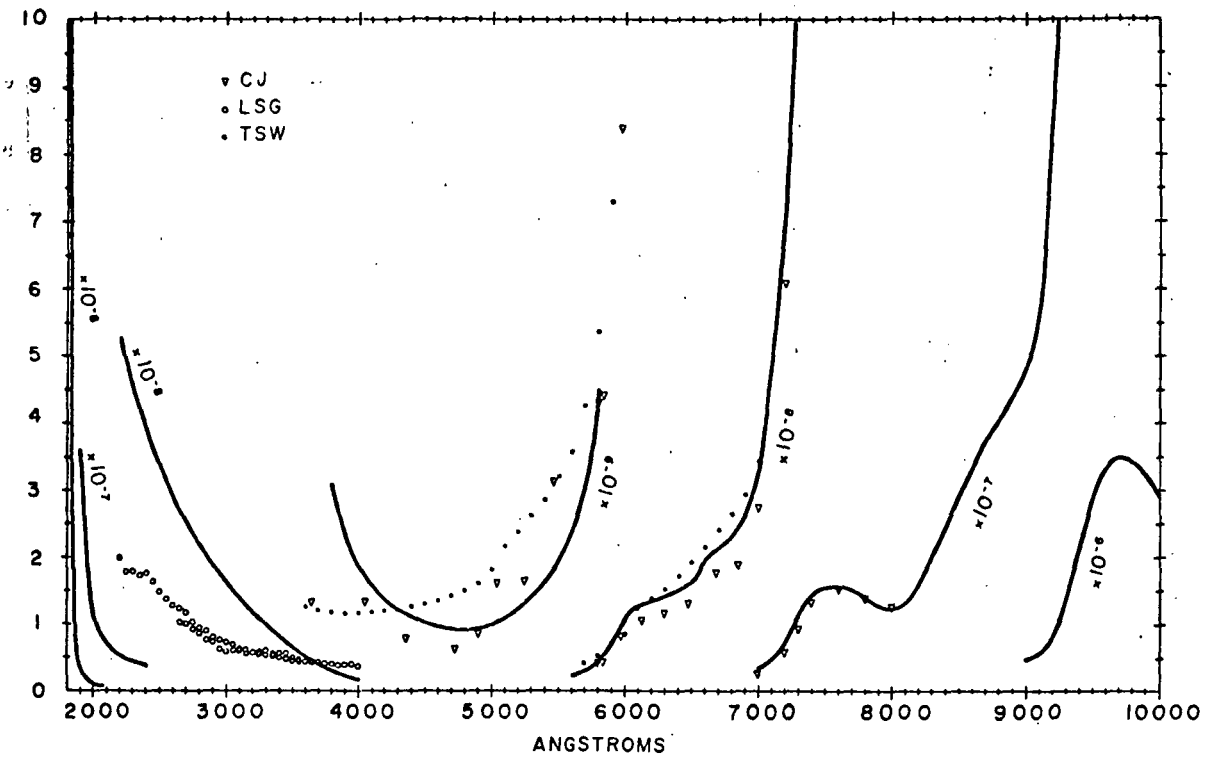

EXTINCTION COEFFICIENTS OF WATER

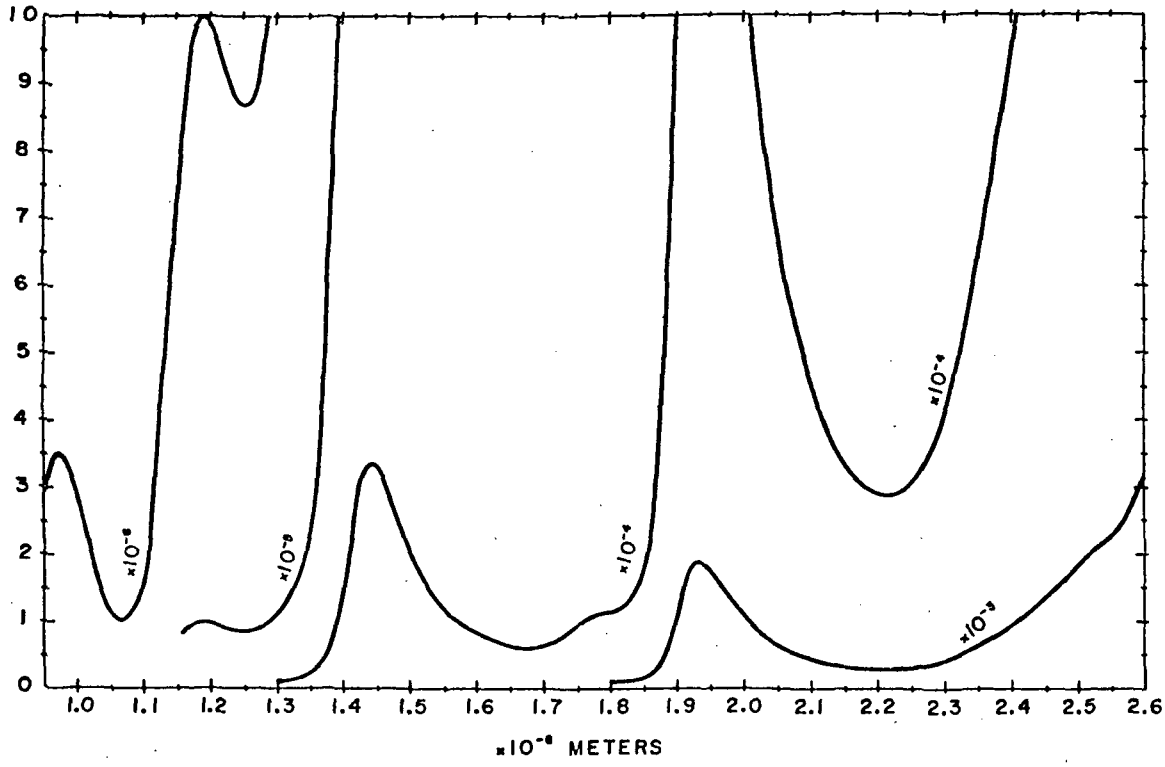

EXTINCTION COEFFICIENTS OF WATER

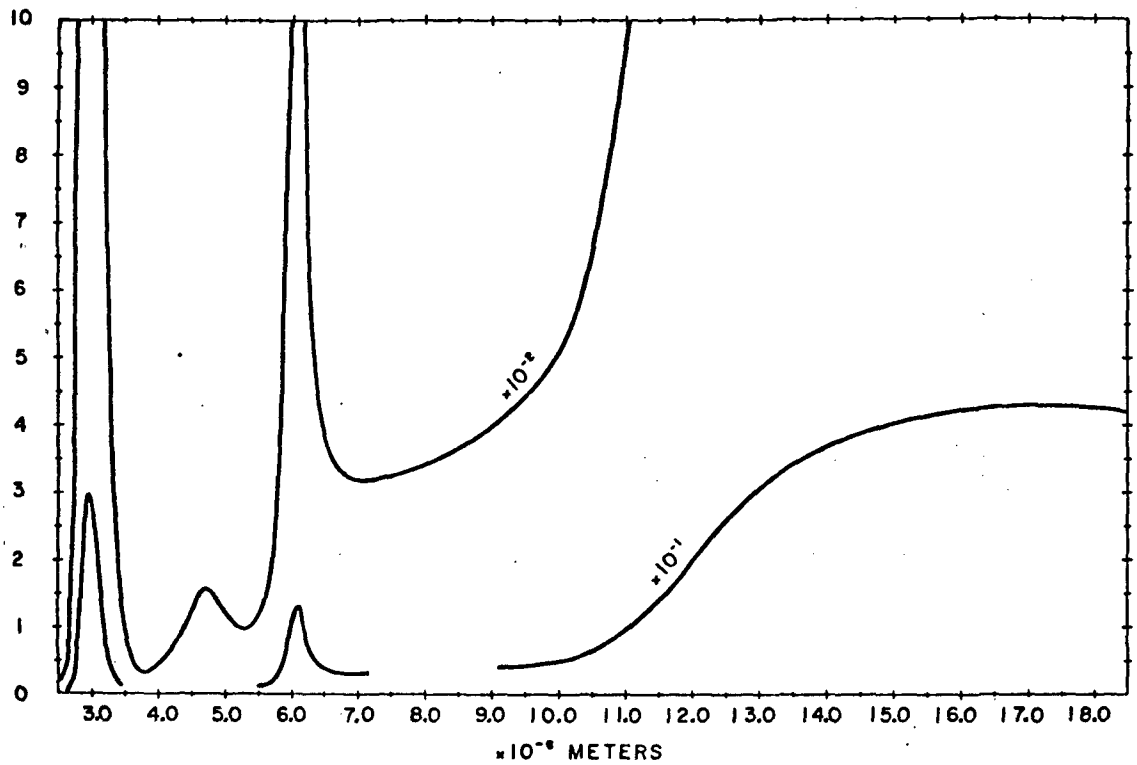

EXTINCTION COEFFICIENTS OF WATER

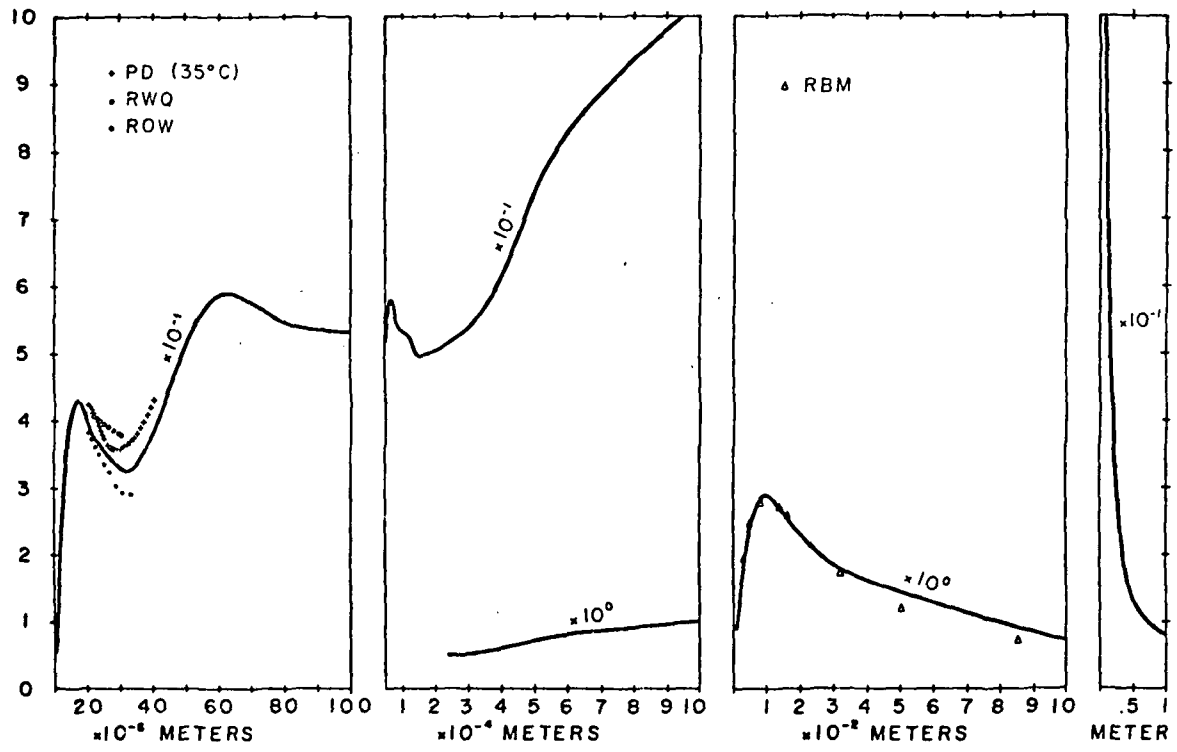

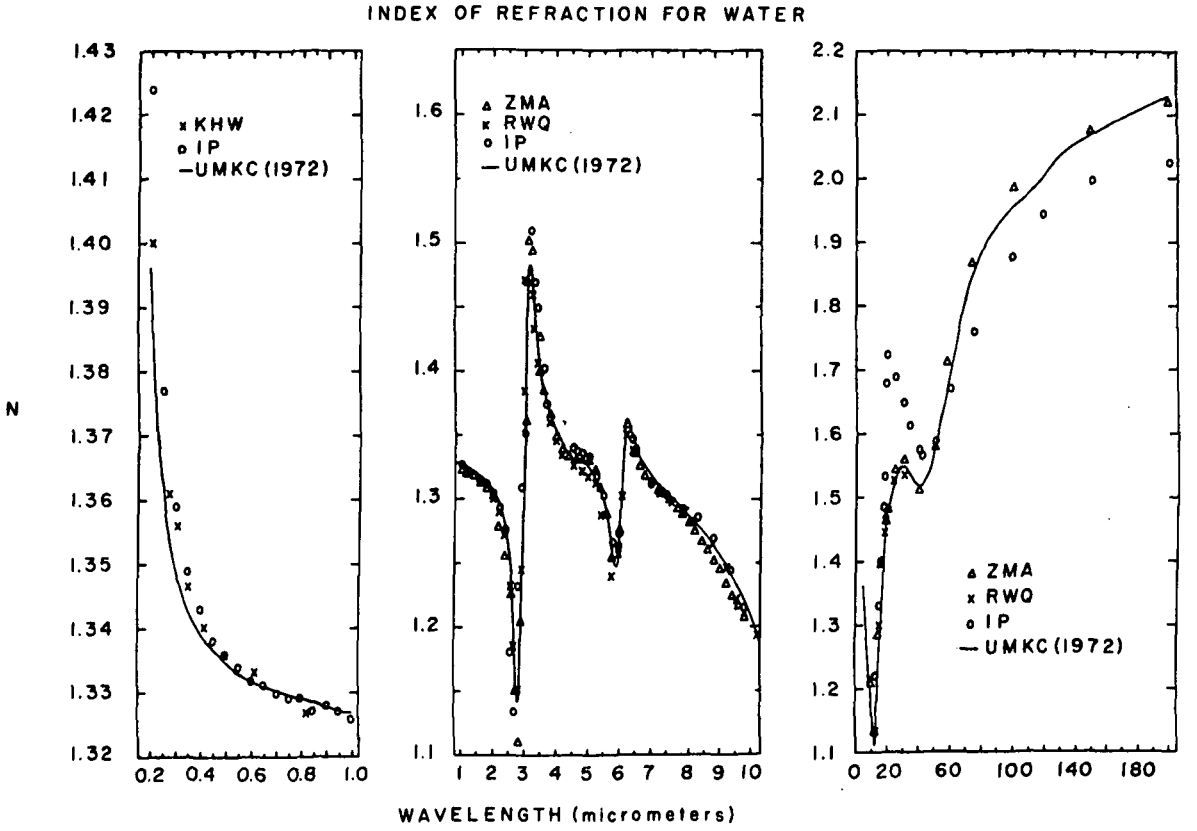
INDEX OF REFRACTION FOR WATER
N
1.43
1.42
1.41
1.40
1.39
1.38
1.37
1.36
1.35
1.34
1.33
1.32
x KHW
o IP
—UMKC (1972)
0.2 0.4 0.6 0.8 1.0
1.6
1.5
1.4
1.3
1.2
1.1
Δ ZMA
x RWQ
o IP
—UMKC (1972)
1 2 3 4 5 6 7 8 9 10
2.2
2.1
2.0
1.9
1.8
1.7
1.6
1.5
1.4
1.3
1.2
1.1
Δ ZMA
x RWQ
o IP
—UMKC (1972)
0 20 60 100 140 180
WAVELENGTH (micrometers)

TABLE I. Optical Constants of Water

$\lambda(\mu m)$	$k(\lambda)$	$n(\lambda)$
0.200	1.1×10^{-7}	1.396
0.225	4.9×10^{-8}	1.373
0.250	3.35×10^{-8}	1.362
0.275	2.35×10^{-8}	1.354
0.300	1.6×10^{-8}	1.349
0.325	1.08×10^{-8}	1.346
0.350	6.5×10^{-9}	1.343
0.375	3.5×10^{-9}	1.341
0.400	1.86×10^{-9}	1.339
0.425	1.3×10^{-9}	1.338
0.450	1.02×10^{-9}	1.337
0.475	9.35×10^{-10}	1.336
0.500	1.00×10^{-9}	1.335
0.525	1.32×10^{-9}	1.334
0.550	1.96×10^{-9}	1.333
0.575	3.60×10^{-9}	1.333
0.600	1.09×10^{-8}	1.332
0.625	1.39×10^{-8}	1.332
0.650	1.64×10^{-8}	1.331
0.675	2.23×10^{-8}	1.331

TABLE I (continued)

λ(μm)	k(λ)	n(λ)
0.700	3.35×10^{-8}	1.331
0.725	9.15×10^{-8}	1.330
0.750	1.56×10^{-7}	1.330
0.775	1.48×10^{-7}	1.330
0.800	1.25×10^{-7}	1.329
0.825	1.82×10^{-7}	1.329
0.850	2.93×10^{-7}	1.329
0.875	3.91×10^{-7}	1.328
0.900	4.86×10^{-7}	1.328
0.925	1.06×10^{-6}	1.328
0.950	2.93×10^{-6}	1.327
0.975	3.48×10^{-6}	1.327
1.0	2.89×10^{-6}	1.327
1.2	9.89×10^{-6}	1.324
1.4	1.38×10^{-4}	1.321
1.6	8.55×10^{-5}	1.317
1.8	1.15×10^{-4}	1.312
2.0	1.1×10^{-3}	1.306
2.2	2.89×10^{-4}	1.296
2.4	9.56×10^{-4}	1.279
2.6	3.17×10^{-3}	1.242
2.65	6.7×10^{-3}	1.219
2.70	0.019	1.188

TABLE I (continued)

λ(μm)	k(λ)	n(λ)
2.75	0.059	1.157
2.80	0.115	1.142
2.85	0.185	1.149
2.90	0.268	1.201
2.95	0.298	1.292
3.00	0.272	1.371
3.05	0.240	1.426
3.10	0.192	1.467
3.15	0.135	1.483
3.20	0.0924	1.478
3.25	0.0610	1.467
3.30	0.0368	1.450
3.35	0.0261	1.432
3.40	0.0195	1.420
3.45	0.0132	1.410
3.50	0.0094	1.400
3.6	0.00515	1.385
3.7	0.00360	1.374
3.8	0.00340	1.364
3.9	0.00380	1.357
4.0	0.00460	1.351
4.1	0.00562	1.346
4.2	0.00688	1.342

TABLE I (continued)

λ(μm)	k(λ)	n(λ)
4.3	0.00845	1.338
4.4	0.0103	1.334
4.5	0.0134	1.332
4.6	0.0147	1.330
4.7	0.0157	1.330
4.8	0.0150	1.330
4.9	0.0137	1.328
5.0	0.0124	1.325
5.1	0.0111	1.322
5.2	0.0101	1.317
5.3	0.0098	1.312
5.4	0.0103	1.305
5.5	0.0116	1.298
5.6	0.0142	1.289
5.7	0.0203	1.277
5.8	0.0330	1.262
5.9	0.0622	1.248
6.0	0.107	1.265
6.1	0.131	1.319
6.2	0.0880	1.363
6.3	0.0570	1.357
6.4	0.0449	1.347
6.5	0.0392	1.339

TABLE I (continued)

λ(μm)	k(λ)	n(λ)
6.6	0.0356	1.334
6.7	0.0337	1.329
6.8	0.0327	1.324
6.9	0.0322	1.321
7.0	0.0320	1.317
7.1	0.0320	1.314
7.2	0.0321	1.312
7.3	0.0322	1.309
7.4	0.0324	1.307
7.5	0.0326	1.304
7.6	0.0328	1.302
7.7	0.0331	1.299
7.8	0.0335	1.297
7.9	0.0339	1.294
8.0	0.0343	1.291
8.2	0.0351	1.286
8.4	0.0361	1.281
8.6	0.0372	1.275
8.8	0.0385	1.269
9.0	0.0399	1.262
9.2	0.0415	1.255
9.4	0.0433	1.247
9.6	0.0454	1.239

TABLE I (continued)

λ(μm)	k(λ)	n(λ)
9.8	0.0479	1.229
10.0	0.0508	1.218
10.5	0.0662	1.185
11.0	0.0968	1.153
11.5	0.142	1.126
12.0	0.199	1.111
12.5	0.259	1.123
13.0	0.305	1.146
13.5	0.343	1.177
14.0	0.370	1.210
14.5	0.388	1.241
15.0	0.402	1.270
15.5	0.414	1.297
16.0	0.422	1.325
16.5	0.428	1.351
17.0	0.429	1.376
17.5	0.429	1.401
18.0	0.426	1.423
18.5	0.421	1.443
19.0	0.414	1.461
19.5	0.404	1.476
20.0	0.393	1.480
21.0	0.382	1.487

TABLE I (continued)

λ(μm)	k(λ)	n(λ)
22	0.373	1.500
23	0.367	1.511
24	0.361	1.521
25	0.356	1.531
26	0.350	1.539
27	0.344	1.545
28	0.338	1.549
29	0.333	1.551
30	0.328	1.551
32	0.324	1.546
34	0.329	1.536
36	0.343	1.527
38	0.361	1.522
40	0.385	1.519
42	0.409	1.522
44	0.436	1.530
46	0.462	1.541
48	0.488	1.555
50	0.514	1.587
60	0.587	1.703
70	0.576	1.821
80	0.547	1.886
90	0.536	1.924

TABLE I (continued)

λ(μm)	k(λ)	n(λ)
100	0.532	1.957
110	0.531	1.966
120	0.526	2.004
130	0.514	2.036
140	0.500	2.056
150	0.495	2.069
160	0.496	2.081
1 70	0.497	2.094
1 80	0.499	2.107
190	0.501	2.119
200	0.504	2.130

PART II

Kramers-Kronig Analysis of Relative Reflectance Spectra Measured at an Oblique Angle*+

George M. Hale, Wayne E. Holland and Marvin R. Querry

Department of Physics

University of Missouri - Kansas City 64110

Relative specular reflectance R is defined as $R = R_s/R_w$, where R_s and R_w are absolute reflectances of a sample material s and a material w for which the index of refraction n_w and the extinction coefficient k_w are known quantities. An algorithm was developed for computing n_s and k_s from the sample's R-spectrum measured for radiant flux polarized perpendicular to the plane of incidence and reflected at oblique angle θ. Kramers-Kronig analysis of the R-spectrum provides $\Delta\phi$ the difference between phase shifts for electromagnetic waves reflected at the surfaces of materials s and w. Real and imaginary parts of a Fresnel equation for relative reflectivity provides equations for computing n_s and k_s when θ, $\Delta\phi$, n_w, and k_w are known quantities. Optical constants for aqueous solutions containing NaCl were computed in this manner; distilled water was the reflectance standard.

I. INTRODUCTION

Robinson,[1] in 1952, was the first to apply what is now known as the Kramers-Kronig (K-K) analysis to a reflectance spectrum obtained for infrared radiant flux nearly normally incident on a bulk sample. The K-K analysis was used to determine $\phi(\lambda)$, the phase-shifts produced when monochromatic waves of wavelength λ were partially reflected from the surface of the sample. The Fresnel reflectivity equation for the case of normal incidence, the measured reflectance, and $\phi(\lambda)$ then provided Robinson with adequate information for computing both n the real and k the imaginary parts of the complex refractive index of the sample. Since 1952 there have been many other discussions and applications of the K-K analysis[2] of reflectance spectra measured at nearly normal incidence. In 1965 Roessler[3] extended the applicability of the K-K analysis by presenting an algorithm for computing $\phi(\lambda)$ and n and k from a reflectance spectrum obtained for radiant flux that was linearly polarized with the electric field intensity vector perpendicular to the plane of incidence and was specularly reflected at an oblique angle $0° \leq \theta < 90°$. Then in 1967 Berreman[4] further extended the applicability of the K-K analysis by presenting an algorithm for computing the phase shifts and n and k from a reflectance spectrum obtained for radiant flux that was linearly polarized either parallel or

perpendicular to the plane of incidence and was specularly reflected at an oblique angle.

Querry et al.[5] recently investigated aqueous solutions by applying a K-K analysis to relative reflectance spectra that were obtained for infrared radiant flux that was linearly polarized perpendicular to the plane of incidence and was specularly reflected at $\theta = 70.03°$. The K-K analysis of the relative reflectance spectra provided the difference $\Delta\phi(\lambda) = \phi(\lambda)_s - \phi(\lambda)_w$ in phase-shifts $\phi(\lambda)_s$ and $\phi(\lambda)_w$ for monochromatic waves of wavelength λ reflected at the surface of the aqueous solution s and at the surface of distilled water w which was used as the reflectance standard. In this paper the applicability of the K-K analysis for computing $\Delta\phi(\lambda)$ from a relative reflectance spectrum is further extended to include an algorithm for computing the optical constants n_s and k_s of the sample when $\Delta\phi(\lambda)$, θ, and the optical constants of the standard reflector are all known quantities. The algorithm is applicable to reflectance spectra obtained for perpendicularly polarized radiant flux specularly reflected at angles $0° \leq \theta < 90°$. As an illustrative example the algorithm was used to successfully compute the optical constants of aqueous solutions containing NaCl. Distilled water was the standard reflector.

II. THE ALGORITHM

Consider plane electromagnetic waves propagating in vacuum or air to be incident at an angle θ relative to the normal of a plane, infinite, smooth surface of a conducting material medium s that is linear, homogeneous, isotropic, and nonmagnetic. The Fresnel equation for the absolute complex reflectivity $\rho_s e^{-i\phi_s}$ of medium s for waves linearly polarized perpendicular to the plane of incidence is

$$\rho_s e^{-i\phi_s} = \frac{Q_s - iP_s - \cos\theta}{Q_s - iP_s + \cos\theta} , \tag{1}$$

where ρ is the modulus of the reflectivity, ϕ is the wave's phase shift caused by the reflection, and Q_s and P_s are parameters that are expressed in terms of θ and the material's index of refraction n_s and extinction coefficient k_s as

$$Q_s = \left\{ \frac{n_s^2 - k_s^2 - \sin^2\theta + [(n_s^2 - k_s^2 - \sin^2\theta)^2 + 4n_s^2k_s^2]^{\frac{1}{2}}}{2} \right\}^{\frac{1}{2}} \tag{2}$$

$$P_s = n_s k_s / Q_s . \tag{3}$$

The index of refraction is expressed in terms of θ, P_s and Q_s as

$$n_s = \left\{ \frac{Q_s^2 - P_s^2 + \sin^2\theta + [(Q_s^2 - P_s^2 + \sin^2\theta)^2 + 4Q_s^2P_s^2]^{\frac{1}{2}}}{2} \right\}^{\frac{1}{2}} . \tag{4}$$

The extinction coefficient is given by Eq. (3). The phase shift $\phi(\lambda)$ may be determined from a K-K analysis of an absolute, spec-

ular, reflectance spectrum for the material;[3]

$$\phi(\lambda) = \text{Prin.} \frac{2\lambda_o}{\pi} \int_o^\infty \frac{\ell n[\rho(\lambda)_s]}{\lambda^2 - \lambda_o^2} d\lambda \quad , \tag{5}$$

where λ is the wavelength, Prin. denotes the Cauchy principal value of the integral, and $\rho(\lambda)_s = R(\lambda)_s^{\frac{1}{2}}$ where $R(\lambda)_s$ is the measured specular reflectance for perpendicularly polarized waves.

The complex relative reflectivity $\rho e^{-i\Delta\phi}$ of the medium s relative to a second medium w for which n_w and k_w are known can be written in two ways for the case of perpendicular polarization

$$\rho e^{-i\Delta\phi} = \frac{\rho_s}{\rho_w} e^{-i(\phi_s - \phi_w)} \tag{6}$$

$$\rho e^{-i\Delta\phi} = \frac{(Q_s - iP_s - \cos\theta)(Q_w - iP_w + \cos\theta)}{(Q_s - iP_s + \cos\theta)(Q_w - iP_w - \cos\theta)} \quad . \tag{7}$$

The ratio $\rho_s/\rho_w = R^{\frac{1}{2}}$ where R is the reflectance of medium s measured relative to the reflectance of medium w. The difference in phase shifts $\Delta\phi$ for waves reflected from media s and w is provided by a K-K analysis of the relative reflectance spectrum

$$\Delta\phi = \phi_s - \phi_w = \text{Prin.} \frac{\lambda_o}{\pi} \int_o^\infty \frac{\ell n[R(\lambda)]}{\lambda^2 - \lambda_o^2} d\lambda \quad . \tag{8}$$

The quantities Q_w and P_w can be calculated by use of expressions similar to Eqs. (2) and (3).

Separating Eq. (6) into real and imaginary parts and then solving the two resultant equations provide expressions for computing Q_s and P_s

$$Q_s = \frac{(A - B)\cos\theta}{A + B - C\cos\Delta\phi - D\sin\Delta\phi} \tag{9}$$

$$P_s = \frac{(D\cos\Delta\phi - C\sin\Delta\phi)\cos\theta}{A + B - C\cos\Delta\phi - D\sin\Delta\phi} \tag{10}$$

where

$$A = (Q_w - \cos\theta)^2 + P_w^2 \tag{11}$$

$$B = R[(Q_w - \cos\theta)^2 + P_w^2] \tag{12}$$

$$C = 2R^{\frac{1}{2}}(Q_w^2 + P_w^2 - \cos^2\theta) \tag{13}$$

$$D = 4R^{\frac{1}{2}}P_w\cos\theta. \tag{14}$$

The optical constants n_s and k_s are determined next by use of Eqs. (4) and (3).

The algorithm is easily checked for correctness by assuming that media s and w are the same. The relative reflectance would be $R(\lambda) = 1$ for all λ and subsequently Eq. (8) shows that $\Delta\phi = 0$ for all λ. In this case Eqs. (9) - (14) reduce to $Q_s = Q_w$ and $P_s = P_w$ which is consistent with the assumption that media s and w are the same.

III. ILLUSTRATIVE EXAMPLE

The relative reflectance spectra and absolute reflectance spectra in the 0.4 - 20-μm wavelength region for 1M, 3M, and 5M aqueous solutions of NaCl are shown in Figures 1 and 2. The specularly reflected radiant flux was linearly polarized perpendicular to the plane of incidence. The angle of incidence was $70.03° \pm 0.23°$. Distilled water was the standard reflector. The experimental methods for measuring relative reflectance were described in a previous paper.[5]

The K-K analysis indicated by Eq. (8) requires a knowledge of the relative reflectance $R(\lambda)$ for all λ. Because the relative reflectance data were only for the 0.4 - 20-μm region we assumed the relative reflectances were R(0.4 μm) and R(20 μm) throughout the $\lambda \leq 0.4$ μm and $\lambda \geq 20$ μm regions respectively. The integration was made with numerical Simpson's rule techniques in the 0.4-20-μm region and analytically in the other regions. The parameters Q_w and P_w were determined by use of the optical constants n_w and k_w of distilled water[6] and equations similar to Eqs. (2) and (3). Next, the parameters Q_s and P_s were calculated by use of Eqs. (9) - (14). And finally, the optical constants n_s and k_s of the aqueous solutions were determined by use of Eqs. (4) and (3). The values for n_s and k_s for the 2-20-μm region are shown graphically in Figure 3. The optical constants computed in this manner

were generally in three significant digit agreement with optical constants previously obtained for the same solutions by KK-analysis of the absolute reflectance spectra[5] shown in Figs. 1 and 2.

A numerical investigation of the propagation of experimental errors through the algorithm was made for typical experimental uncertainties $\Delta R = 0, \pm 0.01R$; $\Delta\theta = 0, \pm 0.23°$; $\Delta n_w = 0, \pm 0.01\ n_w$ and $\Delta k_w = 0, \pm 0.01\ k_w$. As an example, the optical constants for the 3M solution were $n_s = 1.254 \pm 0.012$ and $k_s = 0.046 \pm 0.001$ at $\lambda = 10.05$ μm and $n_s = 1.408 \pm 0.013$ and $k_s = 0.260 \pm 0.005$ at $\lambda = 3.00$ μm. The values for n_s and k_s, and their uncertainties are respectively the average and one standard deviation for individual values of n_s and k_s that were computed for each of the 81 possible different combinations of ΔR, $\Delta\theta$, Δn_w, and Δk_w.

IV. CONCLUSIONS

Before applying the K-K analysis to an absolute reflectance spectrum it is necessary, by either mathematical[2] or semi-empirical[5] methods, to extend the spectrum beyond the wavelength regions where data were obtained experimentally. The algorithm presented in this paper has the principal advantage that physical models are not needed to extend relative reflectance data in order to apply the K-K analysis. By choosing a reflectance standard having optical properties somewhat similar to those of the sample, the relative reflectance will be constant throughout broad spectral regions, such as through the visible region shown in Fig. 1 for the NaCl solutions. The mathematical integration required by the K-K analysis, Eqs. (5) and (8), therefore is more easily applied to relative reflectance data because the relative reflectance more frequently can be assumed to be constant throughout spectral regions where it is difficult to obtain experimental data.

FOOTNOTES AND REFERENCES

*Supported in part by NASA Grant 25-001-012 and by U.S. Department of Interior, Geological Survey Contract 14-08-0001-12636.

+Presented in part at the 1972 June meeting of the American Physical Society, Albuquerque [Bull. Am. Phys. Soc. 17, 672 (1972)].

1. T.S. Robinson, Proc. Phys. Soc. (London) A 65, 910 (1952).
2. A particularly interesting discussion of the K-K analysis is presented by M. Cardona, Optical Properties of Solids, editors S. Nudelman and S. S. Mitra (Plenum Press, New York, 1969) p. 137.
3. D. M. Roessler, Brit. J. Appl. Phys. 16, 1359 (1965).
4. D. W. Berreman, Appl. Opt. 6, 1519 (1967).
5. M. R. Querry, R. C. Waring, W. E. Holland, G. M. Hale, and W. Nijm, J. Opt. Soc. Am. 62, _____ (1972) in press.
6. A. N. Rusk, D. Williams, and M. R. Querry, J. Opt. Soc. Am. 61, 895 (1971).

FIGURE CAPTIONS

Figure 1. Measured relative reflectances and computed absolute reflectances in the 0.4-2.0-μm wavelength region for 1M, 3M, and 5M aqueous solutions of NaCl. The angle of incidence was 70.03° ± 0.23°. Distilled water was the reflectance standard. The radiant flux was linearly polarized perpendicular to the plane of incidence. Standard deviations in measured reflectances were about 1%. The relative reflectance of distilled water is 1.0 at all wavelengths.

Figure 2. Measured relative reflectances and computed absolute reflectances in the 2.0-20-μm wavelength region for 1M, 3M, and 5M aqueous solutions of NaCl. The angle of incidence was 70.03° ± 0.23°. Distilled water was the reflectance standard. The radiant flux was linearly polarized perpendicular to the plane of incidence. Standard deviations in measured reflectances were about 1%. The relative reflectance of distilled water is 1.0 at all wavelengths.

Figure 3. Optical constants in the 2.0-20-μm wavelength region for 1M, 3M, and 5M aqueous solutions of NaCl.

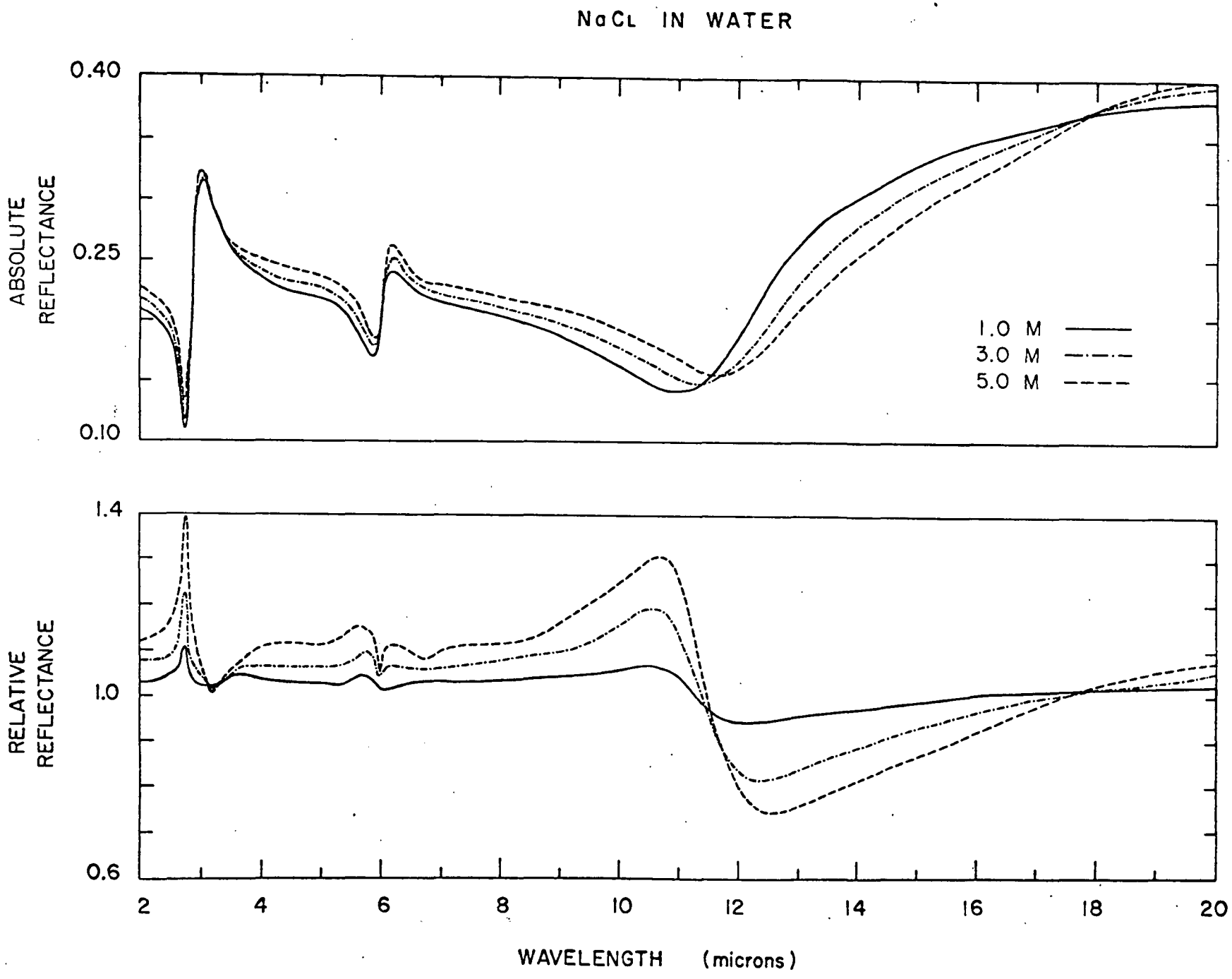
NaCl IN WATER
ABSOLUTE REFLECTANCE
0.40
0.25
0.10
1.0 M
3.0 M
5.0 M
RELATIVE REFLECTANCE
1.4
1.0
0.6
2
4
6
8
10
12
14
16
18
20
WAVELENGTH (microns)

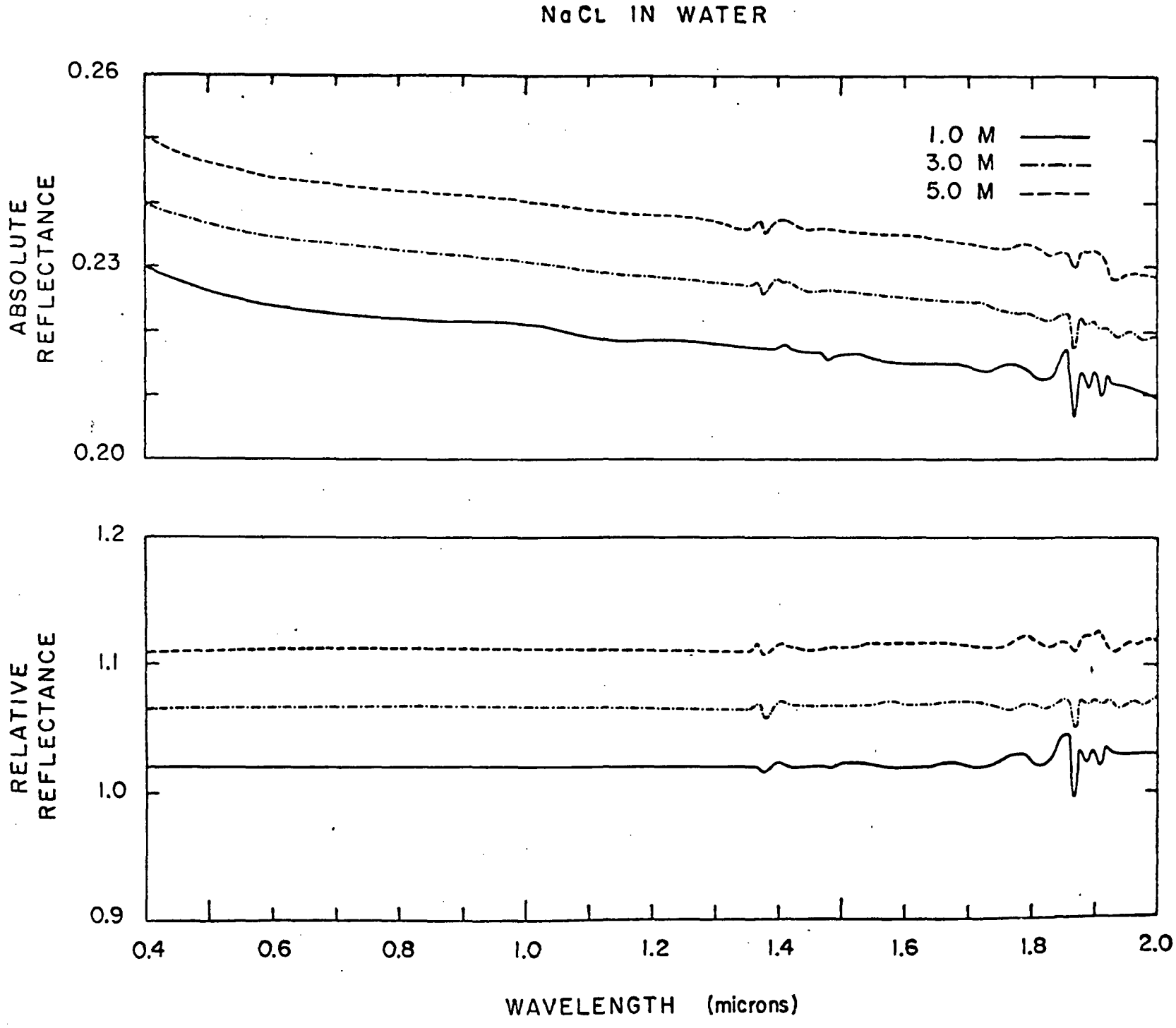
NaCL IN WATER
0.26
0.23
0.20
ABSOLUTE REFLECTANCE
1.0 M
3.0 M
5.0 M
1.2
1.1
1.0
0.9
RELATIVE REFLECTANCE
0.4
0.6
0.8
1.0
1.2
1.4
1.6
1.8
2.0
WAVELENGTH (microns)

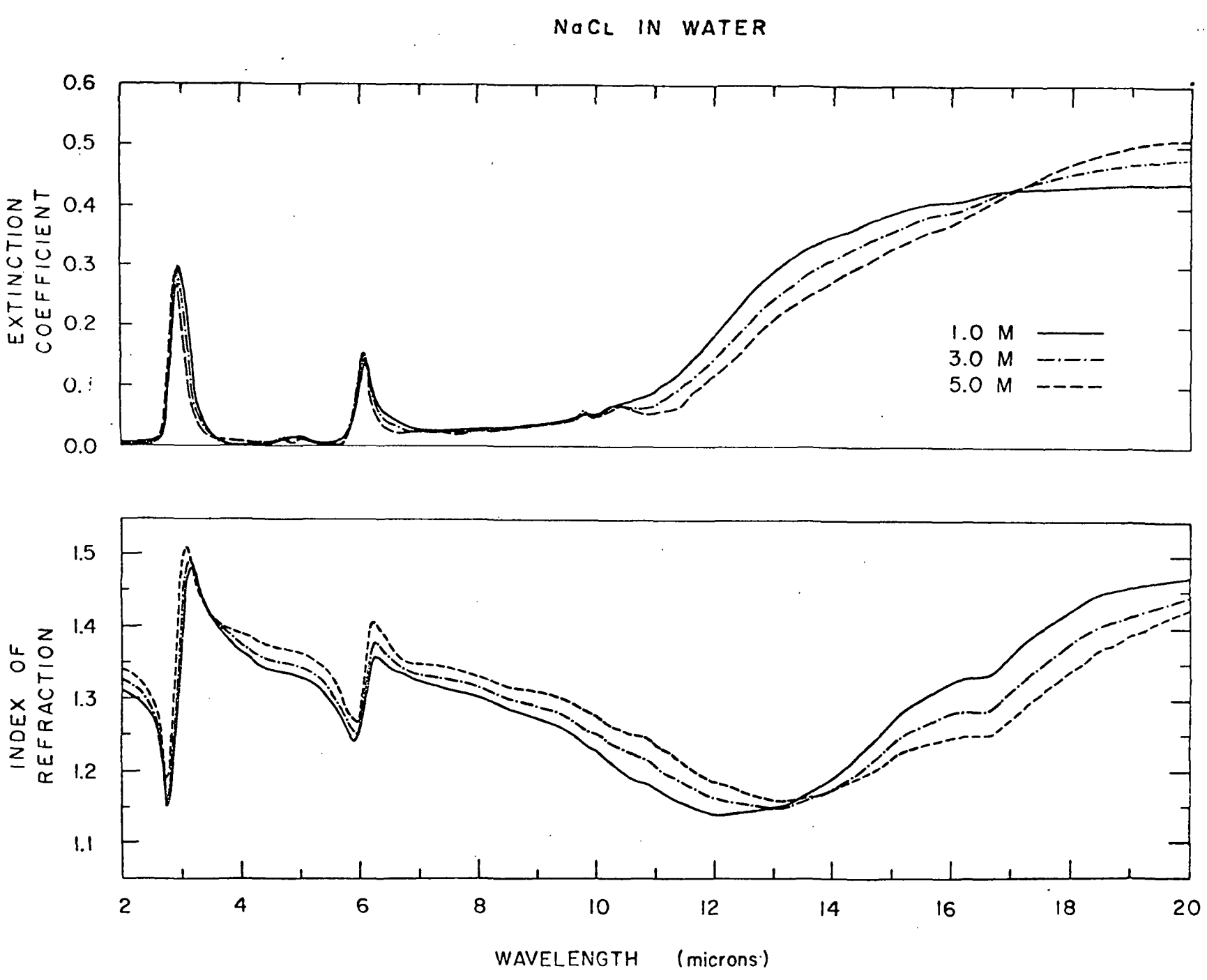
NaCL IN WATER
EXTINCTION COEFFICIENT
0.6
0.5
0.4
0.3
0.2
0.0
1.0 M
3.0 M
5.0 M
INDEX OF REFRACTION
1.5
1.4
1.3
1.2
1.1
2
4
6
8
10
12
14
16
18
20
WAVELENGTH (microns)

PART III

The Influence of Temperature on the Spectrum of Water*

G. Michael Hale and Marvin R. Querry
Department of Physics
University of Missouri--Kansas City, Kansas City, Missouri 64110

AND

Alvin N. Rusk and Dudley Williams
Department of Physics
Kansas State University, Manhattan, Kansas 66502

Abstract

The normal-incidence spectral reflectance of water at 5°C, 27°C, and 70°C has been measured in the spectral region between 5000 and 350 cm^{-1}. From the measured values of spectral reflectance we have determined the optical constants n_r and n_i by Kramers-Kronig methods. The band strengths $S_B = \int n_i(\nu)d\nu$ and band widths have been determined for the absorption bands near 3400 cm^{-1}, 1640 cm^{-1}, and 600 cm^{-1} at each temperature. A similar study of deuterium oxide at 27°C has been conducted for purposes of comparison.

The infrared spectrum of water at ambient temperatures has been the subject of numerous investigations. Irvine and Pollack[1] made a critical survey of work on the subject and emphasized the desirability of further quantitative studies of transmission and reflection with the purpose of obtaining more precise values of the real n_r and imaginary n_i parts of the refractive index in the infrared. Several such quantitative studies have recently been reported.[2-6]

Because the intermolecular structure of water varies with temperature, changes in the infrared spectrum with temperature are to be expected. Draegert *et al*[7] have observed shifts of major band positions in the far infrared and have compared their results with similar studies in the near infrared.[8,9] Falk and Ford[10,11] have also made studies of band positions as a function of temperature and have summarized other recent work on the subject.

The purpose of the present study was to determine the influence of temperature on the optical constants n_r and n_i. In view of the difficulties involved in measuring the Lambert absorption coefficient $\alpha(\nu)$ in spectral regions of strong absorption, we have employed reflection methods. From our measured values of normal-incidence reflectance $R(\nu)$ we have determined $n_r(\nu)$ and $n_i(\nu) = \lambda\alpha(\nu)/4\pi$ by Kramers-Kronig techniques.

EXPERIMENTAL RESULTS

The laboratory procedures employed are essentially the same as those used in our earlier study,[5] in which we measured near-normal reflectance at a free water surface in air. The measured spectral reflectance curves for water samples at 5°C, 27°C, and 70°C are shown in Fig. 1; the sample

temperatures were maintained to within ± 1°C by appropriate thermal baths.[12] The curves shown in Fig. 1 are smoothed curves based on numerous spectral scans. We believe that the spectral reflectance curve for water at 27°C, which is supported by more measurements than the other curves, gives absolute fractional reflectance to within ± 1 percent over most of the spectral range but may involve slightly larger uncertainties at the lowest frequencies. The corresponding uncertainties in the measured fractional reflectance for water at 5°C may be as large as ± 2 percent, because fewer measurements were made.

Unusual difficulties were encountered in establishing the spectral reflectance curves for water at 70°C, at which temperature the vapor pressure is so great that the level of the reflecting surface can change appreciably during a spectral run as a result of evaporation; although we achieved some compensation by addition to the sample at appropriate intervals, evaporation doubtless contributed to the scatter of data points. More serious difficulties were encountered in spectral regions where water vapor has strong absorption bands, since the quantity of water vapor in the reflectometer path was greater for the 70°C water sample than for the reference mirror. This led to possibly spurious results in the vicinity of the strong ν_2 water vapor band near 1625 cm^{-1}; the additional absorption in the sample beam probably reduces the height of the reflectance peak near 1600 cm^{-1} in Fig. 1 and may account in part for the subsequent extremely rapid decrease and the adjacent flat portion of the reflectance curve between 1540 and 1400 cm^{-1}. The presence of additional water vapor did not produce noticeable effects in the vicinity of the ν_3 fundamental water vapor band near 3700 cm^{-1} but did

contribute to the scatter of data points in the low-frequency range where the pure rotational lines of water vapor occur. Except for the regions just noted we believe that the uncertainties in measured reflectance amount to only ± 2 percent.

KRAMERS-KRONIG ANALYSIS

We used the Kramers-Kronig theorem for phase-shift dispersion analysis of reflectance data in order to obtain n_r and n_i from our measured reflectances. According to this K-K theorem, if the modulus $\rho(\nu) = [R(\nu)]^{\frac{1}{2}}$ of the complex reflectivity $\rho(\nu)e^{i\phi(\nu)}$ is known for all frequencies ν, then the phase $\phi(\nu_o)$ at ν_o is given by the expression

$$\phi(\nu_o) = \frac{2\nu_o}{\pi} \int_o^\infty \frac{\ell n \rho(\nu)}{\nu_o^2 - \nu^2} d\nu \qquad (1)$$

where $\rho(\nu)$ and $\phi(\nu)$ must satisfy conditions that allow contour integration in the complex plane. Although the value of $\phi(\nu_o)$ in Eq. (1) is most strongly influenced by values of $\rho(\nu)$ in the immediate vicinity of ν_o, values of $\rho(\nu)$ for all frequencies must be known if the K-K theorem is to be applied with rigor.

Because our own reflectance measurements were limited to the range 5000 to 360 cm^{-1}, it was necessary to make assumptions regarding values of $R(\nu)$ outside this range. Fortunately, values of $R(\nu)$ outside our range can be generated from values of n_r and n_i tabulated by earlier investigators; we used the optical constants published by Zolatarev *et al*,[3] which cover the entire spectral range from the ultraviolet to the radio region. The generated values of $R(\nu)$ were adjusted to provide a smooth fit with our own data at 5000 and 360 cm^{-1}. We assumed that the reflectance of water for all

frequencies above 10,000 cm^{-1} was constant and equal to the reflectance at 10,000 cm^{-1}; this eliminated the remote ultraviolet bands from the integral. Similarly, we assumed that the reflectance of water at extremely low frequencies was equal to its reflectance at 0.37 cm^{-1}, thereby eliminating the effects of absorption bands at lower radio frequencies.

On the basis of the resulting values of $\rho(\nu)$, we performed the integration (1) by techniques involving Simpson's rule. The wave-number interval for the numerical integration was 10 cm^{-1} except in the vicinity of the singularity at $\nu=\nu_o$, where it was reduced to approximately 0.001 cm^{-1}. Phase shifts $\phi(\nu_o)$ were obtained in this manner at 10 cm^{-1} intervals in the range 5000 to 350 cm^{-1}. From the tabulated values ϕ and the measured values of R, the optical constants can be obtained from the Fresnel equation for normal incidence with the results:

$$n_r = (1 - R)/(1 + R_2 - 2R^{\frac{1}{2}} \cos\phi) \tag{2}$$

$$n_i = (-2R \sin\phi)/(1 + R - 2R^{\frac{1}{2}} \cos\phi) \tag{3}$$

where the positive sign is taken for the square root. The resulting values of n_r and n_i in the 5000 - 350 cm^{-1} region for water at 27°C were compared in detail with our earlier values[5] obtained by a different method. Over most of this spectral range there was such close agreement that we concluded that no significant error is introduced by reasonable assumptions regarding reflectance outside the range actually covered in our experimental work. In view of this result, we used the same set of generated values with a smooth fit to our measured values of $R(\nu)$ at 5°C and 70°C. The use of these generated values for $\nu<350$ cm^{-1} may have introduced some uncertainties in the values of n_r and n_i computed for the lowest frequencies

covered in our experimental work, because the absorption for $\nu<350$ cm^{-1} is influenced by temperature change.[7]

The uncertainties in the values of n_r and n_i were estimated by assuming uncertainties of one to three percent in measured reflectance R. On the basis of a one percent uncertainty in R, both n_r and n_i are in general accurate to three significant figures where the first digit to the left of the decimal point is regarded as a significant figure; for example, $n_r = 1.32$ and $n_i = 0.26$. By randomly varying R by one to three percent during successive numerical integrations of (1) we estimate the uncertainty in ϕ to be $\pm$ 0.003 rad. This result leads to an uncertainty of $\pm$ 1 percent n_r except in the vicinity of atmospheric water vapor and carbon dioxide bands, where the uncertainty is $\pm$ 2 percent. The corresponding uncertainties in n_i range from $\pm$ 3 percent at the center of the strong absorption band near 600 cm^{-1}, to $\pm$ 5 percent at the center of the band near 3400 cm^{-1}, and to still larger fractional uncertainties for still smaller values of n_i. For values of $n_i<0.1$, values of n_i based on transmission measurements are to be preferred.

We note that these estimates of uncertainty are based primarily on the random scatter of data points for R and do not include systematic errors such as those noted earlier in connection with the measured reflectance of 70°C water in the vicinity of water vapor bands.

RESULTS

Our values of the refractive index n_r are shown in Fig. 2. Temperature change produces little change in n_r in the 5000 - 4100 cm^{-1} range but produces pronounced changes in the vicinity of the strong 3400 cm^{-1}

absorption band, where temperature increase is accompanied by a decrease in the difference between $n_{r\ max}$ and $n_{r\ min}$ and a slight increase in the difference between the frequencies at which these limiting values occur. The curves for water at 5°C and 27°C are barely distinguishable for most of the range between 2800 and 250 cm^{-1} except near the absorption bands; in the vicinity of the 1640 cm^{-1} band $n_{r\ max} - n_{r\ min}$ is greater for 27°C water than for 5°C water and $n_{r\ min}$ is lower for the 5°C water in the vicinity of 850 cm^{-1}. The n_r values for 70°C water are lower than those for the other samples at nearly all frequencies below 3200 cm^{-1} except in the range between 1000 and 800 cm^{-1}; the steeply rising portion of the n_r curve for 70°C water is shifted to lower frequencies in the range 800 to 400 cm^{-1}. Because of the effect of overlapping absorption by water vapor, we can draw few valid conclusions regarding n_r values for 70°C water in the vicinity of 1625 cm^{-1}.

The present values of n_i, sometimes called the extinction coefficient, are plotted in Fig. 3. As indicated earlier, values of n_i based on reflectance measurements become subject to progressively larger uncertainties as n_i decreases; we have therefore plotted n_i values for only the 27°C sample in the frequency ranges 5000 to 3800 cm^{-1} and 2800 to 1850 cm^{-1}, since the percentage uncertainties for n_i at the other temperatures are greater. We note that the values of n_i in the range 1500 to 1000 cm^{-1} are also subject to large uncertainties.

The major absorption band in the vicinity of 3400 cm^{-1} is a complex band usually attributed to the monomeric fundamentals ν_1 and ν_3; it also includes contributions from $2\nu_2$ and probably from $2\nu_2 + \nu_T$, where ν_T is the

hindered-translation band responsible for absorption near 175 cm^{-1} in the far infrared.[7] With increasing temperature the maximum of this $\nu_{1,2}$ band shifts to higher frequencies and the value of n_i at the maximum decreases. Although the band appears to become narrower with increasing temperature, its full width Γ at half-height actually shows little change.

In making estimates of band strength, the integral $\int \alpha(\nu)d\nu$ is frequently employed; however, the Lambert absorption coefficient $\alpha(\nu)$ is actually proportional to the product[13] of the square of the matrix element for the transition and the frequency ν. In view of the inclusion of ν in $\alpha(\nu)$, the integral $\int \alpha(\nu)d\nu$ as a measure of band strength leads to misleading results when the strengths of bands in widely different spectral regions are to be compared. We have therefore used the definition $S_B = \int n_i(\nu)d\nu$ for comparing band strengths; since $n_i(\nu)$ is proportional to $\alpha(\nu)/\nu$, we have eliminated the influence of ν and can therefore compare the strengths of bands in different regions. The strength of the $\nu_{1,2}$ band decreases with increasing temperature.

The absorption band near 1640 cm^{-1} is usually attributed to the monomeric fundamental ν_2. We note from Fig. 3 that the band maximum does not change appreciably with temperature; the ν_2 band remains narrow at all temperatures covered in the present work. Because the band strength is small and because the band appears as a shoulder on a rising n_i background, it is difficult to determine S_B. The height of the ν_2 peak above the background appears to increase with increasing temperature; although this can be interpreted as evidence for an increase in S_B, the actual maximum values of n_i do not change monotonically with temperature. We also recall

that excess water vapor in the sample beam introduces added uncertainties in our results for water at 70°C.

The large absorption band in the low frequency region in Fig. 3 is usually attributed to hindered rotation or libration of monomeric units in the fields of their neighbors. The librational band ν_L is the strongest band in the spectral range covered in the present work; although the Lambert coefficient is larger for the $\nu_{1,3}$ band, the central frequency of $\nu_{1,2}$ is nearly five times that of ν_L. Although the maximum value of n_i for the ν_L band shows little change with temperature, the band maximum shifts to lower frequencies with increasing temperature. Because the librational band extends well beyond the frequency range of our present measurements, we cannot determine the total band strength S_B; however, we can determine $\int n_i(\nu)d\nu$ from the high-frequency band limit to the band maximum. On the possibly crude assumption that ν_L is symmetrical, we can set S_B equal to twice the measured integral; since the hindered translational band ν_T appears as a shoulder[7] on the low-frequency wing of ν_L, it would have been necessary to make questionable assumptions regarding the contours of ν_L even if our present study had included the entire band.

For purposes of comparison, we have obtained reflection data for D_2O at 27°C in the 5000 - 350 cm^{-1} region. Over much of the high-frequency portion of this range the reflectance of D_2O differed but little from that of H_2O. In Fig. 4 we summarize our results for the portion of the D_2O spectrum that includes its $\nu_{1,3}$, ν_2, and ν_L bands. We note that the results are in general comparable with those obtained for H_2O. However, the three absorption bands in the n_i plot are narrower for D_2O than for H_2O.

The maximum value of n_i for D_2O is significantly smaller for the $\nu_{1,3}$ band but is approximately equal to that for H_2O in the ν_3 and ν_L bands. All D_2O bands appear, of course, at lower frequencies.

DISCUSSION OF RESULTS

The results of the present study in the vicinity of the characteristic bands are presented in the tables. Table I summarizes our results for the refractive index n_r for the bands designated in the first column. The second column in the table gives the minimum values of $n_{r\ min}$ which occurs at the frequency ν_{min} listed in the third column; the fourth and fifth columns, respectively, give corresponding values of $n_{r\ max}$ and ν_{max}. The sixth column gives $\Delta n_r = n_{r\ max} - n_{r\ min}$ and the seventh column lists values of $\Delta\nu = \nu_{min} - \nu_{max}$.

For H_2O the $\nu_{1,3}$ band Δn decreases and $\Delta\nu$ increases with increasing temperature; the values in the table thus give a quantitative measure of the broadening and flattening of feature in the n_r curves in Fig. 2. For the ν_2 band of H_2O, Δn shows a slight increase with temperature and $\Delta\nu$ shows little change; we recall, however, that Δn is small for ν_2 and represents the difference between larger quantities that are subject to uncertainties so large that no significance can be attached to the variation in Δn with temperature. For the H_2O librational band ν_L our data are incomplete, since the values of $n_{r\ max}$ and ν_{max} were not clearly established; the numbers given in parenthesis in Table I assume that the final low-frequency data points actually give the values of $n_{r\ max}$ and ν_{max}. For D_2O at 27°C, the values of Δn for the $\nu_{1,3}$ and ν_2 bands are approximately the same as the corresponding values for H_2O; however, for both bands the values of $\Delta\nu$ are

smaller for D_2O.

Table II summarizes our results for the extinction coefficient n_i for the characteristic bands listed in column one. Columns two and three give, respectively, the maximum values $n_{i\ max}$ observed at frequency ν_{max}. The fourth column gives the band strength S_B and the fifth columns gives the band-width parameter Γ, which represents the full width of the band at half maximum. We shall consider first the H_2O bands.

The $\nu_{1,3}$ band maximum shifts to higher frequencies with increasing temperature; this result is in agreement with the results obtained in transmission studies. The values of $n_{i\ max}$ and S_B for the $\nu_{1,3}$ band clearly decrease with increasing temperature; however, the band-width Γ does not change appreciably with temperature. For ν_2, the frequency ν_{max} does not change with temperature; because this weak band is superposed on a background of absorption, we can draw no firm conclusions regarding S_B and the values listed in the table represent a range of values based on various assumptions regarding the background; similarly, the values of Γ given in the table, which appear to show a narrowing of the band with increasing temperature, are open to question. For the librational band ν_L, the value of $n_{i\ max}$ shows little change with temperature; the band center frequency ν_{max} decreases with increasing temperature as noted in earlier transmission studies.[7] Recalling that our values of S_B and Γ are based on the assumption of a symmetrical band, we note that S_B shows little change and that Γ may increase slightly with increasing temperature.

In comparing D_2O and H_2O at 27°C, we note that $n_{i\ max}$ is slightly smaller for the $\nu_{1,3}$ band of D_2O; for ν_2 and ν_T the values of n_i max

for H_2O and D_2O are not significantly different. The values of S_B and Γ are considerably smaller for each D_2O band than for the corresponding H_2O band.

In comparing Fig. 3 with Table II, we note that there is absorption in the spectral region between ν_2 and ν_L that is not clearly associated with either of these bands. Although the values of n_i throughout this interband region are less than 0.10 and therefore subject to large uncertainties, there is significant integrated absorption $\int n_i(\nu)d\nu$ in this inter-band region. The measured value of $\int n_i(\nu)d\nu$ for the interband region for H_2O is 35 cm^{-1} at 5°C, 31 cm^{-1} at 27°C, and 17 cm^{-1} at 70°C; for D_2O at 27°C, the corresponding value is 22 cm^{-1}. In every case the value of $\int n_i(\nu)d\nu$ is greater than the value of S_B for the sharp ν_2 band. Curnutte and his colleagues[15] have recently interpreted the inter- and intra-molecular spectrum of water by means of a normal-coordinate analysis of a model in which the H_2O monomer is hydrogen-bonded to its four nearest neighbors. Curnutte suggests that the absorption in our interband region may be due to overtones and combinations of ν_L and ν_T.

Table I Refractive Index n_r

Band	$n_{r\ min}$	ν_{min}	$n_{r\ max}$	ν_{max}	Δn_r	$\Delta\nu$
		H_2O at 5°C				
$\nu_{1,3}$	1.104	3560 cm^{-1}	1.501	3155 cm^{-1}	0.397	405 cm^{-1}
ν_2	1.246	1680	1.338	1585	0.092	95
ν_L	1.086	845	(1.544)	(330)	(0.458)	(515)
		H_2O at 27°C				
$\nu_{1,3}$	1.119	3590 cm^{-1}	1.484	3150 cm^{-1}	0.365	440 cm^{-1}
ν_2	1.232	1680	1.349	1600	0.117	80
ν_L	1.116	840	(1.553)	(330)	(0.437)	(510)
		H_2O at 70°C				
$\nu_{1,3}$	1.126	3620 cm^{-1}	1.440	3150 cm^{-1}	0.314	470
ν_2	1.218	1680	1.338	1590	0.120	90
ν_L	1.113	840	--	--	--	--
		D_2O at 27°C				
$\nu_{1,3}$	1.125	2680 cm^{-1}	1.482	2350 cm^{-1}	0.357	330 cm^{-1}
ν_2	1.218	1230	1.332	1180	0.114	50
ν_L	1.090	630	--	--	--	--

Table II Extinction Coefficients n_i

Band	$n_{i\ max}$	ν_{max}	$S_B = \int n_i(\nu)d\nu$	Γ
	H_2O at 5°C			
$\nu_{1,3}$	0.316	3380 cm^{-1}	125 cm^{-1}	370 cm^{-1}
ν_2	0.109	1640	8 - 15	120
ν_L	0.438	590	232*	500*
	H_2O at 27°C			
$\nu_{1,3}$	0.297	3395 cm^{-1}	122 cm^{-1}	390 cm^{-1}
ν_2	0.137	1650	13 - 18	110
ν_L	0.443	580	240*	500*
	H_2O at 70°C			
$\nu_{1,3}$	0.236	3450 cm^{-1}	92 cm^{-1}	380 cm^{-1}
ν_2	0.107	1640	7 - 9	80
ν_L	0.430	510	230*	540*
	D_2O at 27°C			
$\nu_{1,3}$	0.267	2490 cm^{-1}	76 cm^{-1}	280 cm^{-1}
ν_2	0.119	1200	5 - 8	70
ν_L	0.452	460	150*	300*

*These values are based on the assumption that the band is symmetrical about ν_{max}.

LEGENDS FOR FIGURES

Fig. 1 Normal-incidence spectral reflectance of water. The light, continuous curve gives the reflectance at $5^{\circ}C$; the heavy, continuous curve gives the reflectance at $27^{\circ}C$; and the dotted curve gives the reflectance at $70^{\circ}C$.

Fig. 2 The real part n_r of the refractive index of water as a function of frequency. The values of n_r at $5^{\circ}C$, $27^{\circ}C$, and $70^{\circ}C$ are given by the light continuous, the heavy continuous, and the dotted curves, respectively.

Fig. 3 The imaginary part n_i of the refractive index of water, sometimes called the extinction coefficient, is plotted as a function of frequency. The values of n_i at $5^{\circ}C$, $27^{\circ}C$, and $70^{\circ}C$ are given by the light continuous, the heavy continuous, and the dotted curves, respectively.

Fig. 4 The optical constants of D_2O at $27^{\circ}C$. The upper panel gives the normal-incidence spectral reflectance. The center panel gives the real part n_r of the refractive index as a function of frequency. The lower panel gives the extinction coefficient n_i as a function of frequency.

FOOTNOTES AND REFERENCES

*Supported in part at U.M.K.C. by the National Aeronautics and Space Administration and in part at K.S.U. by the Office of Naval Research.

1. W. M. Irvine and J. B. Pollack, Icarus 8, 324 (1968).
2. L. Pontier and C. Dechambenoy, Ann. Geophys. 21, 46 2 (1965); 22, 633 (1966).
3. V. M. Zolatarev, B. A. Mikhailov, L. I. Aperovich, and S. I. Popov, Opt. Spektrosk. 27, 790 (1969). [Opt. Spectrosc. 27, 430 (1969).]
4. M. R. Querry, B. Curnutte, and D. Williams, J. Opt. Soc. Am. 59, 1299 (1969).
5. A. N. Rusk, D. Williams, and M. R. Querry, J. Opt. Soc. Am. 61, 895 (1971).
6. C. W. Robertson and D. Williams, J. Opt. Soc. Am. 61, 1316 (1971).
7. D. A. Draegert, N. W. B. Stone, B. Curnutte, and D. Williams, J. Opt. Soc. Am. 56, 64 (1966).
8. P. A. Giguere and K. B. Harvey, Can. J. Chem. 34, 798 (1956).
9. J. G. Bayly, V. B. Kartha, and W. H. Stevens, Infrared Phys. 3, 211 (1963).
10. M. Falk and T. A. Ford, Can. J. Chem. 44, 1699 (1966).
11. T. A. Ford and M. Falk, Can. J. Chem. 46, 3579 (1968).
12. A. N. Rusk, Doctoral Dissertation, Kansas State University, 1971.
13. G. Herzberg, "Molecular Spectra and Molecular Structure. I. Spectra of Diatomic Molecules" (Van Nostrand, Princeton, 1950), p. 126.
14. J. B. Bryan and B. Curnutte, J. Mol. Spec. (In Press); B. Curnutte and J. Bandekar, J. Mol. Spec. (In Press).

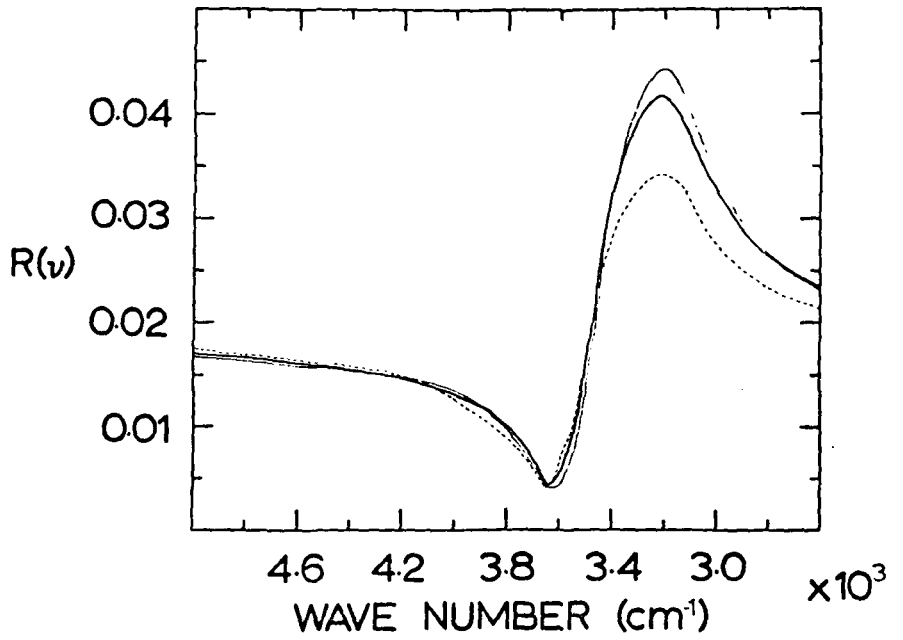
0.04
0.03
R(ν)
0.02
0.01
4.6
4.2
3.8
3.4
3.0
x10³
WAVE NUMBER (cm⁻¹)

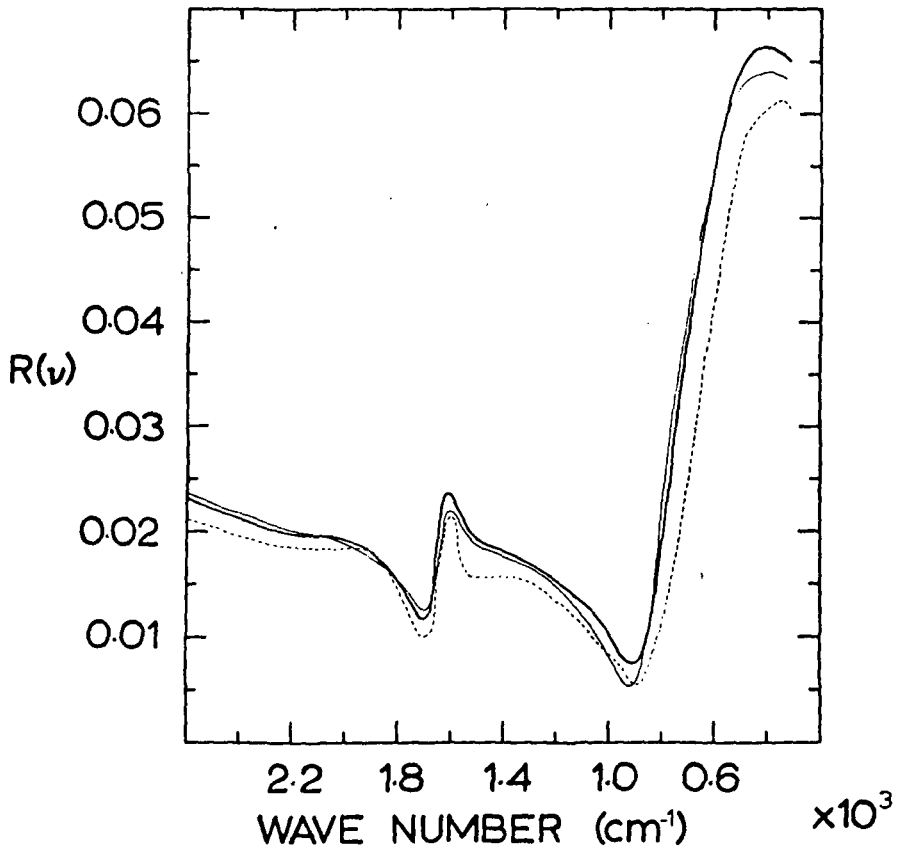
0.06
0.05
0.04
R(ν)
0.03
0.02
0.01
2.2
1.8
1.4
1.0
0.6
x10³
WAVE NUMBER (cm⁻¹)

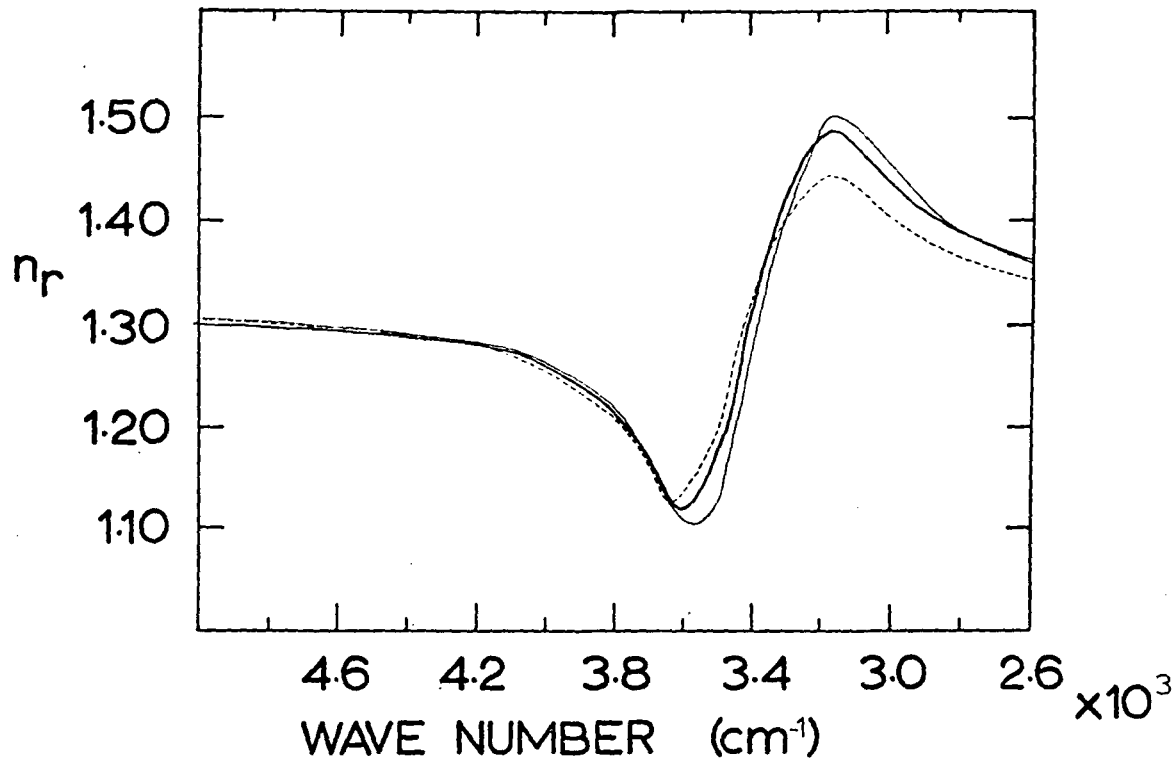
1·50
1·40
n_r
1·30
1·20
1·10
4·6
4·2
3·8
3·4
3·0
2·6
×10³
WAVE NUMBER (cm⁻¹)

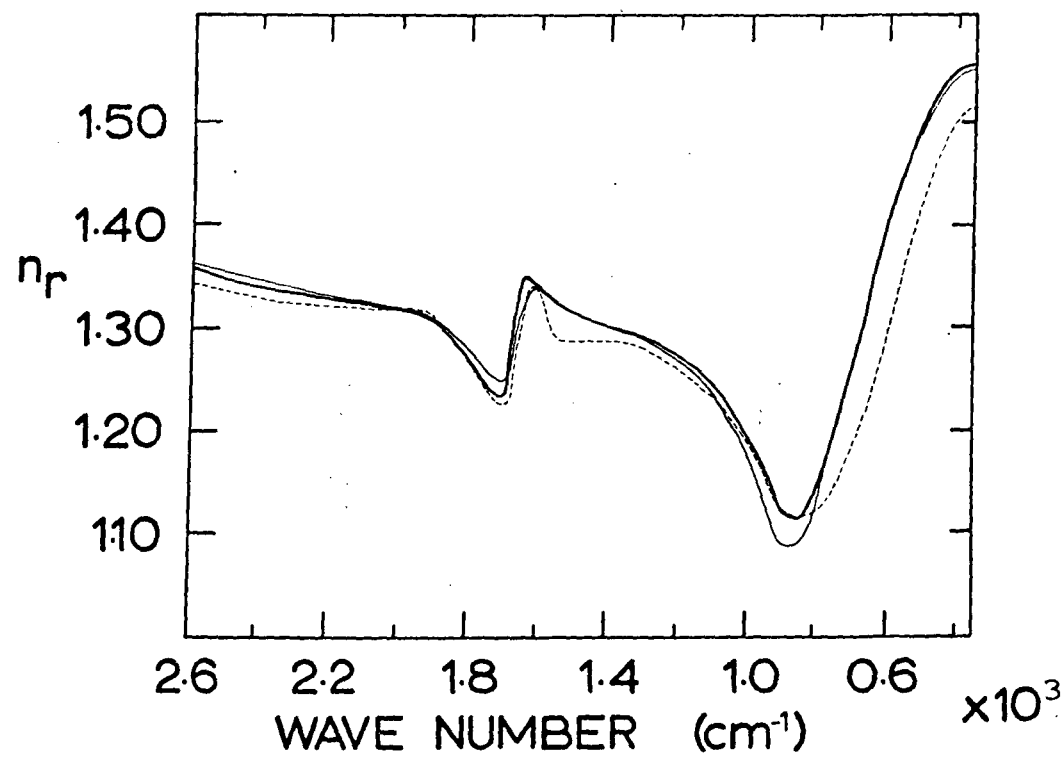
1·50
1·40
n_r
1·30
1·20
1·10
2·6
2·2
1·8
1·4
1·0
0·6
×10³
WAVE NUMBER (cm⁻¹)

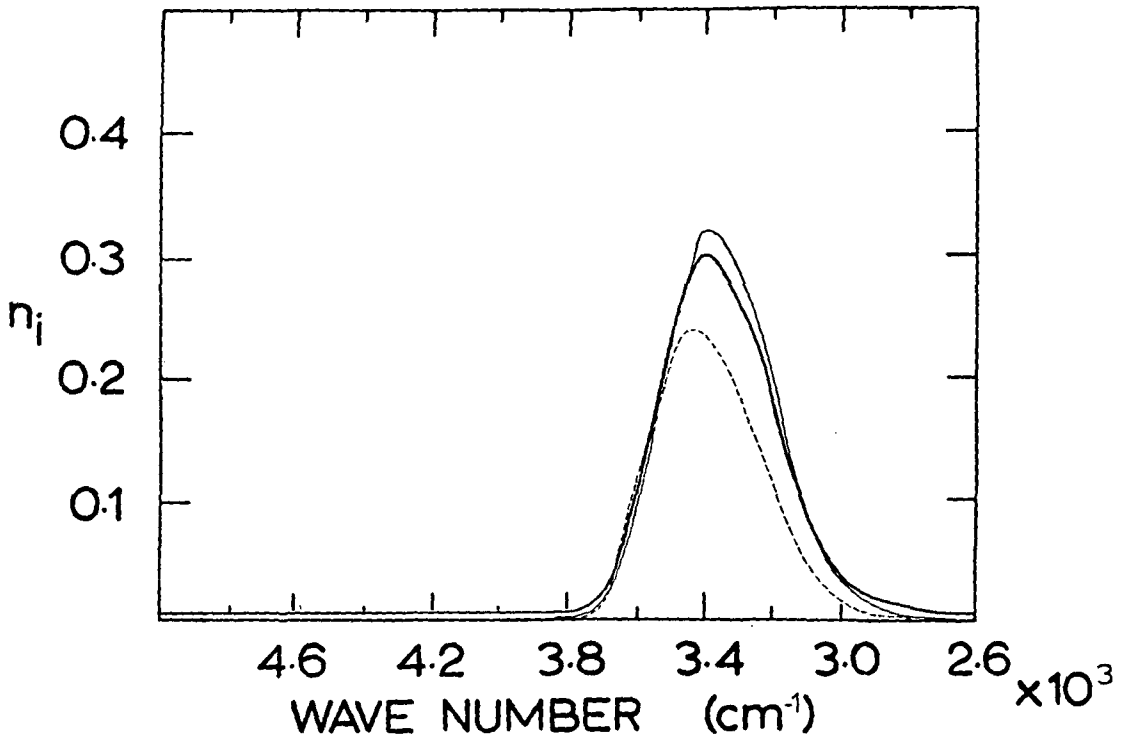
0·4
0·3
n_i
0·2
0·1
4·6
4·2
3·8
3·4
3·0
2·6
x10³
WAVE NUMBER (cm⁻¹)

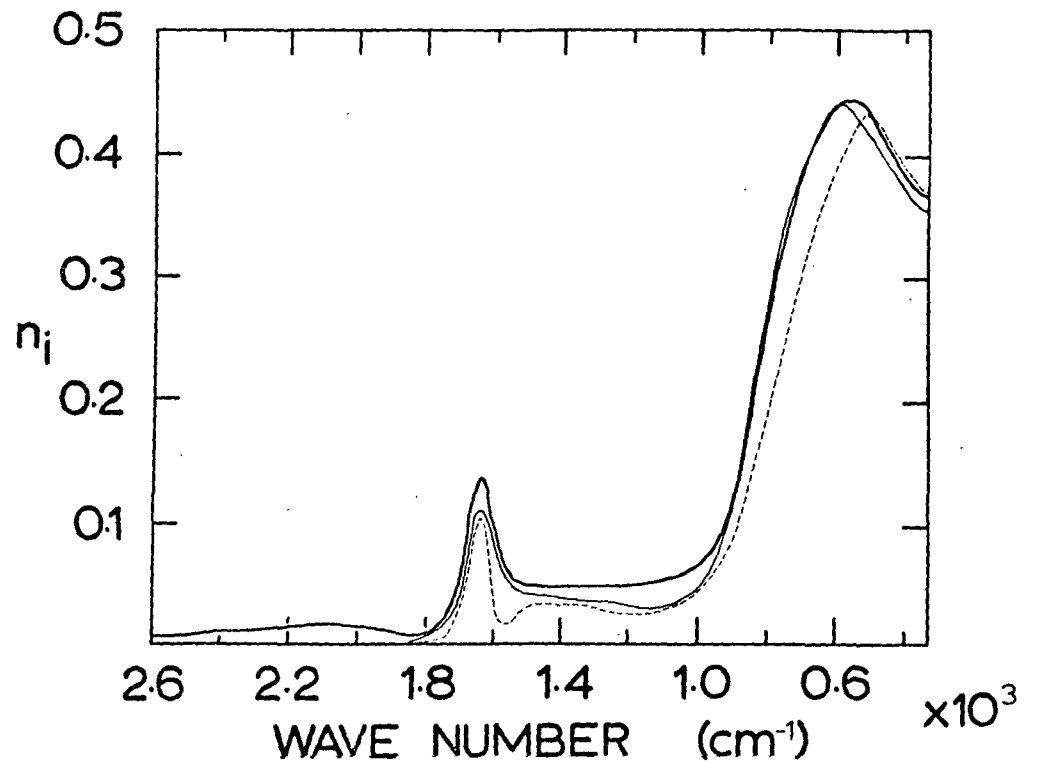
0·5
0·4
0·3
n_i
0·2
0·1
2·6
2·2
1·8
1·4
1·0
0·6
x10³
WAVE NUMBER (cm⁻¹)

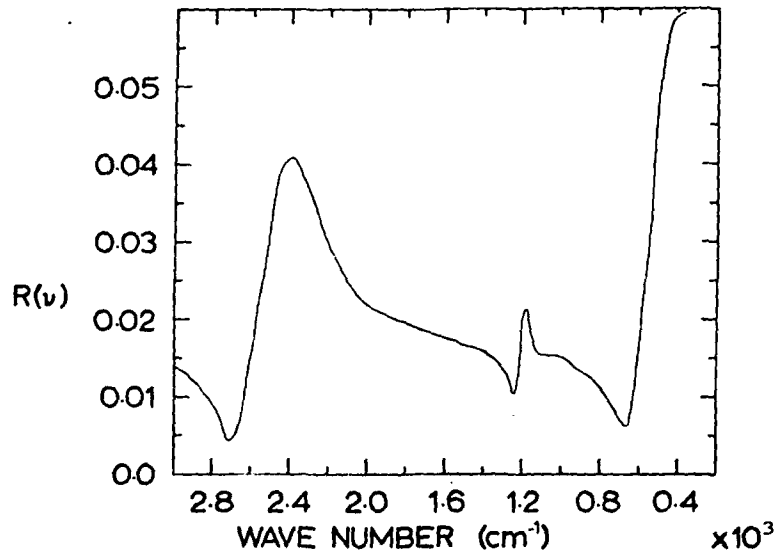
0.05
0.04
0.03
R(ν)
0.02
0.01
0.0
2.8 2.4 2.0 1.6 1.2 0.8 0.4
WAVE NUMBER (cm⁻¹)
x10³

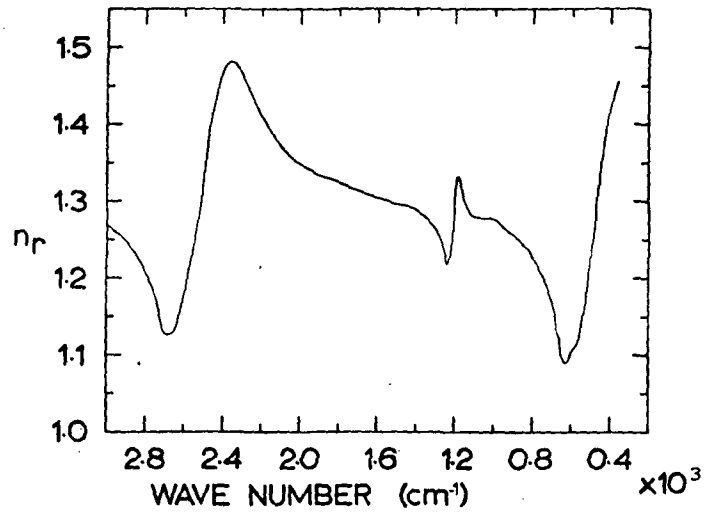
1.5
1.4
1.3
nr
1.2
1.1
1.0
2.8 2.4 2.0 1.6 1.2 0.8 0.4
WAVE NUMBER (cm⁻¹)
x10³

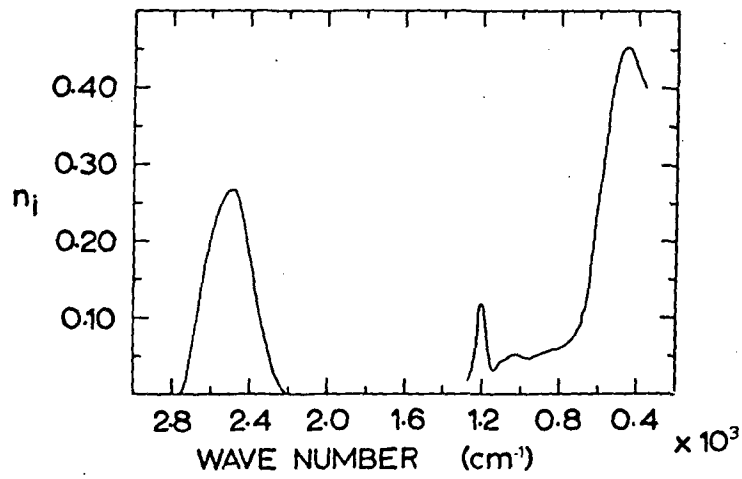
0.40
0.30
ni
0.20
0.10
2.8 2.4 2.0 1.6 1.2 0.8 0.4
WAVE NUMBER (cm⁻¹)
x 10³

PART IV

REFLECTANCE AND OPTICAL CONSTANTS IN THE INFRARED FOR 26 AQUEOUS SOLUTIONS

INTRODUCTION:

In this part of the report we present in graphical form absolute reflectance, phase shifts, index of refraction, and extinction coefficients for water, heavy water, and 26 aqueous solutions. The measurements of absolute reflectance were made by Dr. Paul Rhine and supplied to us by Dr. Dudley Williams of Kansas State University. The reflectance was measured at near normal incidence through the spectral region 5,000 cm^{-1} to 300 cm^{-1}. We made a Kramers-Kronig analysis of the reflectance spectra in order to determine the phase-shift for electromagnetic waves reflected at the surface of the water and the aqueous solutions. We then determined the index of refraction and the extinction coefficients by use of the computed phase-shifts and measured values for reflectance. A full analysis of all the data presented in Part IV will probably take about two more years. Several manuscripts should result from these future investigations. The manuscripts also will be forwarded to the NASA when they are submitted for publication.

The methods for measuring reflectance and computing optical constants were presented in Part III of this report.

FIGURE CAPTIONS

Figure 1. The absolute reflectance at near normal incidence for water and D_2O are represented by graphs having ID symbols nos. 1 and 2 respectively. The spectral region is 5,000 cm^{-1} to 2,600 cm^{-1} wave numbers.

Figure 2. The absolute reflectance at near normal incidence for water and D_2O are represented by graphs having ID symbols nos. 1 and 2 respectively. The spectral region is 2,600 cm^{-1} to 300 cm^{-1} wave numbers.

Figure 3. The phase-shift for electromagnetic waves reflected at near normal incidence for water and D_2O are represented by graphs having ID symbols no. 1 and 2 respectively. The spectral region is 5,000 cm^{-1} to 2,600 cm^{-1} wave numbers. The phase-shifts were computed by using the Kramers-Kronig analysis.

Figure 4. The phase-shift for electromagnetic waves reflected at near normal incidence for water and D_2O are represented by graphs having ID symbols no. 1 and 2 respectively. The spectral region is 2,600 cm^{-1} to 300 cm^{-1} wave numbers. The phase-shfits were computed by using the Kramers-Kronig analysis.

Figure 5. The index of refraction for water and D_2O are represented by graphs having ID symbols no. 1 and 2 respectively. The spectral region is 5,000 cm^{-1} to 2,600 cm^{-1} wave numbers.

Figure 6. The index of refraction for water and D_2O are represented by graphs having ID symbols no. 1 and 2 respectively. The spectral region is 2,600 cm^{-1} to 300 cm^{-1} wave numbers.

Figure 7. The extinction coefficient for water and D_2O are represented by graphs having ID symbols no. 1 and 2 respectively. The spectral region is 5,000 cm^{-1} to 2,600 cm^{-1} wave numbers.

Figure 8. The extinction coefficient for water and D_2O are represented by graphs having ID symbols no. 1 and 2 respectively. The spectral region is 2,600 cm^{-1} to 300 cm^{-1} wave numbers.

Figure 9. The absolute reflectance at near normal incidence for water and 2M, 4M, and 6M aqueous solution of KI are represented by graphs having ID symbols no. 1-4 respectively. The spectral region is 5,000 cm^{-1} to 2,600 cm^{-1} wave numbers.

Figure 10. The absolute reflectance at near normal incidence for water and 2M, 4M, and 6M aqueous solution of KI are represented by graphs having ID symbols 1-4 respectively. The spectral region is 2,600 cm^{-1} to 300 cm^{-1} wave numbers.

Figure 11. The phase-shift for electromagnetic waves reflected at near normal incidence for water and 2M, 4M, and 6M aqueous solutions of KI are represented by graphs having ID symbols no. 1-4 respectively. The spectral region is 5,000 cm^{-1} to 2,600 cm^{-1} wave numbers. The phase-shifts were computed by using the Kramers-Kronig analysis.

Figure 12. The phase-shift for electromagnetic waves reflected at near normal incidence for water and 2M, 4M, and 6M aqueous solutions of KI are represented by graphs having ID symbols no. 1-4 respectively. The spectral region is 2,600 cm^{-1} to 300 cm^{-1} wave numbers. The phase-shifts were computed by using the Kramers-Kronig analysis.

Figure 13. The index of refraction for water and 2M, 4M, and 6M aqueous solutions of KI are represented by graphs having ID symbols no. 1-4 respectively. The spectral region is 5,000 cm^{-1} to 2,600 cm^{-1} wave numbers.

Figure 14. The index of refraction for water and 2M, 4M, and 6M aqueous solutions of KI are represented by graphs having ID symbols no. 1-4 respectively. The spectral region is 2,600 cm^{-1} to 300 cm^{-1} wave numbers.

Figure 15. The extinction coefficient for water and 2M, 4M, and 6M aqueous solutions of KI are represented by graphs having ID symbols no. 1-4 respectively. The spectral region is 5,000 cm^{-1} to 2,600 cm^{-1} wave numbers.

Figure 16. The extinction coefficient for water and 2M, 4M, and 6M aqueous solutions of KI are represented by graphs having ID symbols no. 1-4 respectively. The spectral region is 2,600 cm^{-1} to 300 cm^{-1} wave numbers.

Figure 17. The absolute reflectance of water and 4M aqueous solutions of NaBr, LiBr, and KBr are represented by graphs having ID symbols no. 1-4 respectively. The spectral region is 5,000 cm^{-1} to 2,600 cm^{-1} wave numbers.

Figure 18. The absolute reflectance of water and 4M aqueous solutions of NaBr, LiBr, and KBr are represented by graphs having ID symbols no. 1-4 respectively. The spectral region is 2,600 cm^{-1} to 300 cm^{-1} wave numbers.

Figure 19. The phase-shift for electromagnetic waves reflected at near normal incidence for water and 4M aqueous solutions of NaBr, LiBr, and KBr are represented by graphs having ID symbols no. 1-4 respectively. The spectral region is 5,000 cm^{-1} to 2,600 cm^{-1} wave numbers. The phase-shifts were computed by using the Kramers-Kronig analysis.

Figure 20. The phase-shift for electromagnetic waves reflected at near normal incidence for water and 4M aqueous solutions of NaBr, LiBr, and KBr are represented by graphs having ID symbols no. 1-4 respectively. The spectral region is 2,600 cm^{-1} to 300 cm^{-1} wave numbers. The phase-shifts were computed by using the Kramers-Kronig analysis.

Figure 21. The index of refraction for water and 4M aqueous solutions of NaBr, LiBr, and KBr are represented by graphs having ID symbols no. 1-4 respectively. The spectral region is 5,000 cm^{-1} to 2,600 cm^{-1} wave numbers.

Figure 22. The index of refraction for water and 4M aqueous solutions of NaBr, LiBr, and KBr are represented by graphs having ID symbols no. 1-4 respectively. The spectral region is 2,600 cm^{-1} to 300 cm^{-1} wave numbers.

Figure 23. The extinction coefficient for water and 4M aqueous solutions of NaBr, LiBr, and KBr are represented by graphs having ID symbols no. 1-4 respectively. The spectral region is 5,000 cm^{-1} to 2,600 cm^{-1} wave numbers.

Figure 24. The extinction coefficient for water and 4M aqueous solutions of NaBr, LiBr, and KBr are represented by graphs having ID symbols no. 1-4 respectively. The spectral region is 2,600 cm^{-1} to 300 cm^{-1} wave numbers.

Figure 25. The absolute reflectance at near normal incidence for water and 2M, 4M, 8M, and 16M aqueous solutions of NaOH are represented by graphs having ID symbols no. 1-5 respectively. The spectral region is 5,000 cm^{-1} to 2,600 cm^{-1} wave numbers.

Figure 26. The absolute reflectance at near normal incidence for water and 2M, 4M, 8M, and 16M aqueous solutions of NaOH are represented by graphs having ID symbols no. 1-5 respectively. The spectral region is 2,600 cm^{-1} to 300 cm^{-1} wave numbers.

Figure 27. The phase-shift for electromagnetic waves reflected at near normal incidence for water and 2M, 4M, 8M, and 16M aqueous solutions of NaOH are represented by graphs having ID symbols no. 1-5 respectively. The spectral region is 5,000 cm^{-1} to 2,600 cm^{-1} wave numbers. The phase-shifts were computed by using the Kramers-Kronig analysis.

Figure 28. The phase-shift for electromagnetic waves reflected at near normal incidence for water and 2M, 4M, 8M, and 16M aqueous solutions of NaOH are represented by graphs having ID symbols no. 1-5 respectively. The spectral region is 2,600 cm^{-1} to 300 cm^{-1} wave numbers. The phase-shifts were computed by using the Kramers-Kronig analysis.

Figure 29. The index of refraction for water and 2M, 4M, 8M, and 16M aqueous solutions of NaOH are represented by graphs having ID symbols no. 1-5 respectively. The spectral region is 5,000 cm^{-1} to 2,600 cm^{-1} wave numbers.

Figure 30. The index of refraction for water and 2M, 4M, 8M, and 16M aqueous solutions of NaOH are represented by graphs having ID symbols no. 1-5 respectively. The spectral region is 2,600 cm^{-1} to 300 cm^{-1} wave numbers.

Figure 31. The extinction coefficient for water and 2M, 4M, 8M, and 16M aqueous solutions of NaOH are represented by graphs having ID symbols no. 1-5 respectively. The spectral region is 5,000 cm^{-1} to 2,600 cm^{-1} wave numbers.

Figure 32. The extinction coefficient for water and 2M, 4M, 8M, and 16M aqueous solutions of NaOH are represented by graphs having ID symbols no. 1-5 respectively. The spectral region is 2,600 cm^{-1} to 300 cm^{-1} wave numbers.

Figure 33. The absolute reflectance at near normal incidence for water and 2M, 4M, 8M, and 16M aqueous solutions of KOH are represented by graphs having ID symbols 1-5 respectively. The spectral region is 5,000 cm^{-1} to 2,600 cm^{-1} wave numbers.

Figure 34. The absolute reflectance at near normal incidence for water and 2M, 4M, 8M, and 16M aqueous solutions of KOH are represented by graphs having ID symbols 1-5 respectively. The spectral region is 5,000 cm^{-1} to 2,600 cm^{-1} wave numbers.

Figure 35. The phase-shift for electromagnetic waves reflected at near normal incidence for water and 2M, 4M, 8M, and 16M aqueous solutions of KOH are represented by graphs having ID symbols 1-5 respectively. The spectral region is 5,000 cm^{-1} to 2,600 cm^{-1} wave numbers. The phase-shifts were computed by using the Kramers-Kronig analysis.

Figure 36. The phase-shift for electromagnetic waves reflected at near normal incidence for water and 2M, 4M, 8M, and 16M aqueous solutions of KOH are represented by graphs having ID symbols 1-5 respectively. The spectral region is 2,600 cm^{-1} to 300 cm^{-1} wave numbers. The phase-shifts were computed by using the Kramers-Kronig analysis.

Figure 37. The index of refraction for water and 2M, 4M, 8M, and 16M aqueous solutions of KOH are represented by graphs having ID symbols 1-5 respectively. The spectral region is 5,000 cm^{-1} to 2,600 cm^{-1} wave numbers.

Figure 38. The index of refraction for water and 2M, 4M, 8M, and 16M aqueous solutions of KOH are represented by graphs having ID symbols 1-5 respectively. The spectral region is 2,600 cm^{-1} to 300 cm^{-1} wave numbers.

Figure 39. The extinction coefficient for water and 2M, 4M, 8M, and 16M aqueous solutions of KOH are represented by graphs having ID symbols 1-5 respectively. The spectral region is 5,000 cm^{-1} to 2,600 cm^{-1} wave numbers.

Figure 40. The extinction coefficient for water and 2M, 4M, 8M, and 16M aqueous solutions of KOH are represented by graphs having ID symbols 1-5 respectively. The spectral region is 2,600 cm^{-1} to 300 cm^{-1} wave numbers.

Figure 41. The absolute reflectance at near normal incidence for water and 2M, 4M, 8M, and 12M aqueous solutions of HCl are represented by graphs having ID symbols 1-5 respectively. The spectral region is 5,000 cm^{-1} to 2,600 cm^{-1} wave numbers.

Figure 42. The absolute reflectance at near normal incidence for water and 2M, 4M, 8M, and 12M aqueous solutions of HCl are represented by graphs having ID symbols 1-5 respectively. The spectral region is 2,600 cm^{-1} to 300 cm^{-1} wave numbers.

Figure 43. The phase-shift for electromagnetic waves reflected at near normal incidence for water and 2M, 4M, 8M, and 12M aqueous solutions of HCl are represented by graphs having ID symbols 1-5 respectively. The spectral region is 5,000 cm^{-1} to 2,600 cm^{-1} wave numbers. The phase-shifts were computed by use of the Kramers-Kronig analysis.

Figure 44. The phase-shift for electromagnetic waves reflected at near normal incidence for water and 2M, 4M, 8M, and 12M aqueous solutions of HCl are represented by graphs having ID symbols 1-5 respectively. The spectral region is 2,600 cm^{-1} to 300 cm^{-1} wave numbers. The phase-shifts were computed by use of the Kramers-Kronig analysis.

Figure 45. The index of refraction for water and 2M, 4M, 8M, and 12M aqueous solutions of HCl are represented by graphs having ID symbols no. 1-5 respectively. The spectral region is 5,000 cm^{-1} to 2,600 cm^{-1} wave numbers.

Figure 46. The index of refraction for water and 2M, 4M, 8M, and 12M aqueous solutions of HCl are represented by graphs having ID symbols no. 1-5 respectively. The spectral region is 2,600 cm^{-1} to 300 cm^{-1} wave numbers.

Figure 47. The extinction coefficient for water and 2M, 4M, 8M, and 12M aqueous solutions of HCl are represented by graphs having ID symbols no. 1-5 respectively. The spectral region is 5,000 cm^{-1} to 2,600 cm^{-1} wave numbers.

Figure 48. The extinction coefficient for water and 2M, 4M, 8M, and 12M aqueous solutions of HCl are represented by graphs having ID symbols no. 1-5 respectively. The spectral region is 2,600 cm^{-1} to 300 cm^{-1} wave numbers.

Figure 49. The absolute reflectance at near normal incidence for water and 2M, 4M, 8M, and 12M aqueous solutions of KF are represented by graphs having ID symbols no. 1-5 respectively. The spectral region is 5,000 cm^{-1} to 2,600 cm^{-1} wave numbers.

Figure 50. The absolute reflectance at near normal incidence for water and 2M, 4M, 8M, and 12M aqueous solutions of KF are represented by graphs having ID symbols no. 1-5 respectively. The spectral region is 2,600 cm^{-1} to 300 cm^{-1} wave numbers.

Figure 51. The phase-shift for electromagnetic waves reflected at near normal incidence from water and 2M, 4M, 8M, and 12M aqueous solutions of KF are represented by graphs having ID symbols no. 1-5 respectively. The spectral region is 5,000 cm^{-1} to 2,600 cm^{-1} wave numbers. The phase-shifts were computed by using the Kramers-Kronig analysis.

Figure 52. The phase-shift for electromagnetic waves reflected at near normal incidence from water and 2M, 4M, 8M, and 12M aqueous solutions of KF are represented by graphs having ID symbols no. 1-5 respectively. The spectral region is 2,600 cm^{-1} to 300 cm^{-1} wave numbers. The phase-shifts were computed by using the Kramers-Kronig analysis.

Figure 53. The index of refraction for water and 2M, 4M, 8M, and 12M aqueous solutions of KF are represented by graphs having ID symbols no. 1-5 respectively. The spectral region is 5,000 cm^{-1} to 2,600 cm^{-1} wave numbers.

Figure 54. The index of refraction for water and 2M, 4M, 8M, and 12M aqueous solutions of KF are represented by graphs having ID symbols no. 1-5 respectively. The spectral region is 2,600 cm^{-1} to 300 cm^{-1} wave numbers.

Figure 55. The extinction coefficient for water and 2M, 4M, 8M, and 12M aqueous solutions of KF are represented by graphs having ID symbols no. 1-5 respectively. The spectral region is 5,000 cm^{-1} to 2,600 cm^{-1} wave numbers.

Figure 56. The extinction coefficient for water and 2M, 4M, 8M, and 12M aqueous solutions of KF are represented by graphs having ID symbols no. 1-5 respectively. The spectral region is 2,600 cm^{-1} to 300 cm^{-1} wave numbers.

Figure 57. The absolute reflectance at near normal incidence for water and 4M aqueous solutions of KBr, KF, KCl, and KI are represented by graphs having symbols no. 1-5 respectively. The spectral region is 5,000 cm^{-1} to 2,600 cm^{-1} wave numbers.

Figure 58. The absolute reflectance at near normal incidence for water and 4M aqueous solutions of KBr, KF, KCl, and KI are represented by graphs having symbols no. 1-5 respectively. The spectral region is 2,600 cm^{-1} to 300 cm^{-1} wave numbers.

Figure 59. The phase-shift for electromagnetic waves reflected at near normal incidence for water and 4M aqueous solutions of KBr, KF, KCL, and KI are represented by graphs having ID symbols no. 1-5 respectively. The spectral region is 5,000 cm^{-1} to 2,600 cm^{-1} wave numbers. The phase-shifts were computed by using the Kramers-Kronig analysis.

Figure 60. The phase-shift for electromagnetic waves reflected at near normal incidence for water and 4M aqueous solutions of KBr, KF, KCl, and KI are represented by graphs having ID symbols no. 1-5 respectively. The spectral region is 2,600 cm^{-1} to 300 cm^{-1} wave numbers. The phase-shifts were computed by using the Kramers-Kronig analysis.

Figure 61. The index of refraction for water and 4M aqueous solutions of KBr, KF, KCl, and KI are represented by graphs having ID symbols no. 1-5 respectively. The spectral region is 5,000 cm^{-1} to 2,600 cm^{-1} wave numbers.

Figure 62. The index of refraction for water and 4M aqueous solutions of KBr, KF, KCl, and KI are represented by graphs having ID symbols no. 1-5 respectively. The spectral region is 2,600 cm^{-1} to 300 cm^{-1} wave numbers.

Figure 63. The extinction coefficient for water and 4M aqueous solutions of KBr, KF, KCl, and KI are represented by graphs having ID symbols no. 1-5 respectively. The spectral region is 5,000 cm^{-1} to 2,600 cm^{-1} wave numbers.

Figure 64. The extinction coefficient for water and 4M aqueous solutions of KBr, KF, KCl, and KI are represented by graphs having ID symbols no. 1-5 respectively. The spectral region is 2,600 cm^{-1} to 300 cm^{-1} wave numbers.

Figure 1

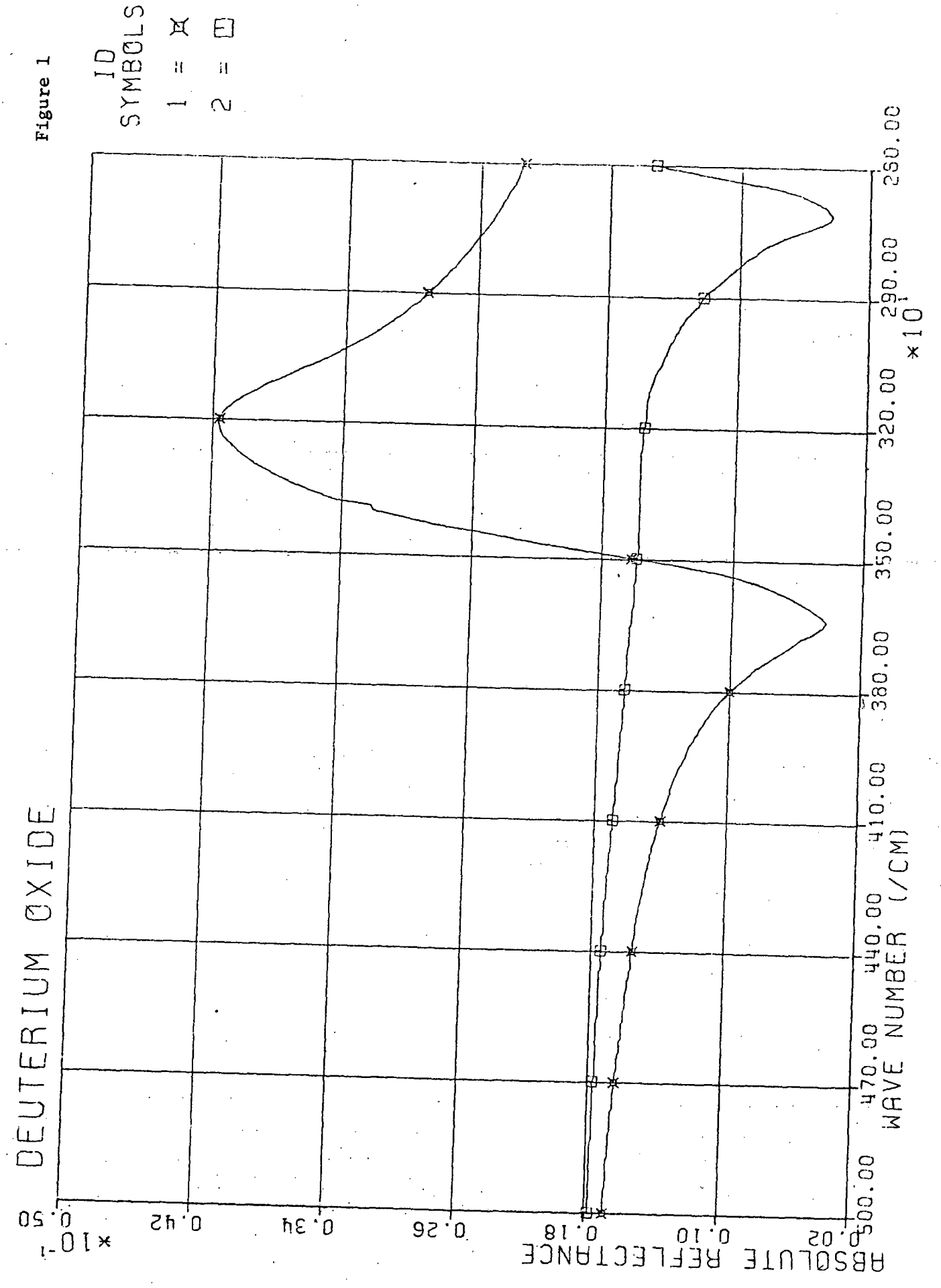
ID
SYMBOLS
1 =
2 =
DEUTERIUM OXIDE
ABSOLUTE REFLECTANCE
*10⁻¹
0.02
0.10
0.18
0.26
0.34
0.42
0.50
WAVE NUMBER (/CM)
*10¹
260.00
290.00
320.00
350.00
380.00
410.00
440.00
470.00
500.00

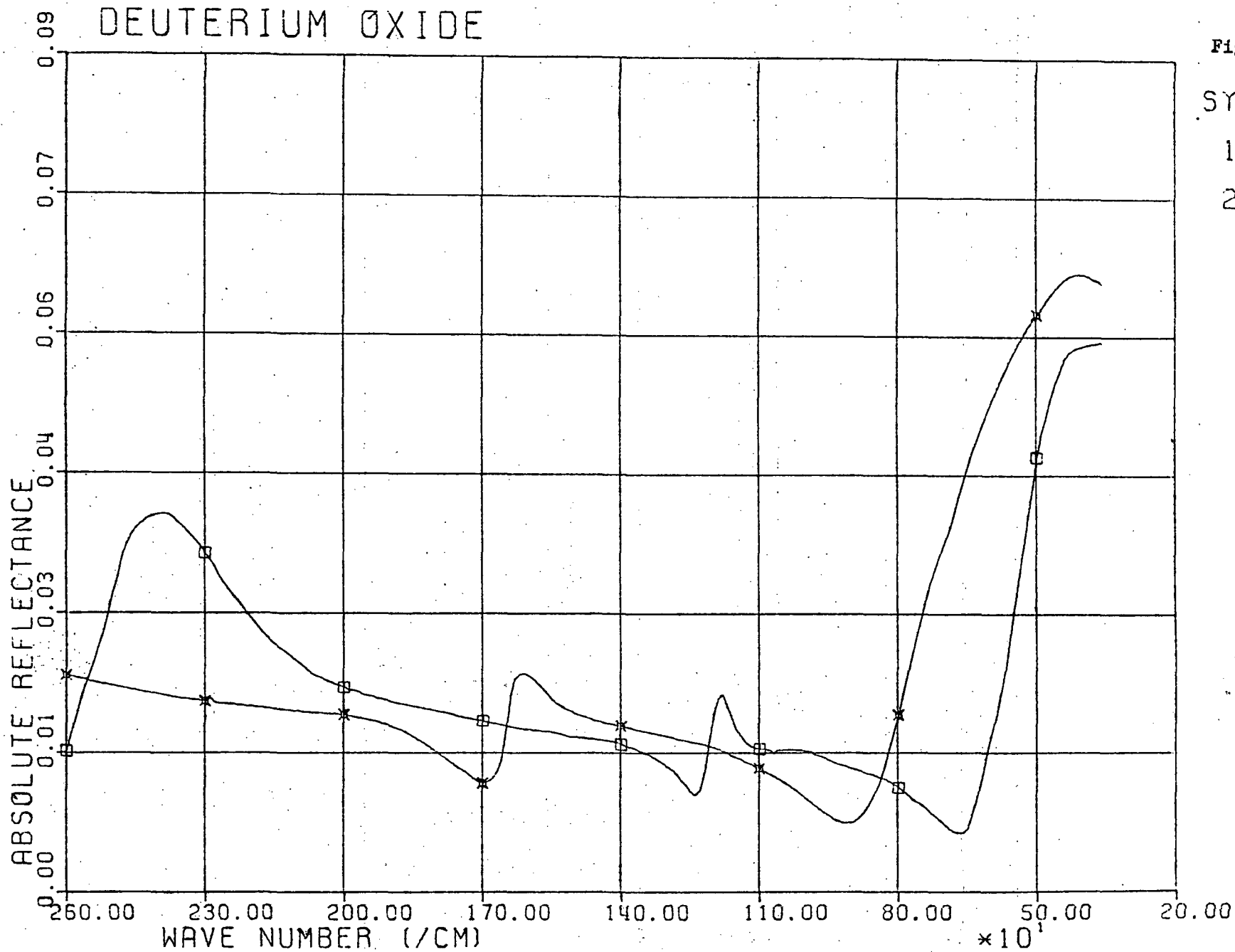
DEUTERIUM OXIDE
ABSOLUTE REFLECTANCE
0.00
0.01
0.03
0.04
0.06
0.07
0.09
260.00
230.00
200.00
170.00
140.00
110.00
80.00
50.00
20.00
WAVE NUMBER (/CM)
×10¹
ID
SYMBOLS
1 =
2 =

Figure 2

Figure 3

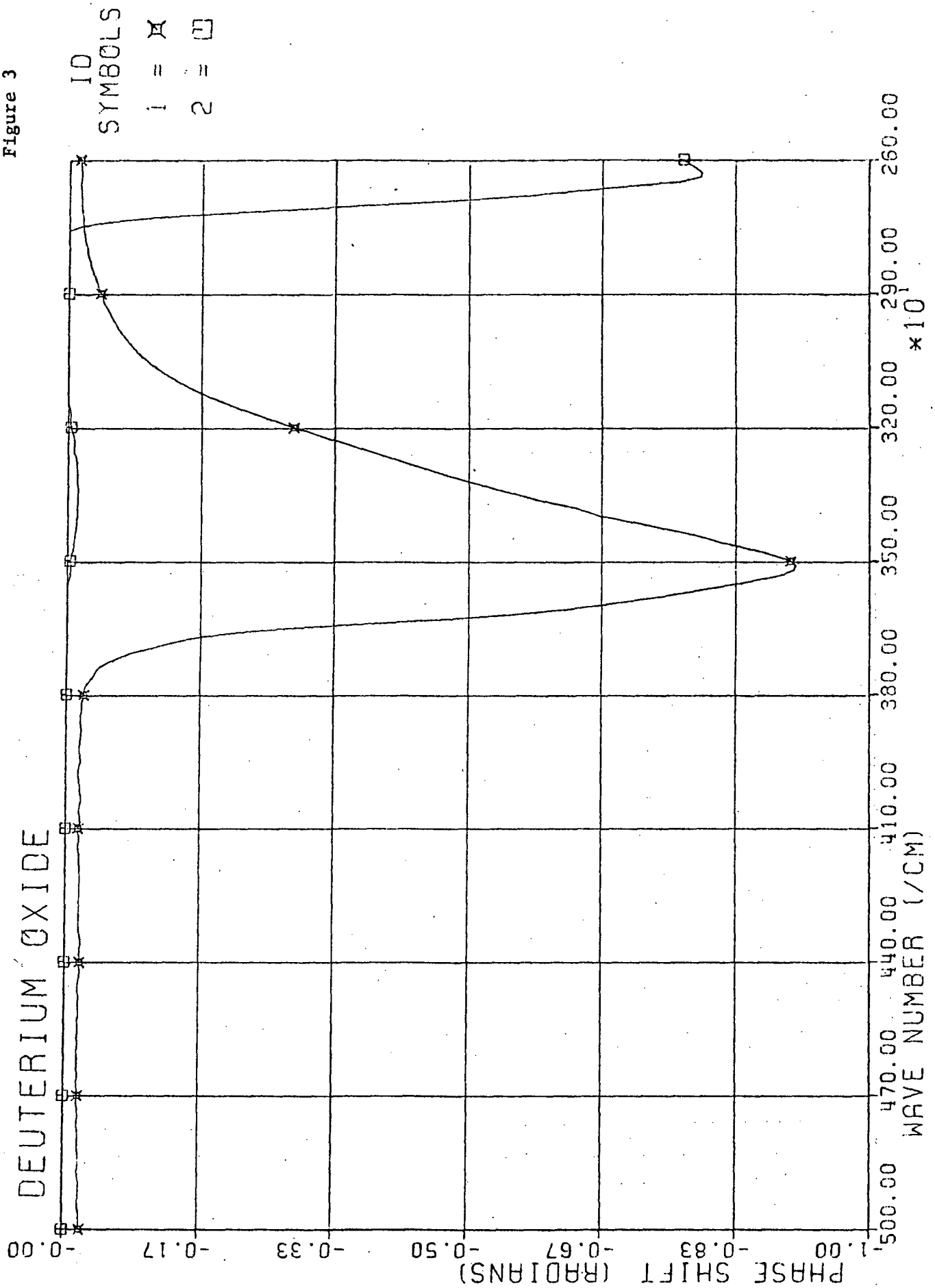
ID
SYMBOLS
1 = X
2 = □
DEUTERIUM OXIDE
PHASE SHIFT (RADIANS)
-0.00
-0.17
-0.33
-0.50
-0.67
-0.83
-1.00
WAVE NUMBER (/CM)
500.00
470.00
440.00
410.00
380.00
350.00
320.00
290.00
260.00
*10¹

Figure 4

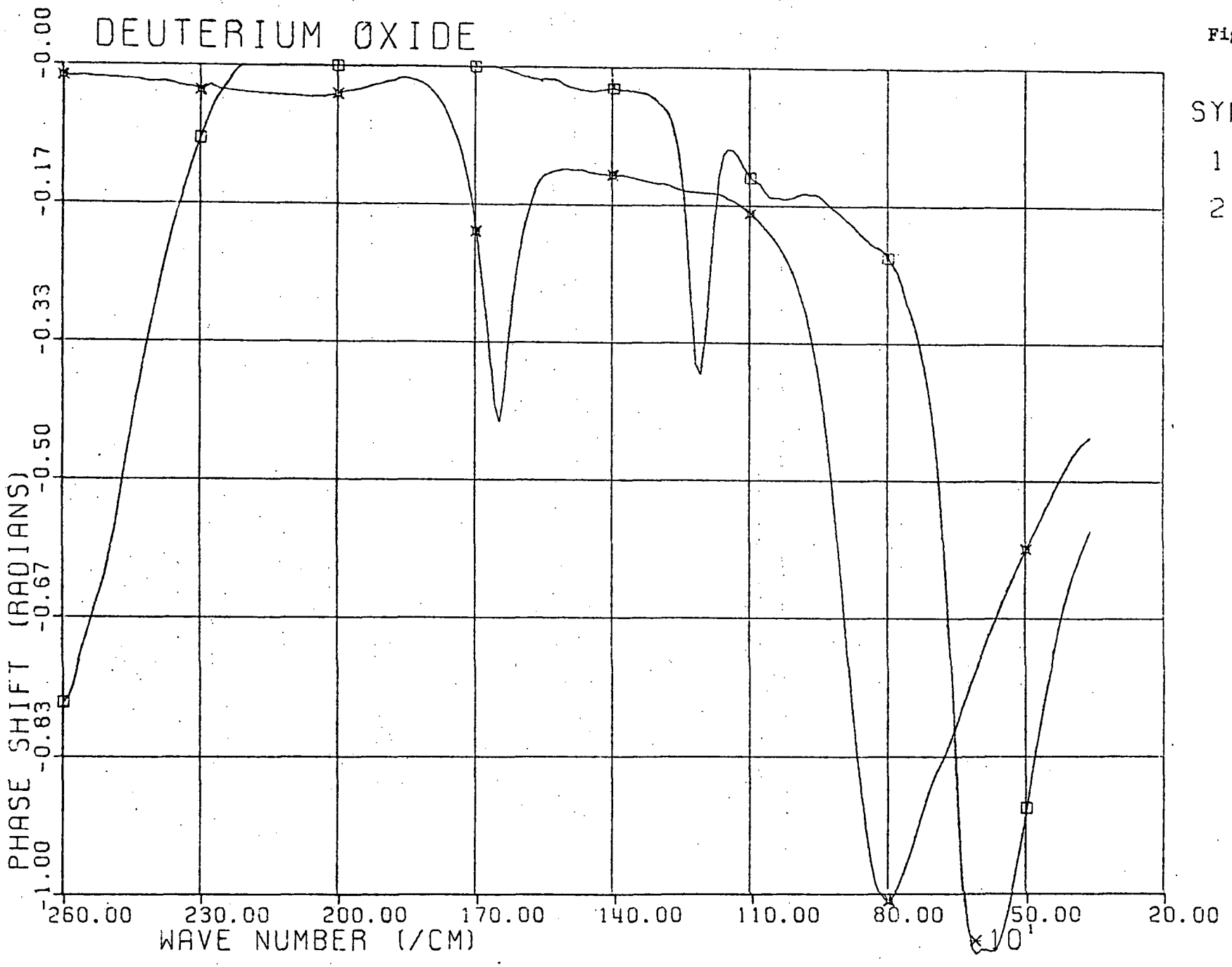
DEUTERIUM OXIDE
ID SYMBOLS
1 =
2 =
PHASE SHIFT (RADIANS)
-0.00
-0.17
-0.33
-0.50
-0.67
-0.83
-1.00
260.00
230.00
200.00
170.00
140.00
110.00
80.00
50.00
20.00
WAVE NUMBER (/CM)
X10¹

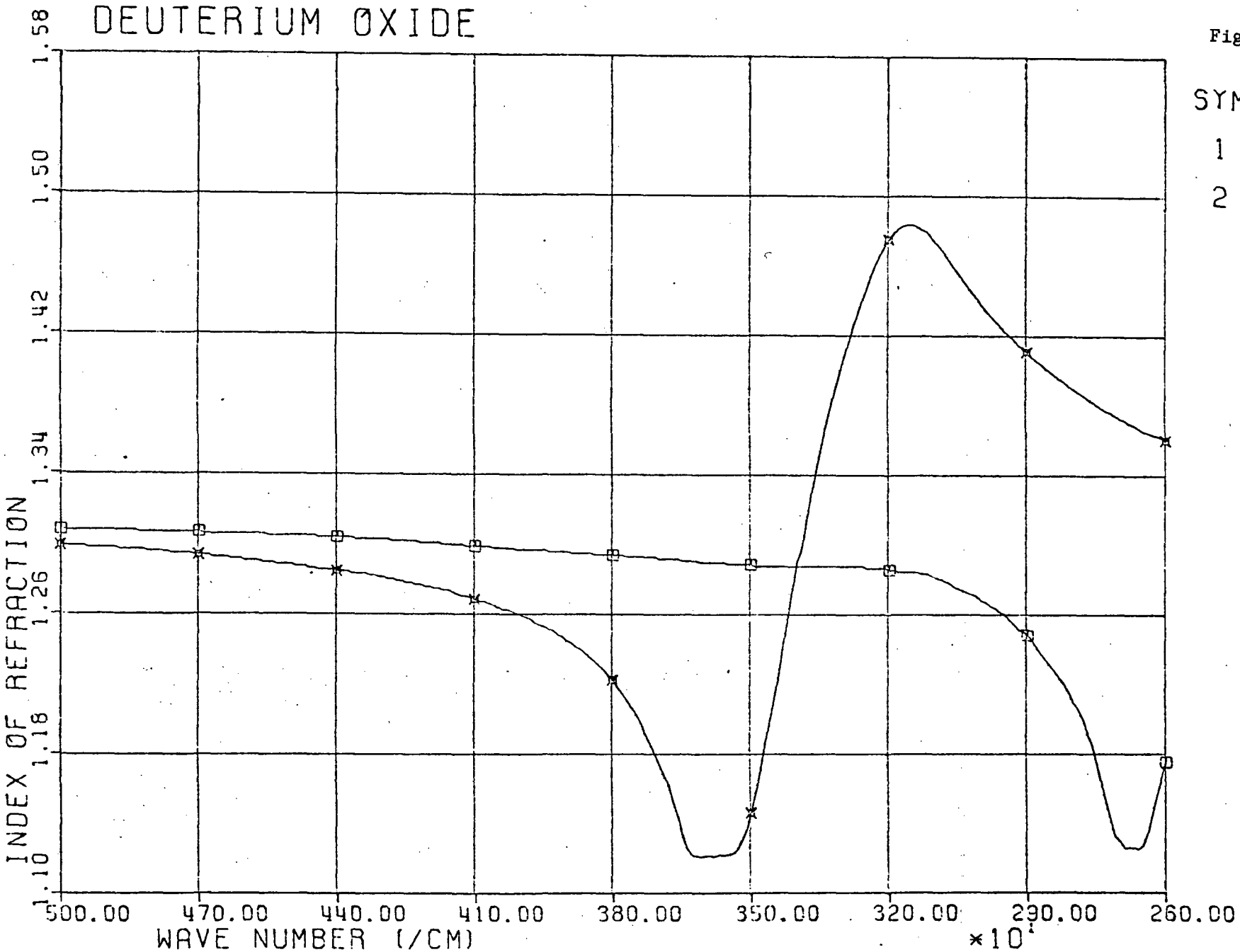
DEUTERIUM OXIDE
INDEX OF REFRACTION
1.58
1.50
1.42
1.34
1.26
1.18
1.10
500.00
470.00
440.00
410.00
380.00
350.00
320.00
290.00
260.00
WAVE NUMBER (/CM)
×10²
ID SYMBOLS
1 =
2 =

Figure 5

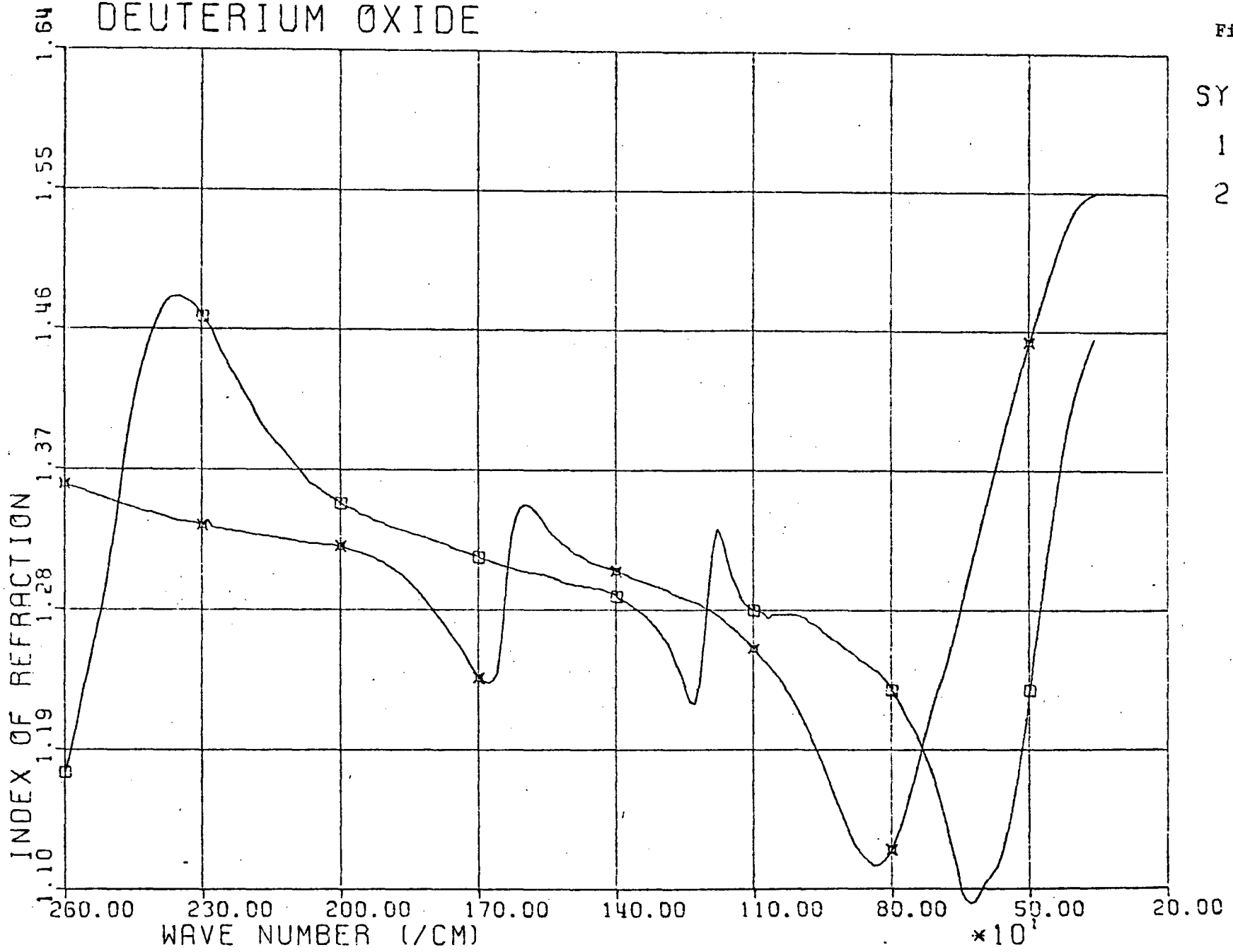
DEUTERIUM OXIDE
INDEX OF REFRACTION
1.64
1.55
1.46
1.37
1.28
1.19
1.10
260.00
230.00
200.00
170.00
140.00
110.00
80.00
50.00
20.00
WAVE NUMBER (/CM)
*10
ID
SYMBOLS
1 =
2 =

Figure 6

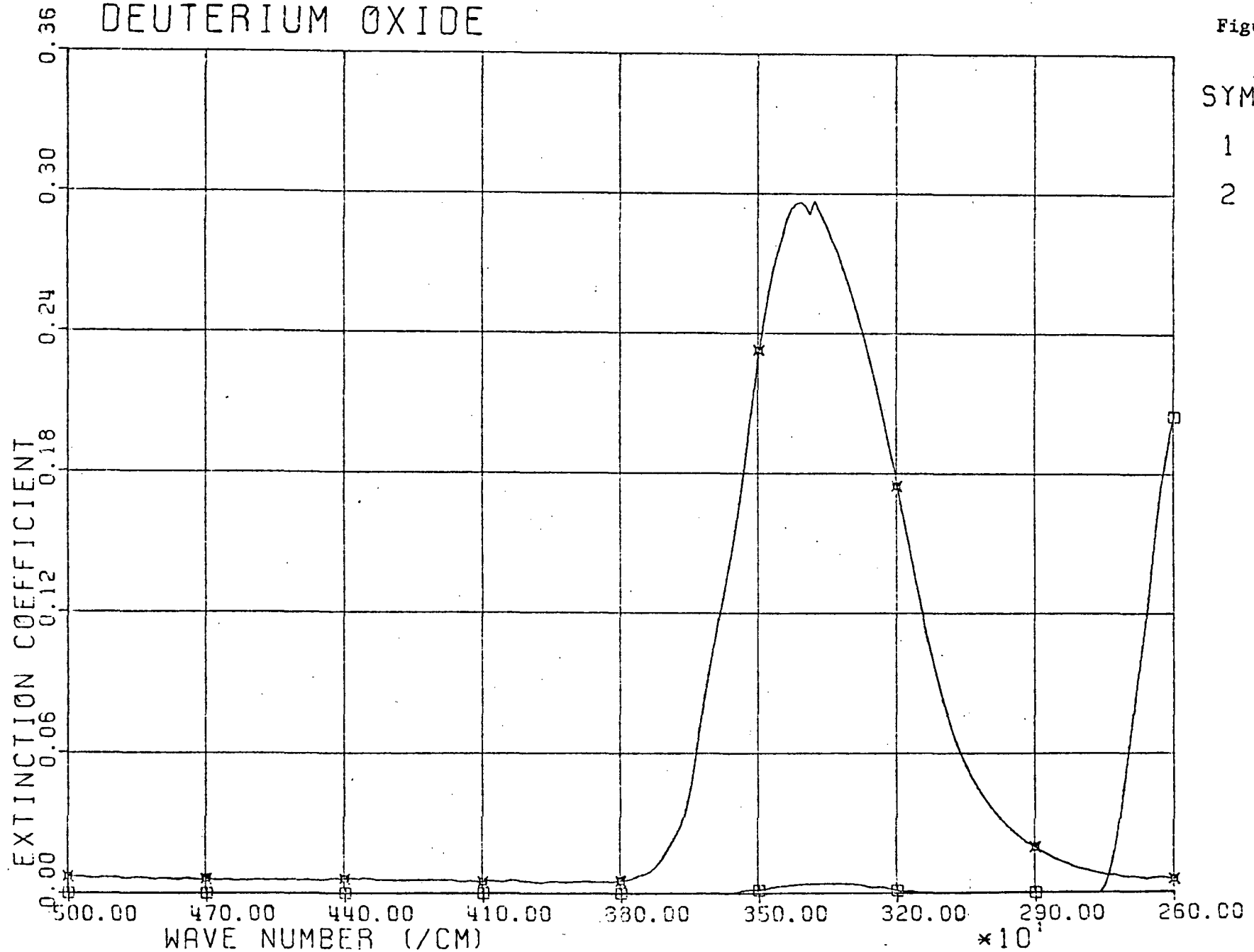
DEUTERIUM OXIDE
EXTINCTION COEFFICIENT
0.00
0.06
0.12
0.18
0.24
0.30
0.36
500.00
470.00
440.00
410.00
380.00
350.00
320.00
290.00
260.00
WAVE NUMBER (/CM)
*10
ID
SYMBOLS
1 =
2 =

Figure 7

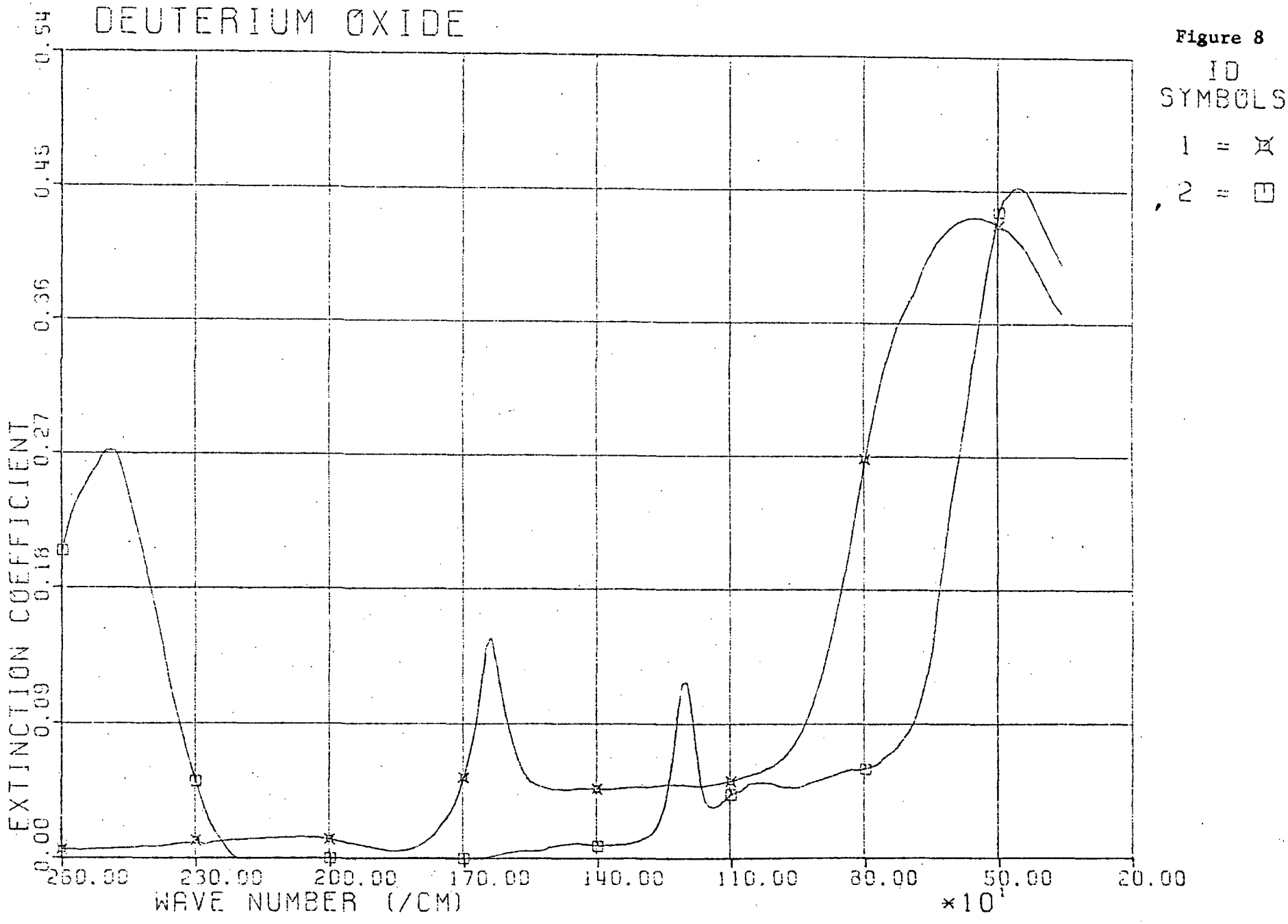
DEUTERIUM OXIDE
EXTINCTION COEFFICIENT
0.00
0.09
0.18
0.27
0.36
0.45
0.54
260.00
230.00
200.00
170.00
140.00
110.00
80.00
50.00
20.00
WAVE NUMBER (/CM)
*10
ID
SYMBOLS
1 =
2 =

Figure 8

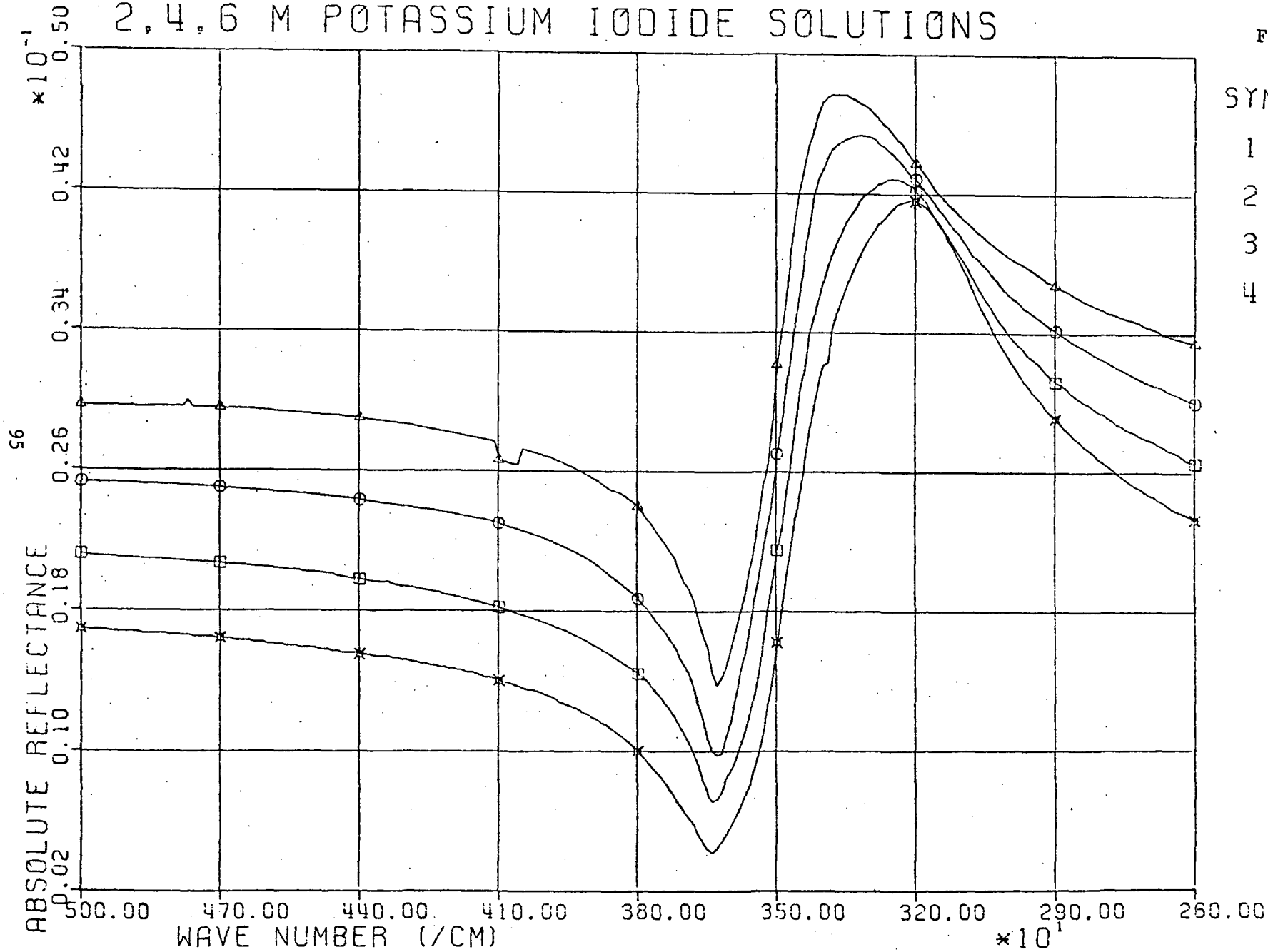
2,4,6 M POTASSIUM IODIDE SOLUTIONS
ABSOLUTE REFLECTANCE
*10⁻¹
0.50
0.42
0.34
0.26
0.18
0.10
0.02
500.00
470.00
440.00
410.00
380.00
350.00
320.00
290.00
260.00
WAVE NUMBER (/CM)
*10¹
ID SYMBOLS
1 =
2 =
3 =
4 =

Figure 9

Figure 10

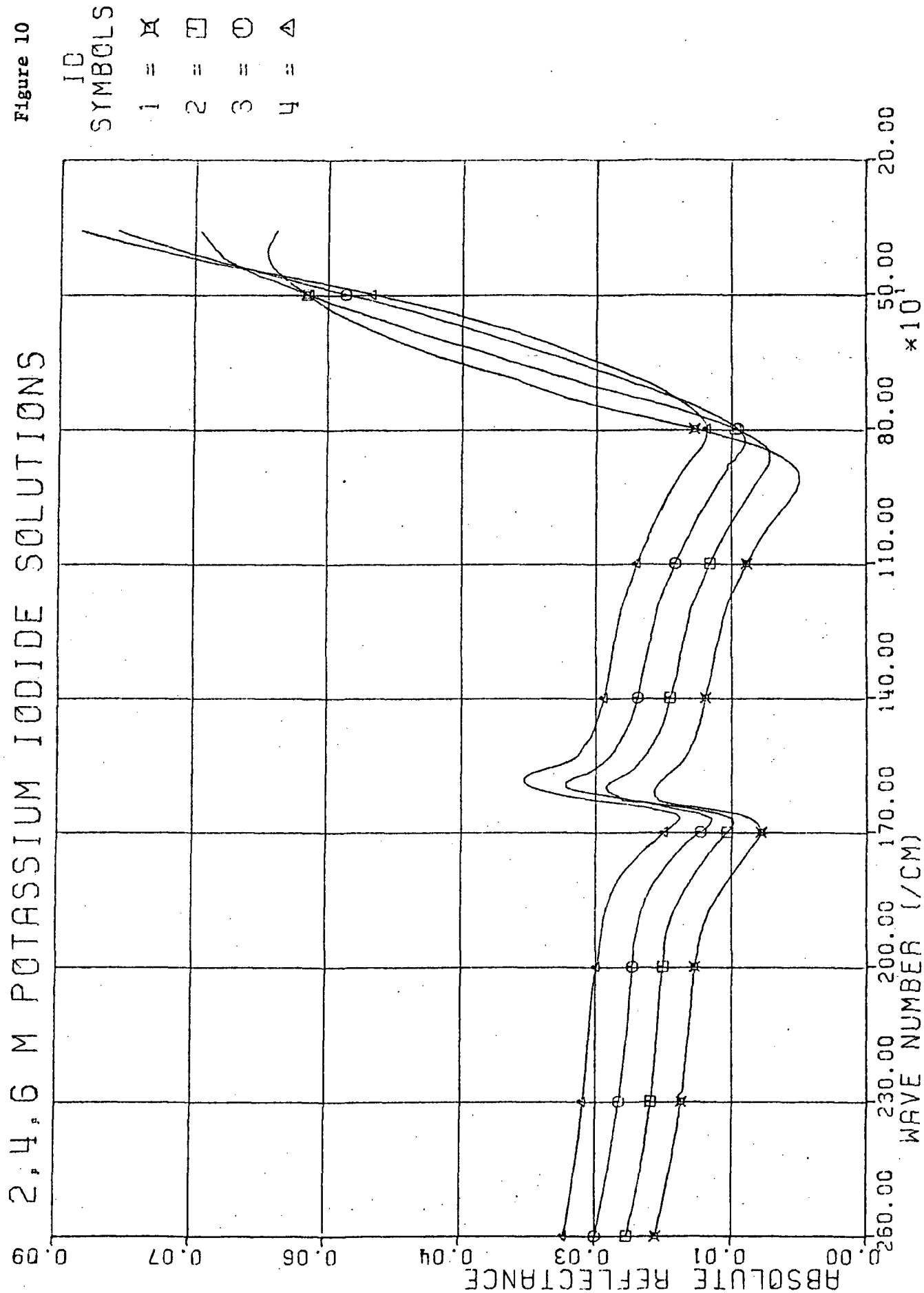
2,4,6 M POTASSIUM IODIDE SOLUTIONS
ID
SYMBOLS
1 =
2 =
3 =
4 =
ABSOLUTE REFLECTANCE
0.00
0.01
0.03
0.04
0.06
0.07
0.09
WAVE NUMBER (/CM)
260.00
230.00
200.00
170.00
140.00
110.00
80.00
50.00
20.00
*10¹

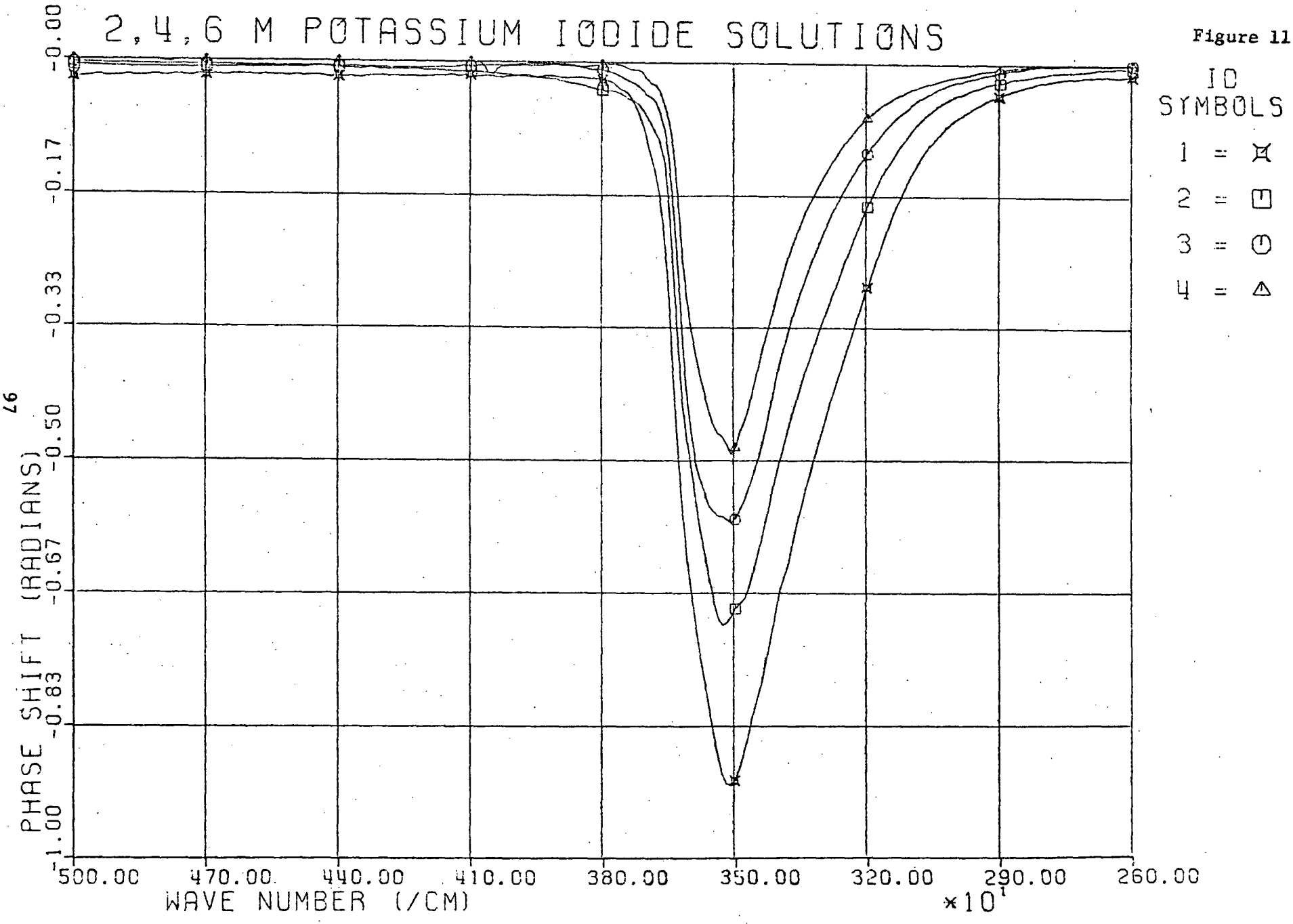
2,4,6 M POTASSIUM IODIDE SOLUTIONS
-0.00
-0.17
-0.33
-0.50
-0.67
-0.83
-1.00
PHASE SHIFT (RADIANS)
500.00
470.00
440.00
410.00
380.00
350.00
320.00
290.00
260.00
WAVE NUMBER (/CM)
×10¹
ID SYMBOLS
1 =
2 =
3 =
4 =

Figure 11

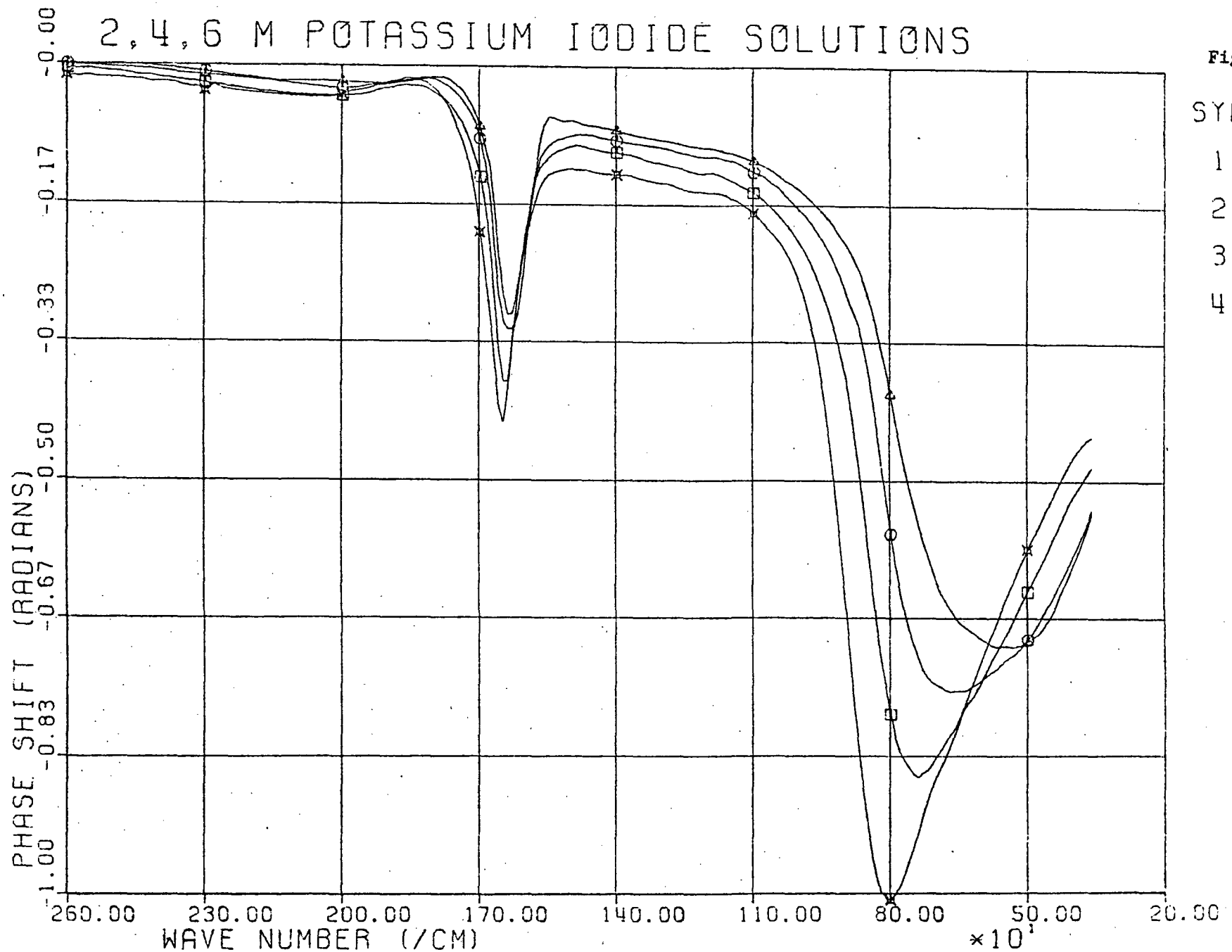
2,4,6 M POTASSIUM IODIDE SOLUTIONS
PHASE SHIFT (RADIANS)
-0.00
-0.17
-0.33
-0.50
-0.67
-0.83
-1.00
260.00
230.00
200.00
170.00
140.00
110.00
80.00
50.00
20.00
WAVE NUMBER (/CM)
×10¹
IO SYMBOLS
1 = ⊠
2 = ⊟
3 = ⊖
4 = △

Figure 12

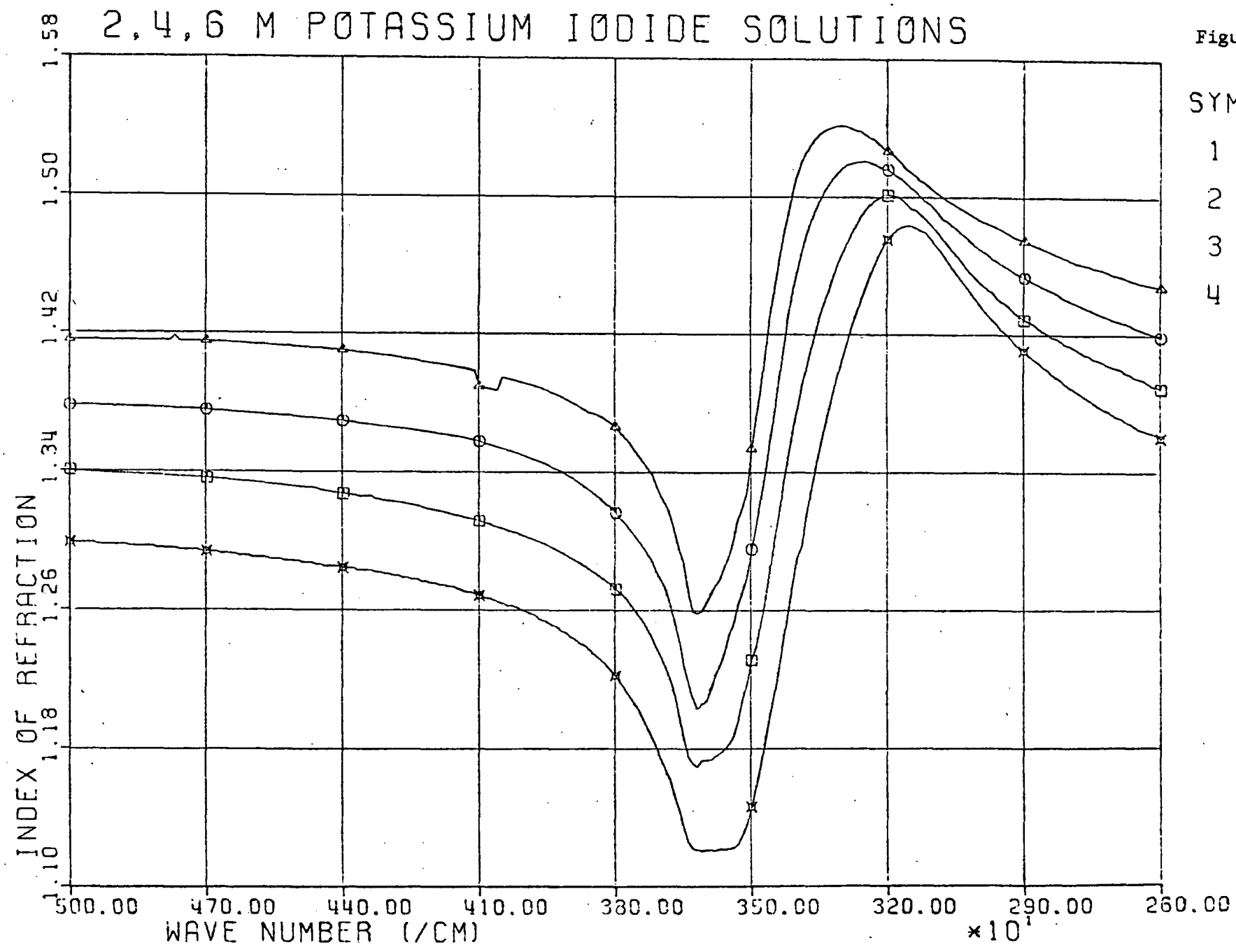
2,4,6 M POTASSIUM IODIDE SOLUTIONS
INDEX OF REFRACTION
1.58
1.50
1.42
1.34
1.26
1.18
1.10
500.00
470.00
440.00
410.00
380.00
350.00
320.00
290.00
260.00
WAVE NUMBER (/CM)
×10¹
ID SYMBOLS
1 =
2 =
3 =
4 =

Figure 13

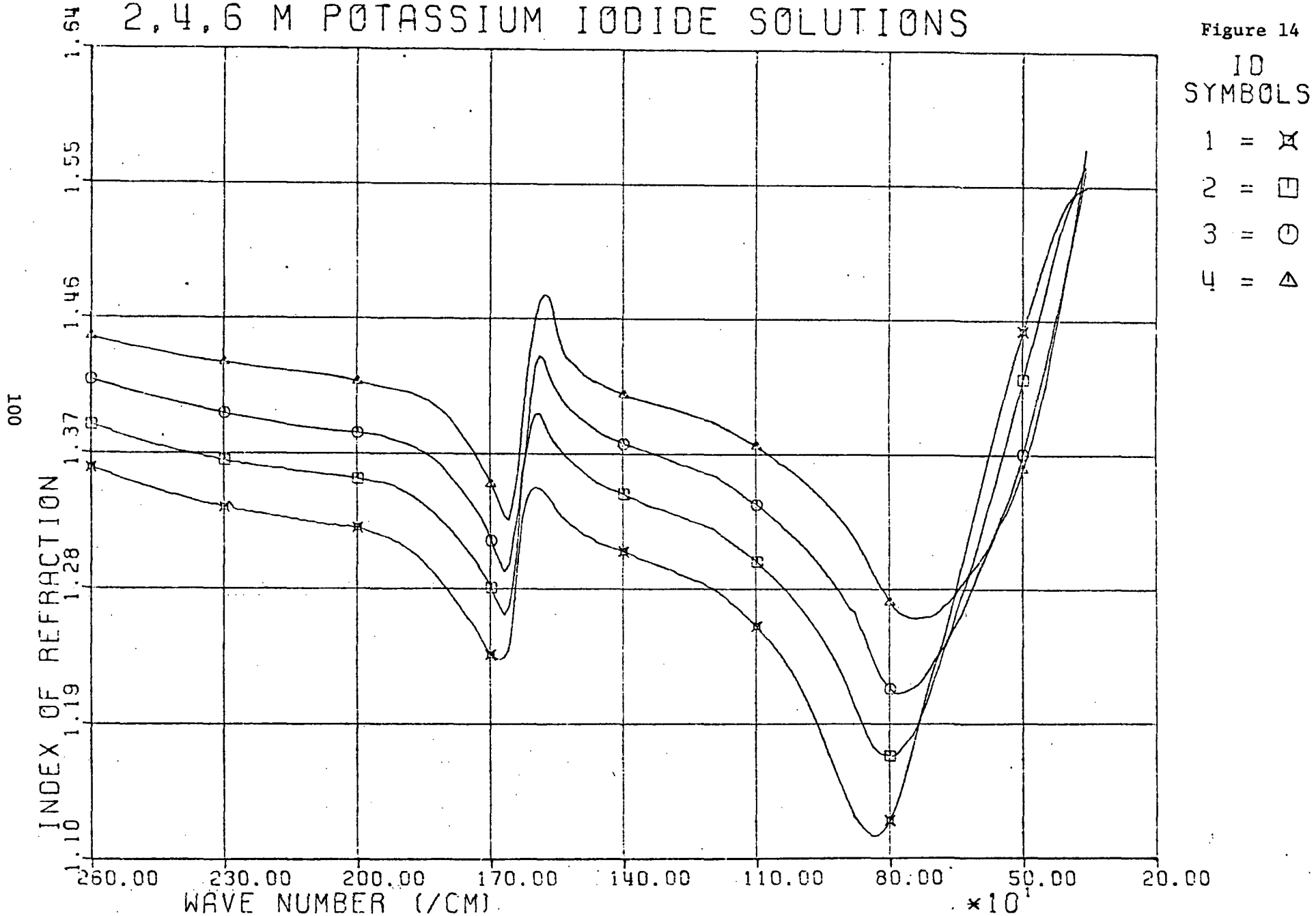
2,4,6 M POTASSIUM IODIDE SOLUTIONS
INDEX OF REFRACTION
1.64
1.55
1.46
1.37
1.28
1.19
1.10
260.00
230.00
200.00
170.00
140.00
110.00
80.00
50.00
20.00
WAVE NUMBER (/CM)
*10
ID SYMBOLS
1 =
2 =
3 =
4 =

Figure 14

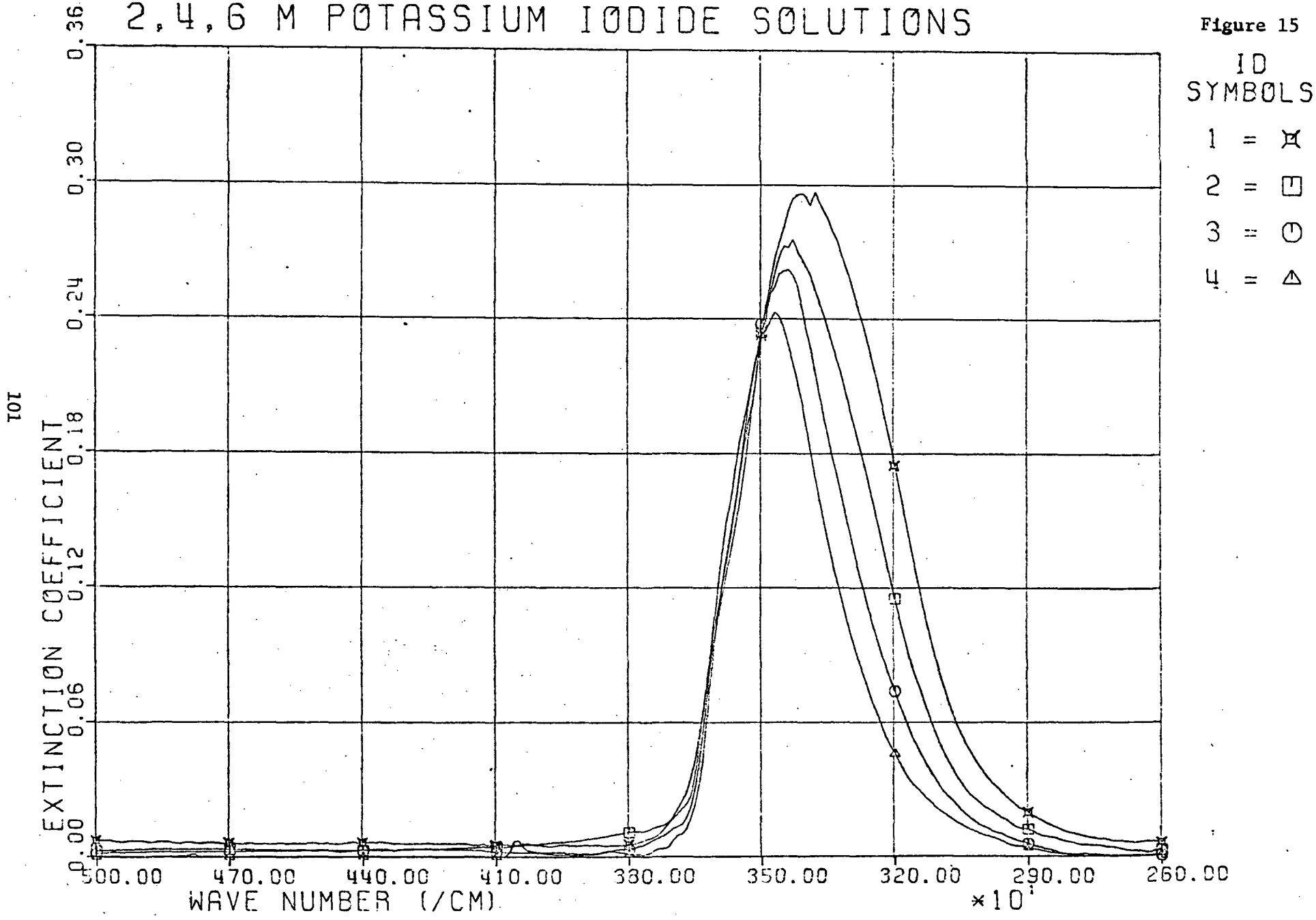
2,4,6 M POTASSIUM IODIDE SOLUTIONS
ID SYMBOLS
1 =
2 =
3 =
4 =
EXTINCTION COEFFICIENT
0.00
0.06
0.12
0.18
0.24
0.30
0.36
500.00
470.00
440.00
410.00
380.00
350.00
320.00
290.00
260.00
WAVE NUMBER (/CM)
×10

Figure 15

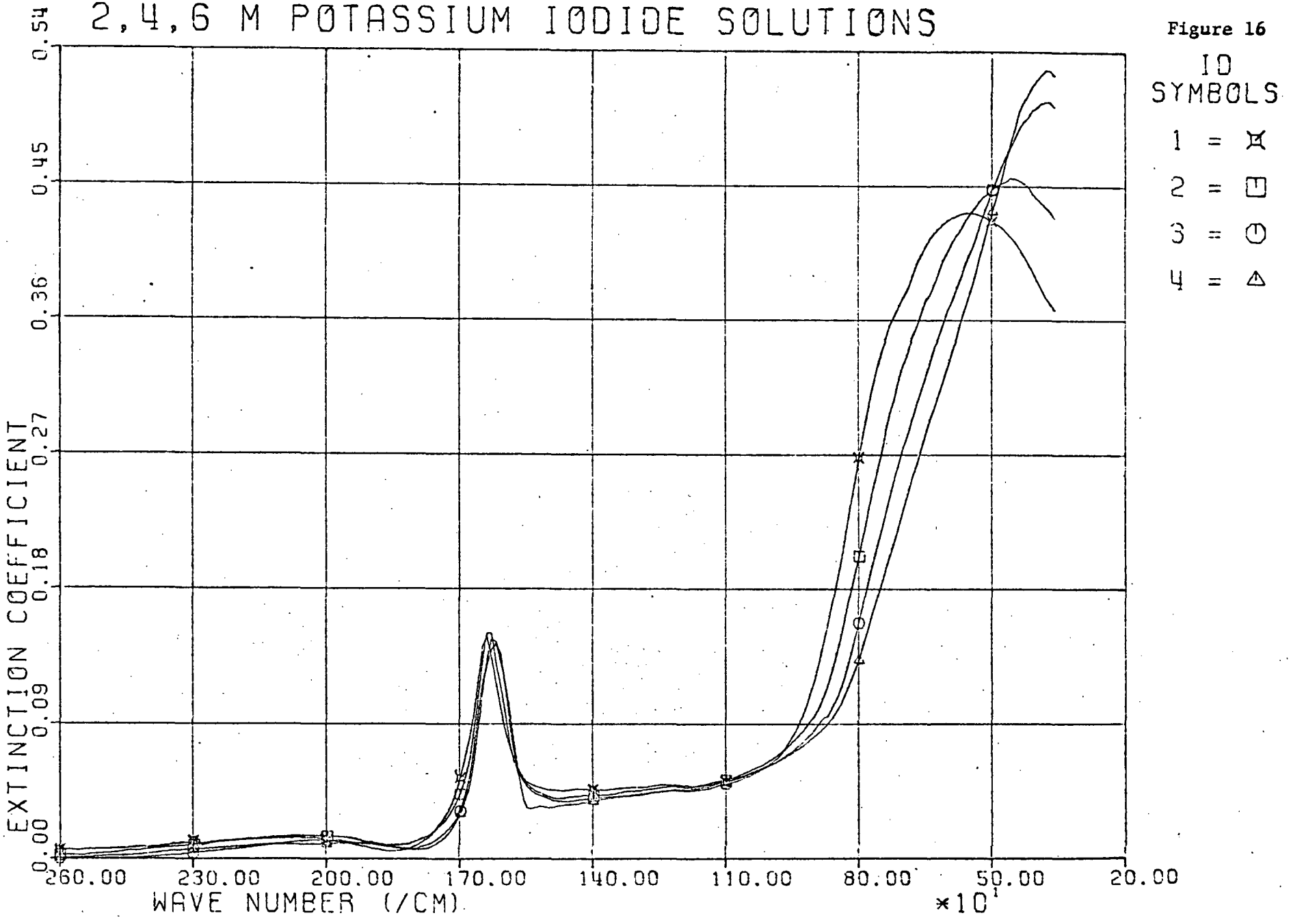
2,4,6 M POTASSIUM IODIDE SOLUTIONS
IO SYMBOLS
1 =
2 =
3 =
4 =
EXTINCTION COEFFICIENT
0.00
0.09
0.18
0.27
0.36
0.45
0.54
260.00
230.00
200.00
170.00
140.00
110.00
80.00
50.00
20.00
WAVE NUMBER (/CM)
*10¹

Figure 16

Figure 17

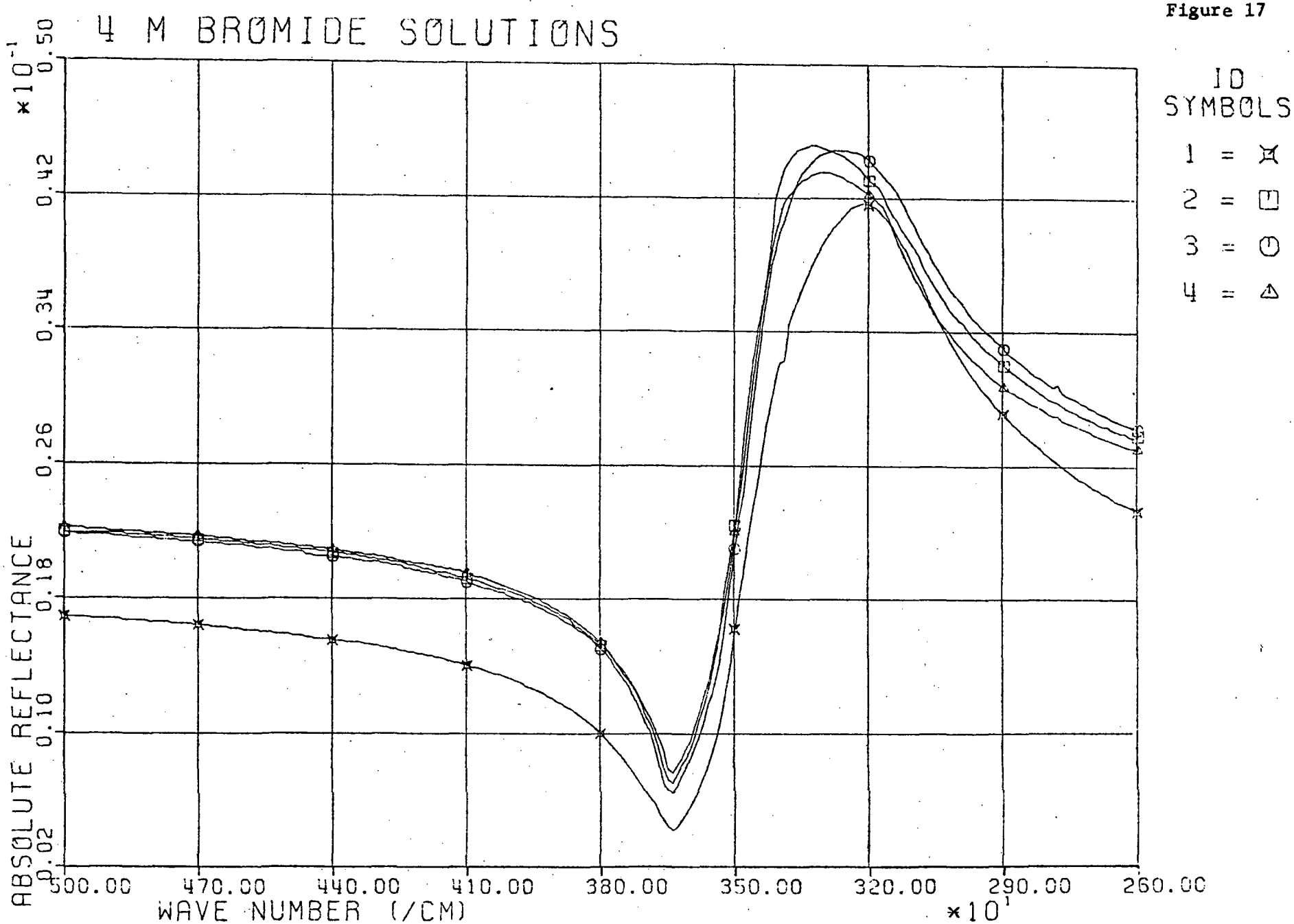
4 M BROMIDE SOLUTIONS
ID SYMBOLS
1 =
2 =
3 =
4 =
ABSOLUTE REFLECTANCE
×10⁻¹
0.50
0.42
0.34
0.26
0.18
0.10
0.02
500.00
470.00
440.00
410.00
380.00
350.00
320.00
290.00
260.00
WAVE NUMBER (/CM)
×10¹

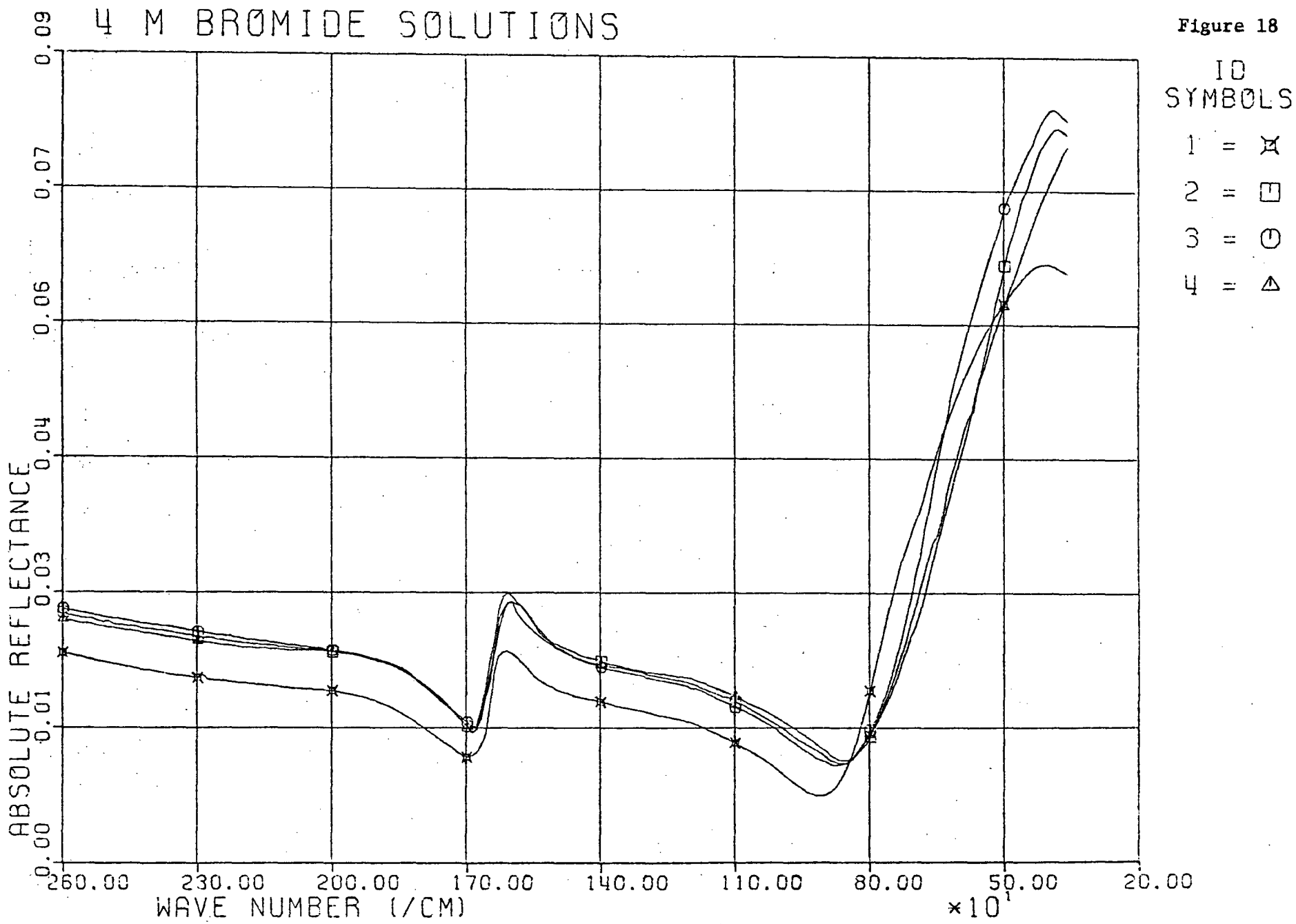
4 M BROMIDE SOLUTIONS
ID SYMBOLS
1 =
2 =
3 =
4 =
ABSOLUTE REFLECTANCE
0.00
0.01
0.03
0.04
0.06
0.07
0.09
260.00
230.00
200.00
170.00
140.00
110.00
80.00
50.00
20.00
WAVE NUMBER (/CM)
×10¹

Figure 18

Figure 19

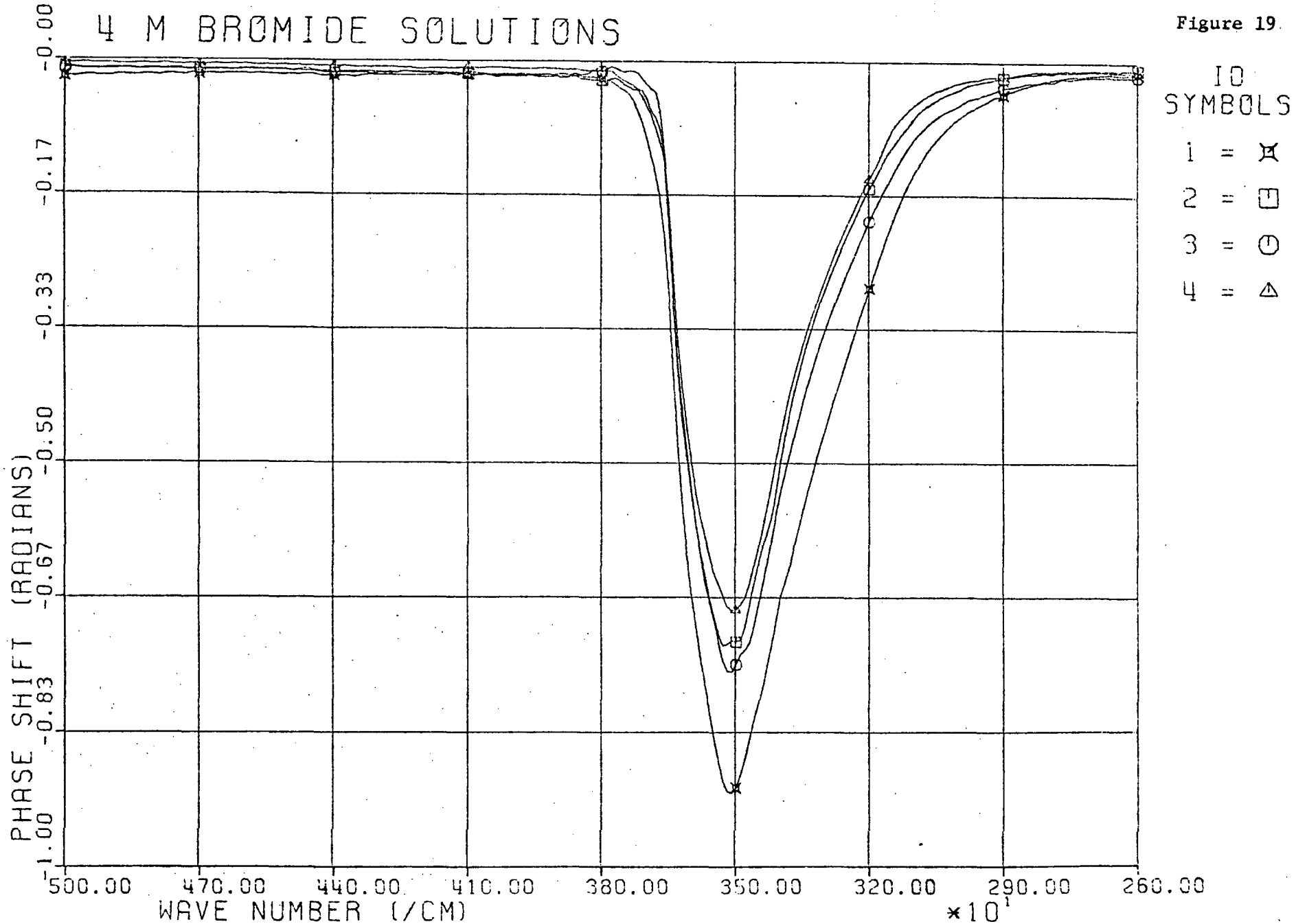
4 M BROMIDE SOLUTIONS
PHASE SHIFT (RADIANS)
-0.00
-0.17
-0.33
-0.50
-0.67
-0.83
-1.00
500.00
470.00
440.00
410.00
380.00
350.00
320.00
290.00
260.00
WAVE NUMBER (/CM)
*10^1
ID SYMBOLS
1 =
2 =
3 =
4 =

Figure 20

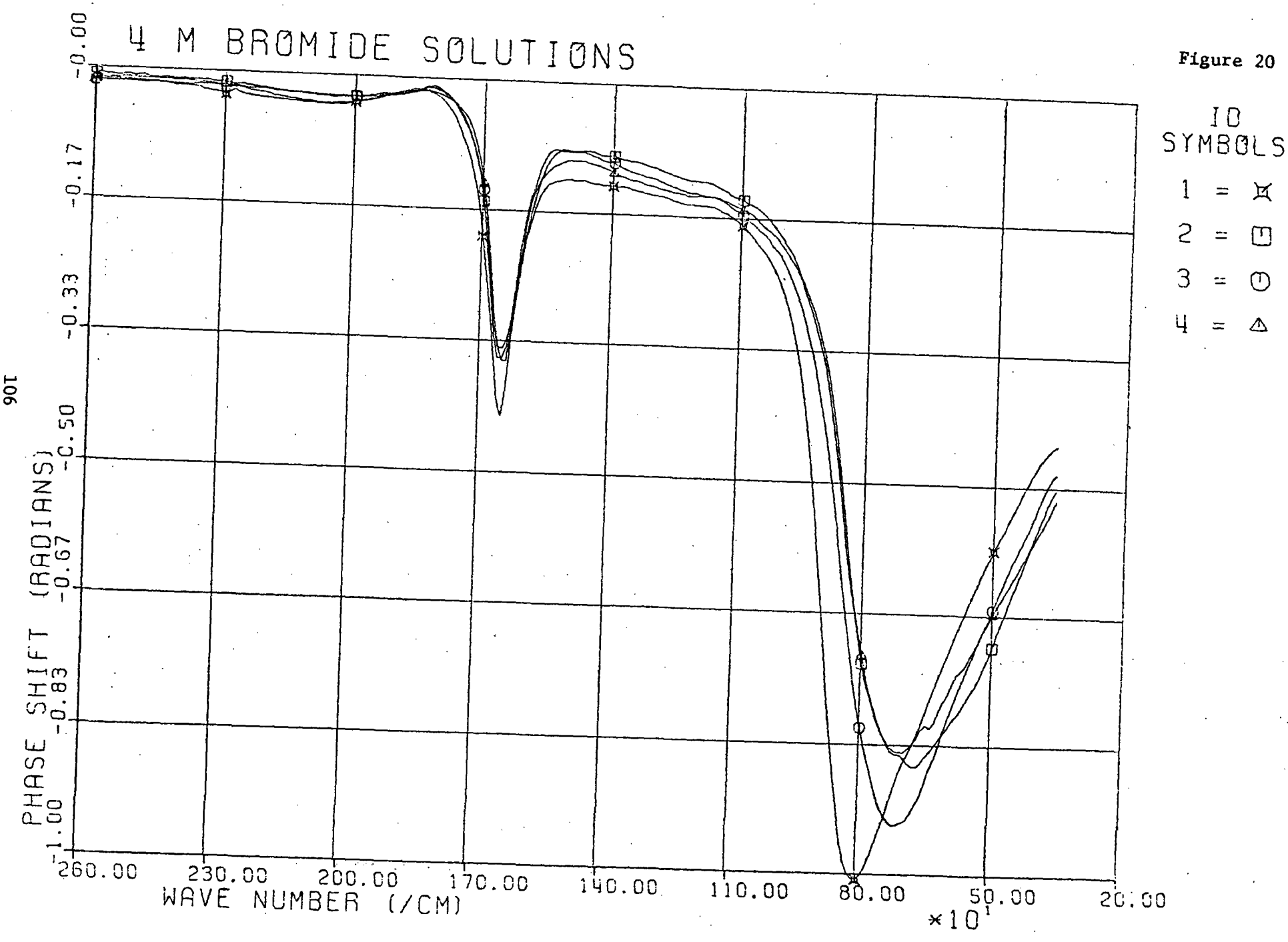
4 M BROMIDE SOLUTIONS
ID SYMBOLS
1 =
2 =
3 =
4 =
PHASE SHIFT (RADIANS)
-0.00
-0.17
-0.33
-0.50
-0.67
-0.83
-1.00
260.00
230.00
200.00
170.00
140.00
110.00
80.00
50.00
20.00
WAVE NUMBER (/CM)
*10¹

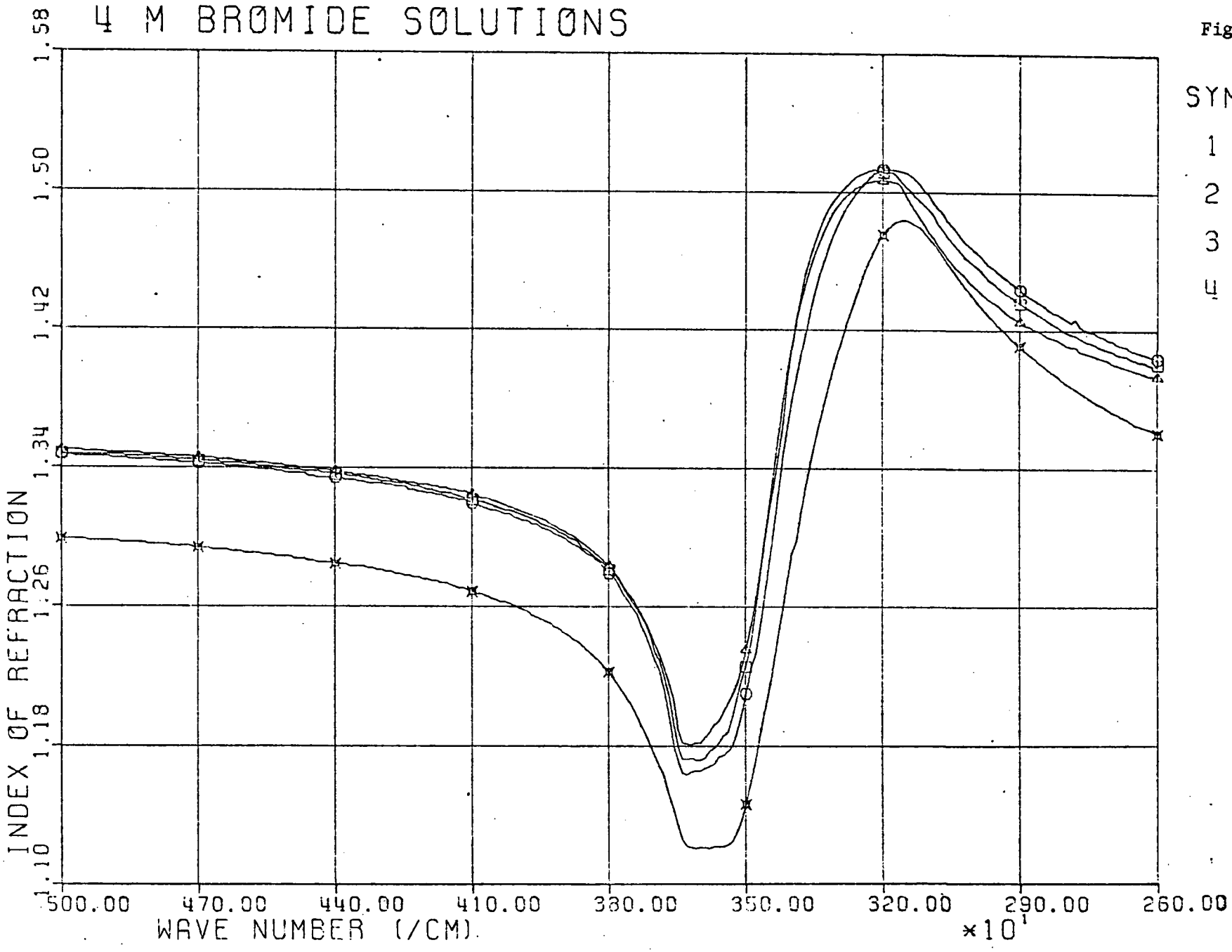
4 M BROMIDE SOLUTIONS
INDEX OF REFRACTION
1.58
1.50
1.42
1.34
1.26
1.18
1.10
500.00
470.00
440.00
410.00
380.00
350.00
320.00
290.00
260.00
WAVE NUMBER (/CM)
*10¹
ID SYMBOLS
1 =
2 =
3 =
4 =

Figure 21

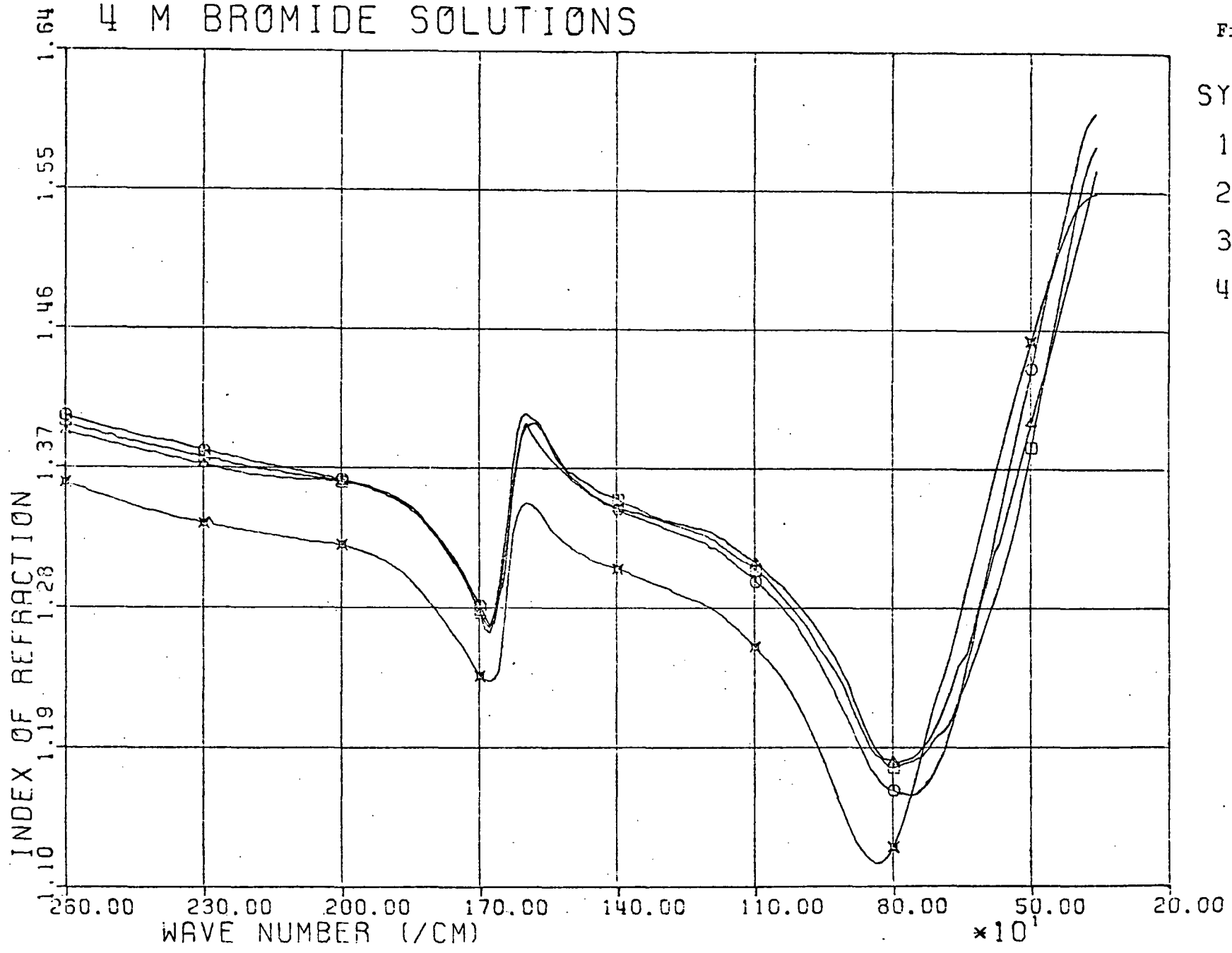
4 M BROMIDE SOLUTIONS
INDEX OF REFRACTION
1.64
1.55
1.46
1.37
1.28
1.19
1.10
260.00
230.00
200.00
170.00
140.00
110.00
80.00
50.00
20.00
WAVE NUMBER (/CM)
*10^1
ID SYMBOLS
1 =
2 =
3 =
4 =

Figure 22

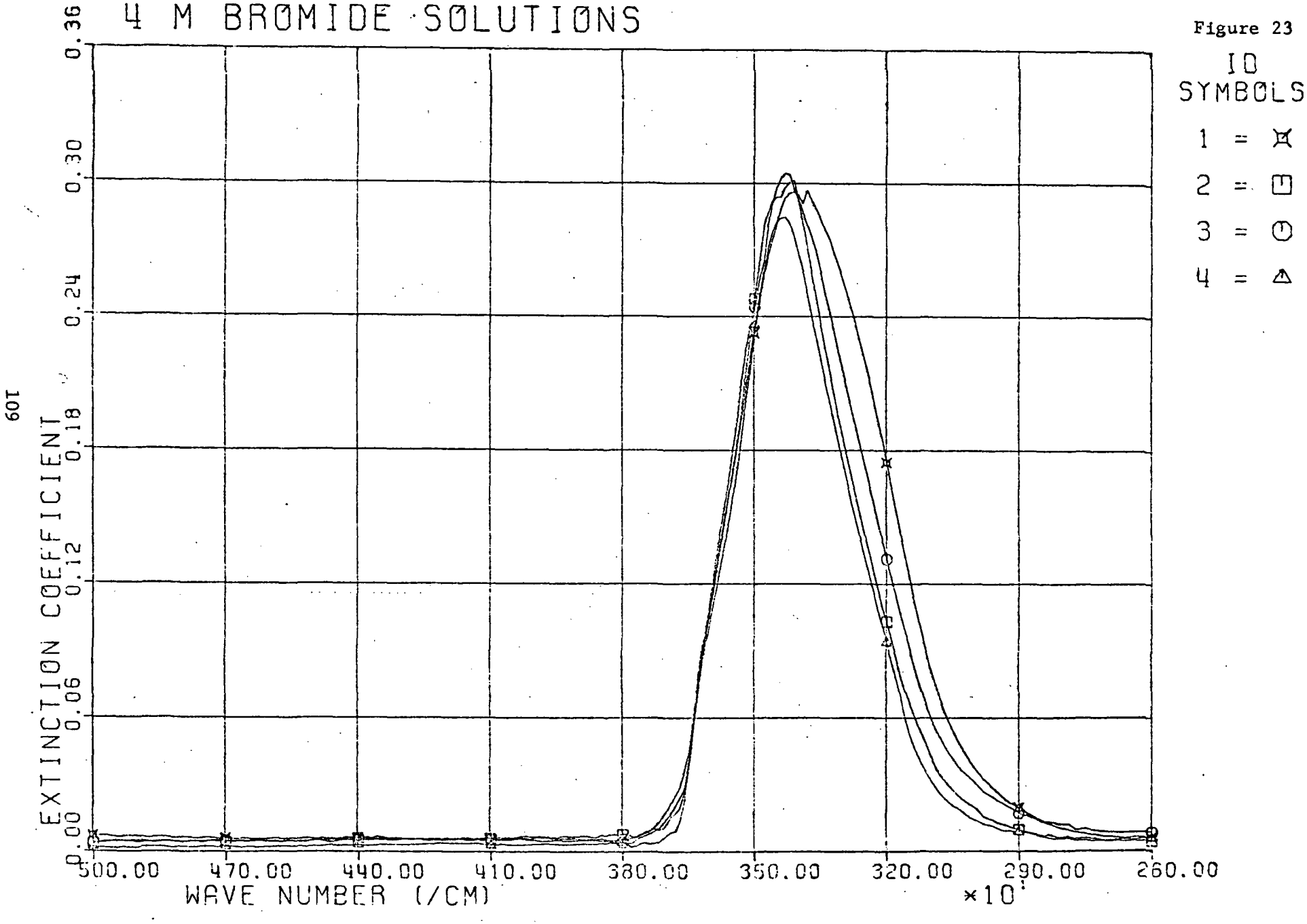
4 M BROMIDE SOLUTIONS
EXTINCTION COEFFICIENT
0.00
0.06
0.12
0.18
0.24
0.30
0.36
500.00
470.00
440.00
410.00
380.00
350.00
320.00
290.00
260.00
WAVE NUMBER (/CM)
×10
ID SYMBOLS
1 =
2 =
3 =
4 =

Figure 23

Figure 24

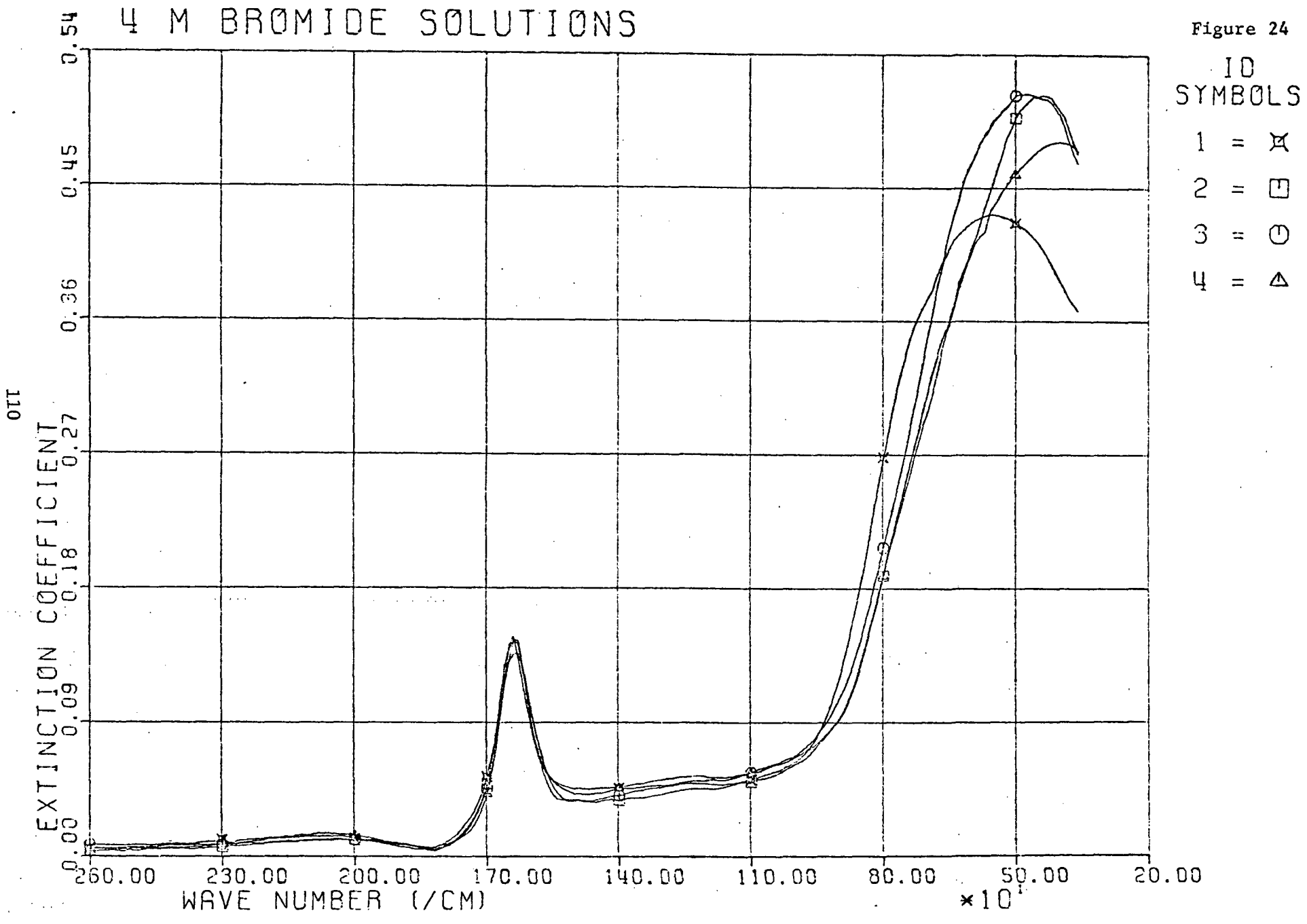
4 M BROMIDE SOLUTIONS
EXTINCTION COEFFICIENT
0.00
0.09
0.18
0.27
0.36
0.45
0.54
260.00
230.00
200.00
170.00
140.00
110.00
80.00
50.00
20.00
WAVE NUMBER (/CM)
×10
ID SYMBOLS
1 =
2 =
3 =
4 =

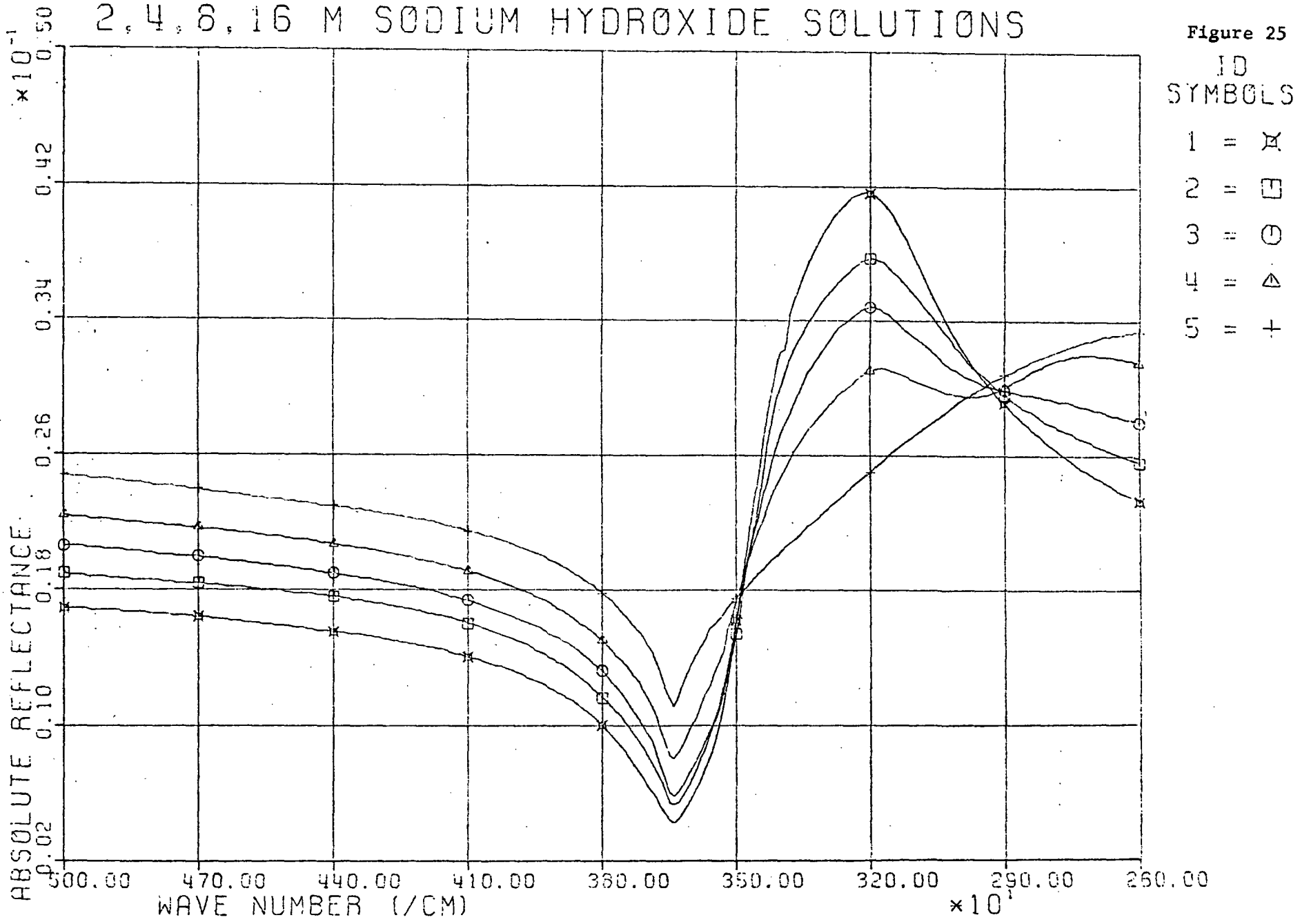
2,4,8,16 M SODIUM HYDROXIDE SOLUTIONS
ID SYMBOLS
1 =
2 =
3 =
4 =
5 =
ABSOLUTE REFLECTANCE
×10⁻¹
0.50
0.42
0.34
0.26
0.18
0.10
0.02
500.00
470.00
440.00
410.00
380.00
350.00
320.00
290.00
260.00
WAVE NUMBER (/CM)
×10¹

Figure 25

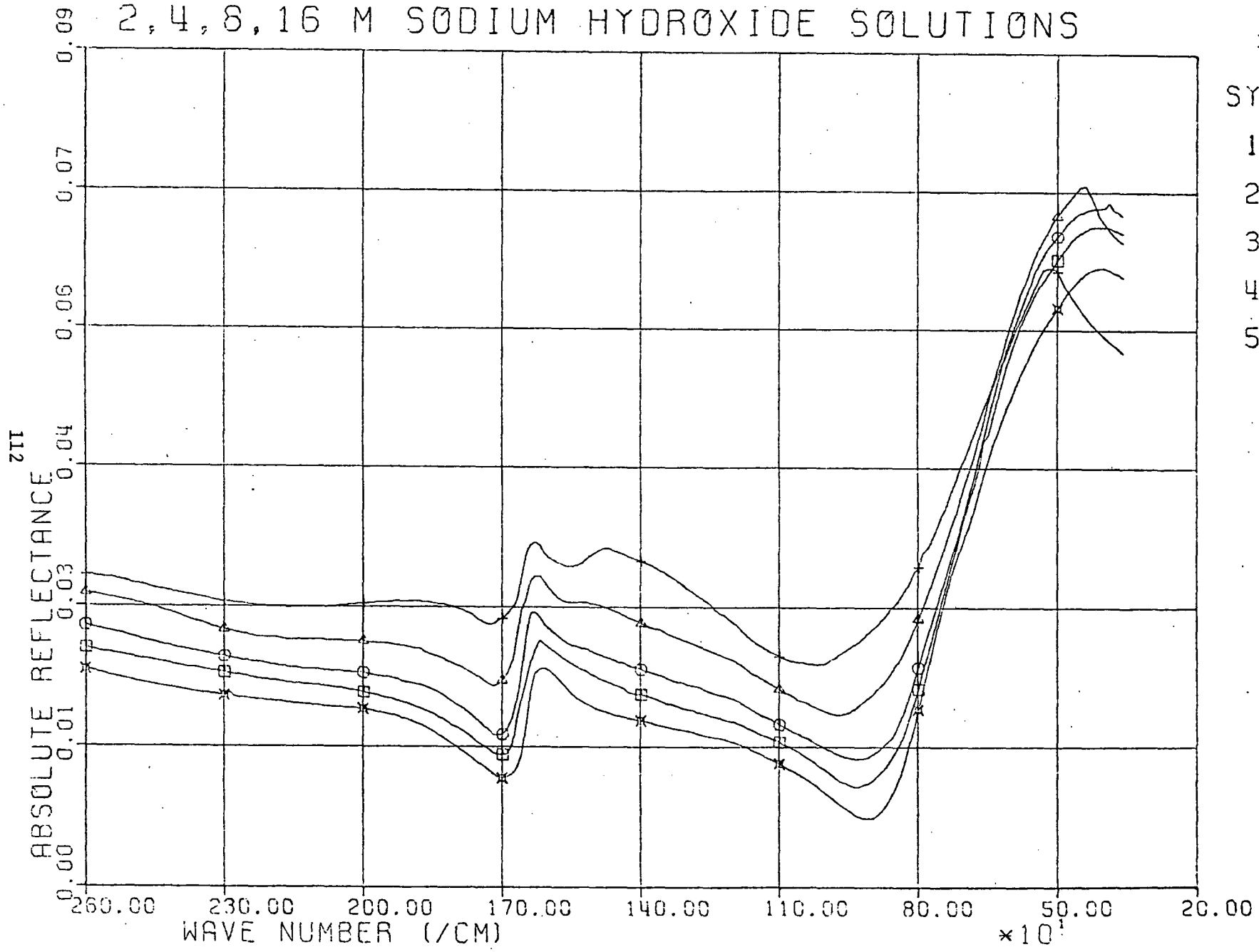
2,4,8,16 M SODIUM HYDROXIDE SOLUTIONS
ABSOLUTE REFLECTANCE
0.00
0.01
0.03
0.04
0.06
0.07
0.09
260.00
230.00
200.00
170.00
140.00
110.00
80.00
50.00
20.00
WAVE NUMBER (/CM)
*10
IO SYMBOLS
1 =
2 =
3 =
4 =
5 =

Figure 26

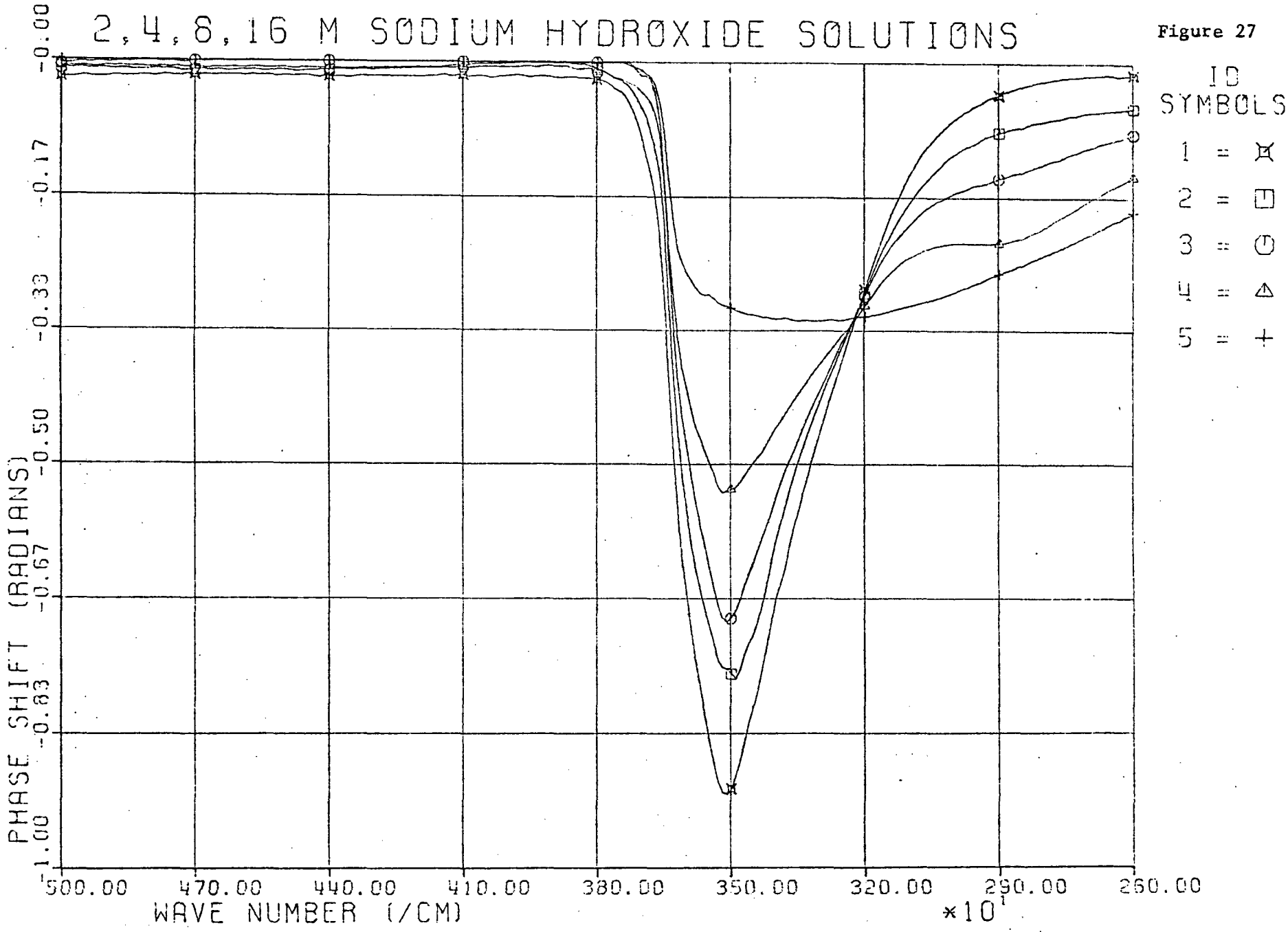
2,4,8,16 M SODIUM HYDROXIDE SOLUTIONS
ID SYMBOLS
1 =
2 =
3 =
4 =
5 =
PHASE SHIFT (RADIANS)
-0.00
-0.17
-0.33
-0.50
-0.67
-0.83
-1.00
500.00
470.00
440.00
410.00
380.00
350.00
320.00
290.00
260.00
WAVE NUMBER (/CM)
*10^1

Figure 27

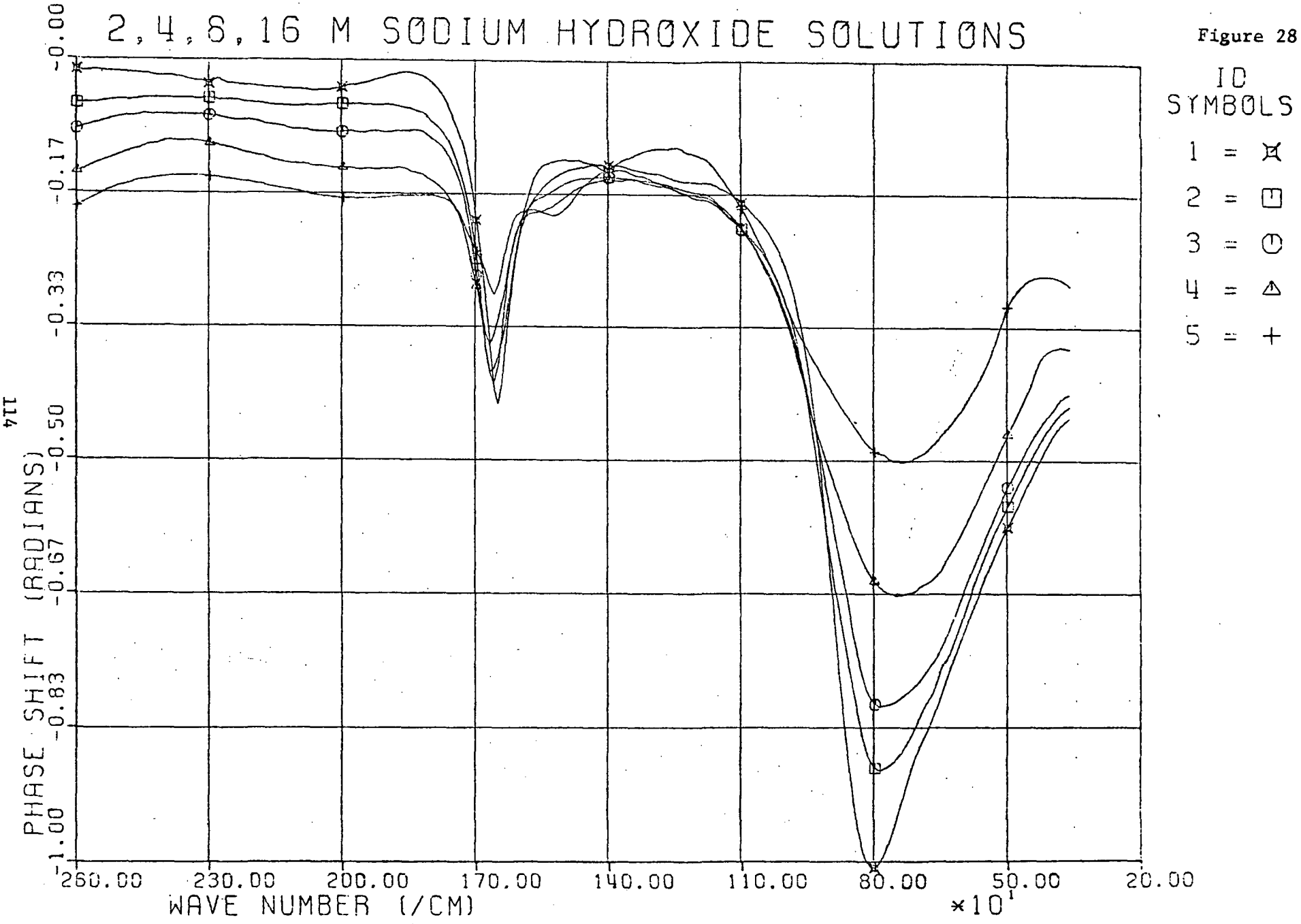
2,4,8,16 M SODIUM HYDROXIDE SOLUTIONS
ID SYMBOLS
1 =
2 =
3 =
4 =
5 =
PHASE SHIFT (RADIANS)
-0.00
-0.17
-0.33
-0.50
-0.67
-0.83
-1.00
260.00
230.00
200.00
170.00
140.00
110.00
80.00
50.00
20.00
WAVE NUMBER (/CM)
*10¹

Figure 28

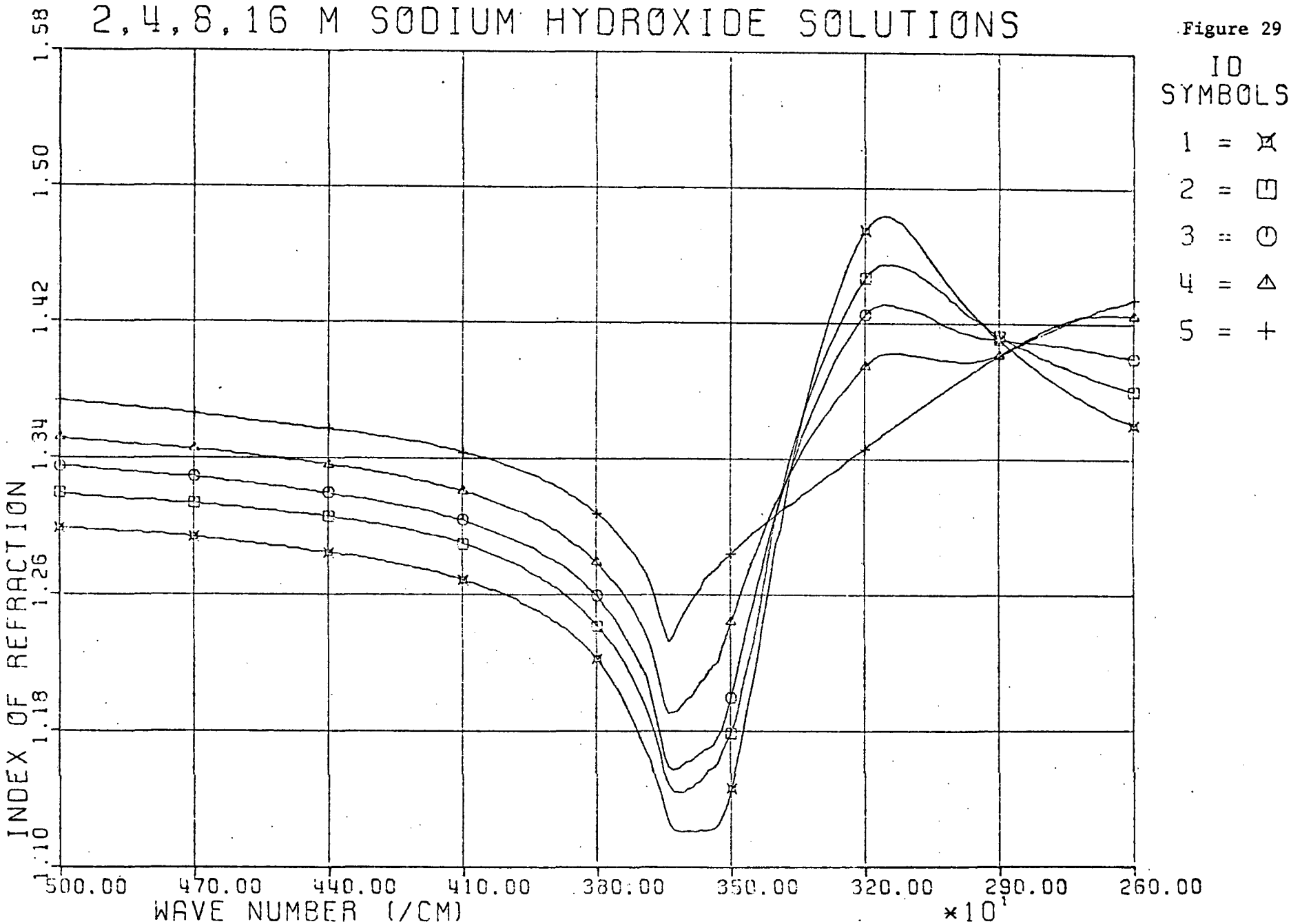
2,4,8,16 M SODIUM HYDROXIDE SOLUTIONS
ID SYMBOLS
1 =
2 =
3 =
4 =
5 =
INDEX OF REFRACTION
1.58
1.50
1.42
1.34
1.26
1.18
1.10
500.00
470.00
440.00
410.00
380.00
350.00
320.00
290.00
260.00
WAVE NUMBER (/CM)
×10¹

Figure 29

Figure 30

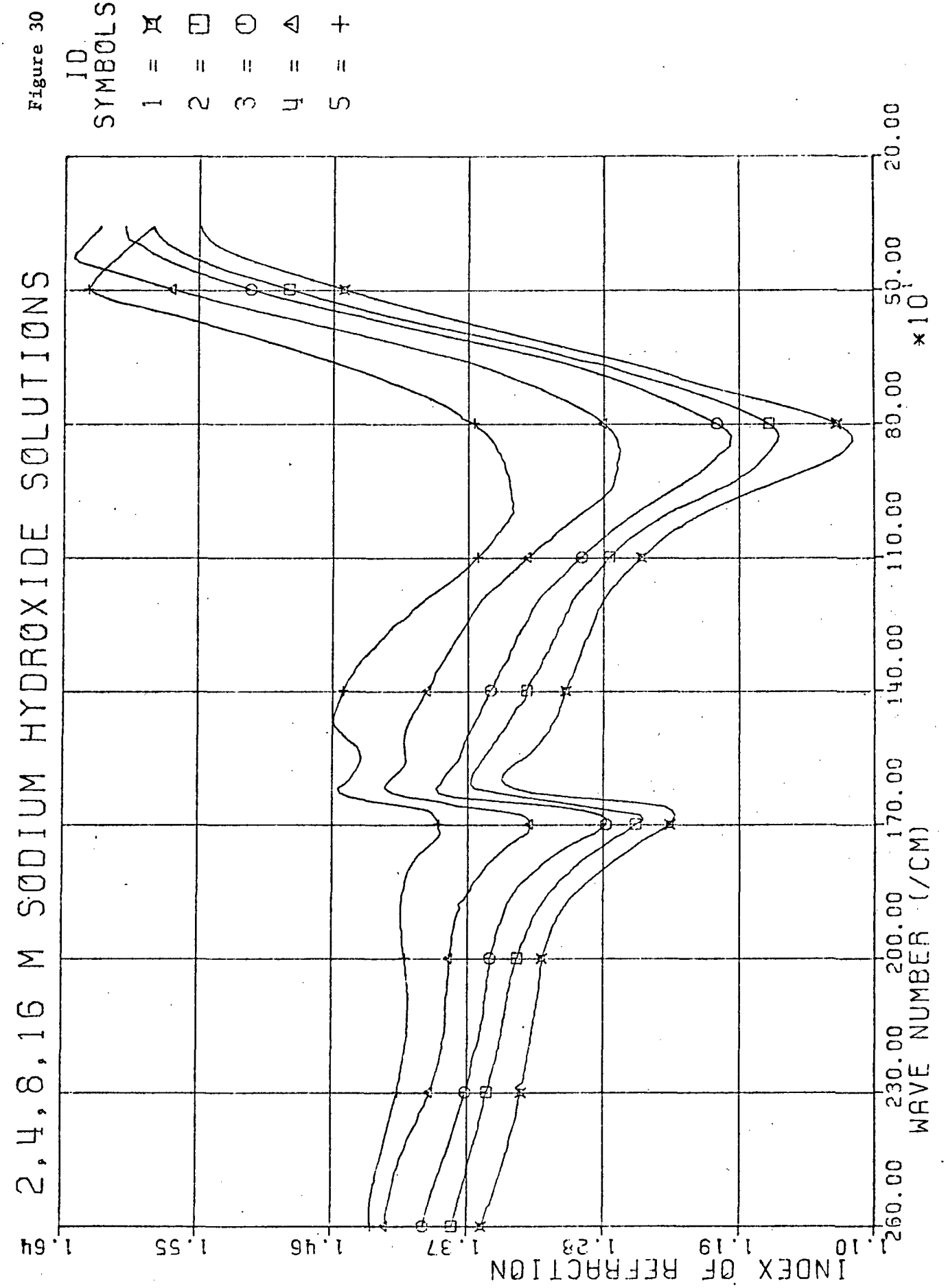
ID
SYMBOLS
1 =
2 =
3 =
4 =
5 =
2,4,8,16 M SODIUM HYDROXIDE SOLUTIONS
INDEX OF REFRACTION
1.10
1.19
1.28
1.37
1.46
1.55
1.64
WAVE NUMBER (/CM)
260.00
230.00
200.00
170.00
140.00
110.00
80.00
50.00
20.00
*10¹

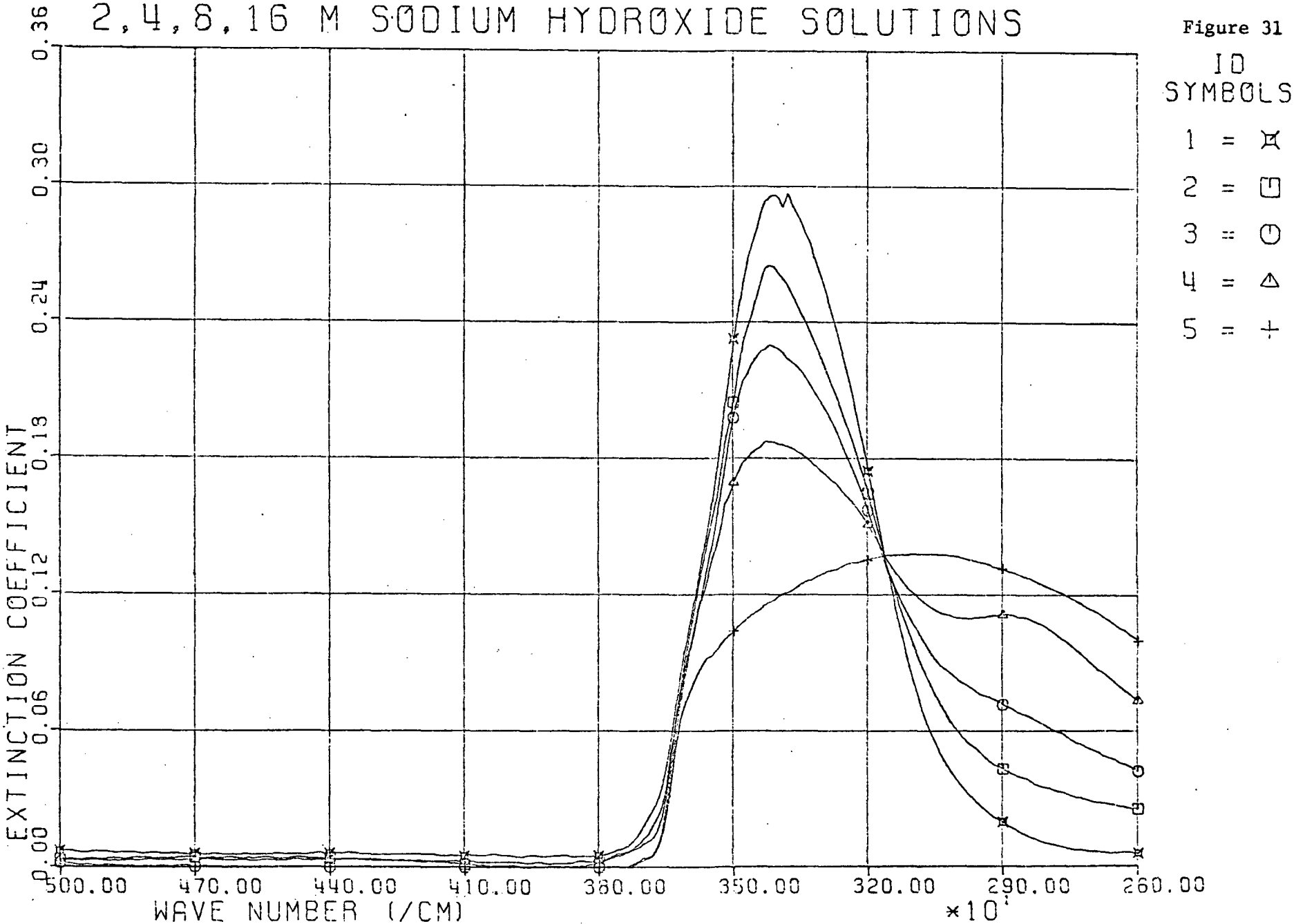
2,4,8,16 M SODIUM HYDROXIDE SOLUTIONS
ID SYMBOLS
1 =
2 =
3 =
4 =
5 =
EXTINCTION COEFFICIENT
0.00
0.06
0.12
0.18
0.24
0.30
0.36
500.00
470.00
440.00
410.00
380.00
350.00
320.00
290.00
260.00
WAVE NUMBER (/CM)
×10³

Figure 31

Figure 32

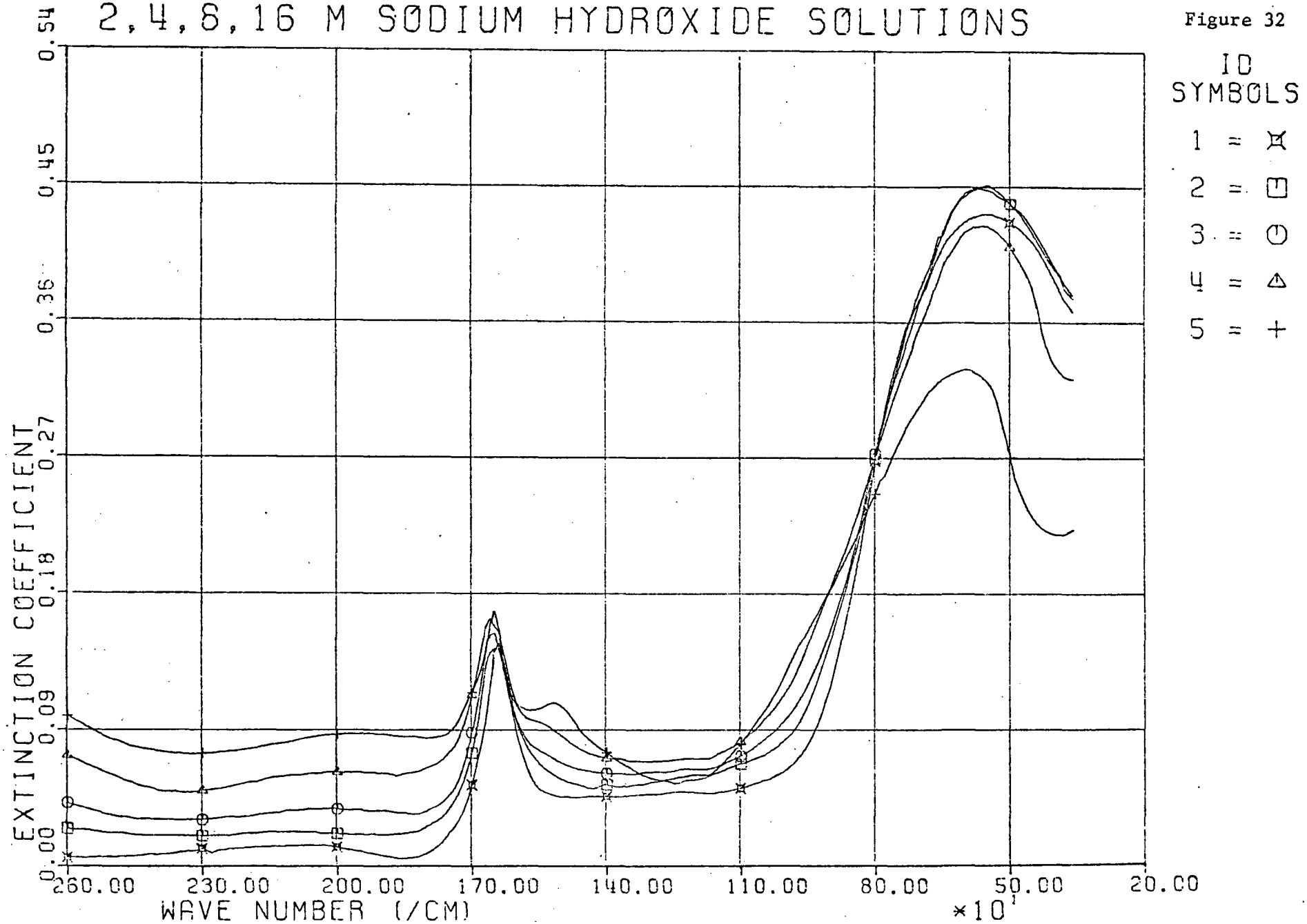
2,4,8,16 M SODIUM HYDROXIDE SOLUTIONS
ID SYMBOLS
1 =
2 =
3 =
4 =
5 =
EXTINCTION COEFFICIENT
0.00
0.09
0.18
0.27
0.36
0.45
0.54
260.00
230.00
200.00
170.00
140.00
110.00
80.00
50.00
20.00
WAVE NUMBER (/CM)
*10¹

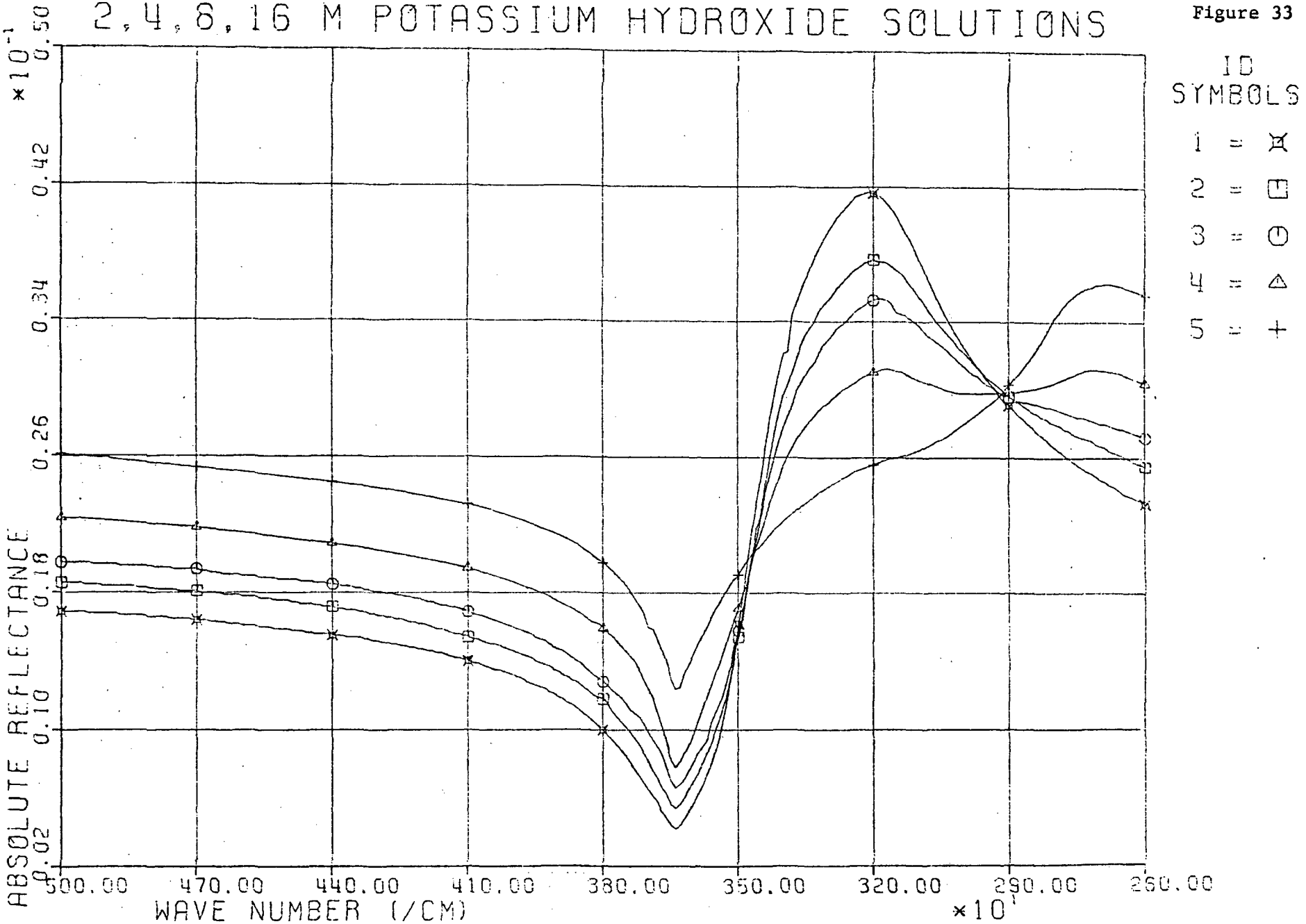
2,4,8,16 M POTASSIUM HYDROXIDE SOLUTIONS
ID SYMBOLS
1 =
2 =
3 =
4 =
5 =
ABSOLUTE REFLECTANCE
×10⁻¹
0.50
0.42
0.34
0.26
0.18
0.10
0.02
500.00
470.00
440.00
410.00
380.00
350.00
320.00
290.00
260.00
WAVE NUMBER (/CM)
×10³

Figure 33

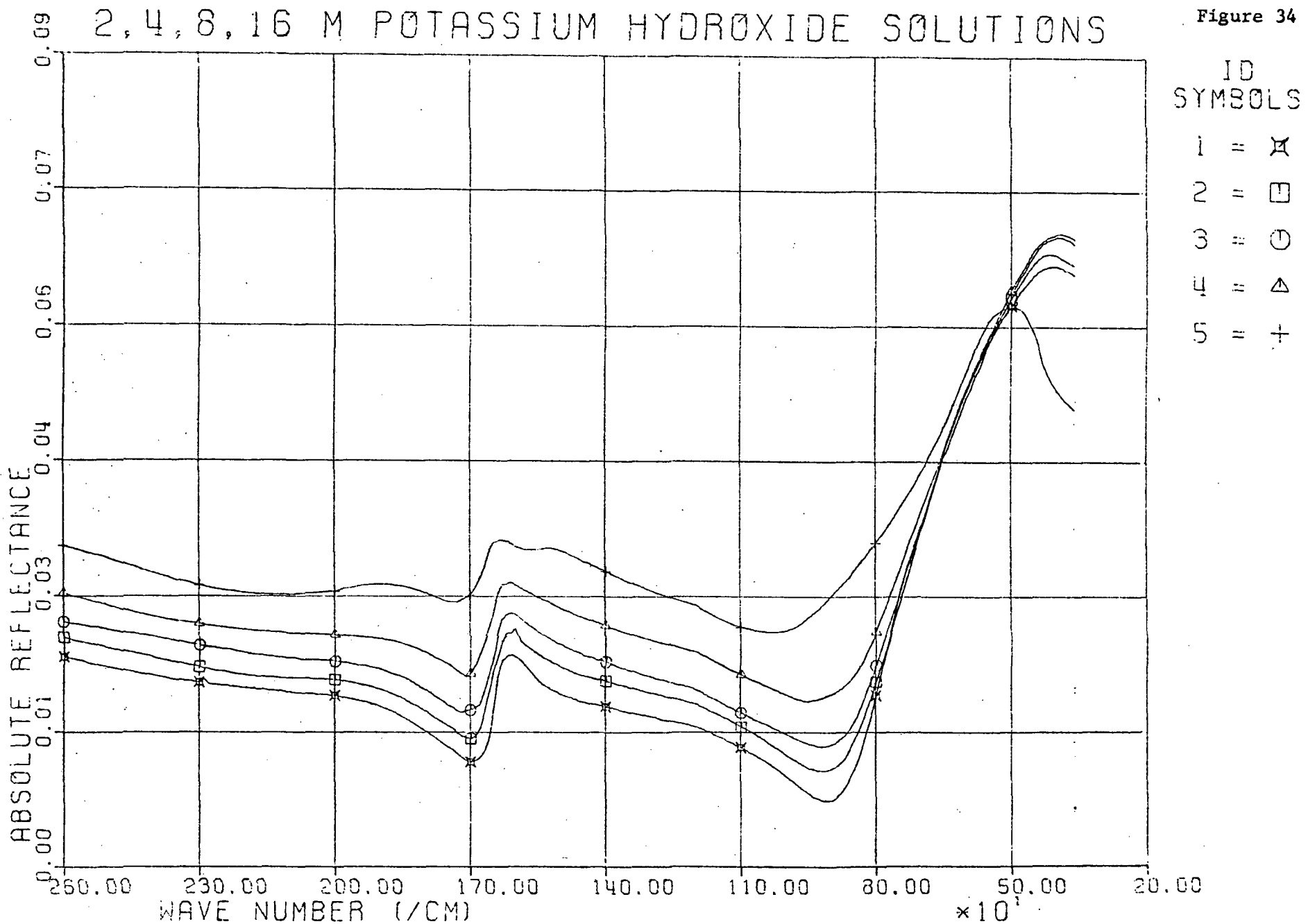
2,4,8,16 M POTASSIUM HYDROXIDE SOLUTIONS
ID SYMBOLS
1 =
2 =
3 =
4 =
5 =
ABSOLUTE REFLECTANCE
0.00
0.01
0.03
0.04
0.06
0.07
0.09
260.00
230.00
200.00
170.00
140.00
110.00
80.00
50.00
20.00
WAVE NUMBER (/CM)
*10¹

Figure 34

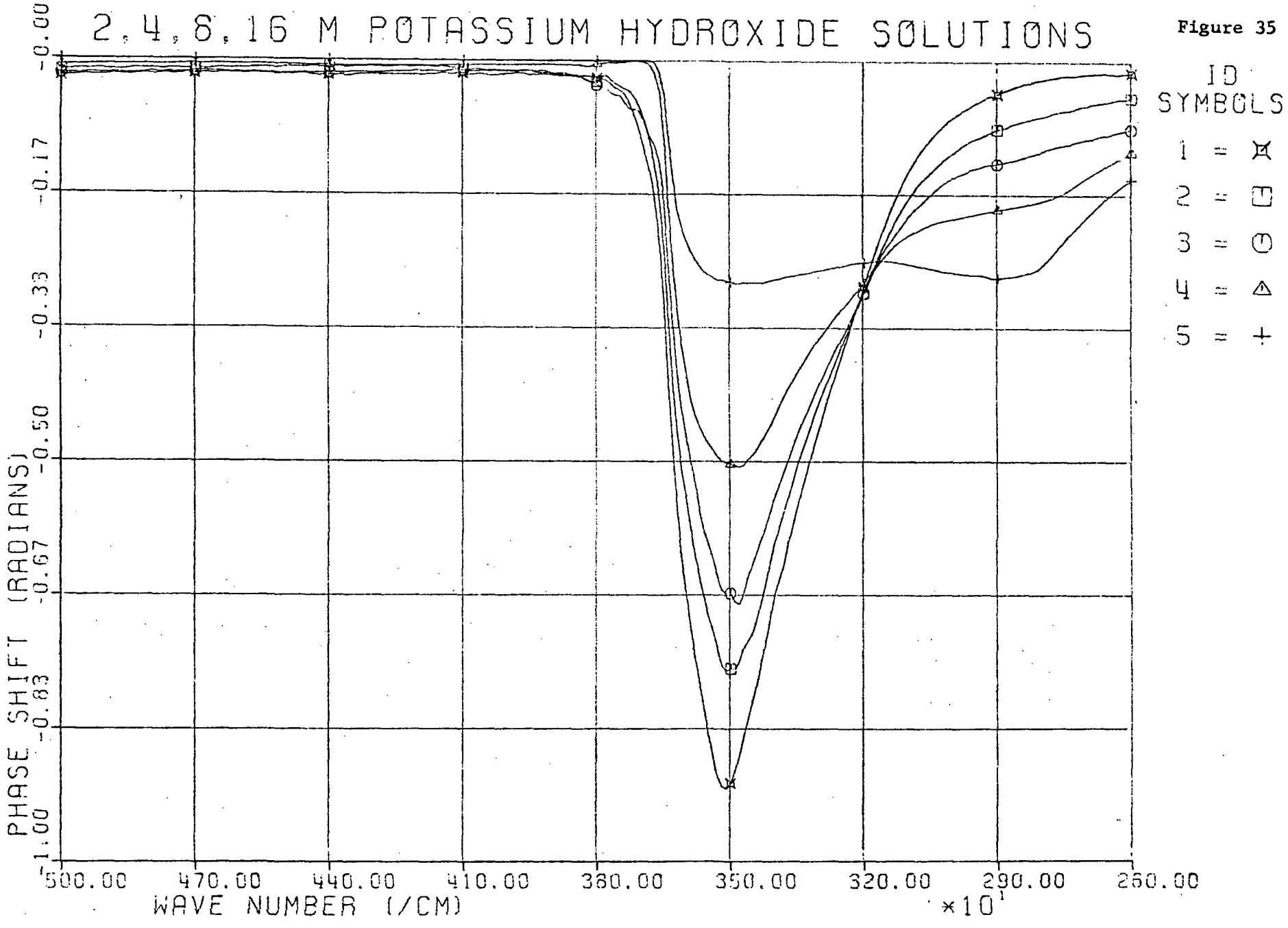
2, 4, 8, 16 M POTASSIUM HYDROXIDE SOLUTIONS
ID SYMBOLS
1 =
2 =
3 =
4 =
5 =
PHASE SHIFT (RADIANS)
-0.00
-0.17
-0.33
-0.50
-0.67
-0.83
-1.00
500.00
470.00
440.00
410.00
380.00
350.00
320.00
290.00
260.00
WAVE NUMBER (/CM)
×10¹

Figure 35

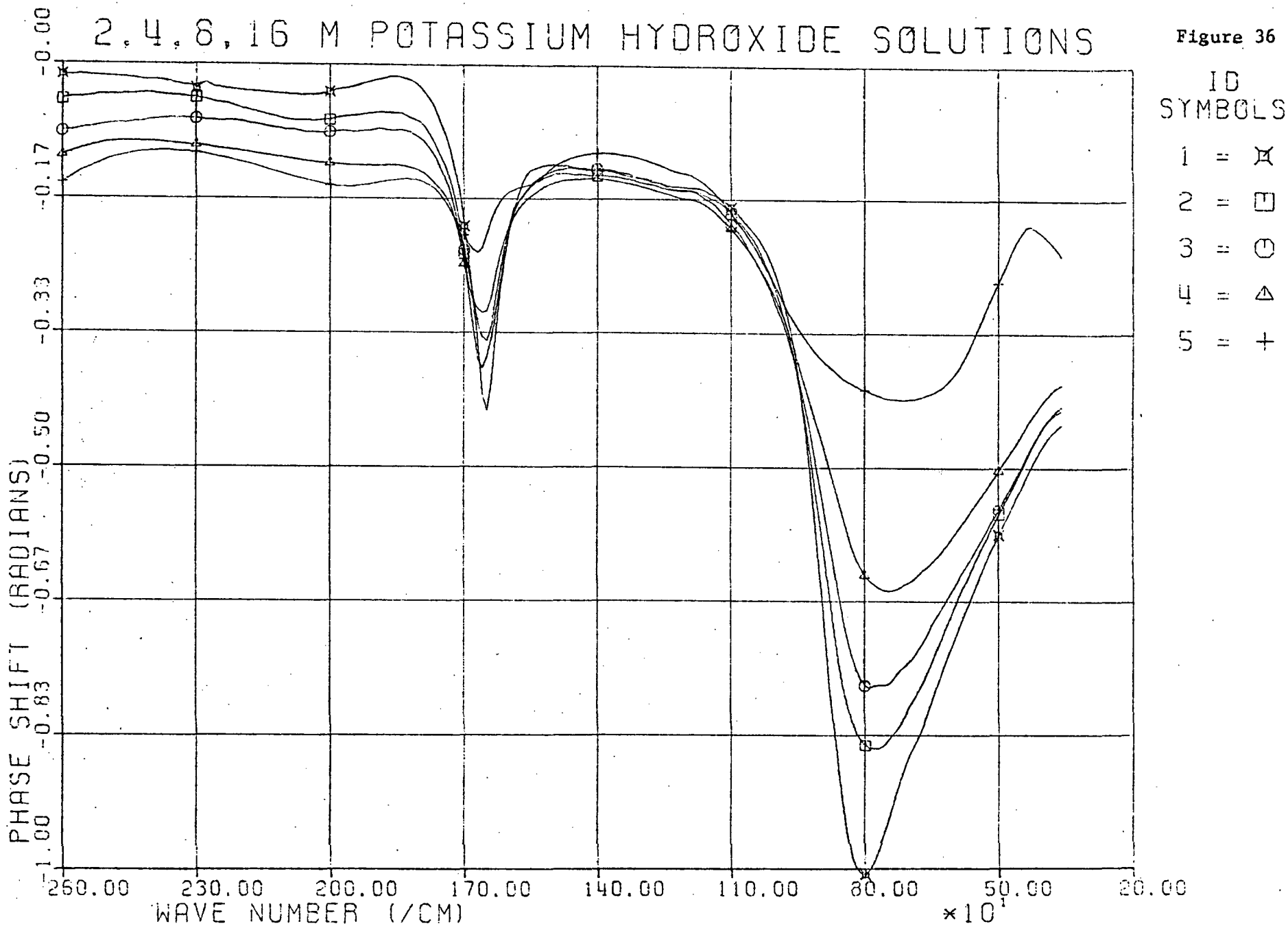
2,4,6,16 M POTASSIUM HYDROXIDE SOLUTIONS
ID SYMBOLS
1 = X
2 = □
3 = ○
4 = △
5 = +
PHASE SHIFT (RADIANS)
-0.00
-0.17
-0.33
-0.50
-0.67
-0.83
-1.00
260.00
230.00
200.00
170.00
140.00
110.00
80.00
50.00
20.00
WAVE NUMBER (/CM)
*10¹

Figure 36

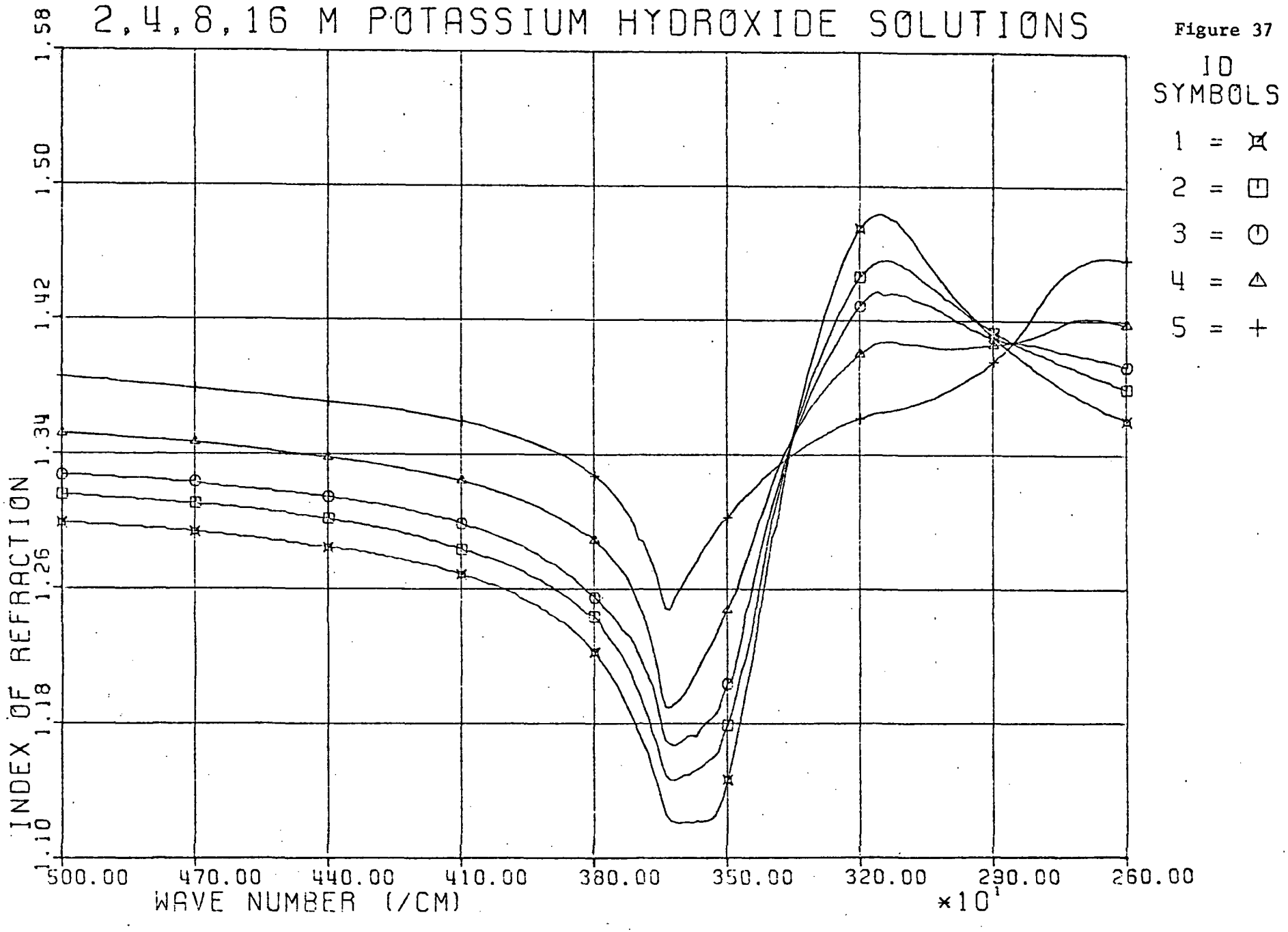
2,4,8,16 M POTASSIUM HYDROXIDE SOLUTIONS
INDEX OF REFRACTION
1.58
1.50
1.42
1.34
1.26
1.18
1.10
500.00
470.00
440.00
410.00
380.00
350.00
320.00
290.00
260.00
WAVE NUMBER (/CM)
*10^1
ID SYMBOLS
1 =
2 =
3 =
4 =
5 =

Figure 37

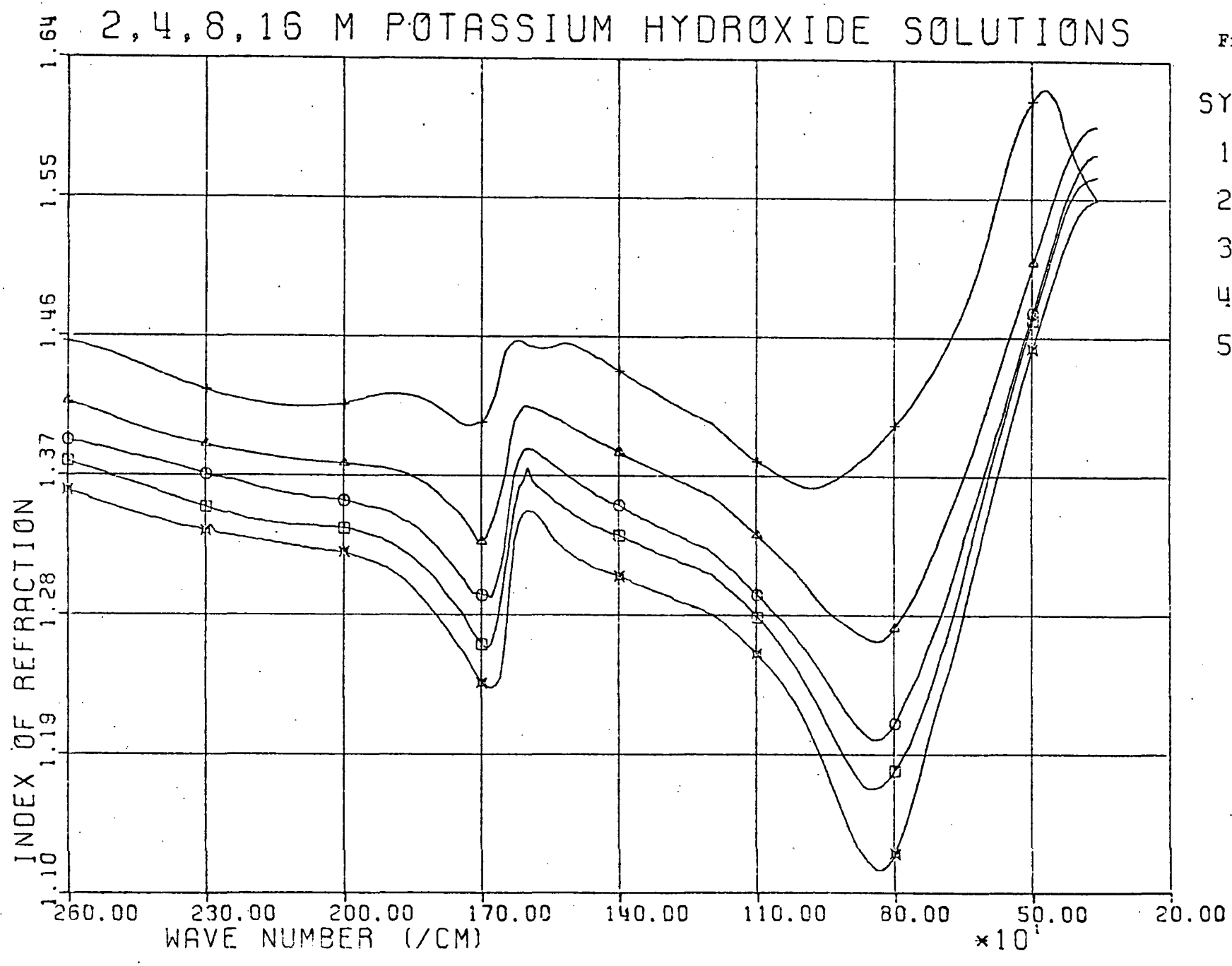
2,4,8,16 M POTASSIUM HYDROXIDE SOLUTIONS
INDEX OF REFRACTION
1.64
1.55
1.46
1.37
1.28
1.19
1.10
260.00
230.00
200.00
170.00
140.00
110.00
80.00
50.00
20.00
WAVE NUMBER (/CM)
*10
ID SYMBOLS
1 =
2 =
3 =
4 =
5 =

Figure 38

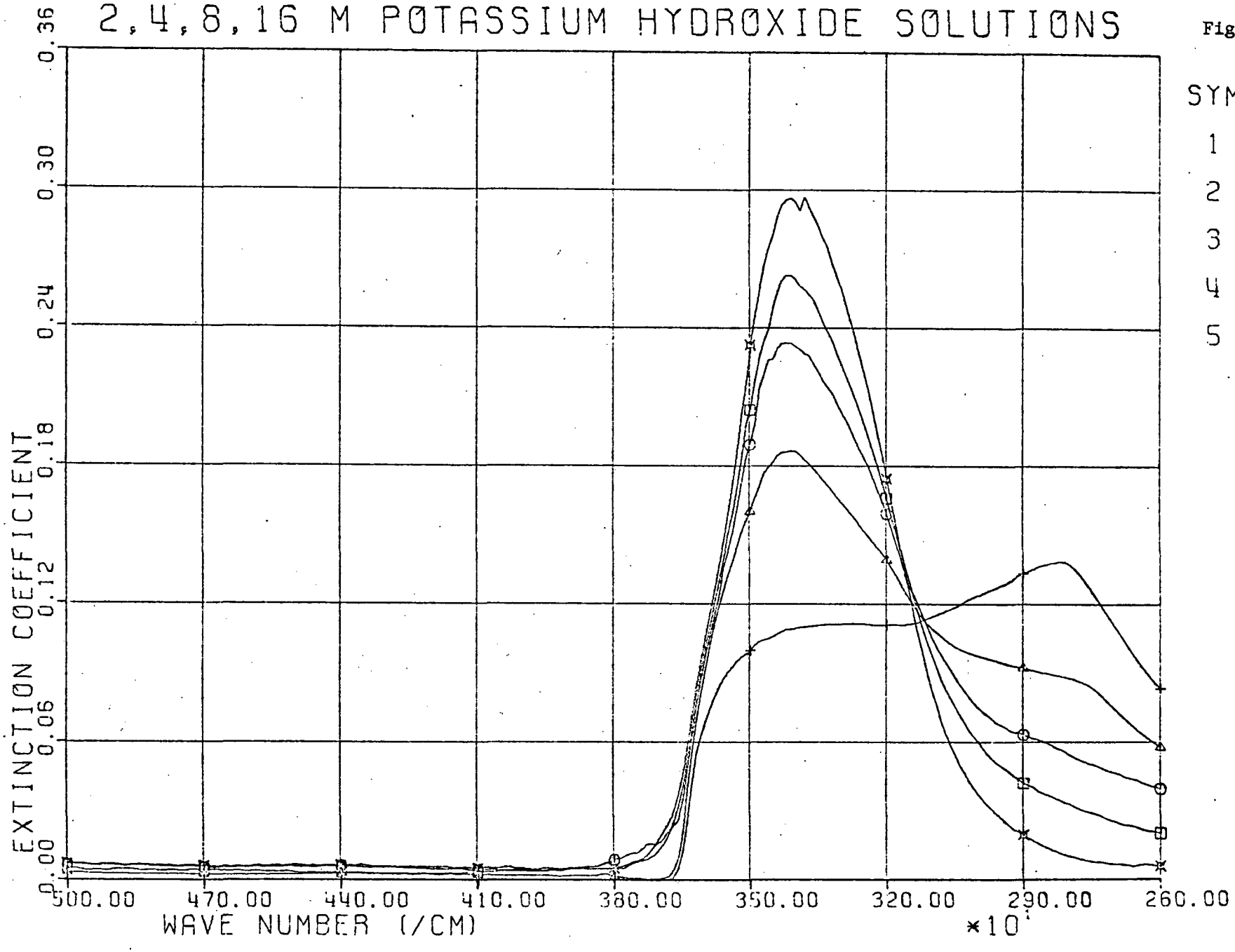
2,4,8,16 M POTASSIUM HYDROXIDE SOLUTIONS
EXTINCTION COEFFICIENT
0.00
0.06
0.12
0.18
0.24
0.30
0.36
500.00
470.00
440.00
410.00
380.00
350.00
320.00
290.00
260.00
WAVE NUMBER (/CM)
*10
ID SYMBOLS
1 =
2 =
3 =
4 =
5 =

Figure 39

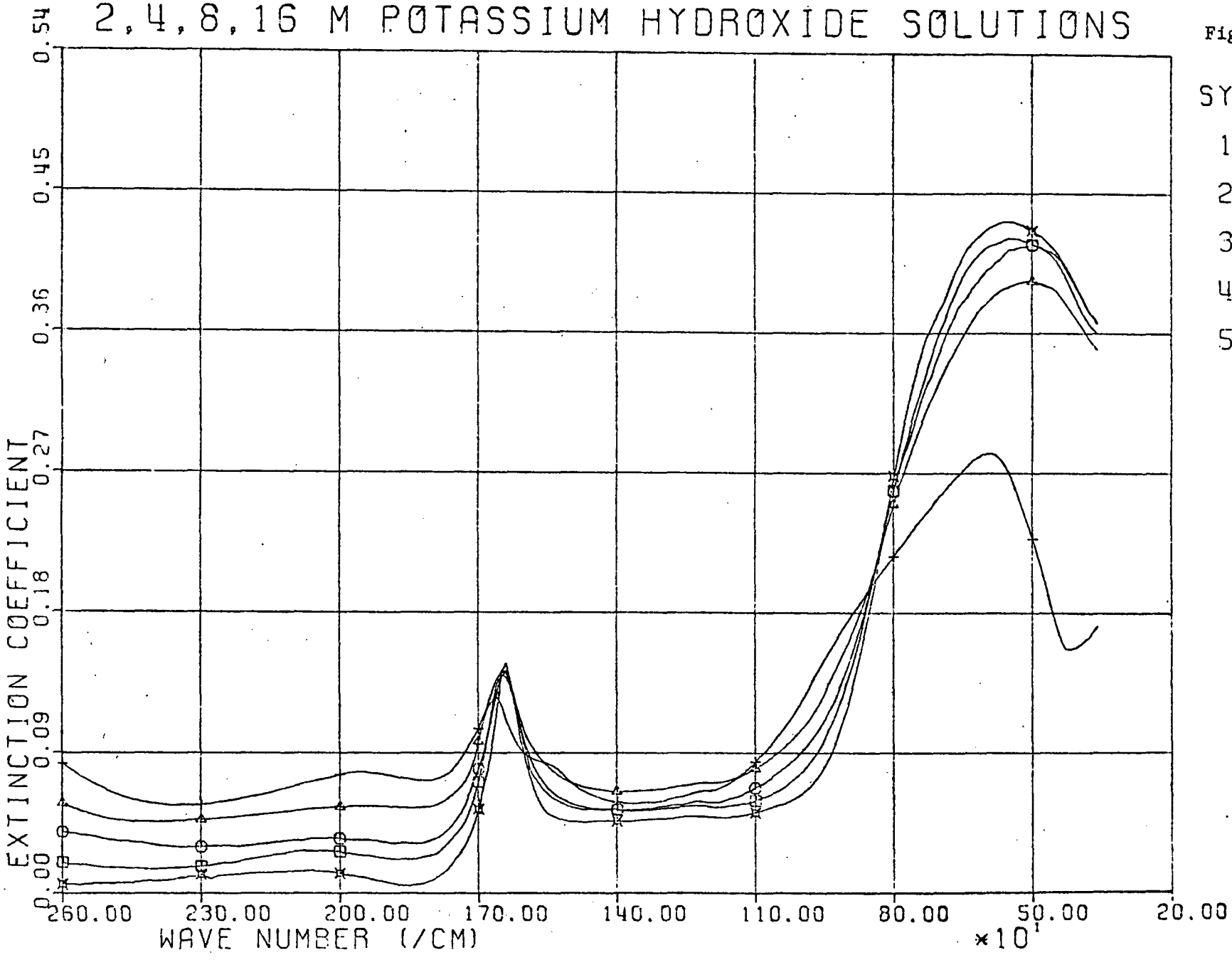
2,4,8,16 M POTASSIUM HYDROXIDE SOLUTIONS
ID SYMBOLS
1 =
2 =
3 =
4 =
5 =
EXTINCTION COEFFICIENT
0.00
0.09
0.18
0.27
0.36
0.45
0.54
260.00
230.00
200.00
170.00
140.00
110.00
80.00
50.00
20.00
WAVE NUMBER (/CM)
×10¹

Figure 40

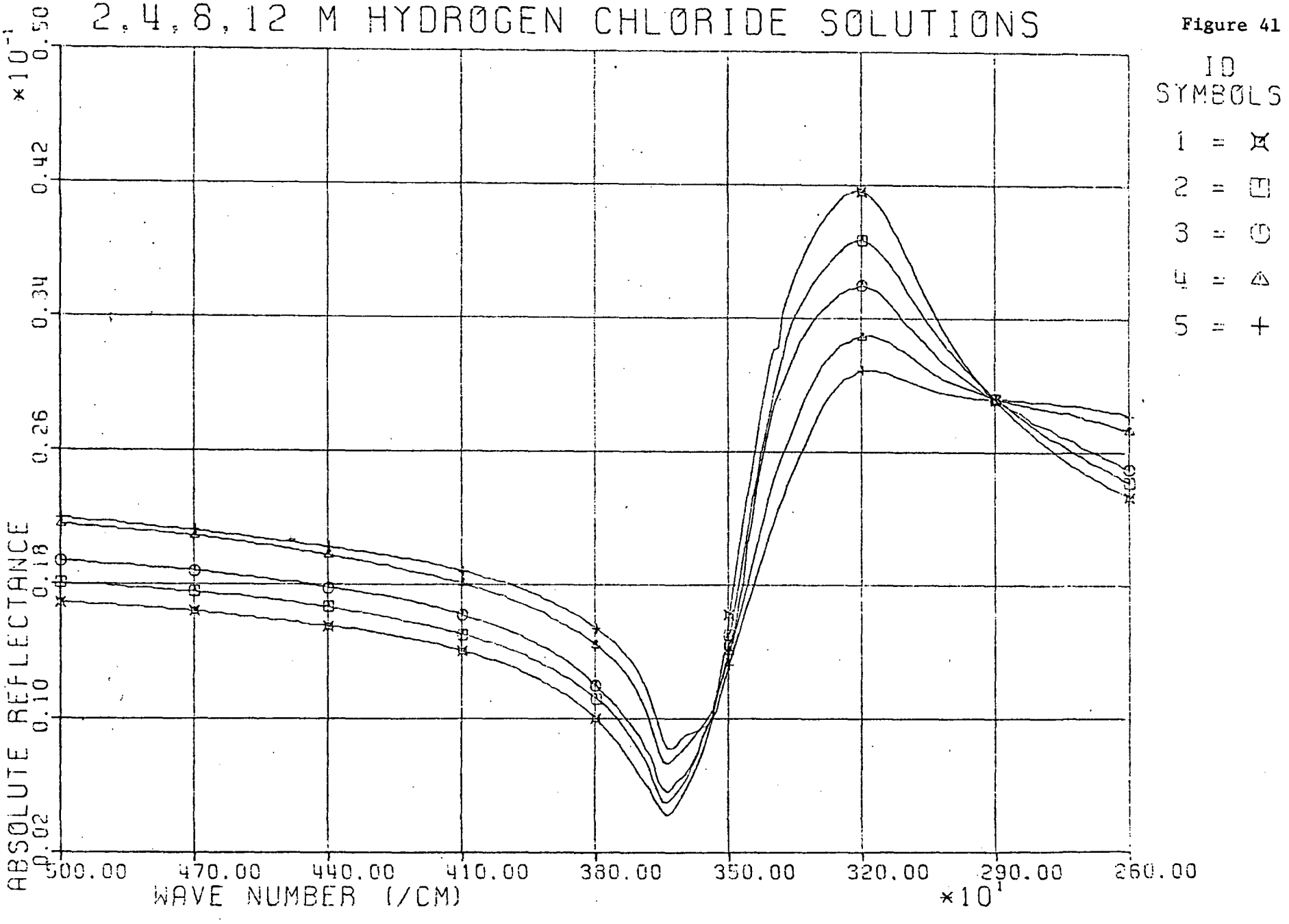
2,4,8,12 M HYDROGEN CHLORIDE SOLUTIONS
ID SYMBOLS
1 =
2 =
3 =
4 =
5 =
ABSOLUTE REFLECTANCE
*10-1
0.50
0.42
0.34
0.26
0.18
0.10
0.02
500.00
470.00
440.00
410.00
380.00
350.00
320.00
290.00
260.00
WAVE NUMBER (/CM)
*10+1

Figure 41

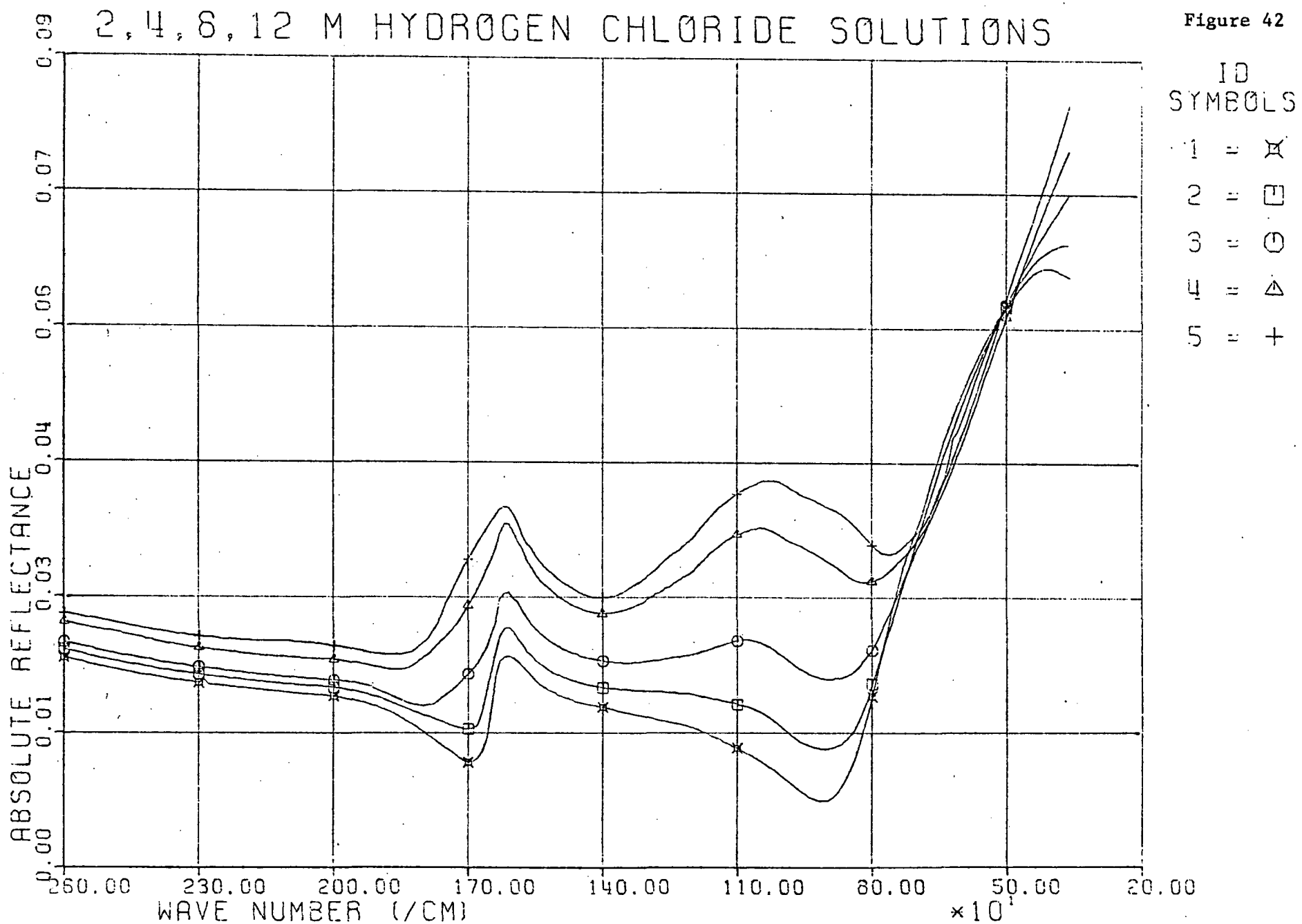
2,4,8,12 M HYDROGEN CHLORIDE SOLUTIONS
ABSOLUTE REFLECTANCE
0.00
0.01
0.03
0.04
0.06
0.07
0.09
260.00
230.00
200.00
170.00
140.00
110.00
80.00
50.00
20.00
WAVE NUMBER (/CM)
×10¹
ID SYMBOLS
1 =
2 =
3 =
4 =
5 =

Figure 42

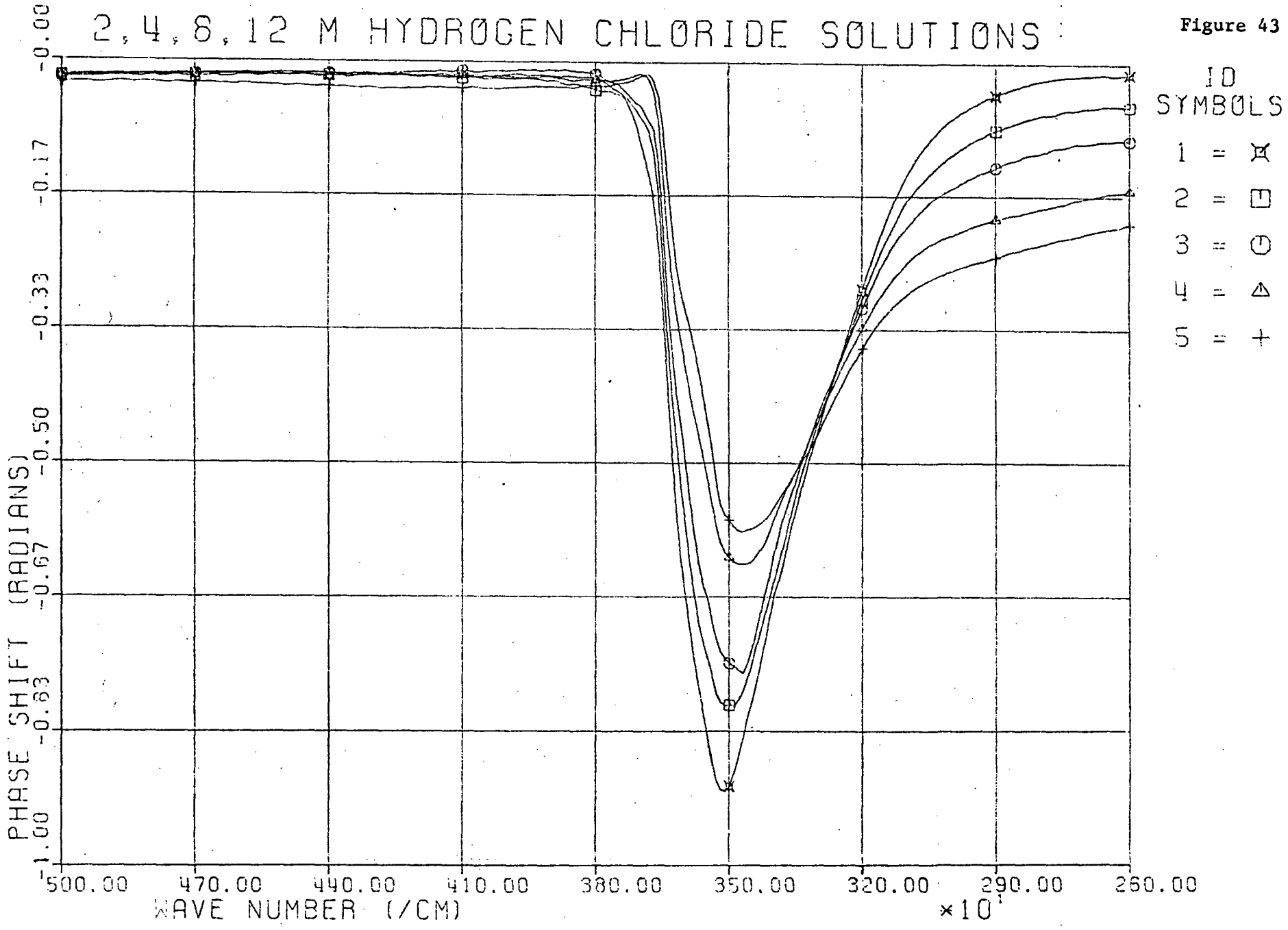
2,4,8,12 M HYDROGEN CHLORIDE SOLUTIONS
ID SYMBOLS
1 =
2 =
3 =
4 =
5 =
PHASE SHIFT (RADIANS)
-0.00
-0.17
-0.33
-0.50
-0.67
-0.83
-1.00
500.00
470.00
440.00
410.00
380.00
350.00
320.00
290.00
260.00
WAVE NUMBER (/CM)
×10¹

Figure 43

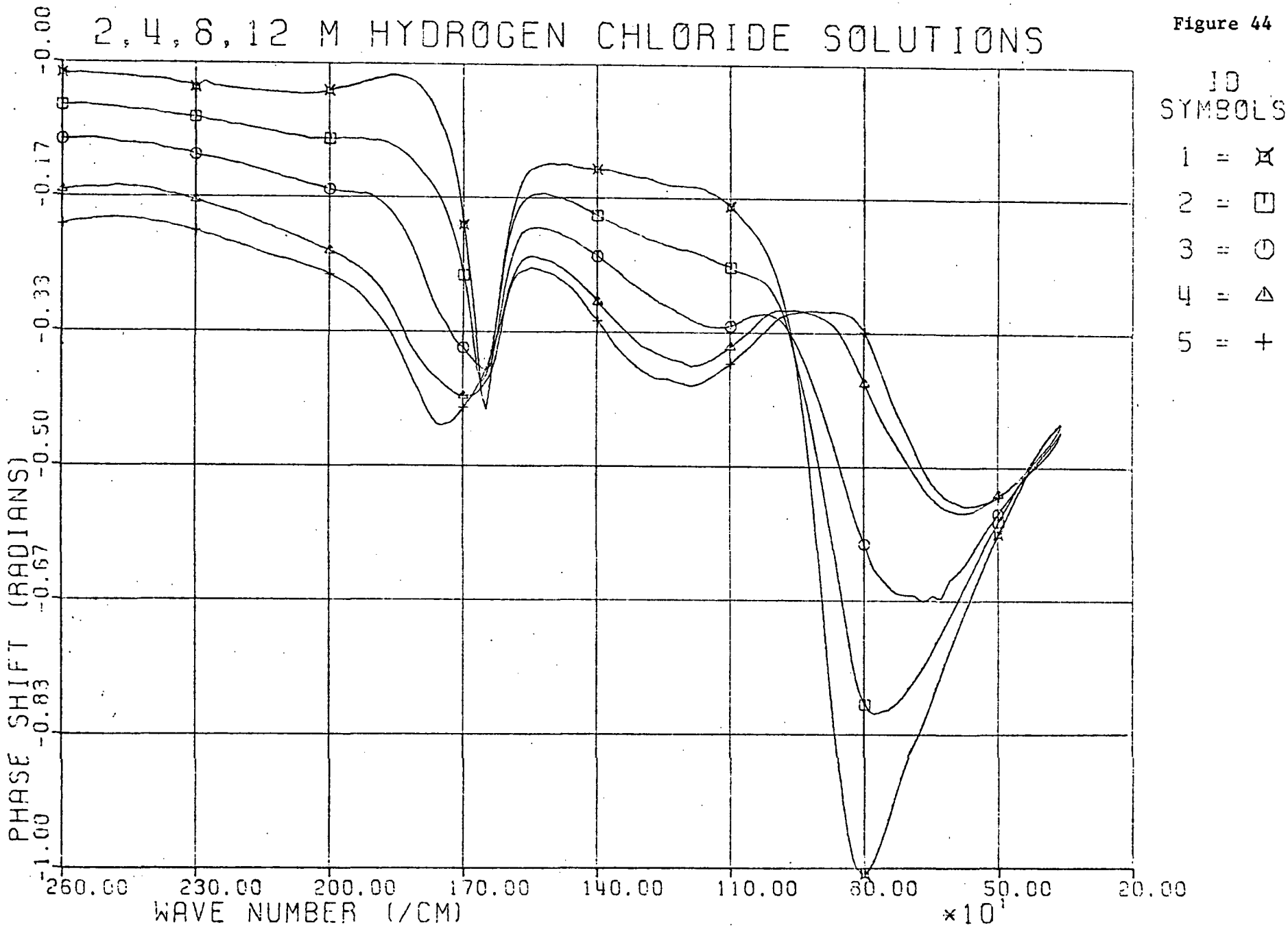
2,4,8,12 M HYDROGEN CHLORIDE SOLUTIONS
ID SYMBOLS
1 =
2 =
3 =
4 =
5 =
PHASE SHIFT (RADIANS)
-0.00
-0.17
-0.33
-0.50
-0.67
-0.83
-1.00
260.00
230.00
200.00
170.00
140.00
110.00
80.00
50.00
20.00
WAVE NUMBER (/CM)
*10¹

Figure 44

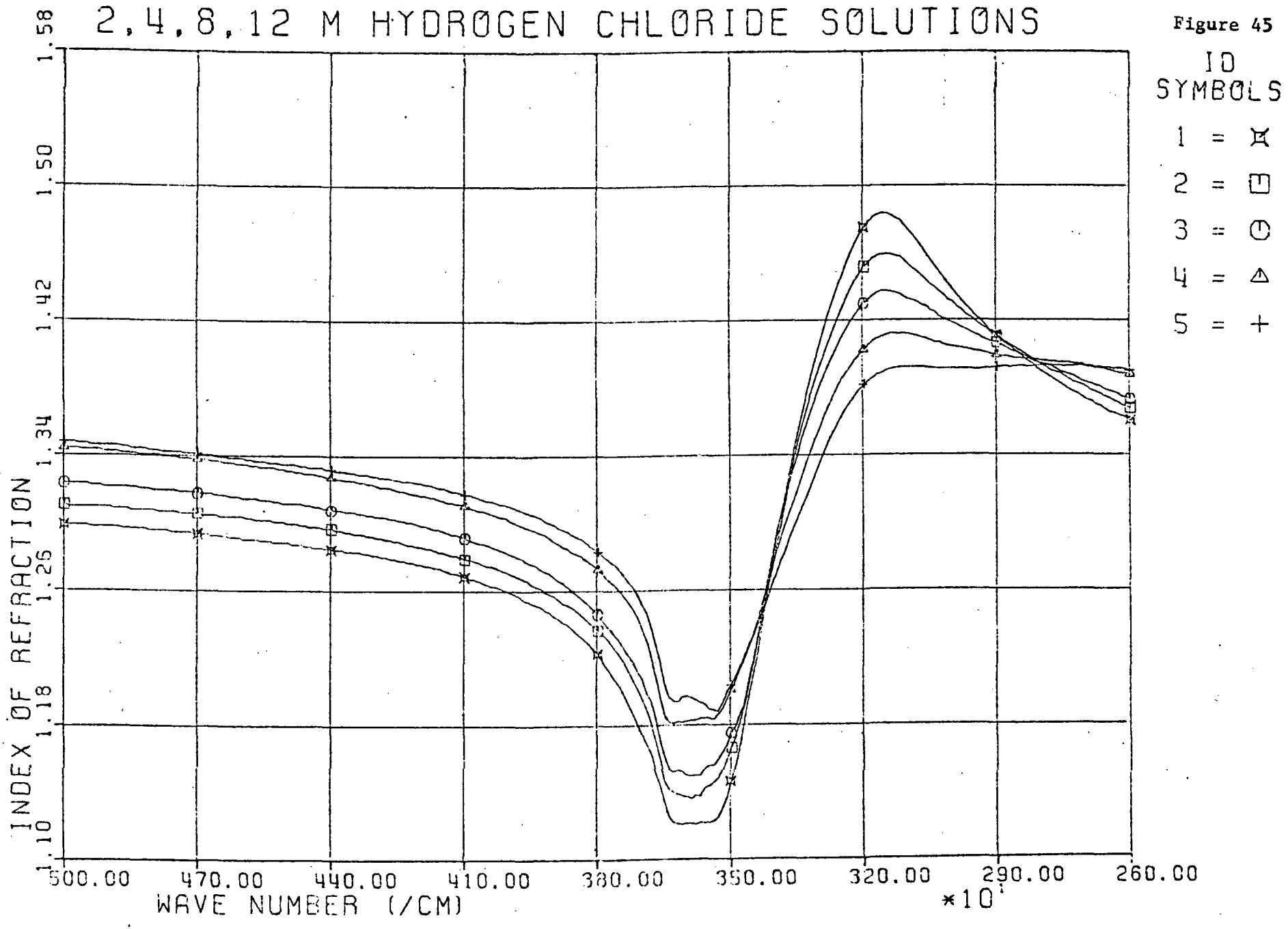
2,4,8,12 M HYDROGEN CHLORIDE SOLUTIONS
ID SYMBOLS
1 =
2 =
3 =
4 =
5 =
INDEX OF REFRACTION
1.58
1.50
1.42
1.34
1.25
1.18
1.10
500.00
470.00
440.00
410.00
380.00
350.00
320.00
290.00
260.00
WAVE NUMBER (/CM)
*10

Figure 45

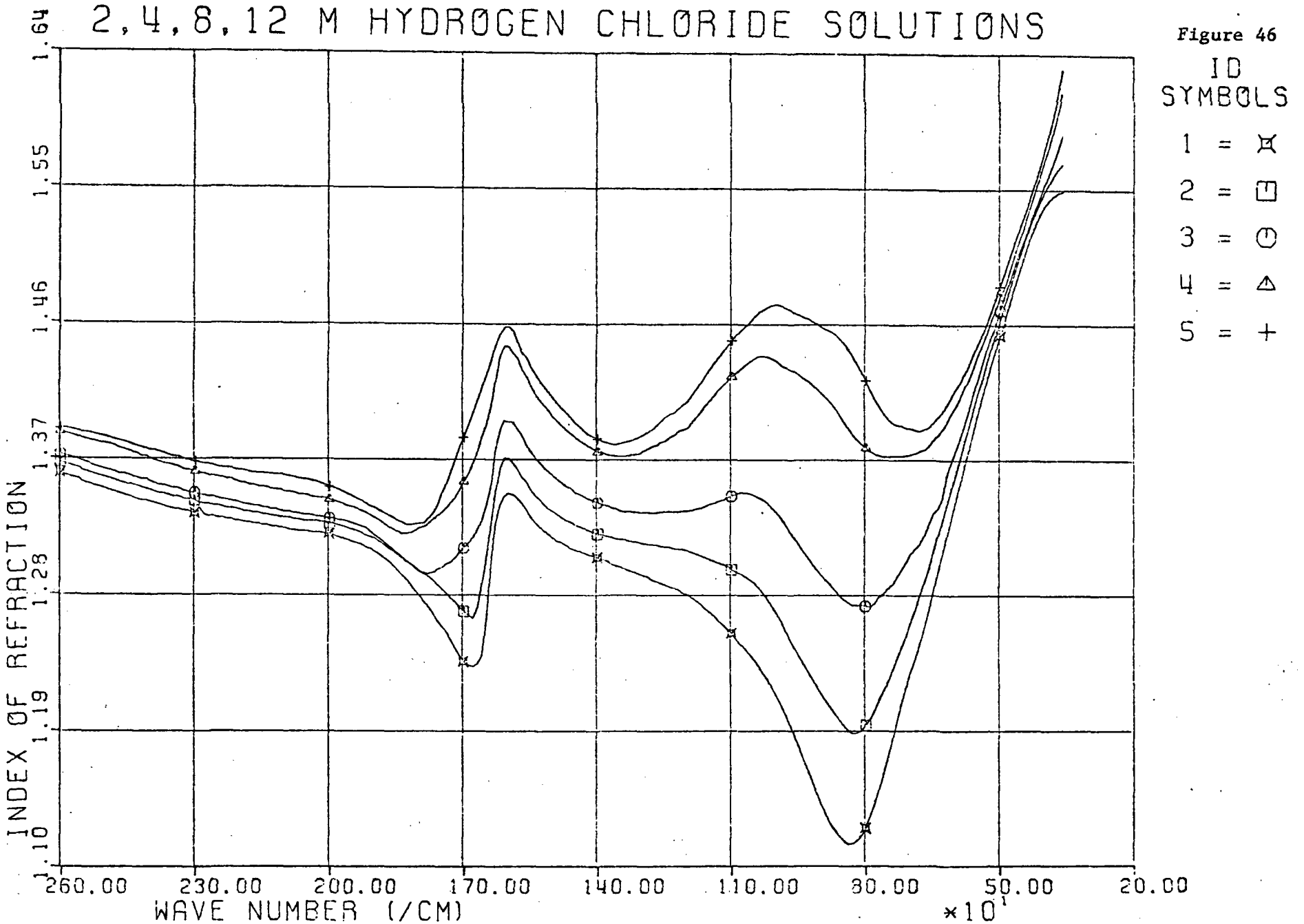
2,4,8,12 M HYDROGEN CHLORIDE SOLUTIONS
INDEX OF REFRACTION
1.64
1.55
1.46
1.37
1.28
1.19
1.10
260.00
230.00
200.00
170.00
140.00
110.00
80.00
50.00
20.00
WAVE NUMBER (/CM)
×10¹
ID SYMBOLS
1 =
2 =
3 =
4 =
5 =

Figure 46

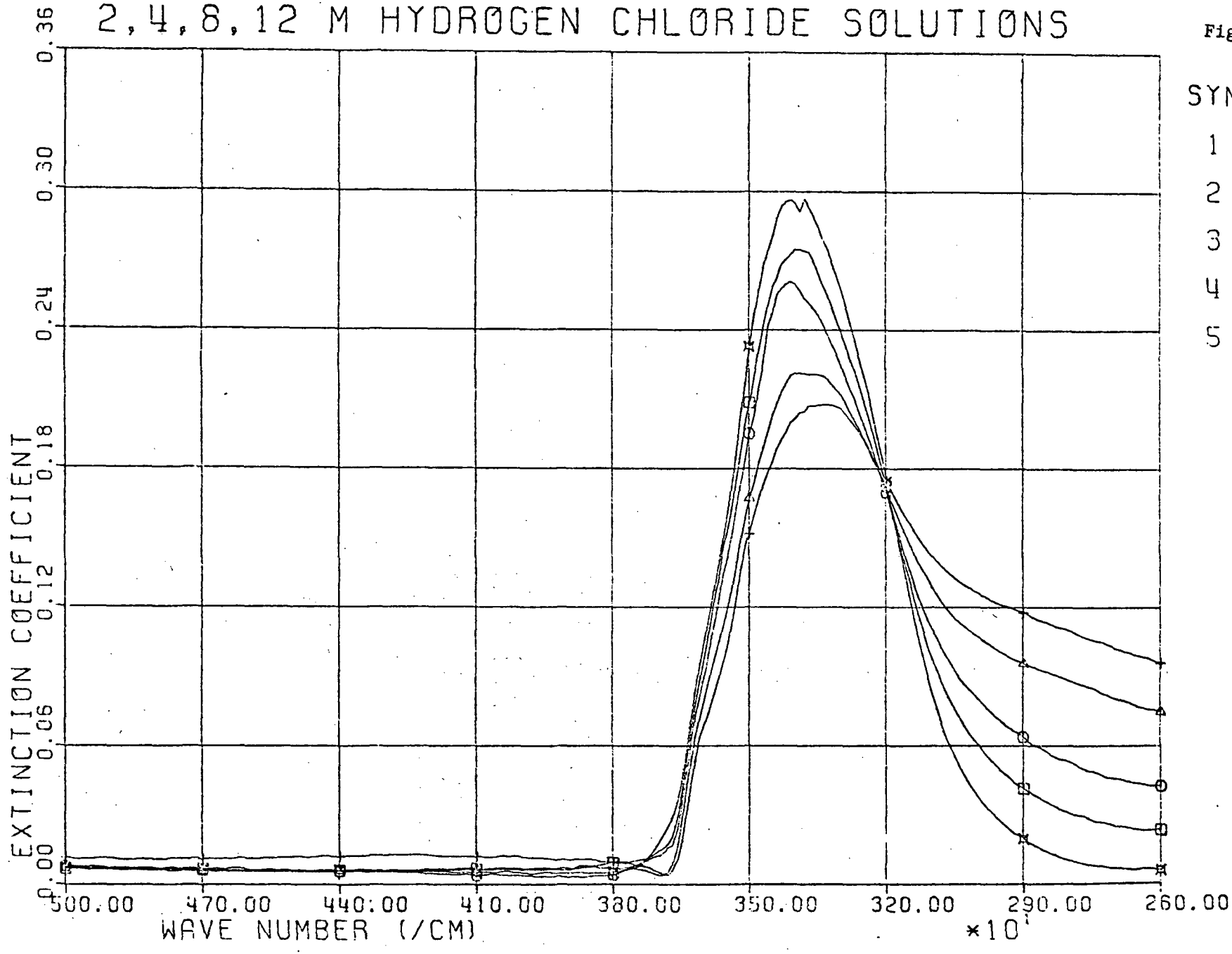
2,4,8,12 M HYDROGEN CHLORIDE SOLUTIONS
EXTINCTION COEFFICIENT
0.00
0.06
0.12
0.18
0.24
0.30
0.36
500.00
470.00
440.00
410.00
380.00
350.00
320.00
290.00
260.00
WAVE NUMBER (/CM)
*10
IO SYMBOLS
1 =
2 =
3 =
4 =
5 =

Figure 47

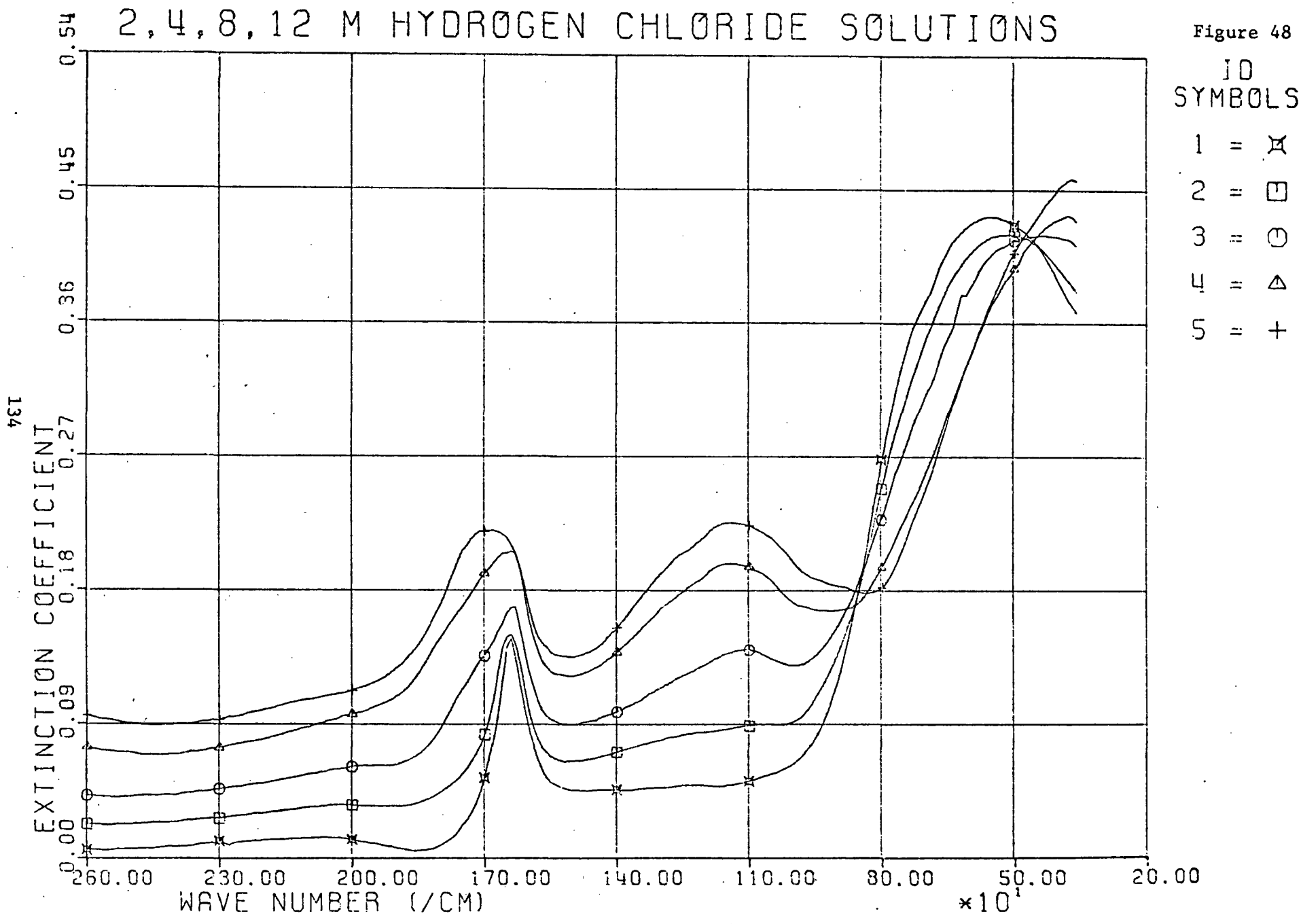
2,4,8,12 M HYDROGEN CHLORIDE SOLUTIONS
ID SYMBOLS
1 =
2 =
3 =
4 =
5 =
EXTINCTION COEFFICIENT
0.00
0.09
0.18
0.27
0.36
0.45
0.54
260.00
230.00
200.00
170.00
140.00
110.00
80.00
50.00
20.00
WAVE NUMBER (/CM)
×10¹

Figure 48

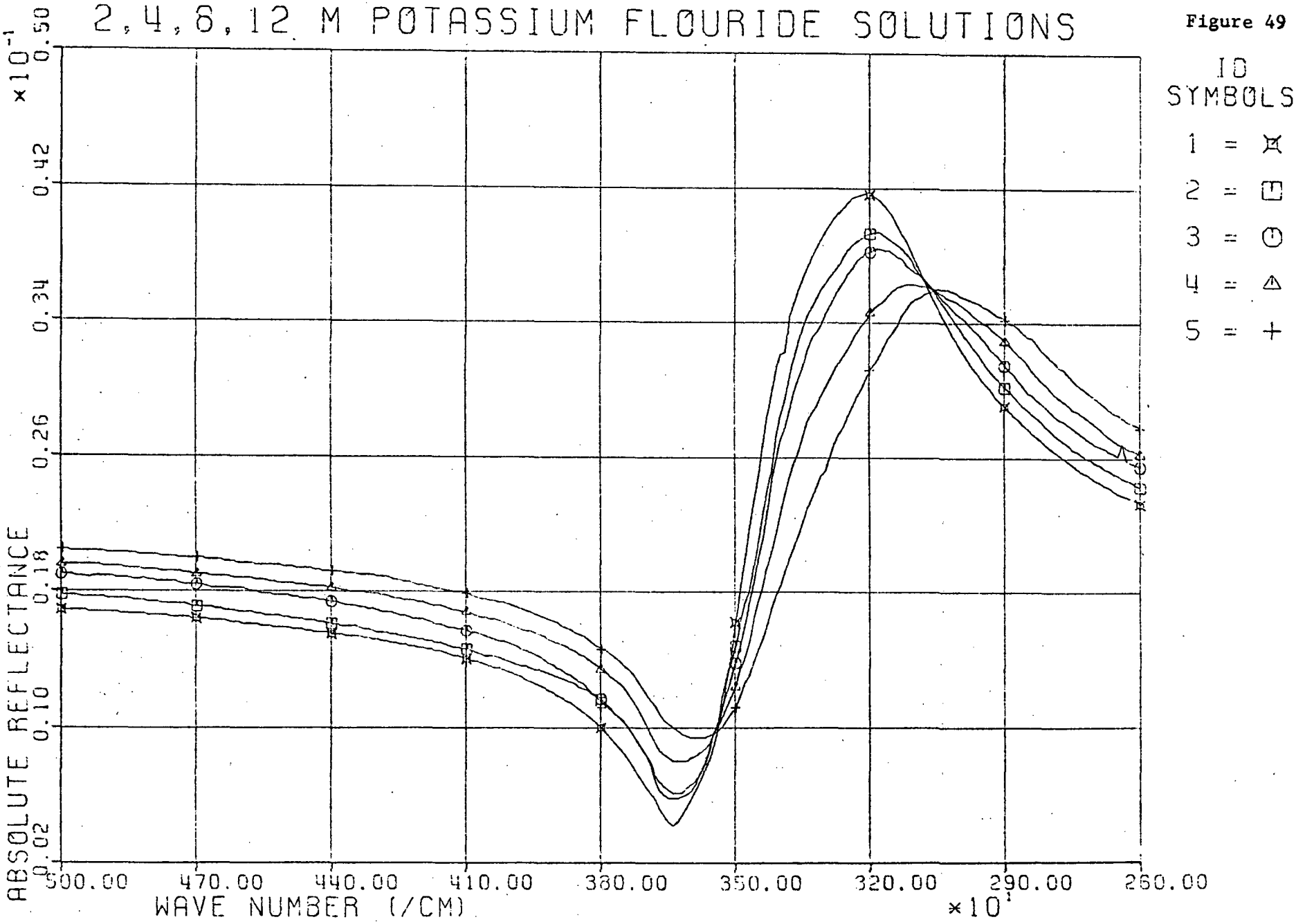
2,4,6,12 M POTASSIUM FLOURIDE SOLUTIONS
ID SYMBOLS
1 =
2 =
3 =
4 =
5 =
ABSOLUTE REFLECTANCE
×10⁻¹
0.50
0.42
0.34
0.26
0.18
0.10
0.02
500.00
470.00
440.00
410.00
380.00
350.00
320.00
290.00
260.00
WAVE NUMBER (/CM)
×10³

Figure 49

Figure 50

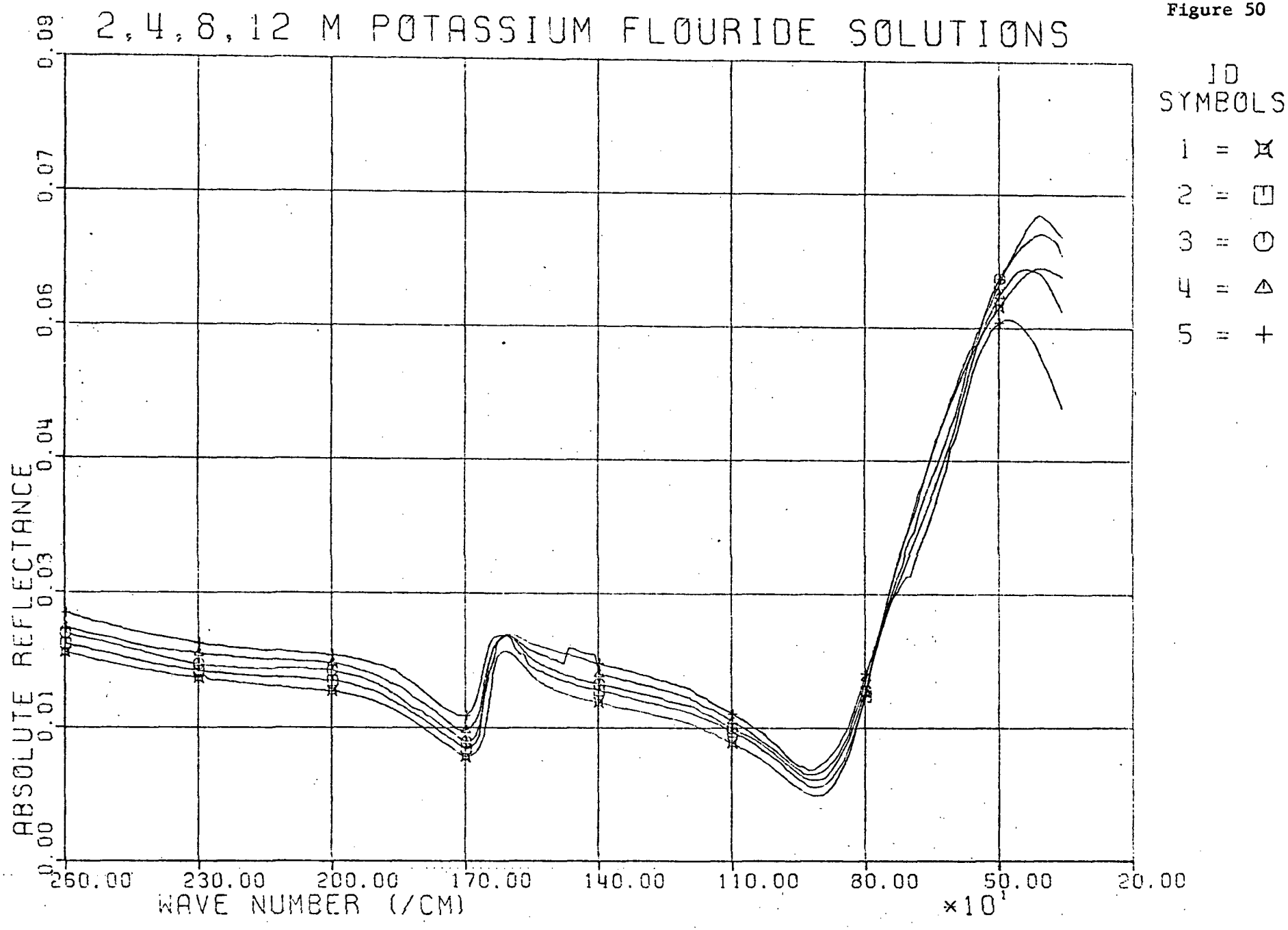
2, 4, 8, 12 M POTASSIUM FLOURIDE SOLUTIONS
ABSOLUTE REFLECTANCE
0.00
0.01
0.03
0.04
0.06
0.07
0.09
260.00
230.00
200.00
170.00
140.00
110.00
80.00
50.00
20.00
WAVE NUMBER (/CM)
×10¹
ID SYMBOLS
1 =
2 =
3 =
4 =
5 =

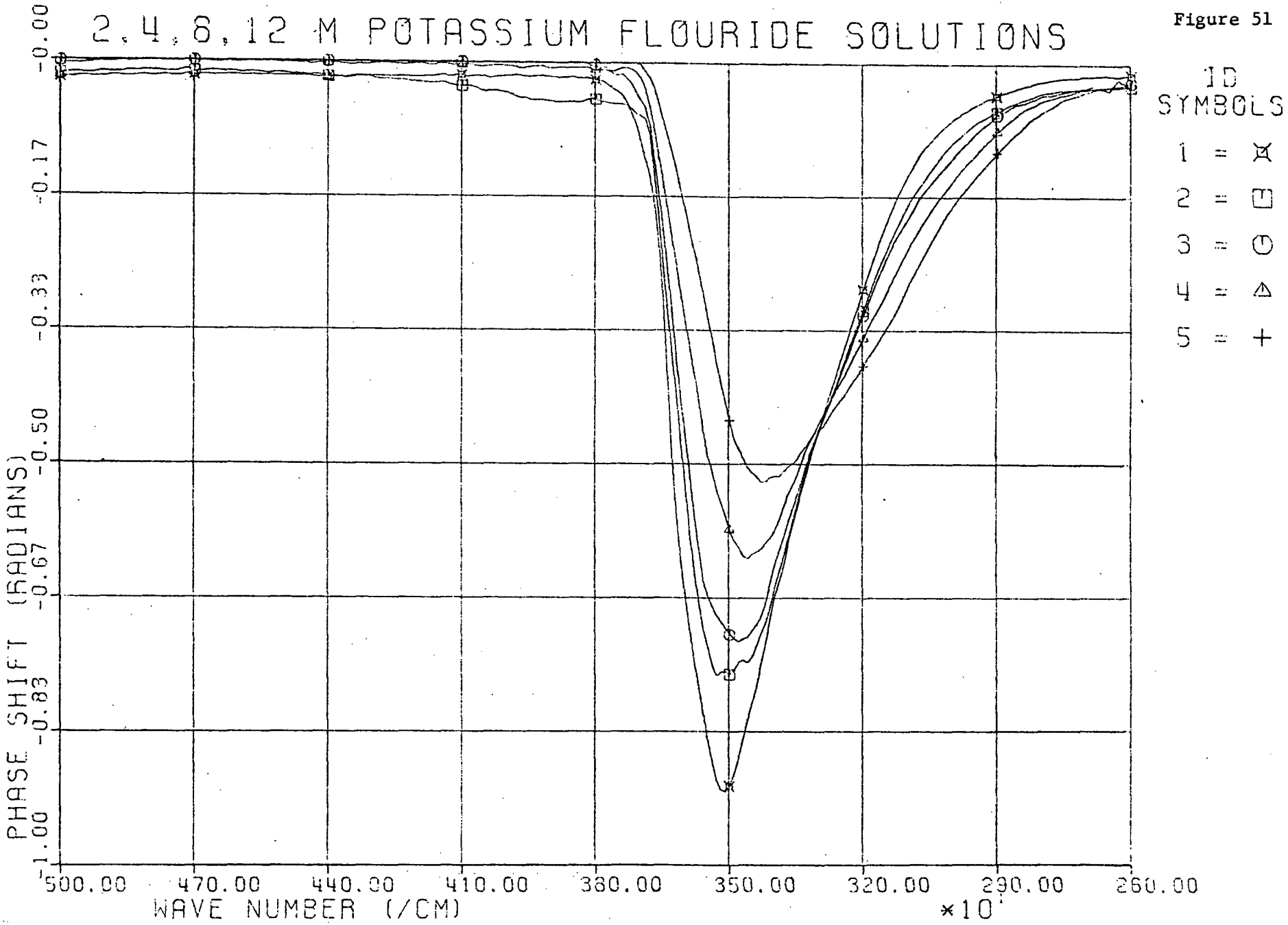
2,4,6,12 M POTASSIUM FLOURIDE SOLUTIONS
ID SYMBOLS
1 =
2 =
3 =
4 =
5 =
PHASE SHIFT (RADIANS)
-0.00
-0.17
-0.33
-0.50
-0.67
-0.83
-1.00
500.00
470.00
440.00
410.00
380.00
350.00
320.00
290.00
260.00
WAVE NUMBER (/CM)
*10

Figure 51

Figure 52

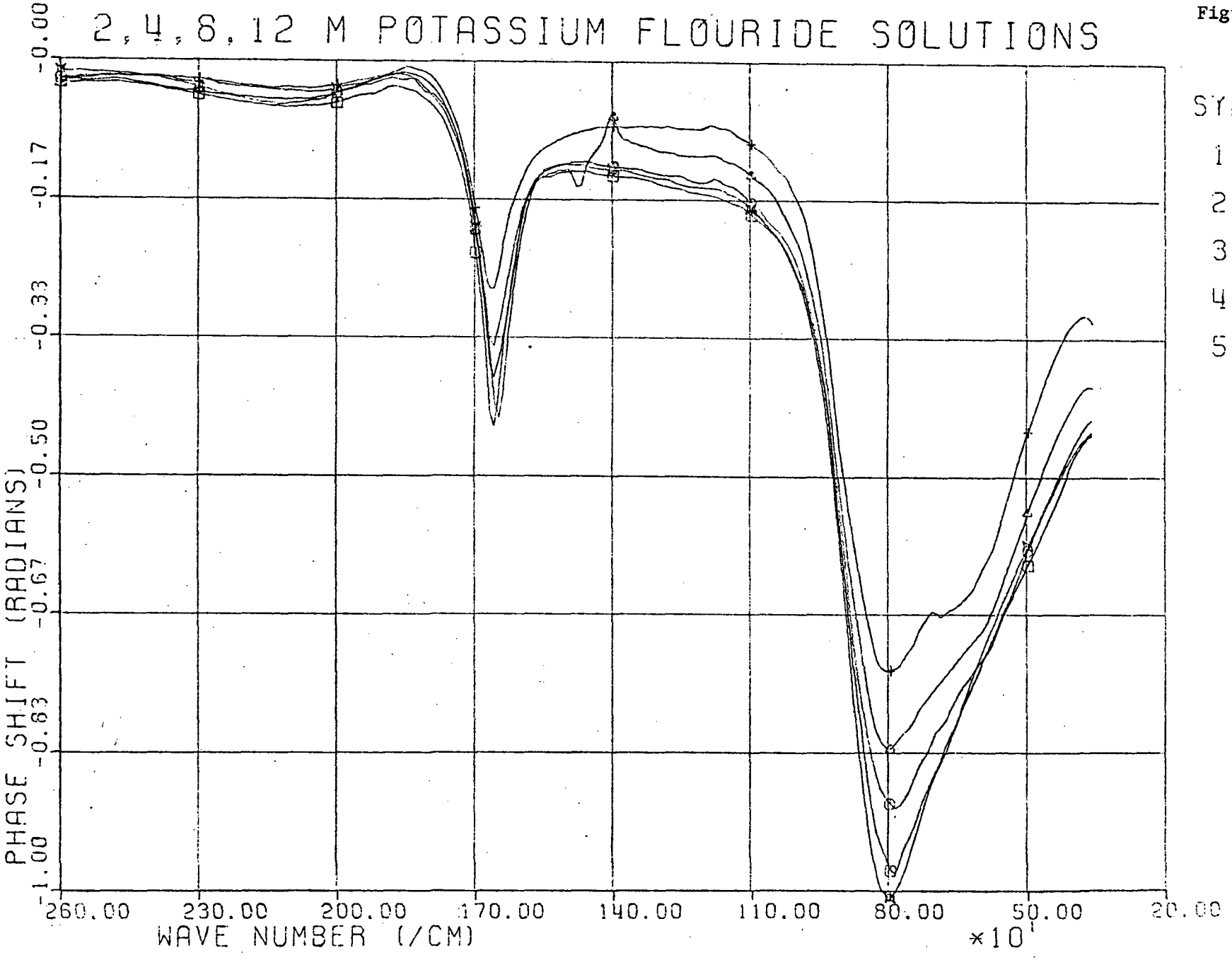
2,4,8,12 M POTASSIUM FLOURIDE SOLUTIONS
ID SYMBOLS
1 =
2 =
3 =
4 =
5 =
PHASE SHIFT (RADIANS)
-0.00
-0.17
-0.33
-0.50
-0.67
-0.83
-1.00
260.00
230.00
200.00
170.00
140.00
110.00
80.00
50.00
20.00
WAVE NUMBER (/CM)
*10

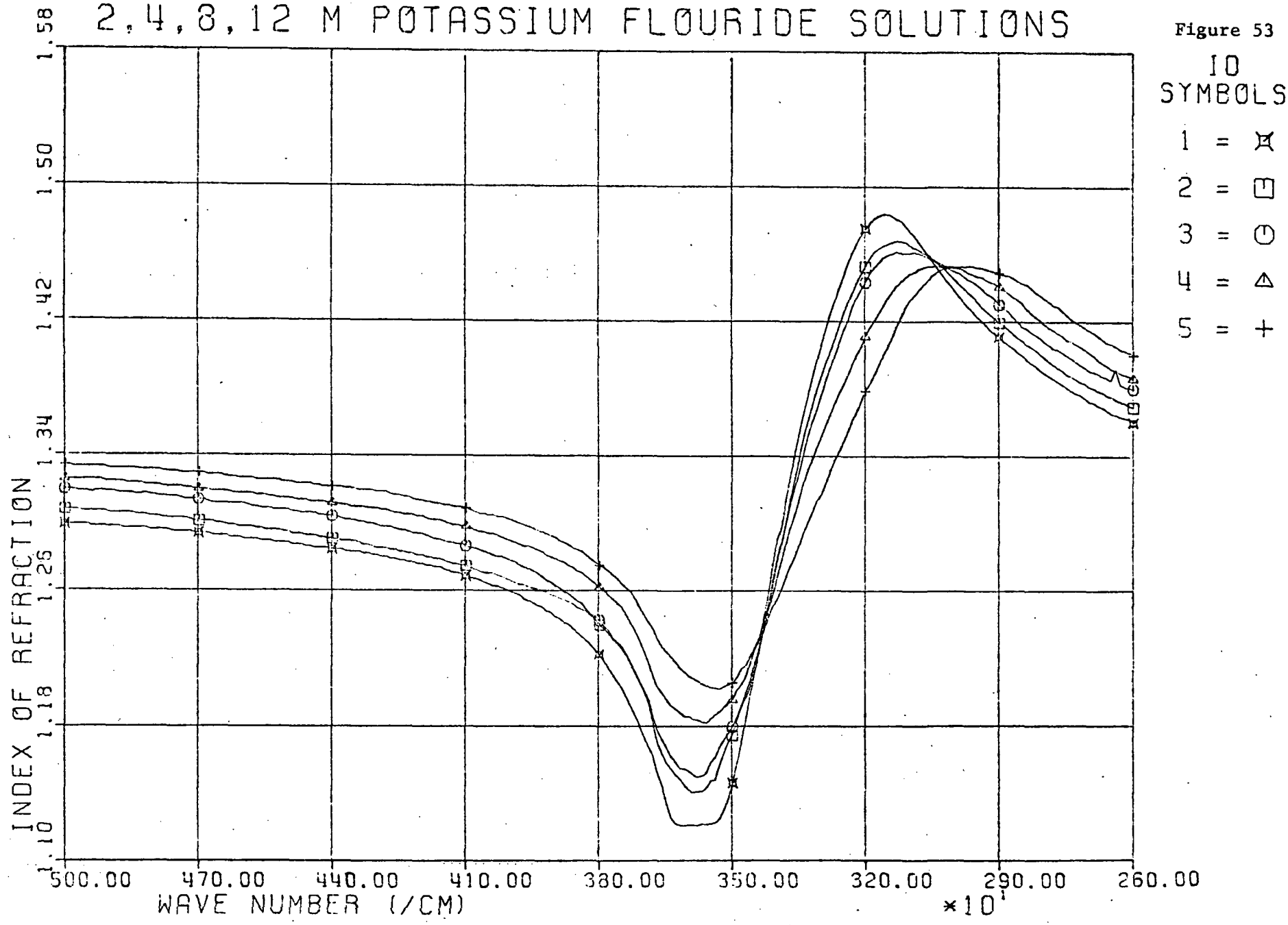
2,4,8,12 M POTASSIUM FLOURIDE SOLUTIONS
INDEX OF REFRACTION
1.58
1.50
1.42
1.34
1.26
1.18
1.10
500.00
470.00
440.00
410.00
380.00
350.00
320.00
290.00
260.00
WAVE NUMBER (/CM)
*10
IO SYMBOLS
1 = X
2 = □
3 = ○
4 = △
5 = +

Figure 53

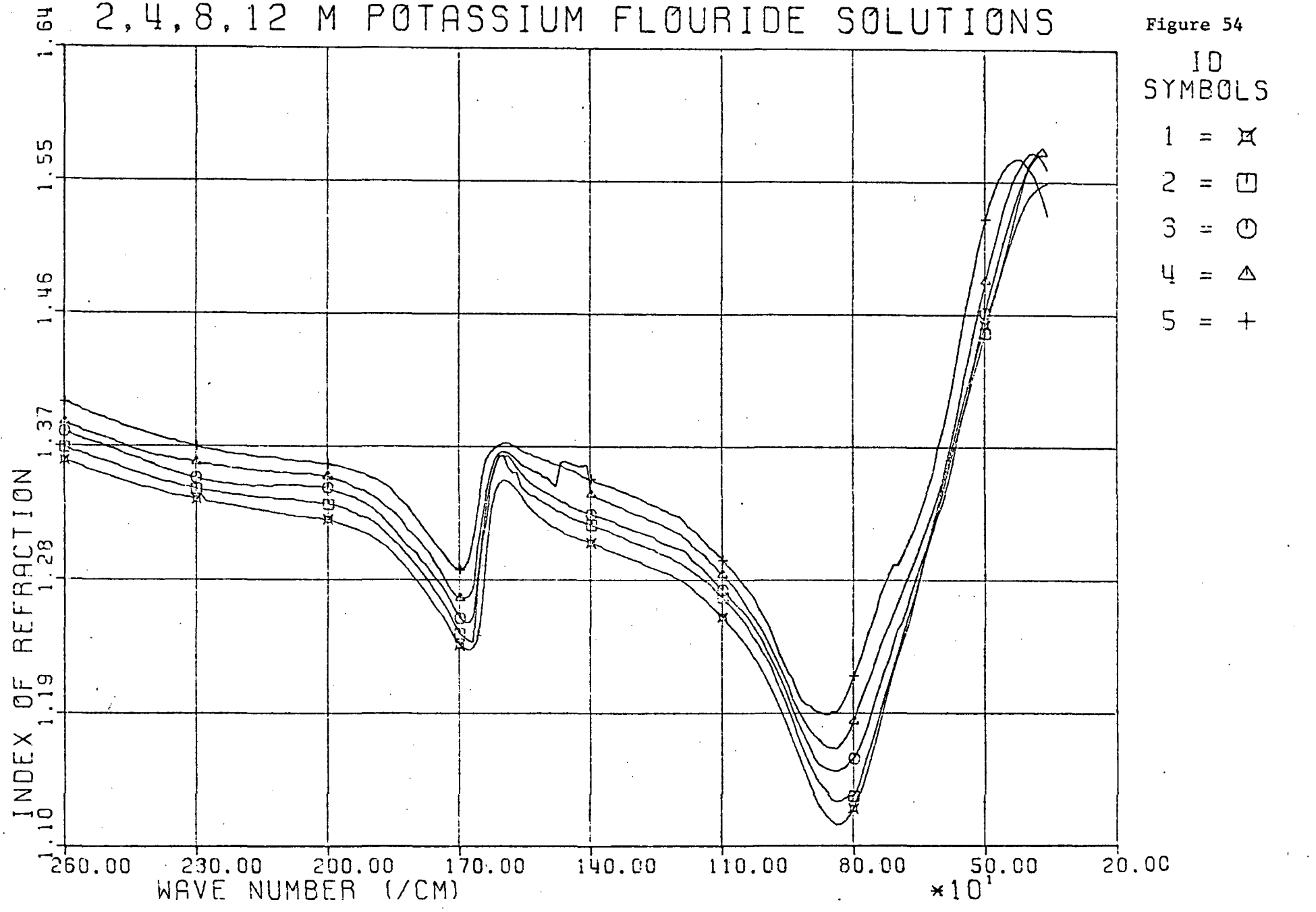
2,4,8,12 M POTASSIUM FLOURIDE SOLUTIONS
INDEX OF REFRACTION
1.64
1.55
1.46
1.37
1.28
1.19
1.10
260.00
230.00
200.00
170.00
140.00
110.00
80.00
50.00
20.00
WAVE NUMBER (/CM)
*10¹
ID SYMBOLS
1 =
2 =
3 =
4 =
5 =

Figure 54

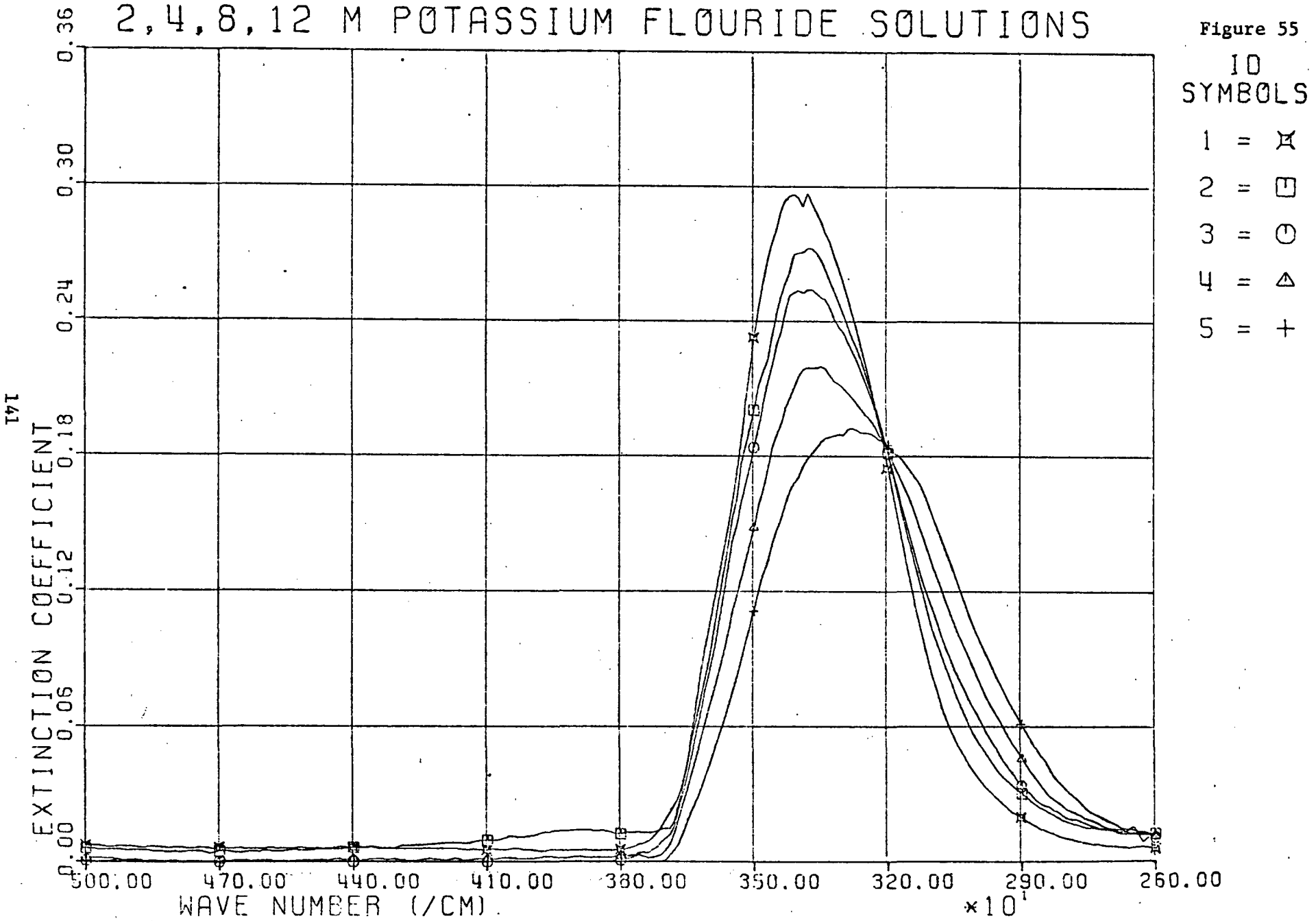
2,4,8,12 M POTASSIUM FLOURIDE SOLUTIONS
EXTINCTION COEFFICIENT
0.00
0.06
0.12
0.18
0.24
0.30
0.36
500.00
470.00
440.00
410.00
380.00
350.00
320.00
290.00
260.00
WAVE NUMBER (/CM)
×10¹
ID SYMBOLS
1 =
2 =
3 =
4 =
5 =

Figure 55

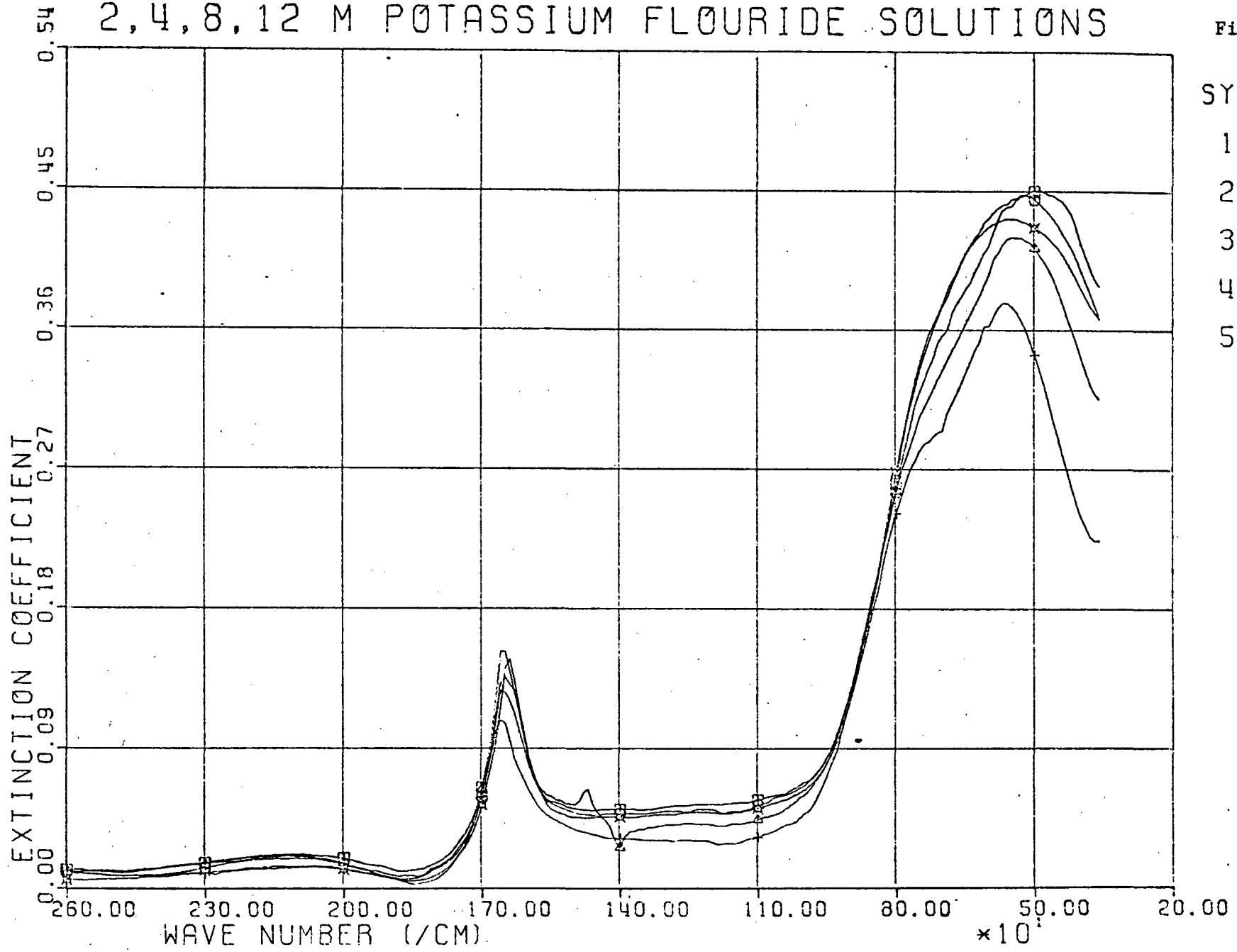
2,4,8,12 M POTASSIUM FLOURIDE SOLUTIONS
EXTINCTION COEFFICIENT
0.00
0.09
0.18
0.27
0.36
0.45
0.54
260.00
230.00
200.00
170.00
140.00
110.00
80.00
50.00
20.00
WAVE NUMBER (/CM)
*10
ID SYMBOLS
1 =
2 =
3 =
4 =
5 =

Figure 56

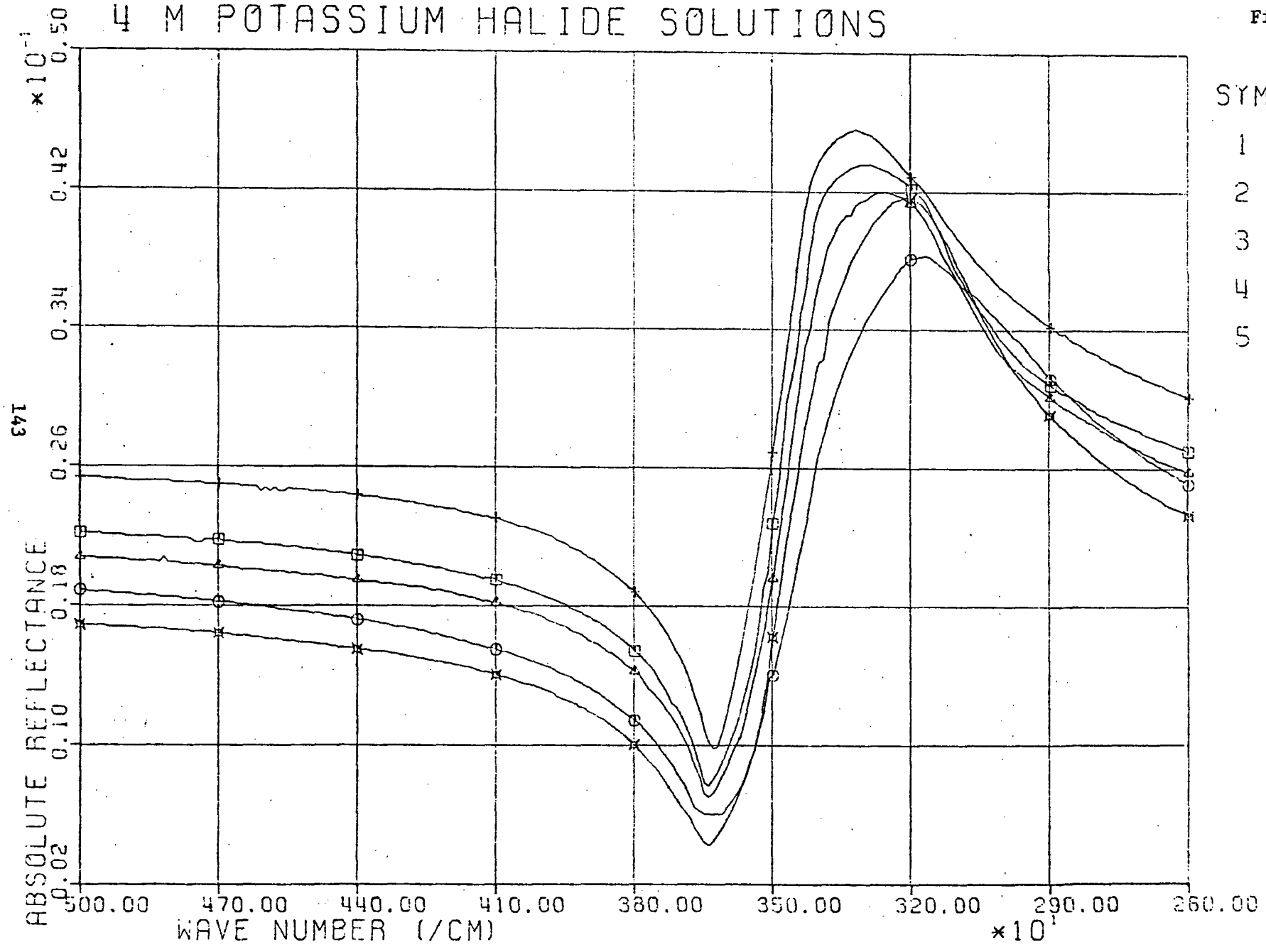
4 M POTASSIUM HALIDE SOLUTIONS
ABSOLUTE REFLECTANCE
*10⁻¹
0.50
0.42
0.34
0.26
0.18
0.10
0.02
500.00
470.00
440.00
410.00
380.00
350.00
320.00
290.00
260.00
WAVE NUMBER (/CM)
*10¹
ID SYMBOLS
1 =
2 =
3 =
4 =
5 =

Figure 57

Figure 58

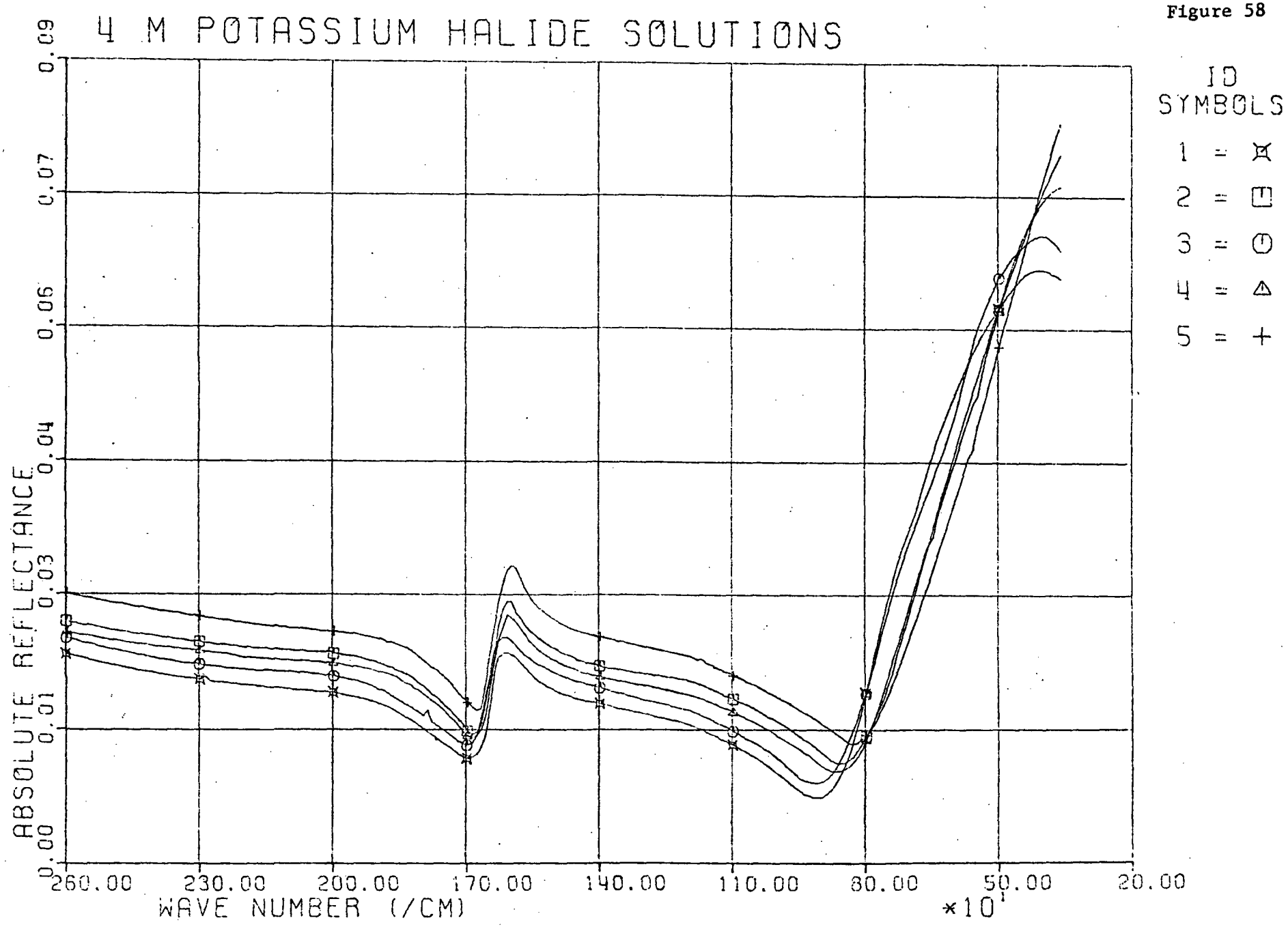
4 M POTASSIUM HALIDE SOLUTIONS
ID SYMBOLS
1 =
2 =
3 =
4 =
5 =
ABSOLUTE REFLECTANCE
0.00
0.01
0.03
0.04
0.06
0.07
0.09
260.00
230.00
200.00
170.00
140.00
110.00
80.00
50.00
20.00
WAVE NUMBER (/CM)
*10

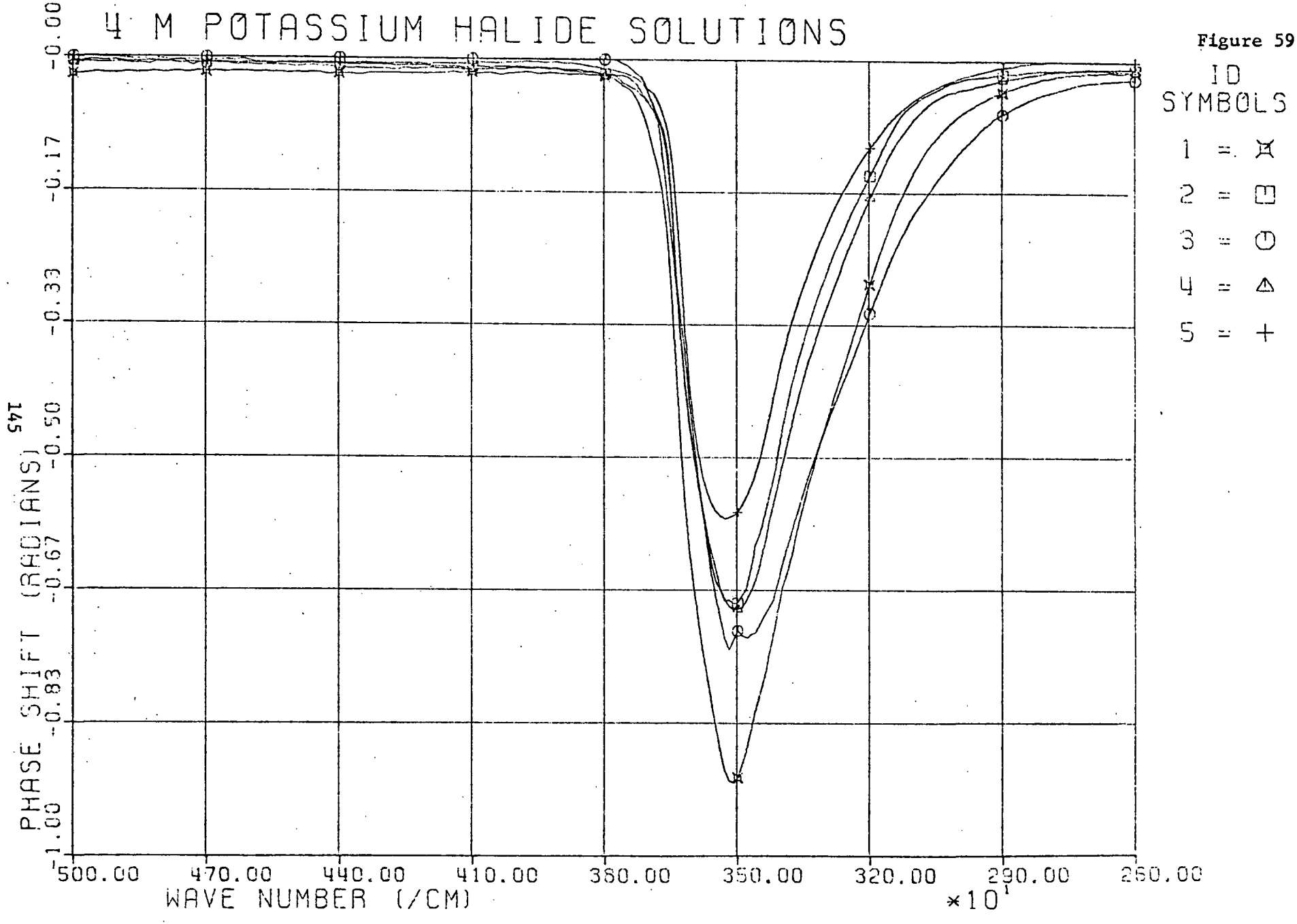
4 M POTASSIUM HALIDE SOLUTIONS
ID SYMBOLS
1 =
2 =
3 =
4 =
5 =
PHASE SHIFT (RADIANS)
-0.00
-0.17
-0.33
-0.50
-0.67
-0.83
-1.00
500.00
470.00
440.00
410.00
380.00
350.00
320.00
290.00
260.00
WAVE NUMBER (/CM)
*10

Figure 59

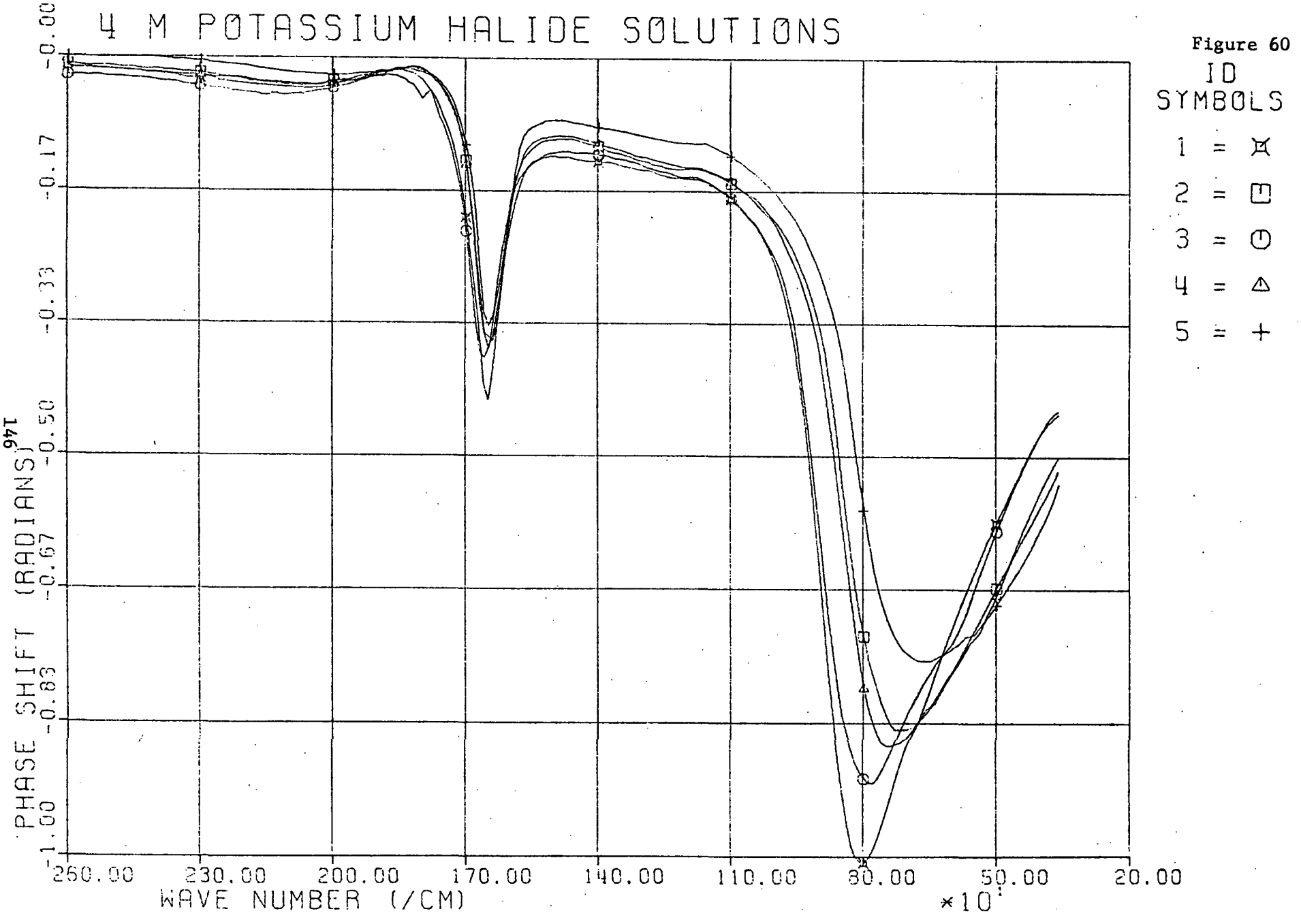
4 M POTASSIUM HALIDE SOLUTIONS
-0.00
-0.17
-0.33
-0.50
-0.67
-0.83
-1.00
PHASE SHIFT (RADIANS)
260.00
230.00
200.00
170.00
140.00
110.00
80.00
50.00
20.00
WAVE NUMBER (/CM)
*10
ID SYMBOLS
1 =
2 =
3 =
4 =
5 =

Figure 60

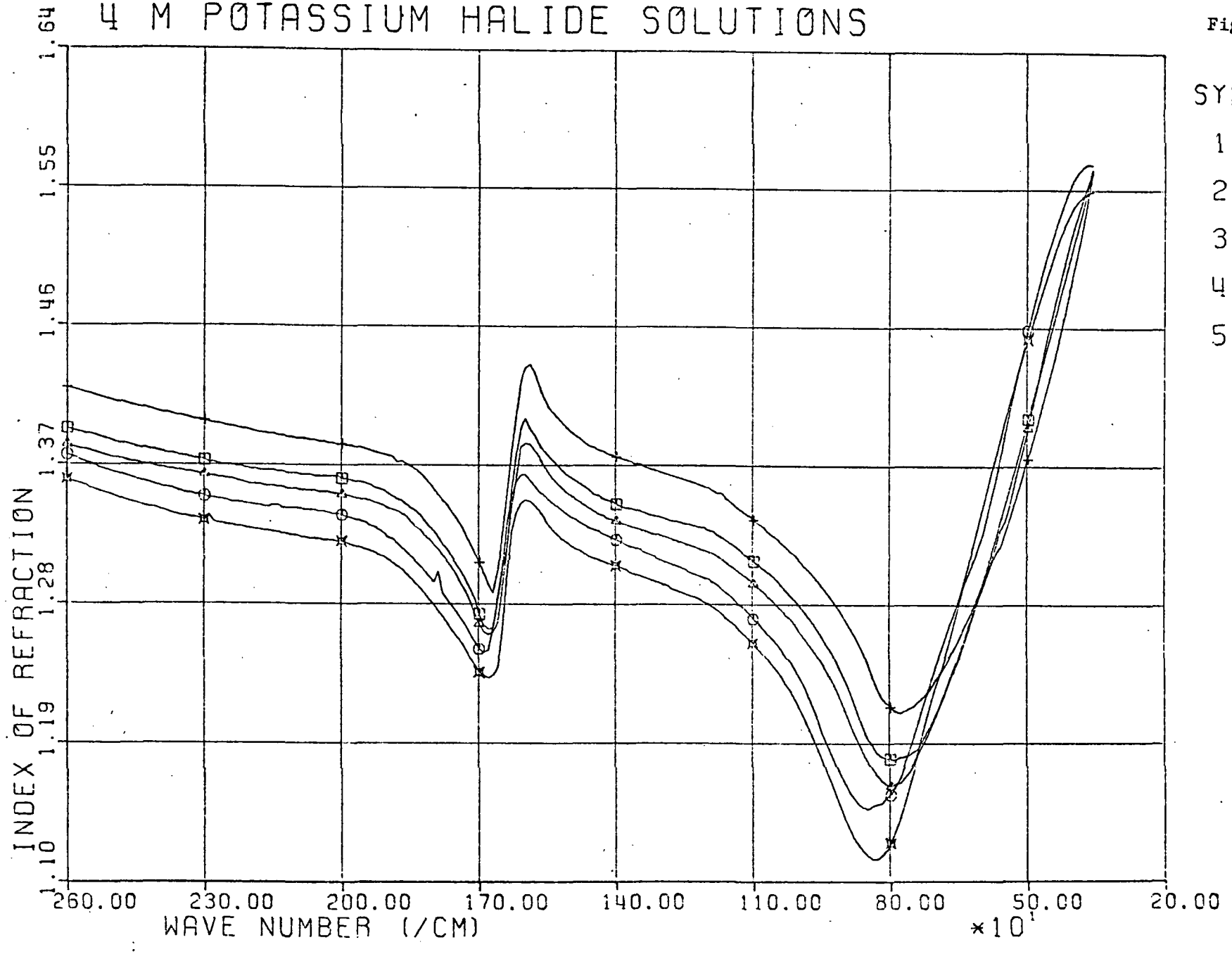
4 M POTASSIUM HALIDE SOLUTIONS
INDEX OF REFRACTION
1.64
1.55
1.46
1.37
1.28
1.19
1.10
260.00
230.00
200.00
170.00
140.00
110.00
80.00
50.00
20.00
WAVE NUMBER (/CM)
*10
ID SYMBOLS
1 =
2 =
3 =
4 =
5 =

Figure 61

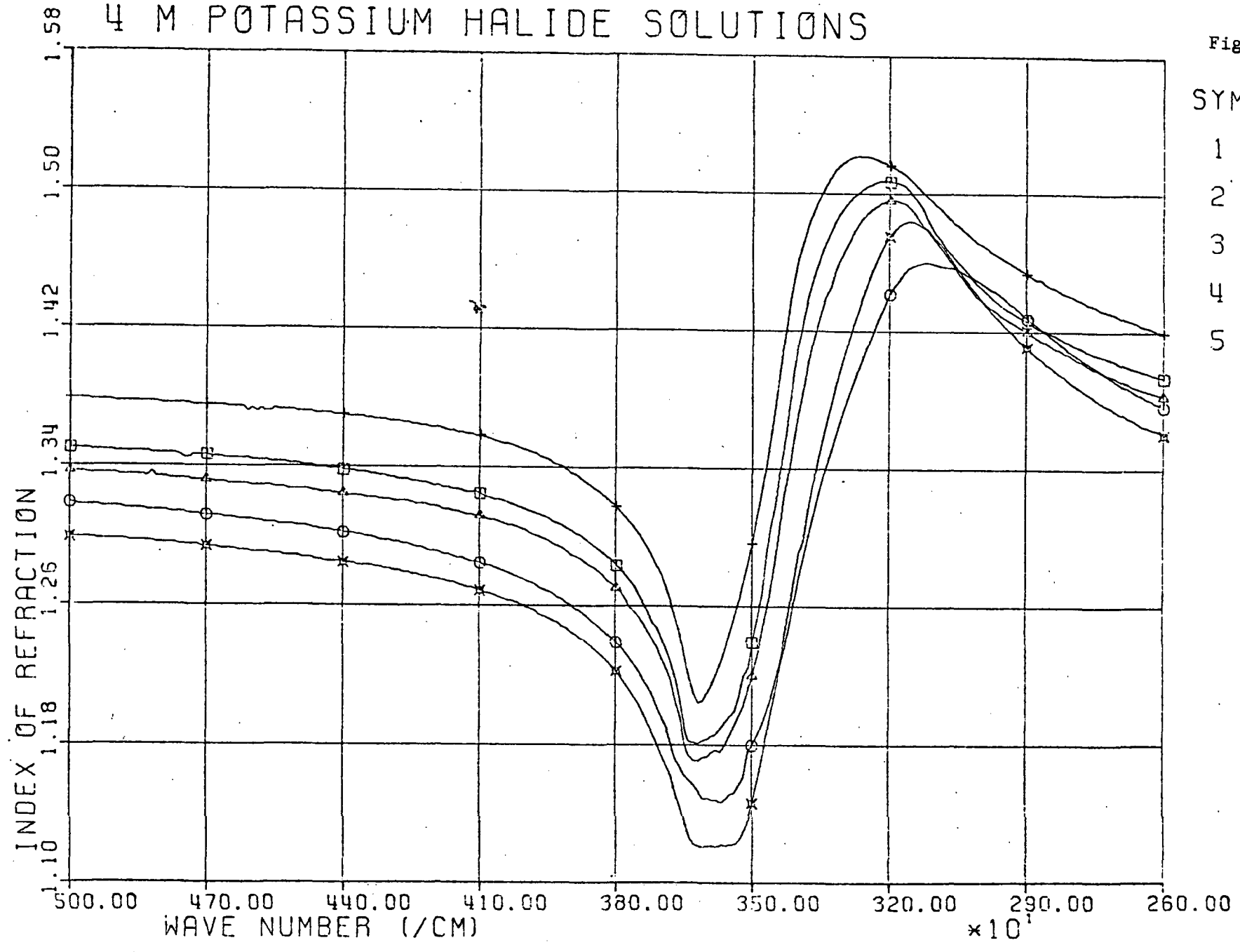
4 M POTASSIUM HALIDE SOLUTIONS
INDEX OF REFRACTION
1.58
1.50
1.42
1.34
1.26
1.18
1.10
500.00
470.00
440.00
410.00
380.00
350.00
320.00
290.00
260.00
WAVE NUMBER (/CM)
×10¹
ID SYMBOLS
1 =
2 =
3 =
4 =
5 =

Figure 62

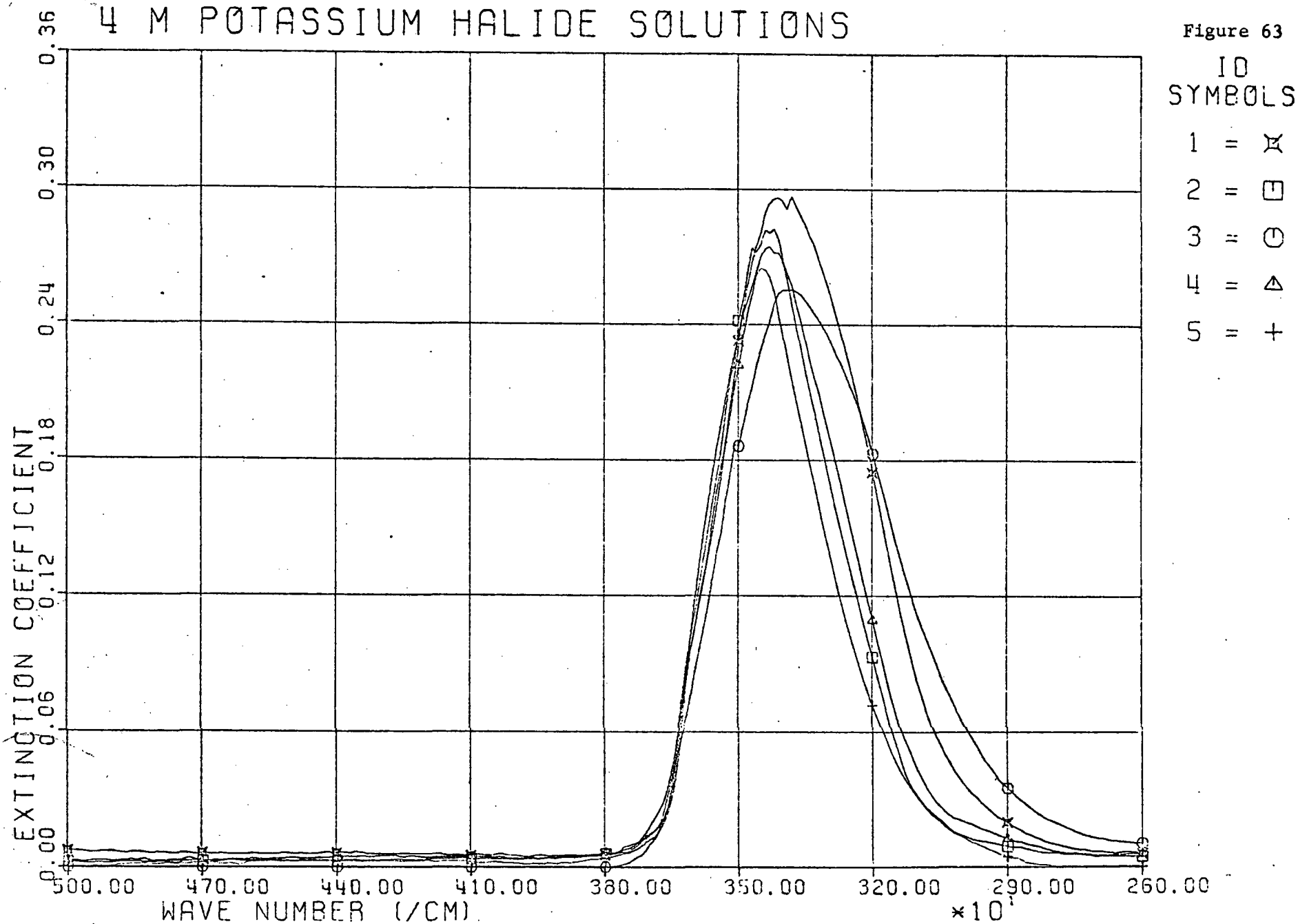
4 M POTASSIUM HALIDE SOLUTIONS
EXTINCTION COEFFICIENT
0.00
0.06
0.12
0.18
0.24
0.30
0.36
500.00
470.00
440.00
410.00
380.00
350.00
320.00
290.00
260.00
WAVE NUMBER (/CM)
×10
ID SYMBOLS
1 =
2 =
3 =
4 =
5 =

Figure 63

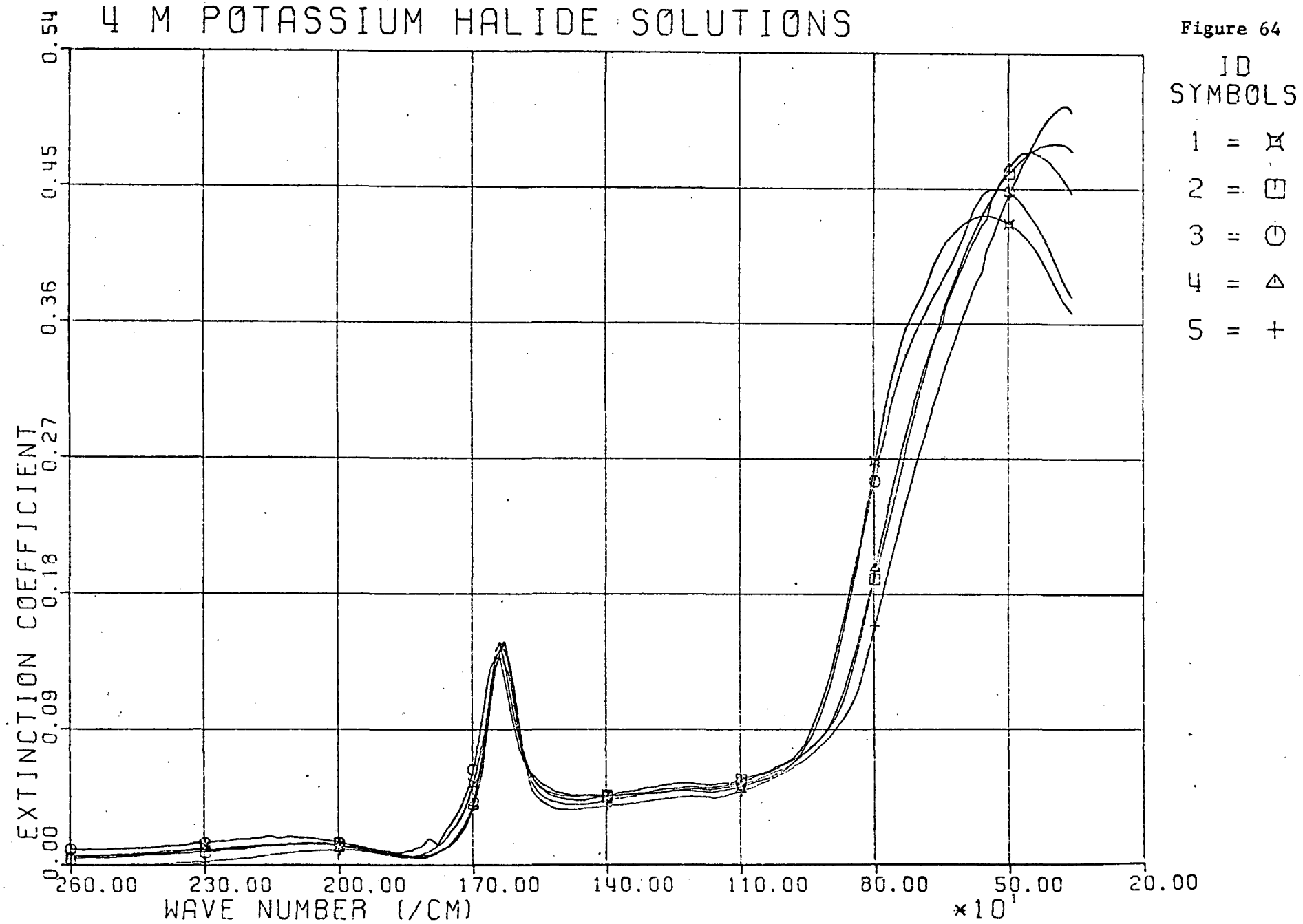
4 M POTASSIUM HALIDE SOLUTIONS
ID SYMBOLS
1 =
2 =
3 =
4 =
5 =
EXTINCTION COEFFICIENT
0.00
0.09
0.18
0.27
0.36
0.45
0.54
260.00
230.00
200.00
170.00
140.00
110.00
80.00
50.00
20.00
WAVE NUMBER (/CM)
*10^1

Figure 64

APPENDIX

LIST OF LASING ORGANIC DYES

Compiled by Wayne E. Holland
Department of Physics
University of Missouri-Kansas City

Definitions of Symbols:

Name = name of organic dye

Ref. = number given to reference from which information was obtained; see list of references at end of table.

Pumping:= F = flash lamp

Nd = neodynium laser

2nd = 2nd harmonic from Nd laser

3nd = 3rd harmonic from Nd laser

4nd = 4th harmonic from Nd laser

R = ruby laser

2R = 2nd harmonic from ruby laser

N = nitrogen laser

Solvent: W = water

M = methanol

E = ethanol

DMF = dimethyl formamide

DMSO = dimethyl sulfoxide

T = toluene

I = isoamyl alcohol

D = dioxane

B = benzene

S = sulfuric acid

G = glycerol

A = acetone

P = pyridine

C = cyclohexane

PMM = polymethylmethacrylate

λ_M = wavelength of maximum laser intensity

λ_C = central wavelength of laser spectral band

Range = spectral range of tunability or spectral band width in Angstrom units.

Name	Ref.	Pumping	Solvent	Conc. of Dye	λ_M or λ_C	Range
Acetamidopyrene Trisulfonate	33	F	W or M	10^{-3}M		
7-Acetoxy-6-allyl-4,8-dimethylcoumarin	16	F	E+NaOH	50mg/l	4750	4580-5140
7-Acetoxy-4-methylcoumarin	16	F	E+NaOH	50mg/l	4600	4410-4860
Acridine Red	2	2Nd	E	10^{-4}M	5840	
		F		$5X10^{-5}$M	6150	
	38	2R	E	10^{-3}M	5800	
	40,39	F	E	10^{-4}M	6015	
	35	F	E	10^{-4}M	6050	
	4	N	E			6015-6250
	21	N	E	$5X10^{-3}$M	5877	
				10^{-3}M	5839	
			DMF	$5X10^{-3}$M	5730	
				10^{-3}M	5760	
	16	F	E	50mg/l	6100	5840-6320
					6090	5820-6340
Acridone (see 9,10-Dihydro-9-oxoacridine)						
Acriflavine	14	F	E	$3.6X10^{-2}$M	5174	
Acriflavine HCl	22	2R	E		5100	
Aluminum Phthalocyanine Chloride (CAP)	38	R	1-Propanol	10^{-3}M	7550	
			E		7555	
			DMSO		7615	
			Ethylene Glycol		7630	
	40	R	E	$8X10^{-5}$-$3X10^{-4}$M	7550	
9-Aminoacridine HCl	17	F	E,W pH 7			4570-4600

Name	Ref.	Pumping	Solvent	Conc. of Dye	λ_M or λ_C	Range
Aminobenzoic Acid	25	N	T			3980-4060
3-Aminofluoranthene	23	F	E@0.0 atm pp O_2	60mg/l		5480-5800
3-Aminophthalimide	28	2R	I		5000	4965-5035
Aquafluor	13	F	E,D	1 part in 5	4200	
BBO (see 2,5-Dibiphenylyl-oxazole						
BBOT (see 2,5-Bis(5-tert-butyl-benzoxazolyl(2))thiopene						
BBP (see Dibiphenylylbenzene)						
BOPOB (see 1,4-Bis(2-(5-biphenyl-oxazolyl))benzene)						
Benzyl-β-methylumbelliferone	17	F	E,W pH>7			4635-4680
3-Benzyl-4-methylumbelliferone	16	F	E+NaOH	50mg/l	4680	4490-4850
2-Biphenyl-5-styryl-1,3,4-oxadiazole	1	3Nd	T	$3.1X10^{-3}M$	3905	3870-3940
			B	$3.1X10^{-3}M$	3915	3890-3940
Bis MSB (see p, p'-Bis(o-methyl-styryl)benzene)						
1,4-Bis(2-(5-biphenyloxazolyl)) benzene (BOPOB)	25	N	Tetrahydrafuran			4280-4500
2,5-Bis(tert-butyl-benzoxazolyl(2))thiopene (BBOT)	14	F	B	$5X10^{-4}M$	4370	

Name	Ref.	Pumping	Solvent	Conc. of Dye	λ_M or λ_C	Range
1,4-Bis(2-(4-methyl-5-phenyloxazolyl))benzene (see 2,2'-p-Phenylene bis(4-methyl-5-phenyl)oxazole)						
p,p'-Bis(o-methylstyryl)benzene	6	2R	E	10^{-4}M	4190	4145-4235
				10^{-3}M	4190	4160-4250
			B	10^{-3}M	4250	4233-4267
	13	F	T	$4X10^{-4}$M	4240	
1,4-Bis(2-(5-α-napthyloxazolyl)) benzene (α-NOPON)	25	N	B			4300-4550
1,4-Bis(2-(5-phenyloxazolyl)) benzene (see2,2'-p-Phenylene bis(5-phenyloxazole))						
Blatt Grun	27	R	S		8000	7830-8170
Brilliant Green	27	R	G		7590	7345-7835
Brilliant Sulphaflavine	23	F	E@0.0 atm pp O_2			5080-5730
Calcein Blue	23	F	E pH>7 @0.0-0.2 atm pp O_2	150mg/l		4490-4900
6-Carboxyfluorescein	23	F	E pH>7 @0.0-0.08 atm pp O_2	30mg/l		5390-5480
Chloro-aluminum Phthalocyanine (see Aluminum Phthalocyanine Chloride)						
Cresyl Violet	23	F	E@0.2 atm pp O_2	100mg/l		6460-7090
Cryptocyanine (see 1,1'-Diethyl-4,4'-carbocyanine Iodide)						

Name	Ref.	Pumping	Solvent	Conc. of Dye	λ_M or λ_C	Range
DDI (see 1,1'-Diethyl-2,2'-dicarbocyanine Iodide)						
DODC (see 3,3'-Diethyl oxodicarbocyanine Iodide)						
DTDC (see 3-Ethyl-2-(5-(3-ethyl-2-benzothiazolinylidene)))						
DTTC (see 3,3'-Diethyl thiatricarbocyanine Iodide)						
Dibiphenylbenzene (BBP)	25	N	B			4000-4159
1,2-Di-4-biphenylylethylene	19	3Nd	T		4080	4063-4097
2,5-Dibiphenylyloxazole (BBO)	6	2R	B	10^{-3}M	4085	4068-4102
	3	N	T	10^{-3}-10^{-4}M	4085	4010-4195
	14	F	B	0.05 S	4100	
	25	N	E			3640-3850
	21	N	DMF	$3X10^{-4}$M	4133	
				$6X10^{-5}$M	4137	
2,5-Di(biphenyl)-1,4-oxazole	1	3Nd	T	$0.7\text{-}2.6X10^{-3}$M	4090	4060-4120
Dibromofluorescein	28	2R	G		5680	
4,4"-Dichlor-1,4-distyrylbenzene	19	3Nd	T		4200	4193-4207
2,7-Dichlorofluorescein	21	N	E+$2X10^{-3}$M NaOH	$1.5X10^{-3}$M	5363	
			E+10^{-3}M NaOH	$3X10^{-4}$M	5442	
	16	F	E+NaOH	50mg/1	5810	5605-5930
2',7'-Dichlorofluorescein	39	F	E			
Dicyanine	27	R	G		7560	7500-7620
			Isobutanol		7650	
			Quinoline		7230,7520	

Name	Ref.	Pumping	Solvent	Conc. of Dye	λ_M or λ_C	Range
1,1'-Diethyl-γ-acetoxy-2,2'-dicarbocyanine Tetrafluoroborate	31	R	M	10^{-3}-10^{-6}M	7970	
7-Diethylamino-4-methylcoumarin	17	2R	E	$2X10^{-3}$M	4550	4450-4750
	11	F	E	10^{-4}M		
	15	F	E	$2X10^{-4}$M		4396-4970
	3	N	E	10^{-2}-10^{-3}M	4555	4385-4820
	26	N	W,E, or T	10^{-2}-10^{-4}M		4450-4900
	4	N	W			4440-4840
	16	F	Isopropyl Alcohol	50mg/1	4550	4360-4800
1,1'-Diethyl-11-bromo-2,2'-quinodicarbocyanine Iodide	24	R	G	10^{-4}M	8150	
1,1'-Diethyl-11-bromo-4,4'-quinodicarbocyanine Iodide	24	R	M	10^{-4}M	8300	
1,1'-Diethyl-4,4'-carbocyanine Iodide (Cryptocyanine)	42	R	G			7500-7900
	48	R	E	10^{-5}M	7370	
3,3'-Diethyl-10-chloro-2,2'-(4,5,4',5'-dibenzo) thiadicarbocyanine Iodide	24	R	A	10^{-4}M	7740	
3,3'-Diethyl-10-chloro-2,2'-(5,5,5',6'-dibenzo) thiadicarbocyanine Iodide	24	R	A	10^{-4}M	7140	
1,1'-Diethyl-γ-cyano-2,2'-dicarbocyanine Tetrafluoroborate	31	R	M	10^{-3}-10^{-6}M	7400	

Name	Ref.	Pumping	Solvent	Conc. of Dye	λ_M or λ_C	Range
3,3'-Diethyl-6,7,6',7'-dibenzo-11-methythiotricarbocyanine Iodide	5	R	E	10^{-5}M		8430-8690
3,3'-Diethyl-2,2'-(4,5,4',5'-dibenzo)thiatricarbocyanine Iodide	24	R	A	10^{-4}M	8600	
3,3'-Diethyl-6,7,6',7'-dibenzothiotricarbocyanine Iodide	5	R	E	10^{-5}M		8240-8530
1,1'-Diethyl-2,2'-dicarbocyanine Iodide	42	R	G			7500-7900
3,3'-Diethyl-2,2'-(5,5'-dimethyl)thiazolinotricarbocyanine Iodide	24	R	G	10^{-4}M	7170	
3,3'-Diethyl-5,5'-dimetoxy-6,6'-bis(methylmercapto)-10-methylthiodicarbocyanine Bromide	5	R	M	10^{-5}M		7270-7390
3,3'-Diethyl-9,12-epoxy-thiatricarbocyanine Iodide	48	R	E	10^{-5}M	7840	
3,3'-Diethyl-12-ethyl-thiotetracarbocyanine Iodide	5	R	E	10^{-5}M		9160-9240
1,1'-Diethylindotricarbocyanine Iodide	48	R	E	10^{-5}M	8040	
3,3'-Diethyl-11-metoxy-thiotricarbocyanine Iodide	5	R	E	10^{-5}M		7730-7980

Name	Ref.	Pumping	Solvent	Conc. of Dye	λ_M or λ_C	Range
1,1'-Diethyl-γ-nitro-4,4'-dicarbocyanine Tetrafluoroborate	31	R	M	10^{-4}M	7960	
			E		8050	
			A		8140	
			DMF		8150	
			P		8210	
			Benzonitrile		8220	
3,3'-Diethyloxadicarbocyanine Iodide (DODC)	30	2Nd	M	10^{-3}M	6580	
3,3'-Diethyl-2,2'-oxa-tricarbocyanine Iodide	24	R	A	10^{-4}M	7420	
	49	R	E	$2X10^{-6}$M	7160	
3,3'-Diethyloxytricarbocyanine Iodide	5	R	E	10^{-5}M		7180-7390
3,3'-Diethyl-9,11,13(penta-1",3",5"-triyl)-thiathiazolino-tricarbocyanine Iodide	48	R	E	10^{-5}M	7240	
3,3'-Diethyl-9,11,13(penta-1",3",5"-triyl)-thiatricarbo-cyanine Iodide	48	R	E	10^{-5}M	7960	
1,1'-Diethyl-4,4'-quinocarbo-cyanine Bromide	24	R	G	10^{-4}M	7540	
1,1'-Diethyl-4,4'-quino-carbocyanine Iodide (Cryptocyanine)	24	R	G	10^{-4}M	7510	
	49	R	E	$2X10^{-6}$M	7260	
1 1'-Diethyl-2,2'-quino-tricarbocyanine Iodide	24	R	A	10^{-4}M	8980	

Name	Ref.	Pumping	Solvent	Conc. of Dye	λ_M or λ_C	Range
1,1'-Diethylquino-2,2'-tricarbocyanine Iodide	5	R	E	10^{-5}M		8860-8980
1,1'-Diethyl-4,4'-quino-tricarbocyanine Iodide	24	R	A	10^{-4}M	10000	
3,3'-Diethyl-2,2'-selena-tricarbocyanine Iodide	24	R	A	10^{-4}M	8260	
	49	R	E	$2X10^{-6}$M	8100	
3,3'-Diethyl-2,2'-(5,6,5',6'-tetramethoxy)thiatricarbo-cyanine Iodide	24	R	A	10^{-4}M	8530	
3,3'-Diethylthiadicarbocyanine Iodide	31	R	M	10^{-4}M	7310	
3,3'-Diethyl-2,2'-thiatricarbo-cyanine Iodide	49	R	E	$2X10^{-6}$M	8010	
3,3'-Diethylthiatricarbo-cyanine Bromide	31	R	M	10^{-4}M	8350	
			A			
	48	R	E	10^{-5}M	8160	
3,3'-Diethylthiatricarbocyanine Iodide (DTTC)	9	R	DMSO	10^{-4}M		7500-9330
	37	R	M,E		8160	
	38	R	M	10^{-5}M	7960	
			A		8015	
			E		8030	
			1-Propanol		8070	
			Ethylene Glycol		8080	
			DMF		8080	
			G		8095	
			Butyl Alcohol		8095	
			DMSO		8160	
	5	R	E	10^{-5}M		7910-8240

Name	Ref.	Pumping	Solvent	Conc. of Dye	λ_M or λ_C	Range
1,2-Dihydro-4-methoxybenzo (C)xanthylium Fluoroborate	8	F			5580	
9,10-Dihydro-9-oxoacridine	13	F	E		4350	
	38	2R	E	$>10^{-3}$M	4370	
Dimethyl POPOP (see 2,2'-p-Phenylenebis(4-methyl-5-phenyl)oxazole						
2,2"-Dimethoxy-1,4-distryl-benzene	19	3Nd	T		4300	4285-4315
1,1'-Dimethyl-11-bromo-2,2'-quinodicarbocyanine Iodide	24	R	G	10^{-4}M	7450	
4,8-Dimethyl-7-hydroxycoumarin	16	F	E+NaOH	50mg/l	4700	4550-5050
3,3'-Dimethyl-2,2'-oxatri-carbocyanine Iodide	24	R	A	10^{-4}M	7440	
3,3'-Dimethyl-9,11(o-phenylene) thiadicarbocyanine Iodide	48	R	E	10^{-5}M	8080	
1,1'-Dimethyl-4,4'-quino-carbocyanine Iodide	24	R	G	10^{-4}M	7490	
1,2-Di-(α-naphthyl)-ethylene	19	3Nd	T		4260	4243-4277
2,5-Di-(α-naphthyl)-1,3,4-oxadiazole (α-NND)	1	3Nd	T	$3.1X10^{-3}$M	3910	3885-3935
			B	$3.1X10^{-3}$M	3910	3885-3935
9,10-Diphenylanthracene	18	2R	C	10^{-2}M	4326	
Diphenylanthracene	25	N	E		4350	
	26	N	W,E, or T	10^{-2}-10^{-4}M		4350-4500

Name	Ref.	Pumping	Solvent	Conc. of Dye	λ_M or λ_C	Range
Diphenylbutadiene	1	3Nd	T	$2.9X10^{-3}M$	3830	3820-3840
2,5-Diphenylfuran (PPF)	3	N	B	10^{-2}-$10^{-3}M$	3735	3690-3795
			E			
	14	F	DMF	$4X10^{-4}M$	3710	
			D		3710	
	28	N	E			3650-3710
1,3-Diphenylisobenzofuran	23	F	E@0.0 atm pp O_2	75mg/l		4840-5180
2,5-Diphenyloxazole (PPO)	3	N	T	10^{-2}-$7X10^{-4}$	3635, 3800	3585-3905
			B	$2X10^{-3}$-$5X10^{-3}M$		
			D	$2X10^{-3}$-$2X10^{-4}M$		
	14	F	D	$7X10^{-3}M$	3810	
	21	N	C	$10^{-3}M$	3570	
				$2X10^{-4}M$	3570	
1,4-Di-(2-(5-phenyloxazyl))-benzene	19	3Nd	T		4170	4155-4185
2,5-Diphenyl-1,3,4-oxydiazole (PPD)	14	F	D	$9X10^{-3}M$	3480	
	25	N	E			3830-3950
Diphenyl Stilbene	25	N	T			4000-4150
			B			4000-4150
	26	N	W,E, or T	10^{-2}-$10^{-4}M$		4000-4200
p,p'-Diphenylstilbene	6	2R	B	$10^{-3}M$	4085	4065-4125
	14	F	B	0.66 S	4090	
			DMF	0.66 S	4090	
3,3'-Diprophylenyl-5,6,5',6'-tetramethoxy-2,2'-thiadicarbocyanine Iodide	49	R	E	$2X10^{-6}M$	7340	

Name	Ref.	Pumping	Solvent	Conc. of Dye	λ_M or λ_C	Range
1,4-Distyrylbenzene	19	3Nd	T		4150	4138-4162
	1	3Nd	T	$1.6X10^{-3}M$	4110, 4170	4090-4130, 4150-4190
Echtblau B	27	R	G		7530	7365-7695
Eosin	38	2R	E	$10^{-3}M$	5400	
	28	2R	E		6000	
	21	N	E+$3X10^{-3}M$ NaOH	$2.5X10^{-3}M$	5577	
			E+$10^{-3}M$ NaOH	$5X10^{-4}M$	5587	
			DMF	$2.5X10^{-3}M$	5680	
			DMF	$5X10^{-4}M$	5705	
Esculin	39	F	W			
	4	N	W			4640-4810
	16	F	E+NaOH	50mg/1	4640	4500-4900
7-Ethylamino-4,6-dimethyl-coumarin	43	F	E		4460	
			E+HCl		4870	
3-Ethylaminopyrene-5,8,10-trisulfonic Acid	30	2R	W	$2.5X10^{-3}M$	4410	
3-Ethyl-2-(5-(3-ethyl-2-benzothiazolinylidene)-1,3-pentadienyl)-benzothiazolium Iodide (DTDC)	18	R				7100-7300
3-Ethyl-3'-methylthiathiazolinotricarbocyanine Iodide	5	R	E	$10^{-5}M$		7380-8010
Fluorescein	10	2R	W	$3X10^{-4}M$	5450	5300-5700
			E	$10^{-3}M$	5500	5400-5800
		2Nd			5500	5420-5800
	26	N	W,E, or T	10^{-2}-$10^{-4}M$		5200-6000
	30	2R	W+NaOH	$10^{-2}M$	5390	

Name	Ref.	Pumping	Solvent	Conc. of Dye	λ_M or λ_C	Range
Fluorescein - continued	19	3Nd	Aqueous Alkaline		5480	5465-5495
	20	N	E	$5X10^{-4}M$		
	21	N	E+$3X10^{-3}$M NaOH	$2.5X10^{-3}M$	5377	
			E+10^{-3}M NaOH	$5X10^{-4}M$	5385	
Fluorescein Diacetate	16	F	E+NaOH	50mg/1	5500	5420-5720
Fluorescein Disodium Salt	2	R	E	$10^{-4}M$	5370	
		F		$5X10^{-5}M$	5600	
	22	2R	W		5350	
	16	F	E	50mg/1	5550	5430-5770
1,3,3,1',3',3'-Hexamethyl-4,5,4'5'-dibenzoindotricarbocyanine Perchlorate	5	R	E	$10^{-5}M$		8160-8330
1,3,3,1',3',3'-Hexamethylindrotricarbocyanine Iodide	5	R	E	$10^{-5}M$		7790-8080
1,3,3,1',3',3'-Hexamethyl-2,2'-indotricarbocyanine Iodide	24	R	A	$10^{-4}M$	8190	
7-Hydroxycoumarin	35	F	W	$10^{-4}M$	4570	
2-Hydroxy-4-methyl-7-aminoquinoline	43	F	E		4130	
7-Hydroxy-4-methylcoumarin (4MU)	10	2R	W	$10^{-3}M$	4550	4300-4850
	34	N	E/various pH			3850-5740
	36	F	W pH>9	$4X10^{-3}M$	4500	4000-5500
	4	N	E			4375-5380
	16	F	E+NaOH			
8-Hydroxy-1,3,6-pyrenetrisulfonic Acid Trisodium Salt	8	F			5500	

Name	Ref.	Pumping	Solvent	Conc. of Dye	λ_M or λ_C	Range
Isopropyl PBD (see Isopropyl-2-phenyl-5(4-biphenylyl)-1,3,4-oxadiazole)						
Isopropyl-2-phenyl-5 (4-biphenylyl)-1,3,4-oxadiazole	14	F	E	$8X10^{-4}M$	3698	
			C	$8X10^{-4}M$	3610	
Isoquinoline Red	28	2R	W		6200	
Kiton Red S	16	F	E	50mg/1	6100	5960-6500
					6030	5900-6420
Lachs	45	2R	G		5400	5375-5425
Liquifluor	13	F	E	1 part in 10	4220	
Lissamine Rhodamine B-200	23	F	E@0.08 atm pp O_2	100mg/1		5750-6450
Lucegenin	28	2R	W+H_2SO_4		6000	5940-6060
Magnesium Phthalocyanine	46	R	Quinoline		7590	7585-7595
7-Methylamino-4,6-dimethyl-coumarin	43	F	E		4430	
			E+HCl		4840	
7-N-Methylamino-4,6-dimethyl-coumarin	43	F	E		4430	
			E+HCl(75% acidified)		4760	
			E+HCl(100% acidified)		4830	
Methylene Blue	27	R	S		8290	8255-8325
	46	R	S		8350	8330-8370
Methylene Green	27	R	S		8230	8130-8330

Name	Ref.	Pumping	Solvent	Conc. of Dye	λ_M or λ_C	Range
4-Methylumbelliferone (see 7-Hydroxy-4-methylcoumarin)						
4,8-Methylumbelliferone (see 4,8-Dimethyl-7-Hydroxycoumarin)						
4-Methylumbelliferone Methyleneiminodiacetic Acid	23	F	E pH 7 @0.2 atm pp O_2	100mg/l		4590-4640
Monobromofluorescein	28	2R	G		5600	
α-NND (see 2,5-Di-(α-naphthyl) -1,3,4-oxadiazole)						
α-NOPON (see 1,4-Bis(2-(5-α-napthyloxazolyl))benzene)						
α-NPO (see 2-(1-Naphthyl)-5-phenyloxazole)						
2-(1-Naphthyl)-5-phenyl-oxazole (α-NPO)	6	2R	E	10^{-3}M	3975	3940-4010
			C		3930	3923-3938
			B		4020	4000-4040
	26	N	W,E, or T	10^{-2}-10^{-4}M		3900-3950
	3	N	E	10^{-2}M	3970	3920-4135
			T			
			B			
			C			
	14	F	E	$2.5X10^{-4}$M	4000	
	25	N	B			3975-4100
			C			3850-4150
	21	N	C	$5X10^{-4}$M	3926	
				10^{-4}M	3923	
Naphthalene Green	27	R	G		7560	7340-7780

Name	Ref.	Pumping	Solvent	Conc. of Dye	λ_M or λ_C	Range
PBD (see 2-Phenyl-5 (4-biphenylyl)-1, 3, 4-oxadiazole)						
POPOP (see 2,2'-p-Phenylene bis(5-phenyloxazole))						
PPD (see 2,5-Diphenyl-1,3,4-oxadiazole)						
PPF (see 2,5-Diphenylfuran)						
PPO (see 2,5-Diphenyloxazole)						
Para-terphenyl	1	4Nd	C	$1.3X10^{-3}M$	3410	3380-3440
Perylene	21	N	DMF	$6.5X10^{-3}M$	4720	
				$1.3X10^{-3}M$	4710	
			C	$1.7X10^{-4}M$	4656	
2-Phenyl-5(4-biphenylyl)-1,3,4-oxadiazole (PBD)	3	N	T	$4X10^{-2}$-$4X10^{-4}M$	3850,3985	3770-4150
	14	F	E	0.1 S	3625	
	25	N	E			3550-3820
2,2'-p-Phenylene bis (4-methyl-5-phenyl) oxazole (Dimethyl POPOP)	6	2R	C	$10^{-3}M$	4230	4220-4240
			E		4310	4270-4350
	3	N	B	$5X10^{-3}$-$5X10^{-4}M$	4295	4235-4410
			T	$5X10^{-3}$-$5X10^{-5}M$		
			C	$10^{-4}M$		
2,2'-p-Phenylene bis (5-phenyloxazole) (POPOP)	6	2R	C	$10^{-3}M$	4105	4080-4130
			E		4210	4160-4260
	10	2R	E	$10^{-3}M$	4300	4200-4460

Name	Ref.	Pumping	Solvent	Conc. of Dye	λ_M or λ_C	Range
2,2'-p-Phenylene bis (5-phenyloxazole) (POPOP) continued	13	F	T	$3.4X10^{-4}M$	4190	
	3	N	B	10^{-3}-$10^{-4}M$		
			T	10^{-3}-$10^{-5}M$	4190	4120-4310
			C	$5X10^{-5}M$		
			D	10^{-2}-$10^{-3}M$		
	25	N	Tetrahydrofuran			4150-4300
	26	N	W,E, or T	10^{-2}-$10^{-4}M$		3900-4450
	4	N	B			4140-4250
2-Phenyl-5-α-naphthyl-1,4-oxazole	1	3Nd	T	$3.7X10^{-3}M$	3995	3960-4025
Phthalocyanine	46	R	S		8630	8625-8635
Pina(orthol)	28	2R	E		5650	5610-5690
Pyronin B	10	2Nd	E	$2X10^{-3}M$	5850	5700-6400
	32	F	W,E	$10^{-3}M$		
	19	2Nd	A,PMM		5760	5740-5780
	17	F	E			6150-6320
	16	F	E+HCl	50mg/1	6160	6005-6400
					6270	6140-6340
Pyronin G	47,28	2R,2Nd	I		5900	5840-5960
	47	F	I		5850	5785-5915
Pyronin Y	23	F	E pH<7 @1.0 atm pp O_2	100mg/1		5900-6350
Pyrylium Salt	29		M			Green
p-Quaterphenyl	14	F	DMF	$7X10^{-3}M$	3740	
	25	N	T			3620-3900
Rapid-filter gelt	28	2R,2Nd	I		6200	6150-6250
	47	F	I		6100	6075-6125

Name	Ref.	Pumping	Solvent	Conc. of Dye	λ_M or λ_C	Range
Rapid-filter Grün	27	R	G		7950	7905-7995
Rhodamine 3B	47,28	2R,2Nd	I		6200	6160-6240
	47	F	I		6100	6060-6140
Rhodamine 6G	10	2R	E	$5X10^{-4}M$	5680	5600-6100
		2Nd			5680	5600-6100
	15	F	E	$10^{-4}M$		5693-6091
	2	2Nd	E	$10^{-4}M$	5620	
		F			5950	
					5990	
	22	2R,2Nd	E	$3X10^{-6}M$	5650	
	38	2R	E	$10^{-5}M$	5550	
	39	F	E	$10^{-4}M$	5850	
	41	F	W,D_2O,DMSO,E			
	32	F	W or E	$10^{-3}M$		
	35	F	E	$10^{-4}M$	5790	
	47,28	2R,2Nd	I		5800	5725-5875
	47	F	I		5800	5725-5875
	19	2Nd	G		5570	5548-5592
	4	N	E			5790-6020
	20	N	E	$5X10^{-4}M$		
	16	F	E	50mg/1	5940	5360-6200
Rhodamine 6GL	21	N	E	$1.5X10^{-3}M$	5686	
				$3X10^{-4}M$	5690	
			DMF	$1.5X10^{-3}M$	5755	
				$3X10^{-4}M$	5773	
Rhodamine B	7	F	E	10^{-4}-$10^{-5}M$		6000-6400
	10	2R,2Nd	E	$5X10^{-4}M$	6000	5800-6400
	15	F	E	$10^{-4}M$		5897-6427
	2	2Nd	M,E	$5X10^{-5}M$	5790	
		F	M		6170	
			E		6220	
	22	2R,2Nd	E		5770	
	41	F	E,W,D_2O			
	26	N	W,E, or T	10^{-2}-$10^{-4}M$		5650-6200

Name	Ref.	Pumping	Solvent	Conc. of Dye	λ_M or λ_C	Range
Rhodamine B - continued	32	F	W,E	10^{-3}M		
	35	F	M	10^{-4}M	6150	
	30	2R	E	$2X10^{-3}$M	6080	
	44,47	2R,2Nd	I		6100	6050-6150
	47	F	I		6100	6040-6160
	4	N	E			6010-6420
	21	N	E+10^{-3}M NaOH	$5X10^{-4}$M	5860	
			E+$3X10^{-3}$M NaOH	$2.5X10^{-3}$M	5817	
	16	F	E	50mg/l	6220	6020-6450
				50mg/l	6100	5900-6520
			E+HCl	50mg/l	6160	5980-6450
			E+NaOH	50mg/l	5900	5800-6100
Rhodamine C	19	2,3Nd	E			5675-5725
Rhodamine G	22	2R,2Nd	E		5850	
Rhodamine S	17	F	E			5780-5945
	16	F	E	50mg/l	5910	5690-6120
					6040	5810-6180
Rhoduline Blue 6G	27	R	G		7580	7455-7705
Saphranine T	19	2Nd	E		6100	5980-6220
Sodium Fluorescein (Uranine)	12	F	W	$2X10^{-4}$M		5360-5450
	15	F	E	$5X10^{-5}$M		5336-5624
	38	2R	W,E	10^{-3}M	5270	
	41,39	F	E,W,D_2O	10^{-4}M	5500	
	35	F	W	10^{-4}M		
	28	2R	E		5600	
	4	N	E			5380-5795
Sodium Salicylate	25	N	E			3950-4180
1-Styryl-4-(ω-vinyl-(n-biphenylyl))-benzene	19	3Nd	T		4320	4305-4335

Name	Ref.	Pumping	Solvent	Conc. of Dye	λ_M or λ_C	Range
p-Terphenyl	14	F	DMF	$8X10^{-4}M$	3410	
			D	$2X10^{-4}$-$4X10^{-4}M$	3425-3555	
Thionin	27	R	S		8500	8395-8605
Toluidine Blue	27	R	S		8480	8425-8535
2,4,6-Triphenyl-pyrilium Fluoroborate	30	2R	M	$1.7X10^{-3}M$	4850	
Trypaflavin	28	2R	E		5050	4995-5105
Uranine (see Sodium Fluorescein)						
Victoria Blue	27	R	G		8090	8035-8145
Victoria Blue R	27	R	G		8140	8035-8245
Violetrot	28	2R,2Nd	I		6200	6150-6250
	47	F	I		6100	6075-6125
Xylene Red B	16	F	E+NaOH	50mg/l	6000,6120	5850-6450

1. Abakumov, G. A., JEPT Letters 9, 9 (1969).
2. Bass, M., Deutsch, T. F., and Weber, M.J., Appl. Phys. Letters, 13, 120 (1968).
3. Broida, H. P., and Hazdon, S. D., Appl. Phys. Letters, 16, 142 (1970).
4. Capelle, G., and Phillips, D., Applied Optics 9, 2742 (1970).
5. Derkacheva, L. D., et al., Optics and Spectroscopy 25, 404 (1968).
6. Deutsch, T. F., and Bass, M., IEEE J. Quantum Electronics, 260 (1969).
7. Deutsch, T. F., Bass, M., and Meyer, P., Appl. Phys. Letters, 11, 379 (1967).
8. Eastman Kodak Co., Data Release: "Dyes for Lasers".
9. Farmer, G. I., et al., Appl. Optics, 8, 363 (1969).
10. Fawcett, B. C., IEEE J. Quantum Electronics, QE6, 473 (1970).
11. Ferrar, C. M., IEEE J. Quantum Electronics, 550 (1969).
12. Ferrar, C. M., IEEE J. Quantum Electronics, 621 (1969).
13. Furomoto, M., and Ceccon, H., IEEE J. Quantum Electronics, 4204 (1969).
14. Furomoto, H., and Ceccon, H., IEEE J. Quantum Electronics, QE6, 262 (1970).
15. Goldstein, A., and Dacol, F. H., Rev. Sci. Inst., 40, 1597 (1969).
16. Gregg, D. W., et al., "Wavelength tunability of new and previously reported flashlamp-pumped laser dyes," Lawrence Radiation Lab., University of California, Livermore, Rept. UCRL-72044, Oct. 15, 1969.
17. Gregg, D. W., and Thomas, S. J., IEEE J. of Quantum Electronics QE5, 302 (1969).
18. Huth, B. G., and Farmer, G. I., IEEE Journal of Quantum Electronics QE4, 427 (1968).
19. Kotzubanov, V. D., et al., Optics and Spectroscopy 25, 406 (1968).
20. Lankard, J. R., and von Gutfeld, R. J., IEEE J. of Quantum Electronics QE5, 625 (1969).
21. Lidholt, L. R., and Wladimiroff, W. W., Opto-Electronics 2, 21 (1970).
22. McFarland, B. B., Appl. Phys. Letters, 10, 208 (1967).
23. Marling, J. B., Gregg, D. W., and Thomas, S. J., IEEE J. of Quantum Electronics QE6, 570 (1970).
24. Miyazoe, Y., and Maeda, M., Appl. Phys. Letters, 12, 206 (1968).
25. Myer, J. A., Itzkan, I., and Kierstead, E., Nature, 225, 544 (1970).
26. Myer, J. A., Johnson, C. L., Kierstead, E., Sharmer, R. D., and Itzkan, I., Appl. Phys. Letters, 16, 3 (1970).

27. Rubinov, A. N., and Mostovnikov, V. A., Zh. Priklad. Spectroskopii 7, 327 (1967).

28. Rubinov, A. N., and Mostovnikov, V. A., Abstracts of the 16th Conference on Luminescence (Molecular Luminesence), Leningrad, 1967.

29. Schafer, F. P., "Organic Dye Lasers," invited paper presented at the 1968 Quantum Electronics Conf., Miami, Fla., May 1968.

30. Schafer, F., Schmidt, W., and Marth, K., Phys. Letters, 24A, 280 (1967).

31. Schafer, F., Schmidt, W., and Volze, J., Appl. Phys. Letters, 9, 306 (1966).

32. Schmidt, W., and Schafer, F. P., Z. Naturforech, 22A, 1563 (1967).

33. Schmidt, W., and Schafer, F. P., Phys. Letters, 26A, 558 (1968).

34. Shank, C. V., Dienes, A., Trozzolo, A. M., and Myer, J. A., Appl. Phys. Letters, 16, 405 (1970).

35. Snavely, B. B., and Peterson, O. G., IEEE J. Quantum Electronics, QE4, 540 (1968).

36. Snavely, B. B., Peterson, O. G., and Reithel, R. F., Appl. Phys. Letters, 11, 275 (1967).

37. Sorokin, P. P., et al., IBM J. of Research and Development, 10, 401 (1966).

38. Sorokin, P. P., et al., IBM J. of Research and Development, 11, 130 (1967).

39. Sorokin, P. P., et al., J. Chem. Phys., 48, 4726 (1968).

40. Sorokin, P. P., and Lankard, J. R., IBM J. of Research and Development, 10, 162 (1966).

41. Sorokin, P. P., and Lankard, J. R., IBM J. of Research and Development, 11, 148 (1967).

42. Speath, M. L., and Bortfeld, D. P., Appl. Phys. Letters, 9, 179 (1966).

43. Srinivasan, R., IEEE J. of Quantum Electronics QE5, 553 (1969).

44. Stepanov, B. I., et al., Zh. Priklo, Spektroskopii, 7, 116 (1967).

45. Stepanov, B. I., and Rubinov, A. N., Soviet Physics Vspekhi, 11, 304 (1968).

46. Stepanov, B. I., Rubinov, A. N., and Mostovnikov, V. A., JEPT Letters 5, 117 (1967).

47. Stepanov, B. I., Rubinov, A. N., and Mostovnikov, V. A., Abstracts of the 3rd Symposium on Nonlinear Optics, Berevan, 1967.

48. Tikhonov, Y. O., and Shpak, M. T., Udrauins 'lyy Fizyehnyy Zhurnal, 12, 2077 (1967).

49. Yamaguchi, G., et al., Oyo Buturi, 37, 346 (1968).